

POLITECNICO DI TORINO

DIPARTIMENTO DI INGEGNERIA MECCANICA E AEROSPAZIALE

Master Degree Thesis

Euro NCAP 2020: the evolution of partial overlap frontal tests and its impact on effective vehicle safety

A simulation analysis of the Euro NCAP ODB and MPDB procedures



Principal Supervisor
prof. Andrea Tonoli

Secondary Supervisors:
prof. Gianpiero Mastinu
prof. Marco Anghileri

Candidate
Tommaso Maria Verri

Industrial Supervisor
Pininfarina Engineering
ing. Francesco Macheda

ACADEMIC YEAR 2017 – 2018

Summary

In the last two decades, consumer testing programmes such as Euro NCAP have driven a substantial improvement in vehicle safety thanks to their effect on public opinion, which was in turn seen as a marketing opportunity by manufacturers. Nonetheless, in the EU, road accidents are still a major cause of death, with over 25 000 people killed every year and a much greater number suffering serious injuries. Out of this number, a substantial part is caused by two car frontal impacts, which are currently tested both by legislation and Euro NCAP with the Offset Deformable Barrier test. However, it has been historically pointed out that this test is not closely representative of real life scenarios as it cannot assess the negative impacts of poor compatibility between vehicle masses, structural designs and front end rigidities. For this reason, a new test procedure has been devised and will be introduced in 2020. The Mobile offset Deformable Barrier test is based on the use of a trolley of a set mass representing the average of the european circulating fleet, which will impact against a vehicle moving at equal velocity in opposite direction. The deformable element used will also allow the assessment of partner protection criteria based on its own deformation. This change represents a new challenge for OEMs and design firms, as it will increase the level of complexity required to design frontal structures, in order for them to guarantee the same level of performance shown in the ODB.

Hence, the aim of this study is to gain an initial understanding of the effects that the new test has on vehicle passive safety by performing comparative simulations between the two procedures on a number of full vehicle mathematical models. The four vehicles to be included were selected in order to have a range of different masses and vehicle design philosophies. Initially, a correlation study based on full width rigid barrier tests was performed in order to understand the level of representativeness of the models. This showed that two out of the four were closely related to physical performance, while other two presented a level of discrepancy. Next, the main part of the study involved the simulation of the vehicles in the ODB and MPDB procedures, which resulted in an in depth analysis completed in terms of crash pulse, section forces, structural deformation and cabin intrusion. The comparative study highlighted an increased harshness of the MPDB test due to its reduced timeframe, in all four vehicles. At the same time it showed a clear correlation between performance and mass: the lighter vehicle underwent substantially higher damage, the model with mass similar to the barrier only minor negative effects, while the two vehicles with heavier mass saw a clear improvement in their deformation, intrusion and acceleration. Furthermore, the deformation of the barrier and the dynamic data of the trolley allowed to assess the partner protection level of the models. The results showed that the performance was closely related to chassis design: the very light and very heavy vehicles achieved comparably negative results, while the vehicle with more advanced frontal structures proved to be substantially better. In conclusion, the study highlighted the very poor results that can currently be obtained when using a ladder chassis design.

Contents

List of Tables	VII
List of Figures	VIII
1 Introduction	1
1.1 The issue of representative crash testing	1
1.2 Aims and objectives	2
1.3 Report structure	3
2 State of the art	5
2.1 The evolution of Euro NCAP	5
2.1.1 Euro NCAP future Roadmaps	9
2.2 From ODB to MPDB	10
2.2.1 The Offset Deformable Barrier test	10
2.2.2 The Mobile Offset Deformable Barrier test	15
2.3 Crash test simulation in the vehicle design process	20
3 Methodology	23
3.1 Simulation softwares	23
3.2 Vehicle models	25
3.2.1 Toyota Yaris	26
3.2.2 Honda Accord	30
3.2.3 Chevrolet Silverado	33
3.2.4 U Model	38
3.3 Barrier models	41
3.4 Schedule of conducted tests	42
4 Correlation Study	45
4.1 The issue of correlating physical crash testing with mathematical models	45
4.2 Correlation methodology	46
4.3 Toyota Yaris	47
4.4 Honda Accord	53
4.5 Chevrolet Silverado	60
4.6 U Model	65
4.7 Conclusions	68

5	Results	71
5.1	Toyota Yaris	71
5.1.1	ODB test	71
5.1.2	MPDB test	78
5.1.3	Comparison	84
5.2	Honda Accord	93
5.2.1	ODB test	93
5.2.2	MPDB test	98
5.2.3	Comparison	102
5.3	Chevrolet Silverado	106
5.3.1	ODB test	106
5.3.2	MPDB test	113
5.3.3	Comparison	117
5.4	U Model	124
5.4.1	ODB test	124
5.4.2	MPDB test	130
5.4.3	Comparison	136
5.5	Conclusions	145
6	Partner protection analysis	147
6.1	Partner protection in Euro NCAP 2020	147
6.2	Analysis methodology in simulation	148
6.3	Partner protection results	149
6.3.1	Toyota Yaris	149
6.3.2	Honda Accord	152
6.3.3	Chevrolet Silverado	155
6.3.4	U Model	158
6.4	Conclusions	161
7	Conclusions and further work	163
7.1	Simulation study conclusions	163
7.2	Further work	166
	Bibliography	I
	A Simulation energy charts	V
	B Correlation study photographs	IX

List of Tables

2.1	ODB test specification	13
2.2	ODB construction specifications	14
2.3	MPDB test specification	18
2.4	PDB construction specifications	19
3.1	2009 Toyota Yaris specifications	26
3.2	2011 Honda Accord specifications	30
3.3	2014 Chevrolet Silverado specifications	34
3.4	Tests schedule	43
4.1	US-NCAP - utilised intrusion measurement points [1]	46
4.2	Toyota Yaris - full width rigid barrier dynamic data	48
4.3	Toyota Yaris - full width rigid barrier deformation measurements [<i>mm</i>]	51
4.4	Honda Accord - full width rigid barrier dynamic data	55
4.5	Honda Accord - full width rigid barrier deformation measurements [<i>mm</i>]	58
4.6	Chevrolet Silverado - full width rigid barrier dynamic data	61
4.7	Chevrolet Silverado - full width rigid barrier deformation measurements [<i>mm</i>]	63
4.8	U Model - ODB 56 <i>km/h</i> intrusion measurements [2]	67
5.1	Toyota Yaris ODB - intrusion measurements	75
5.2	Toyota Yaris MPDB - intrusion measurements	82
5.3	Toyota Yaris - ODB vs MPDB dynamic data	86
5.4	Toyota Yaris - intrusion measurement comparison	90
5.5	Honda Accord ODB - intrusion measurements	97
5.6	Honda Accord MPDB - intrusion measurements	101
5.7	Honda Accord - intrusion measurement comparison	106
5.8	Chevrolet Silverado ODB - intrusion measurements	112
5.9	Chevrolet Silverado MPDB - intrusion measurements	117
5.10	Chevrolet Silverado - ODB vs MPDB dynamic data	118
5.11	Chevrolet Silverado - intrusion measurement comparison	123
5.12	U Model ODB - intrusion measurements	130
5.13	U Model MPDB - intrusion measurements	136
5.14	U model - ODB vs MPDB dynamic data	138
5.15	U Model - intrusion measurement comparison	142

List of Figures

2.1	Progress of adult occupant star rating 1997-2007 [3]	7
2.2	Progress of pedestrian protection star rating 1997-2007 [3]	8
2.3	Euro NCAP future Roadmaps	9
2.4	ODB Normal element with bumper [4]	11
2.5	Car-to-car frontal impact speed and serious or fatal casualties [5]	12
2.6	ODB test infographic [6]	13
2.7	Physical model of ODB [7]	13
2.8	MPDB test infographic [9]	17
2.9	PDB physical model [7] and dimensions [10]	19
2.10	Displacement-strength characteristic corridor of Block B [10]	19
2.11	Progressive Deformable Barrier physical model [7]	20
3.1	The simulation process - softwares utilised	24
3.2	2009 Toyota Yaris Sedan - Physical [11] and CAE models	27
3.3	Toyota Yaris engine compartment - Physical [12] and CAE models	28
3.4	Toyota Yaris - passenger compartment details	28
3.5	Toyota Yaris - model details	29
3.6	2011 Honda Accord - Physical [13] and CAE models	31
3.7	Honda Accord engine compartment - Physical [14] and CAE models	31
3.8	Honda Accord - passenger compartment details	32
3.9	Honda Accord - BIW front section physical [15] and CAE models	32
3.10	Honda Accord - model details	33
3.11	2014 Chevrolet Silverado - Physical [16] and CAE models	34
3.12	Chevrolet Silverado engine compartment - Physical [17] and CAE models	35
3.13	Chevrolet Silverado - passenger compartment details	35
3.14	Chevrolet Silverado - main ladder frame	36
3.15	Chevrolet Silverado - structure details	37
3.16	U Model - CAE model	38
3.17	U Model details - interior and engine compartment	38
3.18	U Model - ladder type chassis	39
3.19	U Model - details	40
3.20	Offset Deformable Barrier - CAE model	41
3.21	Progressive Deformable Barrier - CAE model	41
3.22	Mobile Offset Deformable Barrier - CAE model	42
4.1	Yaris FWRB - simulation snapshot	48
4.2	Yaris FWRB - acceleration	49

4.3	Yaris FWRB - velocity	49
4.4	Yaris FWRB - crush space	50
4.5	Yaris FWRB - LHS and RHS comparison	51
4.6	Yaris FWRB - three quarters and underbody comparison	52
4.7	Yaris FWRB - top view comparison	52
4.8	Honda Accord - front structures modification	54
4.9	Accord - comparison of crash pulse before and after modifications	54
4.10	Accord FWRB - simulation snapshot	56
4.11	Accord FWRB - acceleration	56
4.12	Accord FWRB - velocity	57
4.13	Accord FWRB - crush space	57
4.14	Accord FWRB - LHS and RHS comparison	59
4.15	Accord FWRB - top view comparison	59
4.16	Accord FWRB - three quarters and underbody comparison	60
4.17	Silverado FWRB - simulation snapshot	61
4.18	Silverado FWRB - acceleration	62
4.19	Silverado FWRB - velocity	62
4.20	Silverado FWRB - crush space	63
4.21	Silverado FWRB - LHS and RHS comparison	64
4.22	Silverado FWRB - top view comparison	64
4.23	Silverado FWRB - three quarters and underbody comparison	65
4.24	U Model ODB 56km/h - simulation snapshot	67
4.25	U Model ODB 56km/h - RHS and underbody comparison	68
5.1	Toyota Yaris ODB - simulation snapshot	72
5.2	Toyota Yaris ODB - structural collapse detail	73
5.3	Toyota Yaris ODB - acceleration	73
5.4	Toyota Yaris ODB - section forces	74
5.5	Toyota Yaris ODB - firewall intrusion	76
5.6	Toyota Yaris ODB - firewall deformed region	76
5.7	Toyota Yaris ODB - driver door opening deformation	76
5.8	Toyota Yaris ODB - A-pillar deformation	77
5.9	Toyota Yaris ODB - floor and tunnel deformation	77
5.10	Toyota Yaris MPDB - simulation snapshot	79
5.11	Toyota Yaris MPDB - structural collapse detail	79
5.12	Toyota Yaris MPDB - acceleration	80
5.13	Toyota Yaris MPDB - section forces	80
5.14	Toyota Yaris MPDB - firewall intrusion	82
5.15	Toyota Yaris MPDB - firewall deformed region	83
5.16	Toyota Yaris MPDB - floor and tunnel deformation	83
5.17	Toyota Yaris MPDB - driver door opening deformation	84
5.18	Toyota Yaris MPDB - deformed pillar and interior	84
5.19	Toyota Yaris - comparison between ODB and MPDB energy content	85
5.20	Toyota Yaris - front structures behaviour comparison	86
5.21	Toyota Yaris - crash pulse comparison	87
5.22	Toyota Yaris - velocity trend comparison	87
5.23	Toyota Yaris - section forces comparison	89

5.24	Toyota Yaris - ODB firewall deformation	89
5.25	MPDB	90
5.26	Toyota Yaris - MPDB firewall deformation	90
5.27	Toyota Yaris - interior intrusion comparison	91
5.28	Toyota Yaris - front deformation comparison	92
5.29	Honda Accord ODB- acceleration and section forces	93
5.30	Honda Accord ODB - simulation snapshot	94
5.31	Honda Accord ODB - structural collapse detail	95
5.32	Honda Accord ODB - firewall deformation	96
5.33	Honda Accord MPDB - acceleration and section forces	98
5.34	Honda Accord MPDB - simulation snapshot	99
5.35	Honda Accord MPDB - structural collapse detail	100
5.36	Honda Accord MPDB - firewall deformation	101
5.37	Honda Accord MPDB - A pillar and windscreen deformation	102
5.38	Honda Accord - energy content comparison	103
5.39	Honda Accord - ODB firewall deformation	104
5.40	MPDB	104
5.41	Honda Accord - MPDB firewall deformaton	104
5.42	Honda Accord - front deformation comparison	105
5.43	Chevrolet Silverado ODB - simulation snapshot	108
5.44	Chevrolet Silverado ODB - structural collapse detail	108
5.45	Chevrolet Silverado ODB - acceleration	109
5.46	Chevrolet Silverado ODB - section forces	109
5.47	Chevrolet Silverado ODB - cross section location	110
5.48	Chevrolet Silverado ODB - overall cabin deformation	111
5.49	Chevrolet Silverado ODB - driver side firewall intrusion	111
5.50	Chevrolet Silverado ODB - passenger side intrusion	112
5.51	Chevrolet Silverado MPDB - simulation snapshot	114
5.52	Chevrolet Silverado MPDB - structural collapse detail	114
5.53	Chevrolet Silverado MPDB - acceleration	115
5.54	Chevrolet Silverado MPDB - section forces	115
5.55	Chevrolet Silverado MPDB - driver side firewall intrusion	116
5.56	Chevrolet Silverado MPDB - passenger side intrusion	116
5.57	Chevrolet Silverado - ODB vs MPDB energy content	118
5.58	Chevrolet Silverado - crash pulse comparison	119
5.59	Chevrolet Silverado - velocity trend comparison	119
5.60	Chevrolet Silverado - main rail deformation comparison	120
5.61	Chevrolet Silverado - section forces comparison	121
5.62	Chevrolet Silverado - firewall intrusion comparison	122
5.63	U Model ODB - simulation snapshot	125
5.64	U Model ODB - structural collapse detail	125
5.65	U Model ODB - acceleration	126
5.66	U Model ODB - section forces	126
5.67	U Model ODB - cross section location	127
5.68	U Model ODB - firewall intrusion	128
5.69	U Model ODB - cabin deformation and interior intrusion	129

5.70	U Model MPDB - simulation snapshot	131
5.71	U Model MPDB - structural collapse detail	132
5.72	U Model MPDB - acceleration	132
5.73	U Model MPDB - section forces	133
5.74	U Model MPDB - firewall intrusion	134
5.75	U Model MPDB - cabin deformation and interior intrusion	135
5.76	U Model - energy content comparison	137
5.77	U Model ODB - structural damage	138
5.78	U Model MPDB - structural damage	139
5.79	U Model - crash pulse comparison	139
5.80	U Model - velocity comparison	140
5.81	U Model - RHS section force comparison	141
5.82	U Model - LHS rail section forces comparison	141
5.83	U Model - firewall intrusion comparison	143
5.84	U Model - interior intrusion comparison	144
6.1	Toyota Yaris - barrier deformation in area of interest	150
6.2	Toyota Yaris - overall barrier deformation	150
6.3	Toyota Yaris - barrier and vehicle acceleration comparison	151
6.4	Toyota Yaris - barrier and vehicle velocity comparison	151
6.5	Honda Accord - barrier deformation in area of interest	153
6.6	Honda Accord - overall barrier deformation	153
6.7	Honda Accord - barrier and vehicle acceleration comparison	154
6.8	Honda Accord - barrier and vehicle velocity comparison	154
6.9	Chevrolet Silverado - barrier deformation in area of interest	156
6.10	Chevrolet Silverado - overall barrier deformation	156
6.11	Chevrolet Silverado - barrier and vehicle acceleration comparison	157
6.12	Chevrolet Silverado - barrier and vehicle velocity comparison	157
6.13	U Model - barrier deformation in area of interest	159
6.14	U Model - overall barrier deformation	159
6.15	U Model - barrier and vehicle acceleration comparison	160
6.16	U Model - barrier and vehicle velocity comparison	160
6.17	Comparison between analysed vehicles	161
A.1	Toyota Yaris FWRB - simulation energy	v
A.2	Honda Accord FWRB - simulation energy	vi
A.3	Chevrolet Silverado FWRB - simulation energy	vi
A.4	U Model ODB 56km/h - simulation energy	vii
B.1	Toyota Yaris FWRB - LHS comparison	ix
B.2	Toyota Yaris FWRB - RHS comparison	x
B.3	Toyota Yaris FWRB - top view comparison	xi
B.4	Toyota Yaris FWRB - three quarter view comparison	xii
B.5	Toyota Yaris FWRB - underbody comparison	xiii
B.6	Honda Accord FWRB - LHS comparison	xiv
B.7	Honda Accord FWRB - RHS comparison	xv
B.8	Honda Accord FWRB - top view comparison	xvi
B.9	Honda Accord FWRB - three quarter view comparison	xvii
B.10	Honda Accord FWRB - underbody comparison	xviii

B.11 Chevrolet Silverado FWRB - LHS comparison	xix
B.12 Chevrolet Silverado FWRB - RHS comparison	xx
B.13 Chevrolet Silverado FWRB - top view comparison	xxi
B.14 Chevrolet Silverado FWRB - three quarter view comparison	xxii
B.15 Chevrolet Silverado FWRB - underbody comparison	xxiii
B.16 U Model ODB 56km/h - RHS comparison	xxiv
B.17 U Model ODB 56km/h - underbody comparison	xxv

Chapter 1

Introduction

1.1 The issue of representative crash testing

In the 28 EU member states, road accidents are still a major cause of death, with over 25 000 people being killed every year and a much greater number suffering serious injuries [18]. More than 50% of these fatalities have been shown to be car occupants, involved in either single or multiple vehicle crashes [19]. This clearly poses an important problem firstly for social aspects, but also for economic reasons, as road deaths are a significant expense for european countries both in terms of tangible costs and human costs . For these reasons, throughout the last three decades, national and international institutions have been focusing on creating legislative and consumer tests in order to drive the manufacturers to improve the safety of their products, both to protect the occupants in the event of a crash, and to develop and install systems that could prevent the occurrence from happening in the first place. Among these, one of the projects that has had the most impact has been the European New Car Assessment Programme - Euro NCAP - which completes non legislative tests on the most popular vehicles in the european circulating fleet, assigning a star rating based on the performance shown in a set of standardised procedures. Since its introduction in 1996, the total death toll has been reduced by roughly a quarter, despite the large increase in traffic volume in the same timeframe. A substantial portion of the merit has to be attributed to this institution. In fact, after the first ten years of work, several studies that cross checked test results and accident data proved a positive correlation between occupant protection capabilities and high star rating [20], while vehicles with only 2-3 stars showed worse real life performance. Nonetheless, very relevant differences are present between the results seen in consumer testing procedures and real car-to-car impacts. In fact, the main aim of Euro NCAP was not the prediction of real life behaviour, but the assessment of best practices for specific car models and the overall circulating fleet, mainly due to the boundaries imposed by laboratory testing which could not give a comprehensive overview of the complex phenomena encountered on the roads. To fulfill this goal, the frontal testing procedure that was chosen since the very beginning was very similar to that used for legislative testing: a partial overlap frontal impact against a fixed deformable barrier, or Offset Deformable Barrier test (ODB).

Without diminishing the positive impact that the implementation of such procedure has had on the circulating fleet, which has become much safer, it was pointed out that the

use of the ODB test both in legislative and consumer crash testing has never addressed some important issues, while also being cause to others. Mainly, the research conducted by european entities and projects, such as ADAC and FIMCAR, has shown that the discrepancy between the rating obtained in laboratory testing and the performance in car-to-car accidents can be attributed to issues of compatibility between vehicles. This involves differences in mass, front end structural design and structural rigidity between the two parties, all aspects that have never been considered in safety ratings due to the difficulty of assessment. In addition, the nature of the ODB procedure has worsened the situation by forcing vehicles with higher mass to increase their front end rigidity, due to the much larger amount of energy involved in the impact compared to light vehicles. As a result, in 2009, the accident analysis conducted by ADAC [19] has demonstrated that the probability of serious or fatal injuries in a two car collision were still double if the occupant was in a light vehicle, rather than in one with large mass.

For these reasons and thanks to technological advancements, Euro NCAP has recently decided to revolutionise its frontal impact testing protocol, in order to implement a procedure which represents the real life scenario more closely and also gives the ability to rate the compatibility level of the vehicles, adding to the overall score a number of considerations related to partner protection. The new test, which will be intruduced in 2020, involves the impact with a moving trolley of a mass representing the average vehicle ciruclating on EU roads. The trolley will have a different deformable element mounted on its front, which will replicate more effectively the structural stiffness of an idealised opponnet car and also allow the evaluation of partner protection parameters based on its own deformation. Hence, it was denominated the Mobile offset Progressive Deformable Barrier test, or MPDB.

This change represents an important step forward for vehicle safety, as it will force OEMs and design companies to modify to a great extent current structural design trends in order to obtain the same level of performance that was seen in the past in terms of Euro NCAP rating. For this reason, it is important to start the process of understanding what are the effects of the new test on different vehicle classes and chassis design philosophies, as it represents an important first step towards the definition of the direction that will have to be followed in future vehicle design projects.

1.2 Aims and objectives

The overall aims of the study are to gain a deeper understanding, through the use of mathematical modeling and simulation, of the effects caused by the new Euro NCAP procedure on passive safety performance for a sample of vehicles, selected in order to evaluate the dependency of these effects on the mass of the vehicle and on chassis architecture. Furthermore, a secondary aim is to also understand how these vehicles, designed either today or in the recent past, would perform if partner protection was to be considered, as it will be after 2020.

The objectives set out to achieve these aims are:

- to select a number of suitable mathematical models representing a small number of vehicles with different masses and chassis construction;

- to verify their representativeness by conducting a correlation study between the results obtained in simulation and those coming from physical tests;
- to perform a comparative study, simulating both the current Euro NCAP Offset Deformable Barrier procedure and the new MPDB test, to understand differences and criticalities between the two;
- and finally to assess their performance in terms of partner protection using the results from the MPDB simulations and implementing an analysis methodology that could effectively be used in the consumer testing rating protocol.

1.3 Report structure

This report is subdivided into seven chapters, five of these contain the research and findings of the work, while the initial and final ones are dedicated respectively to the introduction and overall conclusions. The main body of the report is structured as follows:

- the second chapter is aimed at providing a historical review of the evolution of the Euro NCAP programme, from its beginning to the future plans for 2020 and 2025, by analysing the existing literature. In order to have a clear view of the details of the two tests that will be compared in the results section, the procedures and parameters of the Offset Deformable Barrier and Mobile offset Progressive Deformable Barrier tests are presented. In conclusion, a comment on the importance of mathematical modeling and simulation for the vehicle design process and for passive safety is given;
- in the third chapter, the tools and methods utilised to complete the objectives of the study are reported. The initial decisions to be made regarding the choice of softwares to be selected for pre processing, solver and post processing are explained, together with a brief comment on their use. Next, a description and analysis of the four vehicle models adopted for the completion of the comparative study is shown, while the official models of the ODB and MPDB barriers created by the software provider are presented. In addition, the schedule of conducted tests is included for reference;
- the fourth chapter details the work performed to understand the level of correlation between the CAE models used and their physical counterparts. Initially, reasoning is given about the importance and value of this portion of the work, while in the second section the methodology to perform such a study is explained. Finally, the results of the analysis for each vehicle model are reported, together with conclusions regarding the effect of the findings on the following parts of the project;
- in the fifth chapter, the results obtained from the simulations of ODB and MPDB tests are presented. First, the models' structural performance is analysed in terms of the ODB test, to assess their strengths and weaknesses on the current Euro NCAP testing protocol. Next, the MPDB test is analysed and finally a comparison between the two tests is completed. In the final section, conclusions on the findings are drawn;
- lastly, in the sixth chapter the work completed in order to gain an understanding of the partner protection level of the tested vehicles is reported. A brief description

of the procedure that the study is based on and of the methodology used to apply it in the simulation environment is given. The results of barrier deformation and acceleration obtained from the MPDB simulations of the four vehicles utilised are then analysed in order to highlight criticalities and positive achievements. Finally, the performance of the four vehicles is compared to draw conclusions on the findings.

Chapter 2

State of the art

In this chapter, a review of the evolution of the Euro NCAP consumer testing programme is given through the analysis of the existing literature. In addition, the procedure of the current Offset Deformable Barrier test is presented, with details regarding both the setup of the vehicle, the parameters of the test and those of the barrier. The same is presented for the new Mobile offset Progressive Deformable Barrier test in order to have a clear picture of the changes before diving into the details of the results. Finally, a brief comment on the importance of crash test simulations in industry, especially in relation to passive safety, is given.

2.1 The evolution of Euro NCAP

The Euro NCAP (i.e. European New Car Assessment Programme) is a consumer crash testing programme established in order to provide to end users a realistic assessment of the safety level of new vehicles on the European market [21]. The mission of the organisation is to spread knowledge about effective vehicle safety, hence utilising the power of public opinion to push automotive manufacturers to improve safety systems beyond the homologation requirements. In turn, this directly affects the amount of lives saved in real world crash situations [3]. The method to achieve this objective has been based since the very beginning on a star rating system, calculated from the results of a range of tests, but simple enough in its end result to be comprehended by the entire consumer base.

The work of Euro NCAP originated in 1996, from the joint efforts of the Swedish National Road Administration (SNRA), the Federation Internationale de l'Automobile (FIA), the International Testing and the UK's Department for Transport [3]. The initial idea was to move on the line of work of the National Highway Traffic Safety Association (NHTSA, USA) New Car Assessment Programme developed in 1979, where vehicles were tested in a full frontal impact with a rigid wall at 56km/h , although implementing the different testing strategies that had been developed in Europe. Namely, since the beginning the tests included the frontal offset test with ODB barrier at 64km/h , the side impact test with MDB barrier at 50km/h and the pedestrian impact tests for leg, upper leg and head. All tests used in the original round of the programme were based on the developments by the European Enhanced Vehicle-safety Committee (EEVC) for legislation, with the

exception of a higher impact speed for the ODB, raised from 56 to 64km/h [5].

During the first two years of activity, four rounds were completed, starting from the 7 superminis of round one, moving on with a larger batch of family cars for round two, small family cars in round three and executive vehicles in round four. The selection of the cars was based on the highest selling version of the chosen models in the european market; although it is known that different body types, engine sizes and transmission types can influence crashworthiness, Euro NCAP did not aim at testing all vehicles on the road, which would be unrealistic and extremely resource consuming, but at providing information regarding the most significant variants for the road-going fleet. Furthermore, vehicles were only tested in the most basic configuration in terms of safety, meaning that optional equipment offered by the manufacturers at a higher price was not taken into account for the tests funded directly by Euro NCAP. The possibility was given to the manufacturers to fund additional tests in case a certain vehicle was not selected to be in the batch, or to prove the effects of additional safety equipment offered, or to have re-runs whenever an updated version of the vehicle was to come out. In order to ensure unbiased results, the tested vehicles were purchased from normal dealers anonymously, so to minimise the possibility of being given non standard production cars [5].

The initial reaction from the automotive manufacturers was highly critical, as it was believed that it would be impossible to achieve high ratings in the three tested categories due to the very strict evaluation system in place. Soon, however, the tide changed and OEMs started understanding the possible marketing advantage that would have come from scoring a high rating in the test, as public opinion was paying more and more attention to the published results. Not long after the first tests, vehicles were improved greatly and started scoring full marks in all fields, giving the first hint that the method enacted by Euro NCAP was in fact working. At this point, several manufacturers started offering most of the available safety equipment as standard and set the aim of reaching a four star rating as a primary design goal for new models [5].

The first major change to the testing procedures was implemented in 1999, when the pole test was introduced. The procedure was taken directly from the US side impact standard, with the only modification being the introduction of the EUROSID-1 dummy. The decision behind this addition was based on the fact that, due to the Euro NCAP side impact test, manufacturers started introducing measures to reduce head and thorax injuries. However, the standard side impact test did not guarantee a consistent contact with the head of the dummy, hence no significant measure of the effectiveness of the new systems was present. Furthermore, data about road accidents showed that despite the relatively low number of accidents including an impact with a pole, the percentage of serious injuries or deaths caused by this kind of accident was incredibly high. With the new test in place, the scoring system was updated and the number of stars was increased from four to five, and the first vehicles to achieve a five star rating were tested in 2001.

As the years of activity increased, the work of Euro NCAP kept growing consistently, with two batches of tests per year, each containing an ever increasing number of vehicles, as a result of more national stakeholders taking part in the funding and a higher and higher commitment by OEMs. Together with this trend of increased testing volume, the range of areas taken into consideration in the star rating also widened. Amongst all the modifications introduced, the most significant were:

- in 2002, a score for seatbelt reminders was introduced in order to force manufacturers to, at the very least, include intelligent reminders for seatbelt usage for the driver;
- in the same year, the organisation noticed a lack of advancement in the field of pedestrian protection, which was at the time little regarded by the manufacturers, hence a modification to the scoring system for pedestrian protection was put in place, again to push OEMs to take the issue more seriously;
- in 2003, the first child protection rating was introduced, to make sure that vehicle producers took responsibility for the implementation of child restraint systems with the overall structure of the car, including ISOFIX structures as standard and giving customers a range of approved child seats by liaising with the aftermarket industry [3].

At the end of the first decade of testing, the results were very promising, as the amount of vehicles that started achieving a five star rating for adult occupant protection was very high, as highlighted in Figure 2.1. The amount of vehicles with a low star rating kept decreasing, while it was clear that the industry was reacting to all the changes introduced by Euro NCAP to obtain the wanted number of stars.

Furthermore, the results shown in Figure 2.2 clearly show how the modification to pedestrian rating enacted in 2002 drove the wanted outcome, with automakers taking the issue more seriously.

After the success of the first 10 years of work, 2009 was a meaningful milestone for Euro NCAP, as a great deal of modifications was introduced to the rating system. The main drivers for this were the rise of electronic driver assists and crash prevention technologies, not accounted for in the rating system at the time. In addition, the fact that the high number of vehicles achieving a five star rating was leveling the ground and the interest in the results was diminishing. The overhaul of the rating system consisted in the change from three different star ratings to one overall rating, calculated in a more complex way, in order to guarantee that manufacturers could not just achieve positive results in one field and mediocre performance in other less marketable ones. The new rating promoted heavily the use of fully integrated safety systems, comprising of high level technologies in

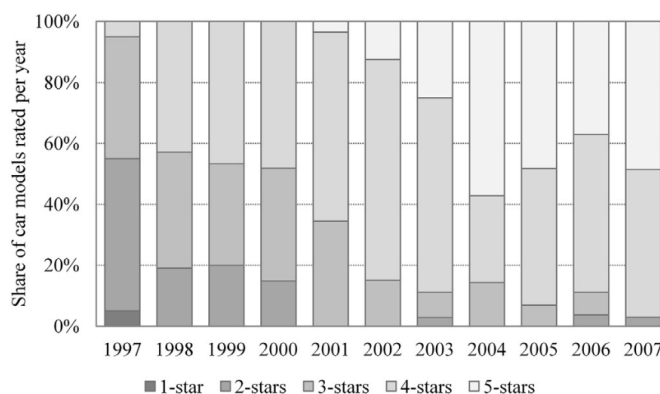


Figure 2.1: Progress of adult occupant star rating 1997-2007 [3]

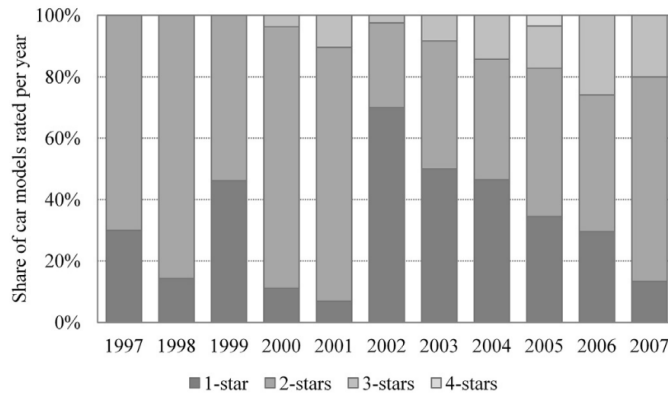


Figure 2.2: Progress of pedestrian protection star rating 1997-2007 [3]

both passive and active safety for adult occupants, children and pedestrians. In this way, it would be easier to discriminate between vehicles performing optimally and vehicles still needing improvements in certain areas, as this would be reflected in a lower overall star rating. In terms of technology, great focus was put on driver assists, the main ones being:

Electronic Stability Control (ESC) Introduced in 2005 as a recommendation by Euro NCAP, in 2009 its integration became part of the rating and in 2011 a functional test was added;

Speed assistance systems (SAS) In 2009, the implementation of manually set speed limitation systems was included in the rating, with incentives for more advanced systems that could be set on the go. Later in 2013, with the advent of intelligent systems for speed limit detection and active assistance, the protocol was updated to include such technology as well;

Autonomous Emergency Braking (AEB) Forward collision warning and AEB systems have represented the biggest revolution in active safety since the introduction of ESC, for this reason, both high speed and low speed AEB systems have been included in the star rating since 2014.

With regards to the field of passive safety, central interest of the work portrayed in this report, it was noted that that the most revolutionary improvements occurred already during the first decade of Euro NCAP's work. The front structures have been gradually improved with the design aim of minimising intrusions in the passenger compartment during the 64km/h ODB test and the level achieved in 2015 was extremely satisfactory for the great majority, if not all, of the tested vehicles. Furthermore, great structural improvements also impacted the side crash occupant protection, which at this moment has reached a high level in terms of Euro NCAP rating. However, Euro NCAP is willing to push the boundaries of development even further, not only by taking into account the latest active safety technologies, but also asking for an extra effort in the area of passive safety to make sure that the structures are designed for impacts that are as similar as possible to real life situations. For this reason, the new Euro NCAP Roadmaps have been devised, giving to the industry an insight into what will be asked in the future by consumer crash testing procedures.

2.1.1 Euro NCAP future Roadmaps

In order to respond to the changes in technology, road accident data and to push the industry to go beyond the status quo, Euro NCAP has, at more or less regular intervals, published their vision and outlook for the future requirements they would be setting in the so called "Roadmaps". In 2015, before the ending of the period concerned by the previous document, set for 2016, the committee published the "2020 Roadmap", where the main objectives and changes for the following years were highlighted. As stated in Chapter 1, the main objective for the near future is to reduce even further the number of casualties and serious injuries on the road, and the way to reach this goal is still quite long. Several changes regarding technological innovation in terms of active safety have been set up for 2020, starting from the update of procedures for AEB, SAS and seatbelt reminders, to the inclusion of procedures for lane departure assists, speeding and impaired driving avoidance, and semi autonomous driving. However, the most substantial change to test procedures for passive safety since the introduction of the pole test has also been included. After 20 years of activity, the Offset Deformable Barrier test procedure at 64km/h will be finally retired. The test procedure will be substituted by the Mobile Offset Deformable Barrier test at 50km/h , with the aim of improving road accident representativeness and begin the very important consideration of compatibility and partner protection [22]. Furthermore, the second challenge will concern the side impact procedure, as a modification to the actual rating will enable the assessment of far side occupant protection for driver and passengers. Finally, the current Hybrid-III anthropomorphic test device will be replaced by the more recently developed THOR Advanced mid-sized male device, which enables a higher level of biofidelity and an unparalleled performance in terms of instrumentation and data acquisition technology [23].



Figure 2.3: Euro NCAP future Roadmaps

Due to the pace at which automotive manufacturers are progressing in the fields of automated driving, active safety assistance and crash testing virtual simulation, Euro NCAP has already set the goals and directions for the more distant future by publishing in 2018 the "2025 Roadmap". The objective set for the future is to achieve the "vision zero", the complete elimination of road casualties. In the pursuit of this goal, the focus is set on primary and secondary safety, with increased focus on driver monitoring, autonomous aids and V2X communication systems for the former, and rear-end collision protection, pedestrian and cyclist safety for the latter. In addition, for the first time in Euro NCAP's history, tertiary safety is introduced: Child Presence Detection systems to solve the problem of children forgotten inside vehicles will be taken into consideration, while an initial assessment at technologies to aid extraction from crashed vehicles will be carried out [24].

Overall, Euro NCAP has been constantly updating and looking to include new aspects in its rating, in order to maintain it pertinent, meaningful and most of all useful for road users. The future shaped by the decisions that have been made in the last few years continues on that path, with the ambitious objective of continuing to push the industry until no more fatalities occur on european roads.

2.2 From ODB to MPDB

Having briefly discussed the advancements completed in the first 20 years of Euro NCAP's path and the ideas put in place for the short and mid term future, focus must be now placed on the matter of most interest to this report: the substitution of the outdated Offset Deformable Barrier test procedure with the newly developed Mobile Offset Deformable Barrier procedure. In order to understand to the full extent the importance of this change, the details of both tests together with their analysis is reported in the following sections.

2.2.1 The Offset Deformable Barrier test

The Offset Deformable Barrier test has been designed by the European Experimental Vehicles Committee (EEVC) in 1994 [4], with the aim of implementing an additional test to the full width rigid wall test used as european legislation at the time. Several studies regarding real world impacts highlighted the issue of high levels of injuries and mortality in frontal car-to-car crashes, which was deemed to be caused by contact between the occupant's body and the vehicle structures due to high levels of intrusion . The discrepancy between the results in full width rigid wall tests and actual road accidents was found to be due to the different kind of loading suffered by the frontal structures of the vehicle: the decreased amount of overlap in the real scenarios had the effect of loading only one of the two sides of the vehicle, hence forcing only half of the structure to absorb all impact energy, thus forcing the cabin to deform to dissipate the residual energy; in addition, the perpendicular surface and extremely high deceleration rate experienced by the face of the front structures impacting against a rigid wall ensured that the collapse of said elements followed the desired buckling sequence, with stiffer structures absorbing most of the energy. This is very different from the real scenario, where the vehicle is impacting against a deformable object (partner vehicle), which does not ensure either a flat, stable surface to load, nor such high decelerations to the front structures. The result

of this occurrence is the inability to collapse the stiffer structures that hence get pushed back in the vehicle as the weaker components fail [25]. Furthermore, in full width rigid barrier tests the engine tends to undergo very high accelerations, which equate to large energy absorption when the block impacts with a stiff firewall. In road impacts, such rigid structures do not exist and the engine cannot be loaded in the same way, and accident analysis had showed that generally a more realistic scenario involves the engine moving sideways and loading the firewall only partially.

For these reasons, the EECV working group designed a test with a limited overlap, set at 40% with the goals of loading mainly one side of the front crash structure and avoiding high engine loading, hence creating a more realistic condition. With regards to the impact face, a deformable barrier was required, aimed at reproducing the softer and more complex shape of a partner vehicle. Hence, several tests were carried out and it was concluded that the most suitable design would be a 450mm deep, 50psi aluminium honeycomb block with a smaller 250psi aluminium block attached to the lower part of the front face, as show in Figure 2.5. This barrier was denominated "normal element with bumper" [4]. In terms of positioning, the deformable face was placed on an "infinitely" rigid block at a height of 200mm from ground level.

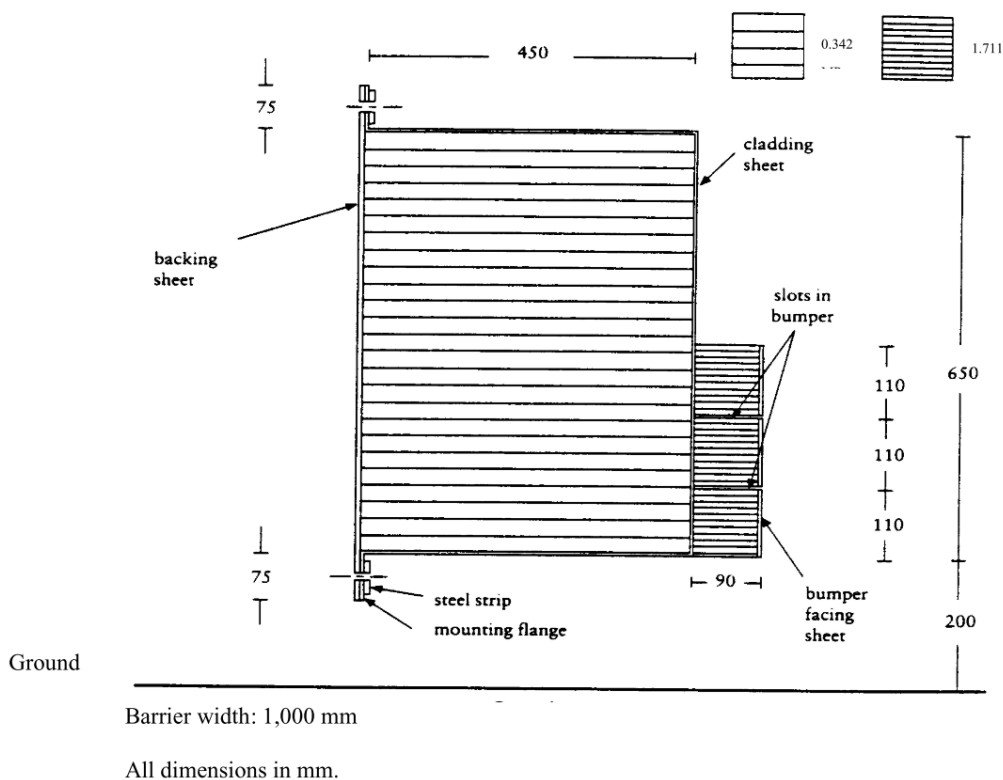


Figure 2.4: ODB Normal element with bumper [4]

Regarding the impact speed, at the time of design of the procedure the decision was made to shape the test in order to reproduce with high fidelity a 50km/h car-to-car crash between identical vehicles with partial overlap. For this reason, the final test speed was set

to 56km/h , although it was already clear at the time that this might be an underestimation, as a speed above 60km/h would have been more representative of the harshness of the majority of real world crashes. Finally, this test represented the first instance in which anthropomorphic test devices were used: the Hybrid III 50th percentile male dummy was chosen in order to record biomechanical parameters and set limits to loads, accelerations and deformations of body components.

Accident Impact Speed* km/h	Casualties Addressed AIS \geq 3
50	Few
55	Just under $\frac{1}{2}$
60	About $\frac{2}{3}$

* 55 km/h approximates to an ODB test at 64 km/h

Figure 2.5: Car-to-car frontal impact speed and serious or fatal casualties [5]

Resulting from the work of EECV WG 11, the UNECE-94 regulation was set up for vehicle homologation in Europe [26]. When Euro NCAP decided what test to include, the choice was made to take the specifications of UNECE 94 in all their declinations. The only change that was made regarded the test speed, set, as mentioned above, at 64km/h . Based on the accident data analysis reported by EECV, it was found that an impact speed of 55km/h in a real life crash would replicate around half of the serious or fatal injuries; at this point, comparative tests were conducted on a medium sized family car and it was found that an ODB test at 64km/h would be around the same severity of a car-to-car impact at 55km/h , due to the amount of energy absorbed by the deformable barrier [5].

Test specifications

The full specifications of the test parameters and barrier construction are here reported. In terms of added mass to the kerb weight of the vehicle, all fluids are topped up to standard running condition, the fuel tank is filled with water (or equivalent) to 90% of its capacity in terms of mass of fuel, and 36kg of ballast are added to the luggage compartment. In addition, the two Hybrid III ATDs placed in the front seats have a mass of 88kg each, while in the rear seats the Q6 and Q10 child dummies have a mass of 23kg and 36kg respectively. The child dummies must also be placed on the child restraints recommended by the OEM; if these are not available, an additional mass of 7kg for the Q6 and 2kg for the Q10 must be included [27].

The barrier is constructed with several layers: a main aluminium honeycomb block with a crush strength of 0.342 Mpa , an aluminium bumper element with crush strength of 1.711 Mpa , an aluminium backing sheet, cladding sheet and bumper facing sheet. The different elements are combined using a specific adhesive bonding procedure [26]. The barrier must be then fixed to a rigid block with a minimum mass of $7 * 10^4\text{kg}$ and the attachment geometry should be such that, during the impact, the vehicle never comes into contact with the rigid block.

Table 2.1: ODB test specification

Vehicle velocity	64km/h
Overlap level	40%
Barrier type	ODB
Front ATDs	Hybrid III 50 th Male [88kg]
Rear ATDs	Q6 [23kg]- Q10 [36kg]
Child restraint mass	7kg (Q6) - 2kg (Q10)
Fuel equivalent mass	90% fuel tank capacity by mass
Luggage mass	36kg

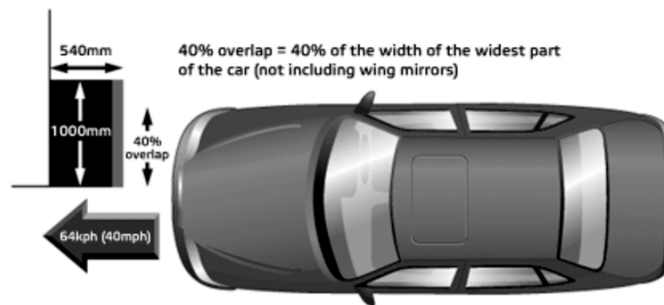


Figure 2.6: ODB test infographic [6]



Figure 2.7: Physical model of ODB [7]

Criticism and issues of the ODB test

Since its introduction, more than 20 years back, the use of ODB test has given the initially desired results, driving OEMs to improve vehicle structures to higher and higher levels. However, many aspects of the test have been criticised and many shortcomings have been identified, both when it was originally design and through the years. At the time of its implementation, it was already clear that the test would not allow the evaluation of the effect on the partner vehicle, as this was not in the objectives of the working group. The

Table 2.2: ODB construction specifications

	Height [<i>mm</i>]	Width [<i>mm</i>]	Depth [<i>mm</i>]	Material	Crush strength [<i>Mpa</i>]
Main block	650	1000	450	Al 3003	0.342
Bumper element	330	1000	90	Al 3003	1.711
Backing sheet	800	1000	2 (thickness)	Al 5251	-
Cladding sheet	1700	1000	0.81 (thickness)	Al 5251	-
Bumper sheet	330	1000	0.81 (thickness)	Al 5251	-

barrier dimensions and material was not designed for this kind of assessment, while the test procedure itself could not assess phenomena of the likes of under- and over-riding, issues that have become more relevant as the level of occupant protection has reached satisfactory levels [28].

Furthermore, as stated above, the ODB test was designed to replicate a car-to-car impact with same vehicle; this poses a big issue in terms of representativeness of real life scenarios, as a light vehicle as a high probability of impacting with a heavier vehicle and vice versa. In the case of a crash between a light and a heavier vehicle, the one with lower mass will experience higher loading due to the law of conservation of momentum [29], hence the structures will have to absorb a level of energy outside of the design range imposed by the ODB test. This results in levels of cabin intrusion substantially higher than tested and also in higher accelerations, again due to the conservation of momentum.

The same issue is reflected in an opposite manner for heavy vehicles in the test. Due to the fixed, and relatively low, amount of energy that the barrier can absorb, the energy that the structure of a heavy vehicle has to absorb is proportionally larger than that of light cars. This lead to a trend of increased stiffness of front structures in already aggressive, large mass vehicles, causing even more compatibility issues when a real impact occurs, while also affecting overall vehicle mass with all its unwanted consequences on performance parameters. Studies have also found that more in general, for all types of vehicles the ODB test has driven a high increase in stiffness of the front crash structures, hence creating a problem for compatibility with partners and adaptability to different impact scenarios [30].

Finally, the soft and shallow ODB barrier has led to a negative design trend in industry: most vehicles nowadays have crash structures which puncture the barrier on purpose, in order to exploit the rigid back plate. This, in a way, makes the test more similar to a partial overlap rigid wall test, hence the type of loading undergone by the crash structures becomes more perpendicular in direction and more abrupt in acceleration, ensuring appropriate collapse in a simpler way. This is clearly an overexaggeration, as the barrier, while being punctured, still does perform partially its function of simulating a partner vehicle. The point that has been raised is, however, that the technological level reached has allowed the implementation of a better approximation of real life conditions compared to what was possible when ODB was designed [31].

2.2.2 The Mobile Offset Deformable Barrier test

Due to the issues stated in the previous section, a new test was studied and devised through the last 15 years with the aim of substituting the UNECE-94 test for homologation to improve the level of safety directly from a legal standpoint. However, an agreement has not been found yet for application on such a large scale, even after the extensive finalisation work by the ADAC MPDB [19] and FIMCAR X projects [32]. The core area to tackle for this new test was the evaluation of compatibility in the broad sense of the term, hence taking into account the effects of the mass of the vehicle, the front end rigidity, the front end structures design, both in regards to **occupant protection** and also in terms of **partner protection**, creating a scenario of higher fidelity to road accidents [19].

The development of the new test took shape from the joint agreement of several organisations, both from Europe and USA, that the most suitable procedure for the evaluation of compatibility would be a mobile barrier test. The underlying idea that drove the design of the ODB test was not modified, as the accident analysis showed that the relevance of an offset test to simulate a car to car impact at a speed between 50 and 60 *km/h* is still valid, and through the years several studies on possibilities for mobile frontal offset tests were carried out. From this starting point, the FIMCAR X project, reuniting the major european organisations and test labs, conducted 15 full scale tests on vehicles of different sizes to determine the parameters of the protocol to be followed, mainly in terms of test speed, barrier mass and overlap. The procedure for of the mobile barrier test involved a test vehicle and a mobile trolley with a front mounted barrier face; the two bodies are positioned facing each other and are launched at the same, and opposite, velocity towards one another. The alignment of the barrier face with the front of the test vehicle will be equal to the desired offset. The study included superminis, small and medium family cars and also SUVs of different sizes, with a minimum vehicle mass of 1000 *kg* and a maximum of 2200*kg* and arrived at the conclusion of a proposal for a new test procedure [33], later to be adopted by Euro NCAP [34], which decided to update its roadmap to put priority on its implementation.

The procedure described above, as opposed to the ODB test, does not intend to replicate for every vehicle a crash with a similarly sized opponent, but an impact with a car of set mass driving on the road. In the case of Euro NCAP and the referenced european project, this mass corresponds to the average of the circulating fleet on european roads. However, the same test could be used, by changing the mass parameter, to replicate other populations of vehicles in different parts of the globe, hence making this procedure an appropriate candidate for worldwide standardisation and harmonisation of tests, while also being extremely robust to future changes without the need for complete redesign and extensive validation tests [35].

As it was far out of the scope of the project to design a new barrier element and a new trolley, the Progressive Deformable Barrier (PDB) face developed in the VC-Compat project [36] and used in FIMCAR V [37] project for the WP2 offset test was selected, while the trolley utilised in side impact tests was deemed to be a suitable base. The design of this barrier element is based on having three different layers, a soft outer bloc, a middle one being capable of absorbing a much larger amount of energy and an inner layer with elevated crush strength. All in all, the PDB barrier is capable of absorbing a significantly higher amount of energy compared to the ODB element. In this way, the vehicle impacting

the barrier finds it considerably more difficult to puncture the whole depth and reach the rigid element of support, with the advantage of both reproducing in a closer way the front end structure of an idealised vehicle and of giving the possibility of assessing the damage inflicted to the barrier by the vehicle in a significative manner. The clear conclusion is that the assessment of the deformation can give a level of insight into the partner protection level of the tested vehicle.

The tests reported in the projects cited above included an assessment of speeds of 45, 50 and 56 km/h for both the vehicle and the impactor, with an overlap set at 50% and an impactor mass of either 1400 kg or 1500 kg . In both [19] and [32] it was found that a test speed of 56 km/h resulted in deformation and acceleration pulses which were significantly higher than the reference car-to-car impact. The opposite occurred when a speed of 45 km/h was utilised, hence the baseline test at 50 km/h was adopted as the most suitable, as in fact it represents closely the reference test. The initial choice of barrier mass of 1500 kg was driven by the results of the GIDAS accident study [29], which highlighted how front seat occupants of vehicles with mass lower than 1500 kg are more likely of being seriously or fatally injured compared to occupants in vehicles heavier than the set threshold. However, for the final proposal of the procedure, the barrier mass was lowered to 1400 kg , as it better represents the average mass of the compact vehicle category in Europe, which is the most widely sold [34]. Regarding the overlap level and direction of impact, the decision was again based on the German (GIDAS), French (LAB) and Swedish (VCTAD) accident data, which highlighted how the 12 o'clock direction would be absolutely relevant and a maximum overlap level of 75% would be representative of most occurrences of serious or fatal injuries in frontal impacts [34]. Finally, the 50% overlap level cited above was chosen.

During the development and after the release of the first drafts of the new procedure, a moderate number of research studies and tests have been completed. These have highlighted how the MPDB is in fact capable of showing the shortcomings of the current standards for passive safety for lighter vehicles, derived from the utilisation UNECE-94 and Euro NCAP ODB, as the crash pulse severity was substantially increased as the whole crash event lasted between 30 and 50 ms less than ODB [38], while in some cases their structures would not be able to guarantee the required levels of intrusion. With regards to vehicles with mass substantially higher than the trolley, the test severity is expected to be lower, which is again more representative of real car-to-car accidents and could lead to a modification of frontal structures' stiffness that could diminish the aggressiveness towards lighter vehicles [35]. Other studies such as [39] have also demonstrated how on certain models with mass comparable or lower to the trolley the levels of intrusion could be far above the required limits, due to the modified behaviour of the crash structures. Finally, for vehicles with mass in the same range or slightly higher than 1400 kg , the crash severity was not substantially diminished and injury assessment values were still more severe than those obtained through ODB: even though the change in velocity is expected to be lower for vehicles with mass above 1400 kg , the PDB structure is much stiffer and loads the structures in a considerably different manner [29]. The general image depicted by the current publications available is that of a high level of variability not only depending on mass, but also on the design of the front end of the vehicle which leads to either high crash pulses, high levels of intrusion or both, when the structural behaviour is incorrect.

With regards to the second, but critical aspect represented by partner protection and compatibility assessment, studies have now been completed mainly with the aim of achieving a proposal for the assessment method to be implemented, as reported by [33] and [19]. The procedure that will be adopted by Euro NCAP in 2020 is still unknown, as its publication is expected through 2019. The aim of the procedure will be to give an objective evaluation of the aggressiveness of a vehicle with regards to its partner, favouring designs that consider the deformation and pulse inflicted to the opponent at a similar level of importance to occupant protection. In order to complete the evaluation, the general agreement is that a 3D scan of the deformed PDB barrier will be used and a quantification of the discrepancies in deformation between different areas of the honeycomb blocks will be the basis for the assessment: a vehicle that is capable of deforming the barrier in a homogeneous manner is far more likely to engage the front structures of the partner vehicle in a positive fashion, driving a deformation similar to a rigid block. Furthermore, the deformation impressed in the barrier can be analysed from a qualitative point of view, to investigate the aggressiveness of the frontal structures and their behaviour, while under or over-riding tendencies will also be highlighted. Only a few published projects have reported the results of the implementation of such procedures, such as [40] and [31], and all have shown extremely poor performance of the tested vehicles due to critical failures of structural elements and interaction with engine block and wheels. This has already proved how the implementation of MPDB as a Euro NCAP standard will drive a heavy improvement in the design of safety structures, shifting the focus from strict self protection to self and partner interaction.

Test specifications

The test specifications published in the aforementioned reports by FIMCAR [32], ADAC [19] and Euro NCAP working group [34] are the most up-to-date drafts available at this time; however, it is recognised that the latest version reported by Volker [34] could very well be identical to the final specification which should be published in the near future, at least for the most part. For this reason, this draft is taken as the full specification for the work portrayed in this report and its details are highlighted in this section. Furthermore, the specifications for the barrier face and trolley have also been published as a draft, directly by Euro NCAP in 2017 [10]. Similarly to what has been stated for the test procedure, this draft will be taken as definitive for the purpose of this project.

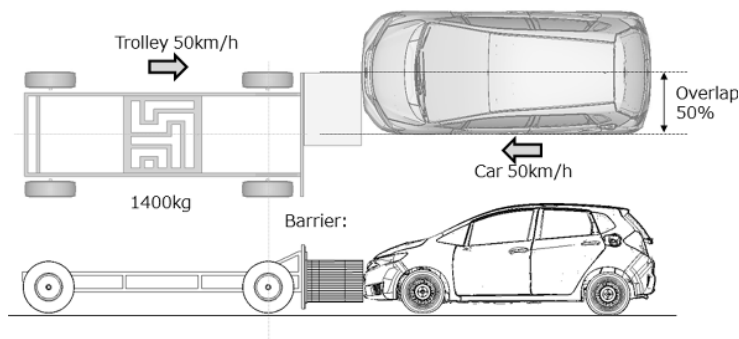


Figure 2.8: MPDB test infographic [9]

The specifications of the test regarding the vehicle present few differences in terms of added mass: the THOR ATDs are placed in the front seat and their mass is slightly lower compared to Hybrid III dummies, setting the scale at 80 kg . The rest of the procedure in these terms remains unchanged, with Q6 and Q10 child dummies in the back seats, 90% of fuel by mass in the fuel tank and 36 kg of mass in the luggage compartment. As stated previously, the test speed has been set to 50 km/h both for the vehicle and for the trolley while the overlap has been fixed to 50%.

Table 2.3: MPDB test specification

Vehicle velocity	50 km/h
Overlap level	50%
Barrier type	PDB
Barrier velocity	50 km/h
Front ATDs	THOR ADV 50 th Male [80kg]
Rear ATDs	Q6 [23kg]- Q10 [36kg]
Child restraint mass	7 kg (Q6) - 2 kg (Q10)
Fuel equivalent mass	90% fuel tank capacity by mass
Luggage mass	36 kg

Regarding the barrier face, the Progressive Deformable Barrier is composed of three different aluminium honeycomb deformable cores fixed one in front of the other, denominated A, B and C starting from the one closer to the trolley face. The blocks have the dimensions shown in Figure 2.9, with blocks A and C showing a homogeneous crush strength characteristic. The first honeycomb core (A) must have a strength between 1.540 MPa and 1.711 MPa when statically loaded in accordance with procedure NHTSA TP-214D, while for the third (C) the value must be between 0.308 MPa and 0.342 MPa when tested in the same manner. Block B is effectively the "Progressive" element in the barrier's construction: its crush strength must be variable in accordance with compression, with a characteristic within the boundaries shown in Figure 2.10, when tested with a compression rate of 100 mm/min from 0 to 355 mm . Additionally, the barrier comprises of a back mounting plate, three intermediate plates, a contact plate and a cladding sheet, as shown in Figure 2.11. The dimensions and material characteristics of all elements are reported in Table 2.4. All components of the barrier are held together by a two-part polyurethane adhesive agent.

With respect to the mobile element, or trolley, the Euro NCAP specification sheet sets a total mass of 1400 kg and the constructive constraint of no deformation after the impact with the vehicle. Front and rear track are fixed at 1500 mm , while wheelbase must be equal to 3000 mm . The centre of gravity of the barrier should be located on the vertical plane connecting the centres of the two axles, 1000 mm behind the front axle and at a height of 500 mm .

Table 2.4: PDB construction specifications

	Height [mm]	Width [mm]	Depth [mm]	Material	Crush strength [Mpa]
Block A	568	1000	90	Al 3003	1.540-1.711
Block B	568	1000	450	Al 3003	Progressive
Block C	568	1000	250	Al 3003	0.308-0.342
Backing sheet	720	1000	3 (thickness)	AlMg2/3	-
Cladding sheet	720	1000	0.8 (thickness)	Al 5754	-
Intermediate sheet	566	1000	0.5 (thickness)	Al 5754	-
Contact sheet	566	1000	1.5 (thickness)	Al 1050A	-

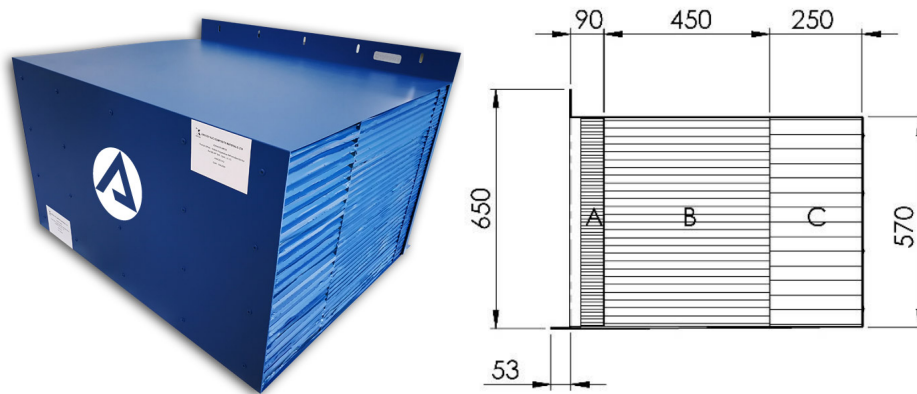


Figure 2.9: PDB physical model [7] and dimensions [10]

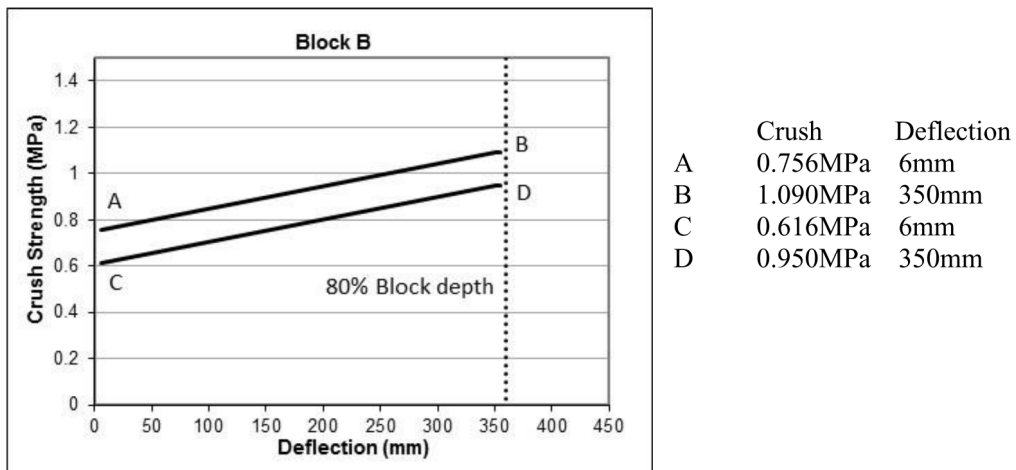
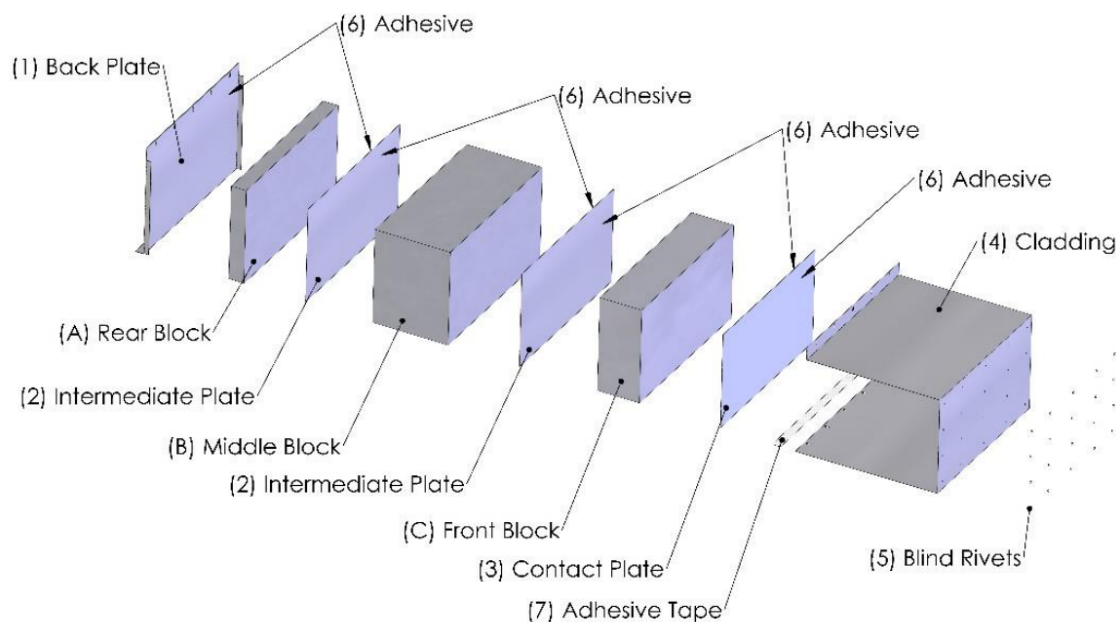


Figure 2.10: Displacement-strength characteristic corridor of Block B [10]



- | | |
|-----------------------------|---|
| (1) One back plate | (A) One rear deformable honeycomb core |
| (2) Two intermediate plates | (B) One progressively deformable honeycomb core |
| (3) One contact plate | (C) One front deformable honeycomb core |
| (4) One outer cladding | |
| (5) Blind rivets | |
| (6) Adhesive | |

Figure 2.11: Progressive Deformable Barrier physical model [7]

2.3 Crash test simulation in the vehicle design process

For the past 15 to 20 years, the vehicle design process has been highly influenced by the development of Computer Aided Engineering and Finite Element modeling and simulation, as the advancements in such fields, combined with the ever increasing availability and affordability of powerful computing hardware, have brought much higher flexibility to the design cycle. With regards to crash testing, the advent of simulation has impacted heavily the possibilities of car makers and researchers since the earliest stages of its introduction [41], as the possibilities to gather data from full scale physical tests has always been extremely restricted due to budget constraints. In fact, one of the main issues in the advancement of vehicle safety is the extremely high cost of physical tests, especially during the design process, when prototypes have to be crashed: it would be absolutely unfeasible to conduct a full scale physical test every time a modification is performed to vehicle structures, restraint systems, ATD positioning, test procedure and so on. This is even more valid when research projects are concerned and a high number of variations to the subject under study are undertaken. The evolution from linear static to non linear dynamic finite element modeling in commercial codes such as LS-DYNA and PAM-Crash

has allowed engineers to improve their understanding in terms of full vehicle structural behaviour and crash dynamics [42], thanks to the possibility of visualising every step of the impact event and repeating simulations with design improvements and variations at an extremely high pace compared to the past. The evolution of both vehicle mathematical models and simulation codes has also enabled designers to take advantage not only of the qualitative assessment of simulated crash events, but also to utilise the resulting quantitative data regarding deformations, accelerations, forces and more as a close guideline to direct the vehicle design process. In fact, the simulation of crash events constitutes, nowadays, one of the pillars of every design cycle: since the initial stages of the chassis design, simulations are performed in order to verify if the direction taken by engineers is consistent with the expectations and objectives set for passive safety. As the process continues, the mathematical model of the vehicle becomes more and more similar to the finalised product, with every component eventually being represented with a high level of fidelity, both in terms of shape and mechanical-physical qualities. As a result, the simulations that derive from such detailed models become closely representative of the results that will be obtained in physical testing.

The level of accuracy and confidence with whom the full scale crash test simulations represent reality is difficult to be judged from a theoretical point of view, and the scarcity of publications on the matter does not allow to quantify with absolute certainty the representativeness of the results. However, the extensive use of such tools in industry and the verifications that have been performed through the years as several design projects developed has ensured that using simulations as a research and design aid is extremely valuable and closely representative. Although the variability of the results in physical tests and the complexity of the calculation of full scale crashes are both considerable, the qualitative and quantitative data obtained in simulation gives information that is consistently in the same region of interest of the physical scenario. In conclusion, this proves how advanced simulation tools can be effectively utilised in order to perform research analyse to evaluate new scenarios, such as that of interest of this report, with a considerable amount of confidence that the results be in line with reality.

Chapter 3

Methodology

In this chapter, the tools and methods utilised to complete the work anticipated in Chapter 1 are reported. The initial decisions to be made regarding the choice of softwares to be selected for pre processing, solver and post processing are explained, together with a brief explanation of their use. Next, a description and analysis of the four vehicle models adopted for the completion of the comparative study is shown, while the official models of the ODB and MPDB barriers created by the software provider are presented. In conclusion, the schedule of conducted tests is included for reference.

3.1 Simulation softwares

The first step in the process of completing the simulation analysis was the choice of appropriate software for the application. Whenever FEM crash analysis is to be completed, three pieces of software are needed to perform a simulation from the starting point of having a complete mathematical model, hence disregarding the pure model design phase.

First of all, a pre-processor is required to create the context in which the simulation will be evaluated: models of the vehicle and of the barrier are here placed in relation to each other with the required geometrical parameters, the initial and boundary conditions such as initial velocity, gravitational load and contact definitions are also set. More importantly, the pre-processor can be used to modify the geometry of the utilised model and to perform the discretisation of the components into a finite element mesh. Finally, the control parameters required for correct performance of the solver are input, both in terms of basic conditions such as timestep size and simulation duration, and more advanced settings to ensure flawless advancement of the simulation steps. In addition, the data logging functions are set up so that the output files of the solver contain exactly the parameters required for the post-processing. All in all, the pre-processor can be seen as an user entrance interface to the solver, where parameters that would have to be manually encoded in the input file of the simulation can be defined in a more user friendly manner. For the study here reported, the software chosen for this part of the work was ANSA Pre-processor, created and distributed by BETA CAE Systems [43]. The choice was made mainly due to the advantages in terms of compatibility with the solver of choice, discussed next in this chapter, flexibility and advanced functionalities for model preparation and modification.

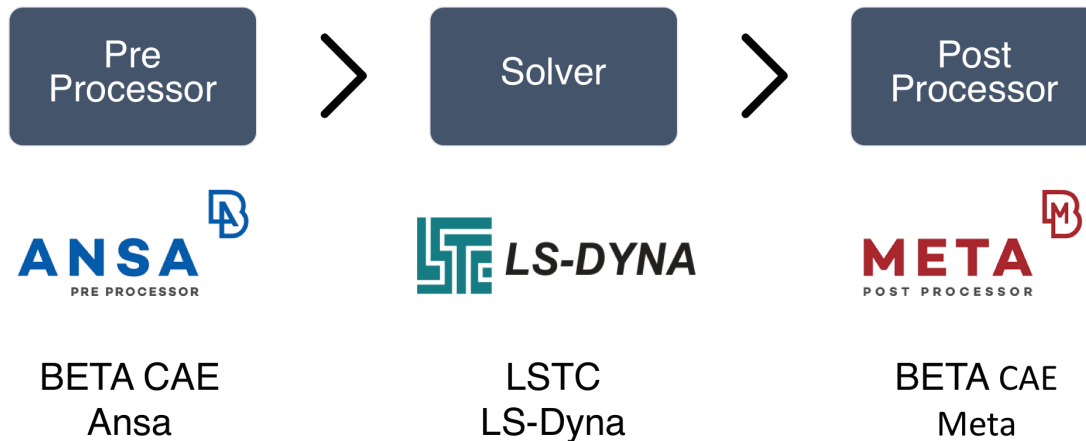


Figure 3.1: The simulation process - softwares utilised

In fact, ANSA is currently seen as the industry standard in terms of pre-processing capabilities, although the utilisation of the software requires more getting used to compared to other competitors such as Altair Hypermesh due to its less intuitive UI, as stated in the early stages of this project by engineers of the Simulation department at Pininfarina Engineering s.r.l.. The software version utilised in this project was ANSA v18.1.0.

The second step in the process involves the use of a solver code, which effectively performs all the mathematical operations to simulate the interactions set in the input file, calculating a log of deformations, forces, accelerations, moments and so forth, while also creating the visualisation frames of the event at pre-set intervals. The code utilised in this instance was LSTC LS-DYNA, an explicit "one code strategy" platform that enables a wide variety of dynamic non linear applications. It is regarded as the most advanced code for full scale automotive crash simulations available at the present time and it is widely used in industry for this type of application. This code is currently used by the great majority of research institutions and automotive manufacturers, both due to its superior level of representativeness of physical behaviour, its extremely extensive material definition possibilities, flexibility of application and robustness towards imperfections in the input file preparation, which give great advantage in terms of working efficiency [44]. Furthermore, most full scale vehicle models are currently developed for simulation in LS-DYNA, while the providers of additional modeling components such as crash barriers, airbags and dummies tend to also develop their products primarily for this code. For these reasons and to be in line with the standards utilised in the most recent studies in the field of vehicle simulation for safety, choosing to use the LSTC software is both appropriate for compatibility and an assurance of meaningful results. The utilisation of this software is not based on a standard user interface, but the input file is simply launched through the Terminal interface, in this case from a Linux OS, and the output files are compiled as the simulation runs, together with a live log of the steps and working messages for debugging. The version utilised was LS-DYNA v8.1.

Finally, the third and final software required is a post-processor. This is needed in order to visualise and analyse the output files from the solver, which comprehend, as stated

above, both graphical representations of crash event and data logs of selected variables. The performance of the post-processor is not only limited to visualisation but it includes powerful data manipulation tools to aid in the analysis of the crash, also allowing the extraction of processed data for further analysis in other softwares. The software chosen for this task was BETA CAE Systems' META, developed to work in combination with ANSA pre-processor. The software version was, as for ANSA, META v18.1.0.

Software utilisation issues

It has to be noted that, although the packages utilised are extremely advanced, their utilisation is neither simple in principle nor unaffected by unexpected problems, which can be at least partially avoided by acquiring extensive experience. The main problems encountered during the development of this work regarded primarily the acquisition of the knowledge necessary to create simulations that would run without encountering fatal errors during the calculation with the solver, also by learning how to select the appropriate hardware parameters on which to launch the simulation. In second instance, when the simulations eventually ran through until their preset end, the complicated task became the troubleshooting of unexpected results, such as anti-physical behaviours of structures, extreme deformations in soft components or wrong interactions between elements in contact (barrier-vehicle interaction), which took arguably more time and effort than learning to have fully running simulations. Analysing the path retrospectively, it can be stated with confidence that one should not underestimate the time and effort required to obtain meaningful output data when simulations of this level of complexity are involved.

3.2 Vehicle models

As anticipated in Chapter 1, the work performed included the study on four different vehicle models:

- a **Toyota Yaris sedan M.Y. 2010**, representing a typical light B-segment car;
- an **Honda Accord sedan M.Y. 2011**, a D-segment sedan with average mass;
- a **Chevrolet Silverado M.Y. 2014**, selected due to its higher mass;
- a medium sized SUV with ladder chassis, designed for the asian market, which will be denominated **U Model** for the sake of simplicity.

The first three models here presented were obtained through the National Highway Traffic Safety Administration (NHTSA - USA) portal [45]. The models were developed and validated by the George Washington University National Crash Analysis Centre in Virginia (USA), and are freely available for public usage. The choice to utilise these vehicle models was made for several reasons:

- The models made available are suitable for the aims of the project as they represent three very different mass categories and two different chassis designs, while being vehicles of moderate age, hence still relevant in terms of design trends;

- They were originally developed specifically for crash simulation in LS-Dyna and are already set-up as a rigid wall test, which makes their implementation into a new environment less troublesome;
- Full scale complete vehicle models are generally not publicly available and finding a suitable one developed for LS-DYNA is a difficult task, let alone models with different masses. A different approach was pursued in the initial stages of the project, when an attempt was made to convert a PAM-Crash model to LS-Dyna; the amount of modifications to make to the formulation of materials and specific components such as joints and springs made it impossible to ensure the representativeness of the model, hence the idea was abandoned;
- Being available to all researchers and institutions, the models have been used in various projects [46] already and are continuously updated and improved, making them a suitable base for this work. Furthermore, the results can in this way be replicated if necessary, without issues of ownership if needed;

The U Model, on the other hand, cannot be discussed in the details of its origin due to confidentiality, its design details and specifications will be however discussed in Section 3.2.4.

3.2.1 Toyota Yaris

The first model utilised is a 2010 Toyota Yaris Sedan, a small four door B-segment car sold on the American market, which shares the same structures as the hatchback model, apart for the rear section. For what concerns the crash structures, this vehicle is very similar to the version sold in Europe, with no major redesign performed between the two markets. The model represents a typical light vehicle on the road, which in the current Euro NCAP ODB test performed extremely well, achieving a 5 star rating for adult occupant protection, while in the NHTSA full width rigid barrier test was awarded 4 stars both for driver and passenger. The kerb weight of the vehicle as tested in the European and American ratings was 1050 kg, placing it well under 1400kg of the MPDB barrier, hence at a theoretical disadvantage in the comparative study. It has to be noted, however, that the test weight will be closer to the mass of the barrier due to the presence of dummies, fuel ballast and luggage ballast.

Table 3.1: 2009 Toyota Yaris specifications

Model	Toyota Yaris Sedan 1.5
Year	2010
Chassis type	Steel unibody
Kerb weight	1050 kg
Safety rating	5 Star Euro NCAP 4 Star NHTSA

Overall model completeness

The mathematical model provided by NHTSA is for the most part complete, although a level of simplification in the engine bay components is present. As shown in Figure 3.2, the model represents closely the overall shape of the vehicle, with surfaces clearly modeled accurately for the base version with no additional aesthetic elements such as sideskirts and modified plastic bumpers.



Figure 3.2: 2009 Toyota Yaris Sedan - Physical [11] and CAE models

Regarding the **engine bay**, Figure 3.3 shows how most components have in fact been modeled, but with some idealisation of shapes: the airbox, engine and fuse box are simply represented by blocks, while a number of components filling the compartment between the engine and the radiators is not represented at all. This will have an effect on the representativeness of the model, as the front structures will have more space available to compress before being limited by the compacting of the components against the firewall.

Looking at the **interior**, all the main components are represented, including complete models of seats, dashboard, steering wheel and column, and also less relevant details such as door panels, trim components and handbrake. Although these components will not have a great effect on the results of this study, they all indicate that a high standard was meant when designing the mathematical model.

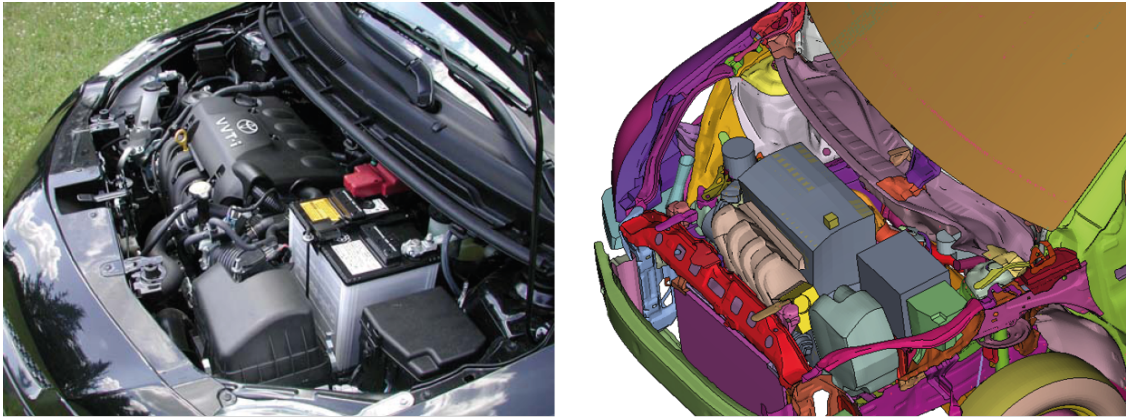


Figure 3.3: Toyota Yaris engine compartment - Physical [12] and CAE models

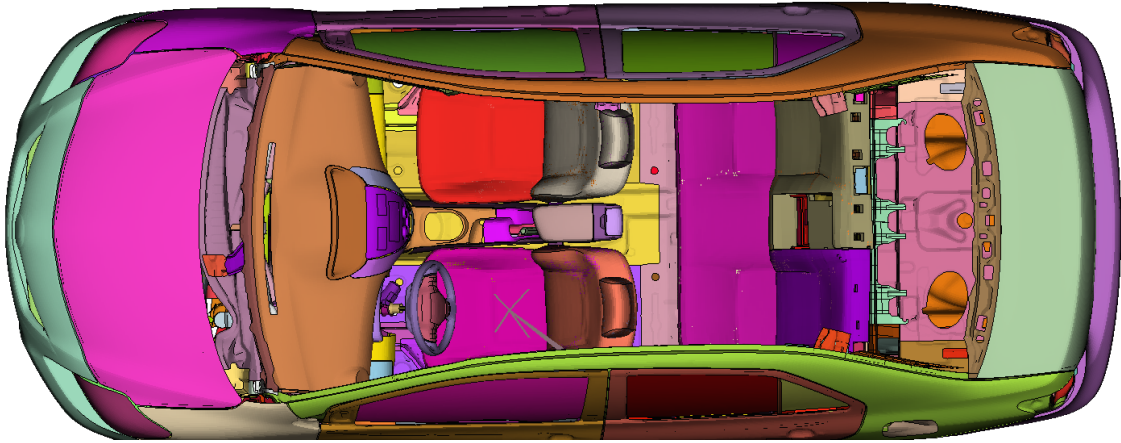
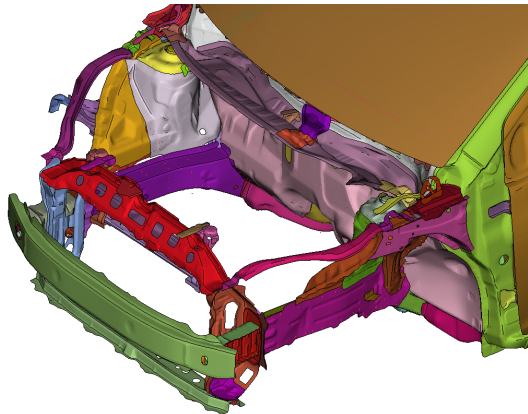


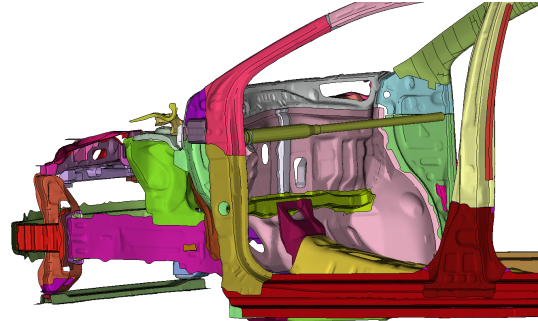
Figure 3.4: Toyota Yaris - passenger compartment details

Structural design

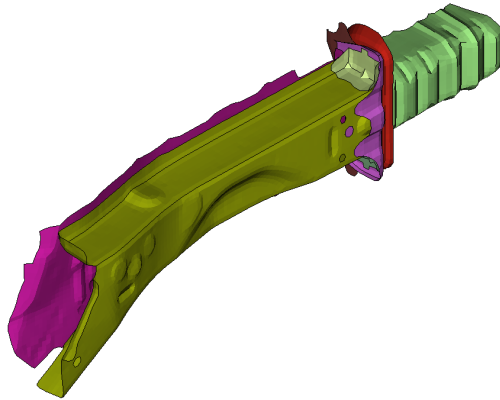
Naturally, the most relevant aspect for what concerns this study is represented by the **vehicle structure**. Unfortunately it is not possible to obtain a clear representation of the body in white of the physical model, hence the structures can only be assessed by their precision on a visual level, which is demonstrated by the details and the complexity of the surfaces, as exemplified in Figure 3.5c. Overall, the front structures are composed of one main load path, which includes large main rails, followed by long crash boxes connected through a large front cross beam. The configuration in itself is extremely simple, with upper rails of minute size and no third load path. The main crash structure rails continue on the underbody, as highlighted in Figure 3.5d, into two underbody rails of reduced length, while load is also transferred to two inner main rails that elongate until the end of the cabin on either side of the central tunnel. Additional elements are present to transfer part of the load to the sills, from which the rear rails develop after the end of the cabin. From the point of view of the passenger compartment, the firewall is reinforced with two internal structures, one horizontal and one vertical, both visible in Figure 3.5b.



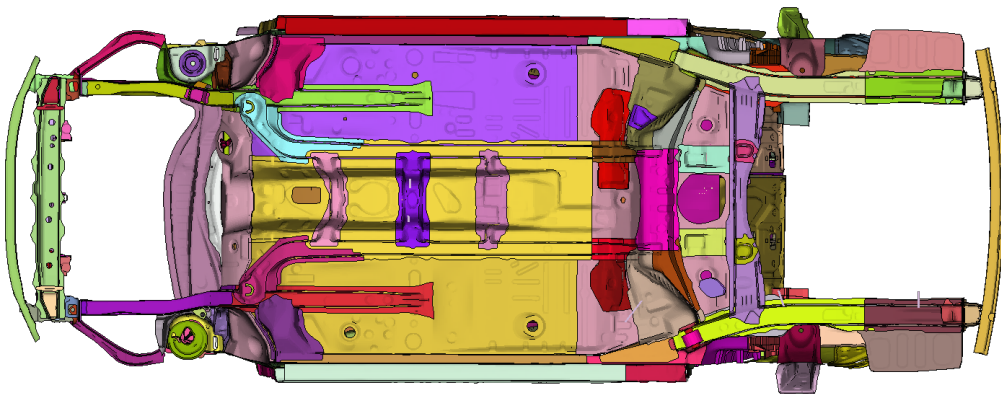
(a) Front crash structures



(b) Interior firewall reinforcements



(c) Detail of front main rail and crash box



(d) Underbody structures

Figure 3.5: Toyota Yaris - model details

3.2.2 Honda Accord

The second chosen model is that of a 2011 Honda Accord four door sedan. This is a typical modern large family car, representative of the D-segment, which, with a kerb weight of 1420kg , sits at a very similar mass to the MPDB barrier. This should theoretically mean that no major disadvantage should be seen with regards to occupant protection, as the amount of energy involved in the crash event should remain fairly unchanged. The model is, again, the version sold on US soil, which is considerably different in terms of trim levels, engine characteristics and accessories from the Euro model; nevertheless, as the structural design of the two vehicles remains the same, the meaningfulness of the results of this study will not be affected. The vehicle obtained a five star safety rating in the NHTSA tests for both front occupants, while in Euro NCAP it also achieved full marks, with a five stars award achieved.

Table 3.2: 2011 Honda Accord specifications

Model	Honda Accord EX-L 2.4
Year	2011
Chassis type	Steel unibody
Kerb weight	1420 kg
Safety rating	5 Star Euro NCAP 5 Star NHTSA

Overall model completeness

Compared to the Yaris model, the representation presents a lower level of completeness. While the body panel components are evidently designed to a high standard, as shown in Figure 3.6, the accuracy of other mechanical and interior trim elements is not exceptional.

In fact, the number of components present in the **engine bay** is extremely limited: the engine and automatic gearbox are represented with a good level of fidelity, but a number of important auxiliary components is missing including battery, brake booster and a portion of the intake system (Figure 3.7). These components, especially the former two cited, play a relatively important role in crash simulation, as they are virtually rigid and do not deform to a high extent. For this reason, the assessment of their impact on the firewall, consequently to the deformation of the frontal structures, can cause a level of structural damage. In this case, it will not be possible to assess these effects and, as explained for the Yaris model, the incompleteness of the engine bay’s representation will cause the frontal structures to have a longer range of action in terms of backwards deformation.

The same comments can be done for the interior of the vehicle: all major elements such as steering column and wheel, seat frames and dashboard support structures are modeled, while trim components and plastics are not. Contrary to the engine bay, these imperfections do not affect the results of this study’s simulations, as no biomechanical measurements will be taken and no ATDs will be simulated.



Figure 3.6: 2011 Honda Accord - Physical [13] and CAE models

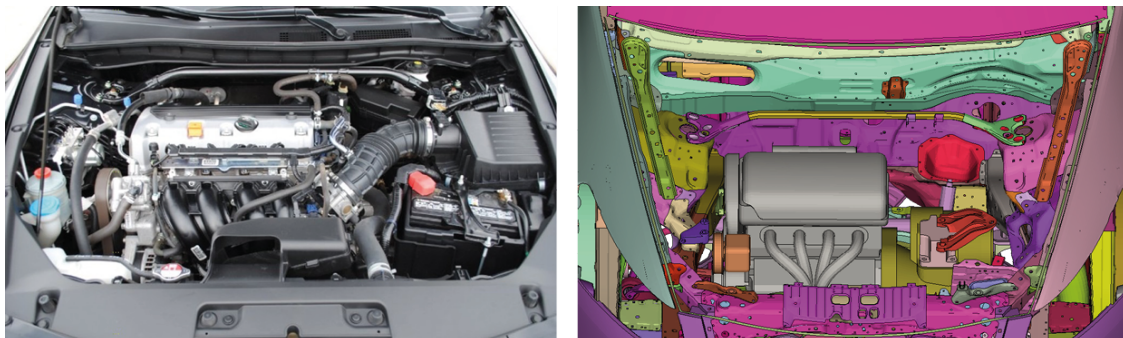


Figure 3.7: Honda Accord engine compartment - Physical [14] and CAE models

Structural design

If the model can be criticised for the aspects reported above, it has to be highly praised for its quality and details in terms of structural design. As it is possible to see in Figure 3.9, the complex shapes of the front end structures are presented without compromise and the same intention is reflected on the design of the rest of the chassis.

At first glance, the front end design appears much more complex than that of the Yaris. In fact, the number of load paths in this case increases, with the addition of a long and complex upper structure, joining at the front of the vehicle in a secondary cross beam. The main load path is still represented by the main rail, with a wide cross section and substantial length, followed by a short crash box to which the principal cross beam is

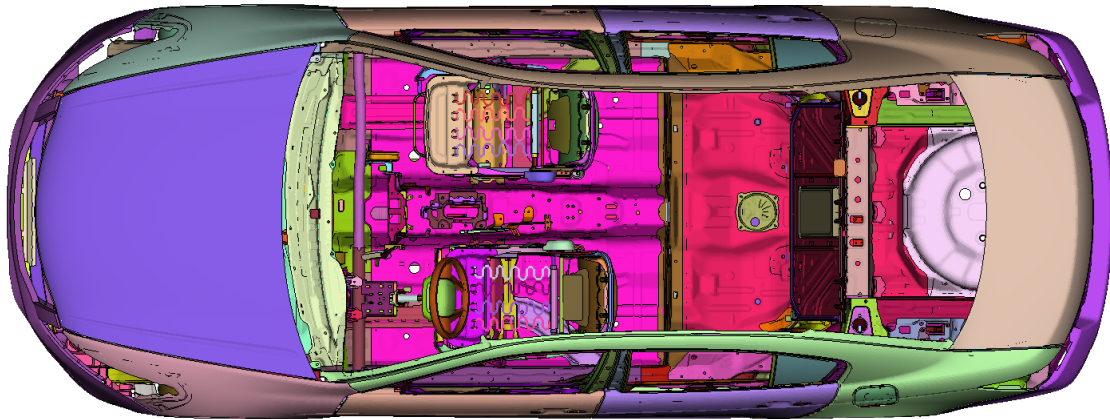


Figure 3.8: Honda Accord - passenger compartment details

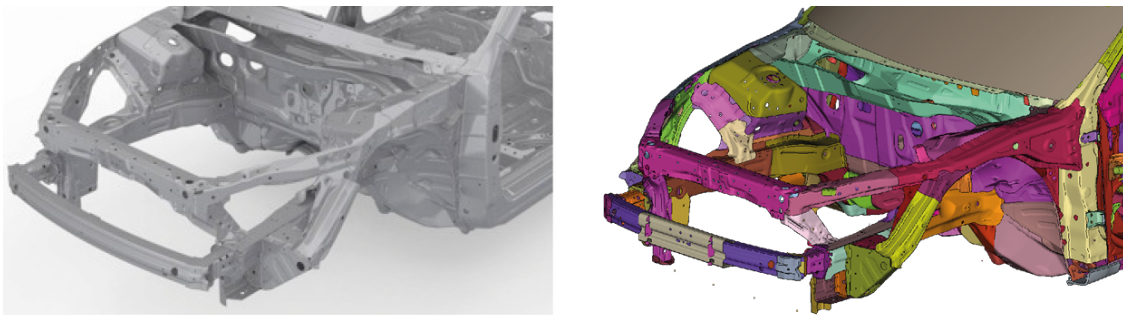


Figure 3.9: Honda Accord - BIW front section physical [15] and CAE models

connected. It can be noted how from the main load path, a connection with the upper shotguns is created in order to share the load between the two paths and exploit the role of both the underfloor rails and the a-pillars. Additionally, a large engine subframe is present and its size and shape allow it to be loaded early in the crash event, unloading some of the energy on the engine mounts that will detach when reaching a pre-set load limit and make the engine drop towards the ground. This more complex front end design was denominated by honda the Advanced Compatibility Engineering™(ACE™) body structure [47], which is the result of a study to improve the vehicle's compatibility during frontal impacts. For this reason, this model is expected to perform positively not only with respect to occupant protection, but also in terms of PDB deformation. As the upper load path terminates at the a-pillars, the main rails continue towards the rear of the vehicle, with c-sections placed above the floor of the vehicle, inside the cabin. These bend and join with the sills in correspondence of the B-pillars. Secondary rails reinforce the central tunnel and the rear engine subframe mounting points, while additional elements transfer part of the load to the sills at their frontmost part. The rear structures are designed as an extension of the sills until the rear cross beam (Figure 3.10c). In addition, the C-pillars continue along their line until the end of the luggage compartment (Figure 3.10b), to finally join with a large panel also connected to the rear cross beam.

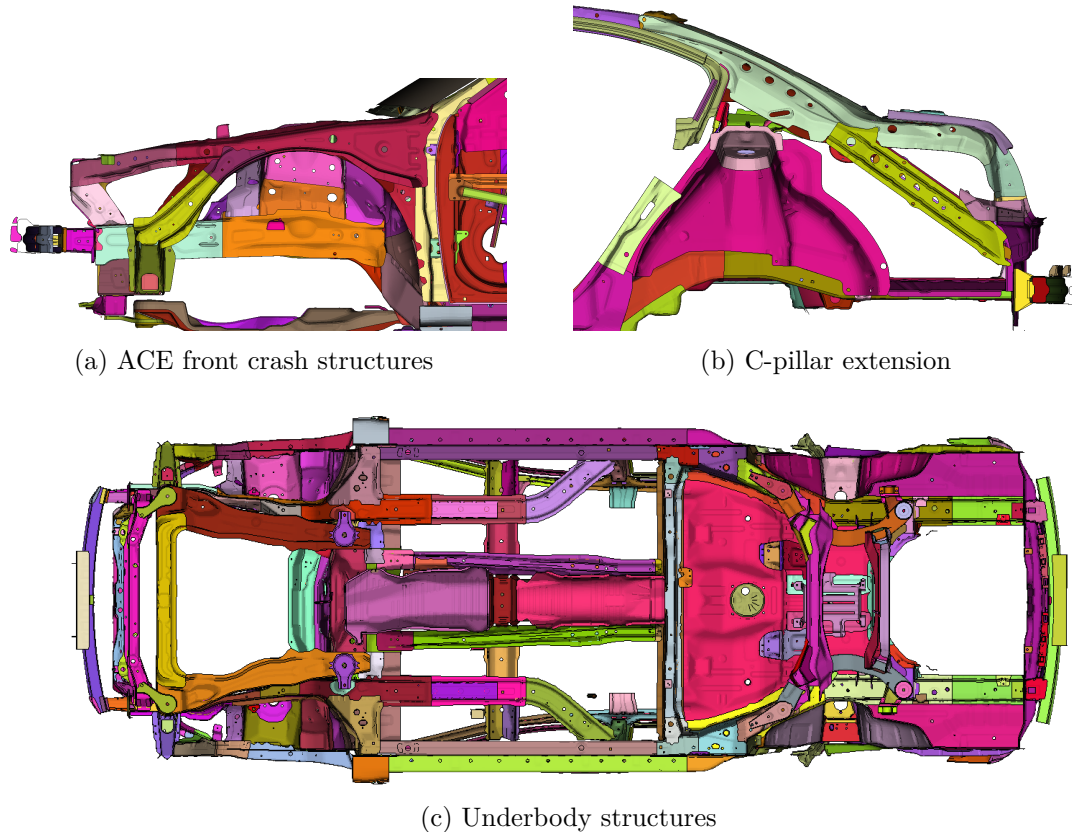


Figure 3.10: Honda Accord - model details

3.2.3 Chevrolet Silverado

The third vehicle model selected is a Chevrolet Silverado 1500 Crew Cab pick-up, which represent an extreme in terms of mass and it is utilised with the aim of assessing to the full extent the expected structural advantages of the MPDB test on heavy vehicles. The Silverado has a kerb weight of 2367kg and it is only sold in the USA, while it can be imported in Europe. For this reason, it has never been a test subject for Euro NCAP and, as a consequence, the star rating is not available. However, the vehicle has been tested by US' Insurance Institute for Highway Safety (IIHS) in their moderate overlap frontal test, which shares the same specifications as the Euro NCAP ODB impact, apart for having only a single Hybrid III dummy in the front driver seat and no other ATDs for front and rear passengers. In this test, the Silverado scored a **GOOD** rating, which represents the maximum available score on a scale of 4 possible achievements (**POOR-MARGINAL-ACCEPTABLE-GOOD**). This proves that its design would have, indeed, been able to achieve a positive score for the european consumer test. Furthermore, in the NHTSA full width rigid barrier test it achieved a rating of five stars for the driver and five stars for the front passenger.

Table 3.3: 2014 Chevrolet Silverado specifications

Model	Chevrolet Silverado 1500 Crew Cab 4WD
Year	2014
Chassis type	Steel ladder chassis with separated cabin
Kerb weight	2367 <i>kg</i>
Safety rating	GOOD IIHS 5 Star NHTSA

Overall model completeness

As for the previous two models, the Chevrolet Silverado is represented with good quality for what concerns the external appearance, as all surfaces are modeled accurately with regards to the physical counterpart, as shown in Figure 3.11. The front grille and badge are missing as they have been removed due to their behaviour in simulation: their extreme deformation could not be dealt with by the code and, although several attempts were made, the decision was made to remove the component as its importance and effect on the results of the impact is absolutely negligible.



Figure 3.11: 2014 Chevrolet Silverado - Physical [16] and CAE models

Considering the engine bay, several components haven't been modeled in this case as well. Although the most important equipment is present - engine and gearbox assembly, battery, brake booster, steering system, radiators and pulleys - a considerable amount of empty space is left in the compartment, compared to the physical model. This will yield the same effects described for the Accord model, permitting a better performance of the front structures.

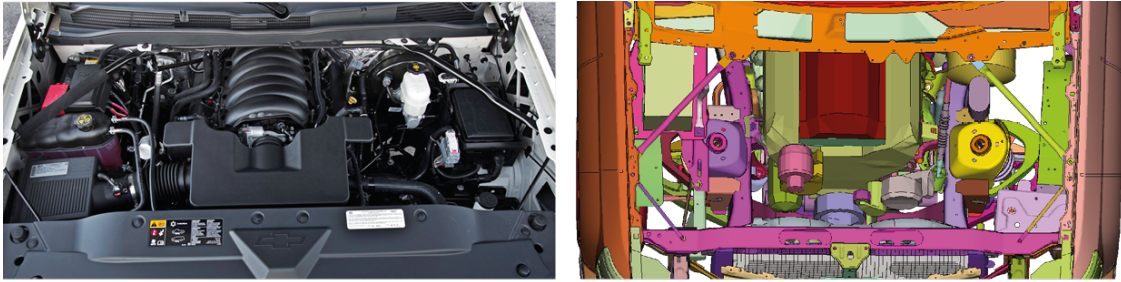


Figure 3.12: Chevrolet Silverado engine compartment - Physical [17] and CAE models

With regards to the interior trim and parts, this is by far the least equipped model out of the three. Only basic features are modeled: steering wheel and column, cross car beam, seat frames. No plastic components or accessories have been developed at this time.

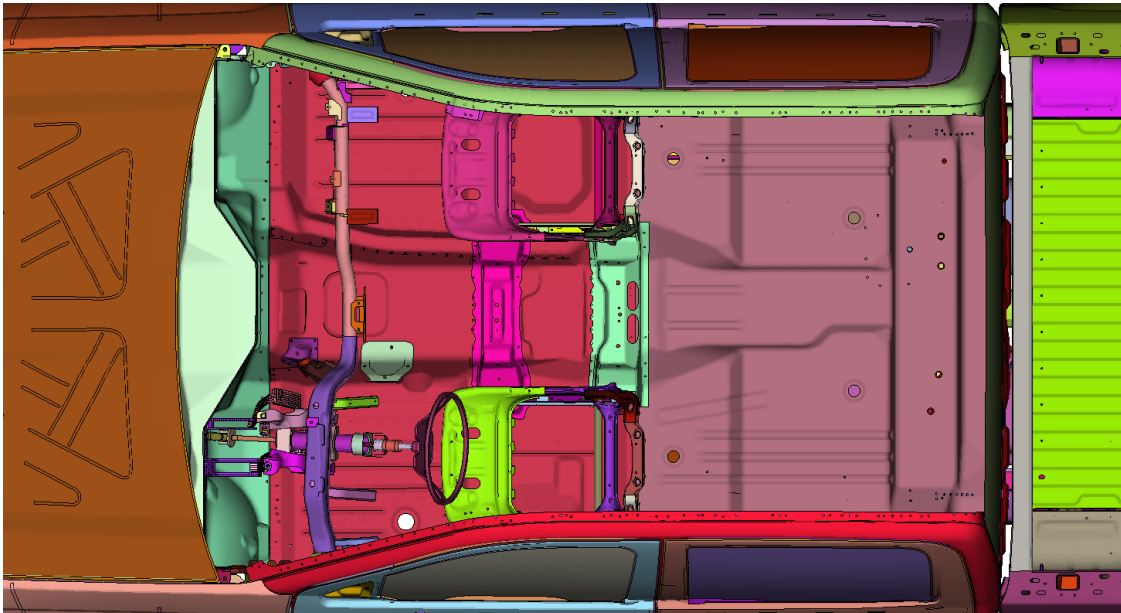


Figure 3.13: Chevrolet Silverado - passenger compartment details

Structural design

Once again, the lack of details of the engine compartment and interior is not reflected on the structural components of the chassis and the cabin. In this case, the vehicle is supported by a ladder chassis, typical choice for heavy duty and off-road applications. Two box section steel rails are employed as main structural components, running from the front to the rear of the vehicle, connected by a series of cross beams. The rail structure supports all parts of the vehicle, from the engine, to the wheels and suspension, to the full cabin. In terms of frontal crash structures, the foremost part of the main rails acts as the principal, and only, load path. No crash boxes are employed in this instance and only two minute u-shaped components are attached to the front of the rails. In order to drive a correct deformation during impact, the main structures are designed including three sets of triggers of decreasing size, with the larger ones at the front. These will allow buckling of the steel box sections in a controlled manner, hence absorbing the most amount of energy possible. Other load paths are not present, hence the residual energy will be absorbed by the same rails, moving towards the rear of the vehicle. Regarding the cabin, its structures are not designed to absorb a significant portion of the frontal impact energy, however, the firewall components are designed to sustain the load applied by the engine, which is still considerable. The large size of the A-pillars and the sills will also contribute towards cabin integrity and load transfer from the front wheels and possible impacting objects (Eg. barrier in small overlap test).

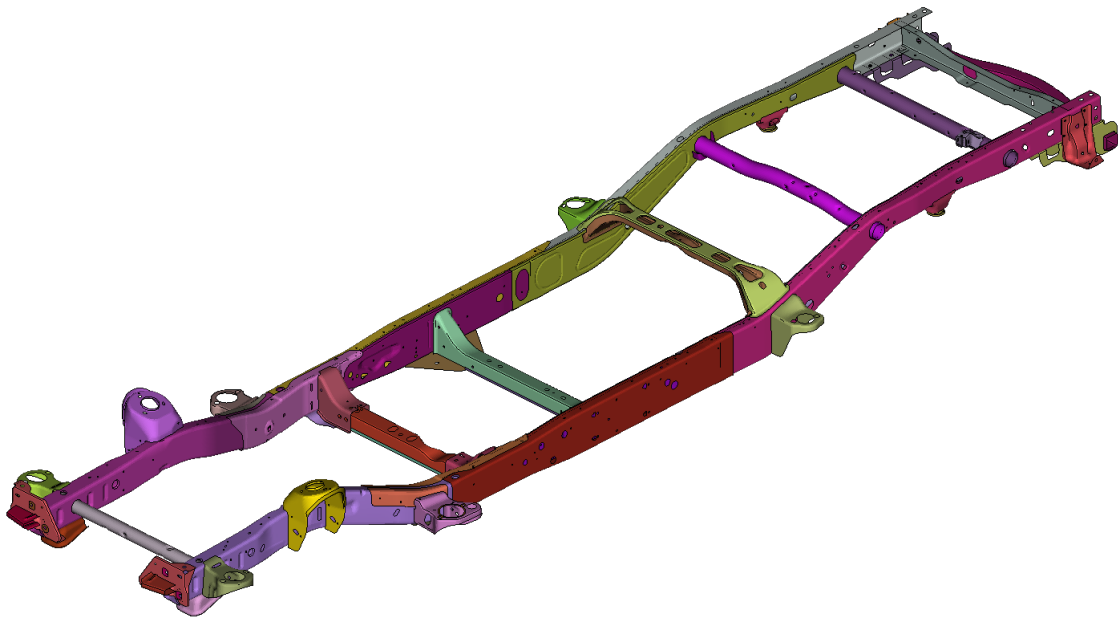
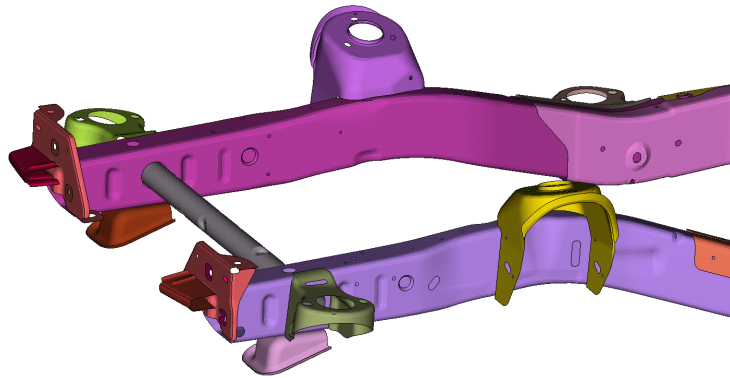
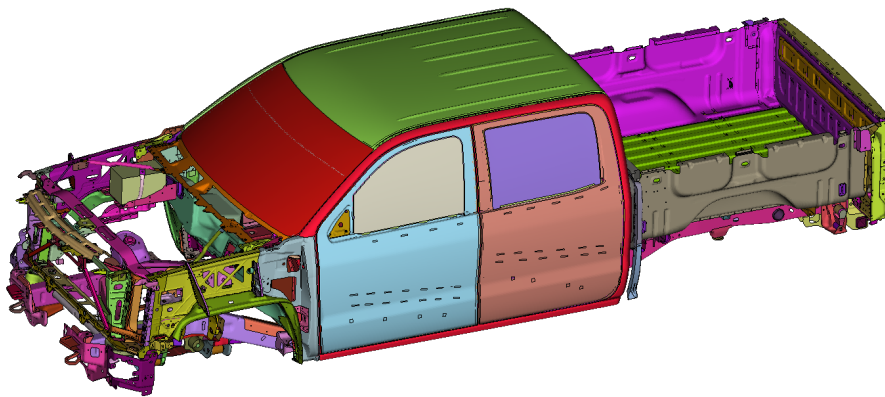


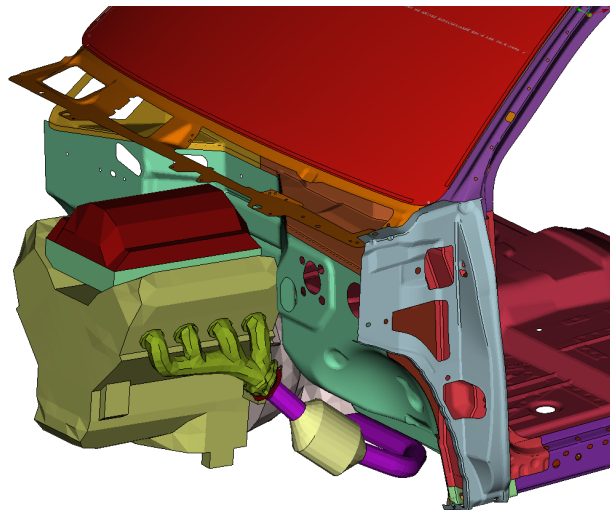
Figure 3.14: Chevrolet Silverado - main ladder frame



(a) Front structures detail



(b) Cabin structure



(c) Firewall, A-pillar, sill

Figure 3.15: Chevrolet Silverado - structure details

3.2.4 U Model

The last model under consideration is that of a medium-sized SUV designed for asian market, which is denominated for this study U Model. The vehicle was designed to undergo the EU homologation tests, hence an ODB at 56km/h . The Euro NCAP rating was not within the design parameters, therefore it is expected that it will underperform quite heavily in the current ODB 64km/h . Its mass is expected to be above 1700kg in roadgoing condition, hence considerably above the mass of the Honda Accord. The reason to analyse the performance of this vehicle lie in the interest in seeing how a vehicle that was not designed for the Euro NCAP ODB would perform in the MPDB. The expectation is that, due to its mass, the results for occupant protection in terms of intrusion and acceleration will be substantially better in MPDB.

Regarding the completeness of the model, it is not possible to assess it due to the impossibility to obtain photos of the real vehicle, its engine bay and its interior in detail. What can be said, however, is that the model utilised represents the vehicle in the final stages of the design process, hence includes a high level of detail both for the chassis, for the components in its front section, for the interior dashboard and for the seat frames. The body of the vehicle is also finalised for the most part, although certain components have been removed for disclosure issues.



Figure 3.16: U Model - CAE model

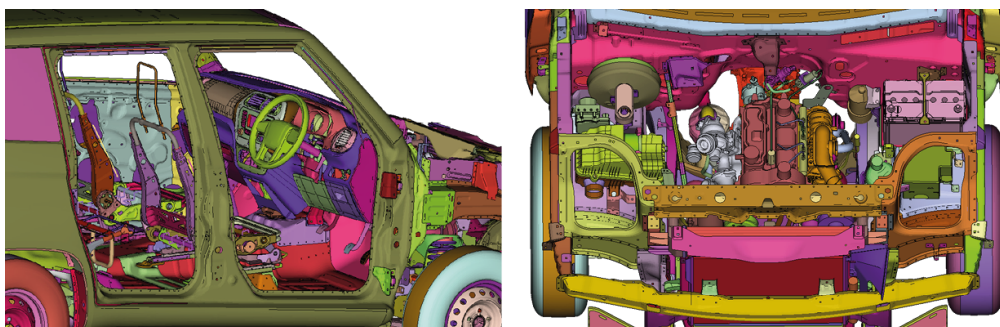


Figure 3.17: U Model details - interior and engine compartment

Structural design

Regarding the structural design of the SUV, the main frame is, similarly to the Silverado, of the ladder type, with a separated cabin mounted on top. The front crash structures show a large cross beam attached to two different sets of crash boxes placed subsequently one to the other, as reported in Figure 3.19a.

These are designed with several collapse triggers, with a function akin to that explained for the large pickup. Moving backwards in the central part of the front compartment, the actual main rails begin in correspondence with the engine subframe and show a cross section that enlarges until the S shaped transition towards the bottom of the cabin. It is expected that the smaller front part of the rails will collapse after the crash boxes have failed, while excess load will be absorbed by the deformation of the weak spot corresponding with the first part of the S curve.

In contrast with the design shown with the Silverado, the front part of the U Model's cabin does include some impact structures. Two additional box sections are attached to the A-pillar and protrude forwards until reaching the same axis as the front main cross beam (Figure 3.19b).

These additional crash structures bend downwards in their front part in order to absorb some energy during the ODB impact and unload it on the most rigid parts of the cabin. The cross beam that connects them is also aimed at sharing part of the load during the ODB test, this time with the crash structure on the opposite side of the vehicle. This seems to be reasonable also due to the size of the bottom part of the A-pillars, which is relatively large.

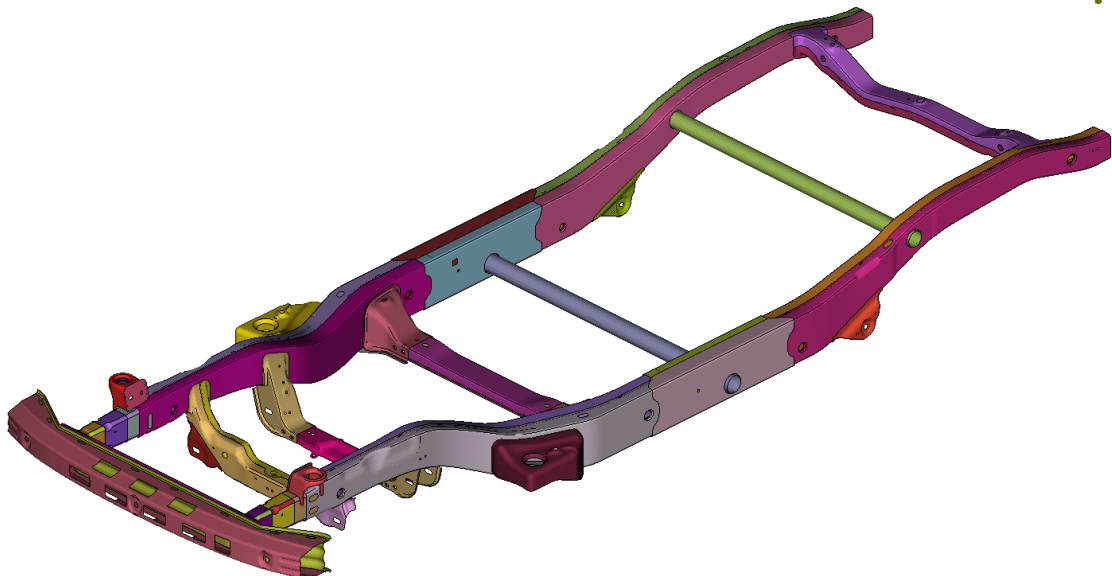
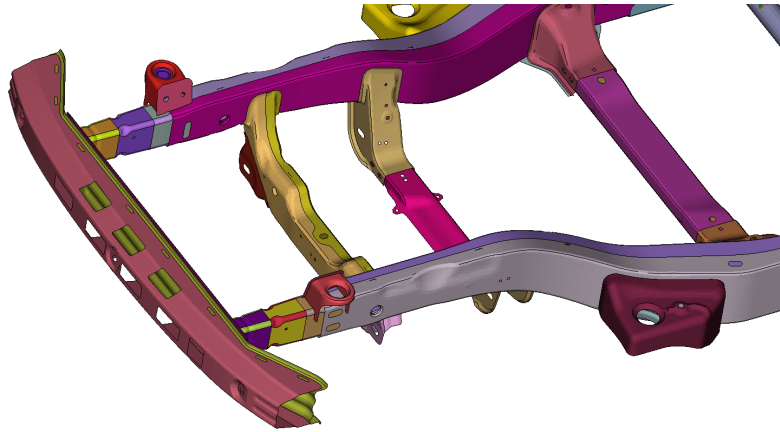
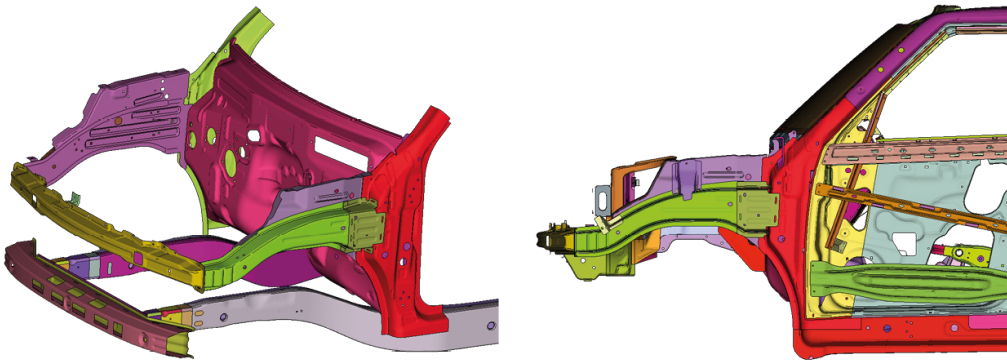


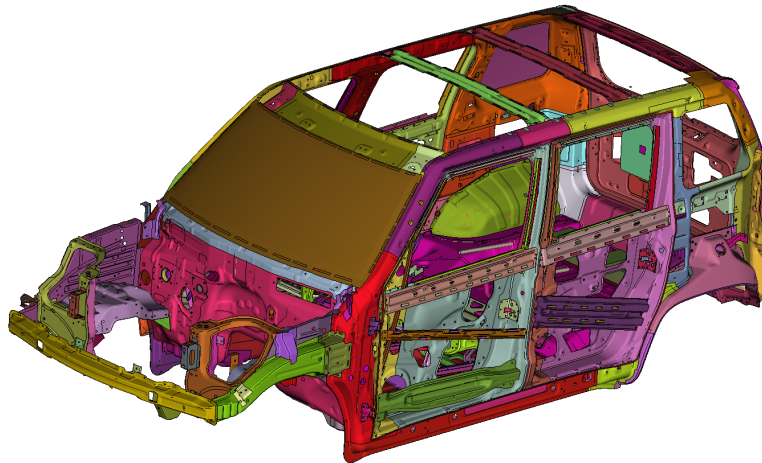
Figure 3.18: U Model - ladder type chassis



(a) Main crash structures detail



(b) Cabin frontal crash structures



(c) Cabin structure

Figure 3.19: U Model - details

3.3 Barrier models

The models of the ODB and MPDB impactors and ancillaries were provided by Livermore Software Technology Corporation (LSTC) [48], which is the company selling the LS-DYNA code. These were, therefore, specifically created to perform in the LS-DYNA environment.

The ODB model, portrayed in Figure 3.20, is based on the UNECE-94 regulations and is available in several different versions that allow the user to compromise between accuracy of representation and computational time. The honeycomb structure can be modeled as a solid, creating a very cost effective solution, or through shell elements, which increases the accuracy of the behaviour but increases the cost by roughly 20 times. For this study, the model chosen is a combination of shell and solid elements, which guarantees a high level of accuracy and does not require the increased computational efforts of a shell-shell model [49]. The shell elements are used to represent the main block, while the solids are employed for the bumper element.

The MPDB model (Figure 3.22, on the other hand, is based on the Research Moving Deformable Barrier Version 1.0 specification [50]. It is the first model released by an official software provider and it is expected to be updated in the future in order to be in line with the most up-to-date specifications published by Euro NCAP. The only formulation available includes a barrier face completely modeled with shell elements, attached to a solid trolley body.

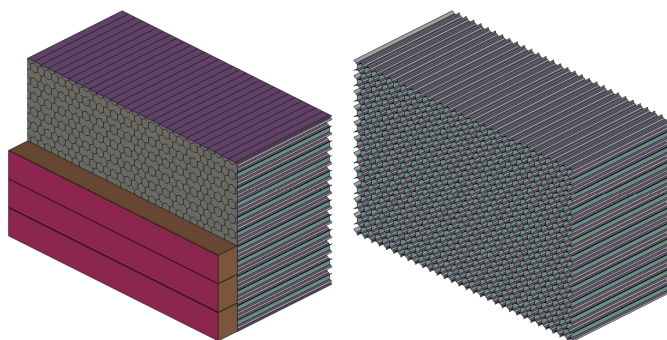


Figure 3.20: Offset Deformable Barrier - CAE model

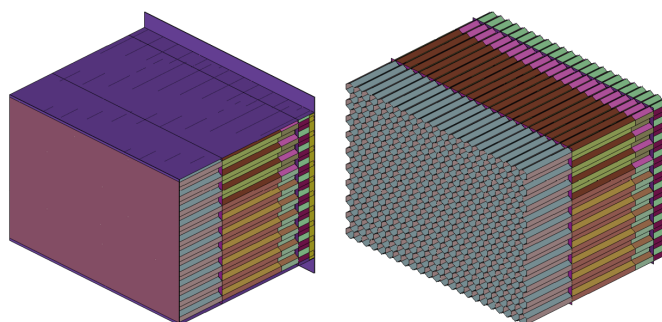


Figure 3.21: Progressive Deformable Barrier - CAE model

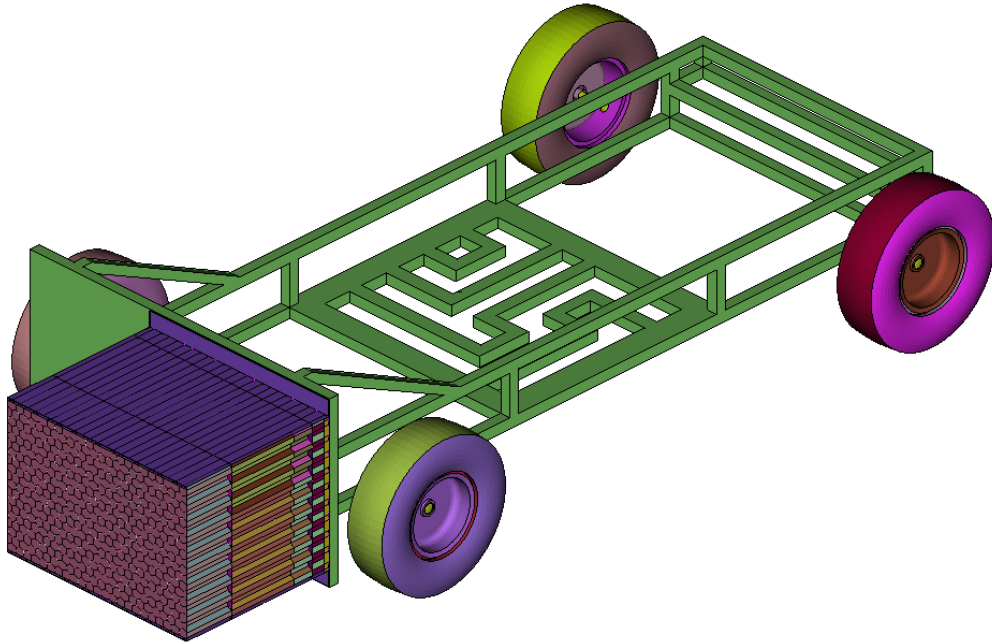


Figure 3.22: Mobile Offset Deformable Barrier - CAE model

3.4 Schedule of conducted tests

The testing schedule is reported in Table 3.4. First of all, all models were ran in the rigid wall setup at 56km/h , both to perform the correlation study and to test that the model was not incurring in any internal issues: the rigid wall test is a simple setup in simulation as it does not involve interaction with a complex element such as a deformable barrier. In this way, the model could be also checked to find critical points and address them before moving onto the more complicated scenarios. The next step was running the ODB simulations, which were also a well understood scenario, due to the large number of tests performed to simulate the standard Euro NCAP procedure. Finally, the MPDB simulations were completed: even though at this point the familiarity with the softwares was at a satisfactory level, the increased complexity of the barrier, together with the fact that not many tests were ran in this scenario made it quite a challenge. It has to be noted that most of the tests had to be ran several times, in order to troubleshoot the issues with the models themselves and their interaction with the barriers; these repetitions will not be highlighted.

Table 3.4: Tests schedule

		First batch	Second batch	Third batch
Rigid Wall	Yaris	X		
	Accord	X		
	Silverado	X		
	U Model	X		
ODB	Yaris		X	
	Accord		X	
	Silverado		X	
	U Model		X	
MPDB	Yaris			X
	Accord			X
	Silverado			X
	U Model			X

Chapter 4

Correlation Study

In this chapter, the work performed to understand the level of correlation between CAE and physical models is portrayed. Initially, reasoning is given about the importance and value of this portion of the work, while in the second section the methodology to perform such a study is explained. Finally, the results of the analysis for each vehicle model are reported, together with conclusions regarding the effect of the findings on the following parts of the project.

4.1 The issue of correlating physical crash testing with mathematical models

As anticipated in Chapter 1, the first part of the analysis performed in this project has involved a qualitative and quantitative comparison between the results obtained through the vehicle mathematical models and the ones deriving from physical tests. This study was undertaken in order to understand, to an extent, the level of correlation and representativeness of the simulated models and of the simulation capabilities themselves, so that a level of confidence in the results of the actual ODB-MPDB comparison can be obtained.

Several studies have surely been completed in the past on the same subject as this section of the work, as correlation studies between models and physical crash tests can be performed through the vehicle design process whenever a full scale physical example is constructed and tested. However, works of this type do not get published by automakers, who tend to keep them within the boundaries of industrial confidentiality for obvious reasons. In addition, a correlation study for the first three models utilised is not present in literature, even though the models are freely available and so is the physical tests data. For this reason, it seems appropriate to put effort into utilising all available resources to understand the significance of the models used and of the simulation tools, before drawing conclusions on the effects of the Euro NCAP test modification. Regarding the U Model, a brief correlation analysis was performed during the final stages of the design process by Pininfarina s.p.a.; hence, a sample of the achieved results will be reported to give an understanding of the significance of the model.

4.2 Correlation methodology

Considering the first three models, Toyota Yaris - Honda Accord - Chevrolet Silverado, the correlation analysis consisted in replicating the full width rigid barrier test as performed by NHTSA's (USA) NCAP, in accordance with the specification of the Laboratory Test Procedure for NCAP Frontal Impact Testing [51]. The test consists in the vehicle impacting with a rigid wall at a speed of 56km/h , at 12 o'clock with a 0° angle. The test dummies utilised in this instance are a 50th male Hybrid III, sat in the driver seat and a 5th female Hybrid III for the front passenger seat. To obtain the correct test weight, the fuel tank must be filled to its full capacity, while the luggage compartment must host a mass equal to:

$$RCLW = VCW - (68.04 \times DSC) \quad (4.1)$$

where: $RCLW$ = Rated Cargo and Luggage Weight
 VCW = Vehicle Capacity Weight
 DSC = Designated Seating Capacity

The test was performed in simulation and the results were confronted with those obtained through US NCAP database. The provided information includes a full report comprising measurements of intrusions [52], shown in Table 4.1, and photographs from most relevant angles of the vehicle pre and post crash. Furthermore, the accelerometer data recorded during the event is also freely available, with a very high number of channels from which to extract the crash pulse data points, and was downloaded from [53].

Table 4.1: US-NCAP - utilised intrusion measurement points [1]

Door Opening Width	Left side upper
	Left side lower
	Right side upper
	Right side lower
Wheelbase	Left side
	Right side
Driver compartment	Inside window jam
	Foot rest

Considering the physical test data available, the areas of interest for the comparison included the acceleration pulse, velocity against time and crush space (deformation) against time. The acceleration data for both CAE and physical result was post-processed using a SAE J211 filter, while the velocity and deformation are obtained through integration of the filtered acceleration signal. As it will be more evident by looking at the graphical representations, the more significant results are those of velocity and deformation, as the crash pulse has both an intrinsic level of variability according to the position where it is taken and of low repeatability between tests, hence it is very hard to reproduce it

perfectly with a simulation. Nevertheless, the locations of peaks and the amplitude of the maximum peaks should remain in the same range in a repeatable and representative way. Furthermore, intrusions measurements were taken from the CAE model and compared to those of the physical test, in order to ensure that no large discrepancies were present.

Finally, the visual comparison between the deformed CAE model and crashed vehicle is performed. This allows to get an overall view of how realistic the simulation is, as the structural elements should deform in a similar way. It is expected, due to the suboptimal level of completeness and approximation of certain components in the models, that the whole behaviour will not be represented perfectly in all its aspects. The core idea of the comparison lies in the structural similarity.

4.3 Toyota Yaris

Despite the simplifications highlighted in Section 3.2.1, the model replicates with a good level of similarity the physical behaviour in the full width rigid barrier test. The similarities and discrepancies are here analysed first with regards to dynamic data, then to deformation and intrusions, and only in the end in terms of visual representation.

Dynamic data

As reported in Table 4.2, the CAE model underestimates the peak acceleration by roughly $3.6g$, which is equal to less than 7% difference out of the $52.5g$ experienced in the physical test. During the vehicle design process, this is seen as a positive results as a difference below 10% means that using the simulation with a reasonable safety factor will result in a high level of confidence that the structures will perform as expected. However, the difference in the peak can be blamed both on the level of accuracy of the calculation process itself, and on the amount of missing components in the front part of the vehicle. As expected, the diminished compacting effect of the rigid parts in the engine bay allows better employment of the crash structures and results in lower maximum acceleration, which also occurs later in the crash event as shown in Figure 4.2. Analysing in more detail the pulse, it is possible to appreciate how the shape and timing of most of the peaks is consistent with the physical test. This is especially true for the first, second and third lower peaks, which occur with exact timing. These correspond to the first engagement of the cross beam and crash boxes, their collapse, followed by the onset of deformation of the main crash structures. The main peaks region represents the actual progressive failure of the crash structures and bottoming out of the engine, hence in this part a level of discrepancy is understandable, due to the aforementioned reasons. One section that cannot be easily explained, however, is that occurring in the CAE model during the first $5ms$: in this timeframe, only the front part of the plastic bumper is in contact with the barrier and deflects, no structural element is loaded and forces on the crash structures are still irrelevant. The narrow peak of $13g$ seems unreasonable. The section here analysed could also partially explain the reduced peak later in the crash: the bottoming out of the structure will occur with less residual energy, since part of it has been consumed in the earlier stages.

Considering the velocity graph (Figure 4.3) it is possible to appreciate better the level of similarity of the two crash events, as this gives a reading of the overall trend of deceleration, filtering out the very specific instantaneous behaviour. In the first $30ms$, the trend of the

CAE model seems more aggressive than that occurring in reality. This can be mostly blamed on the initial peak (first $5ms$) that has been discussed above, as after the initial dip the two lines proceed in parallel until $30ms$. After a central section in which the change in velocity of the CAE model appears to be almost identical to the real one, the final part shows how the absence of the same level of compacting leads to a more gentle slope. Finally, the time to reach zero velocity results $2.7ms$ greater for the simulation, which equates to 4.4% .

Moving the attention on the maximum crush space, the simulation slightly underestimates this parameter, as it did for peak acceleration. Although a greater crush space would be expected when lower accelerations are achieved, the data in Table 4.2 shows a difference of 2.2% , equal to roughly $14mm$, which is minute compared to the $600+mm$ of deformation. Nevertheless, the difference could be due to the same reasons explained for the lower peak acceleration: the higher amount of energy used earlier in the crash means that at the end of the impact less energy is present to deform the structure. However, since an equal mean acceleration is present, the differences in deformed length could also be more due to oscillation than to significant phenomena.

Table 4.2: Toyota Yaris - full width rigid barrier dynamic data

	Physical	CAE	Difference	% Difference
Peak acc. [$-g$]	52.46	48.87	3.59	6.84
Mean acc. [$-g$]	25.09	25.11	-0.02	-0.08
Max crush space [mm]	631.43	617.67	13.76	2.18
Time to zero velocity [s]	61.3	64	-2.70	-4.40

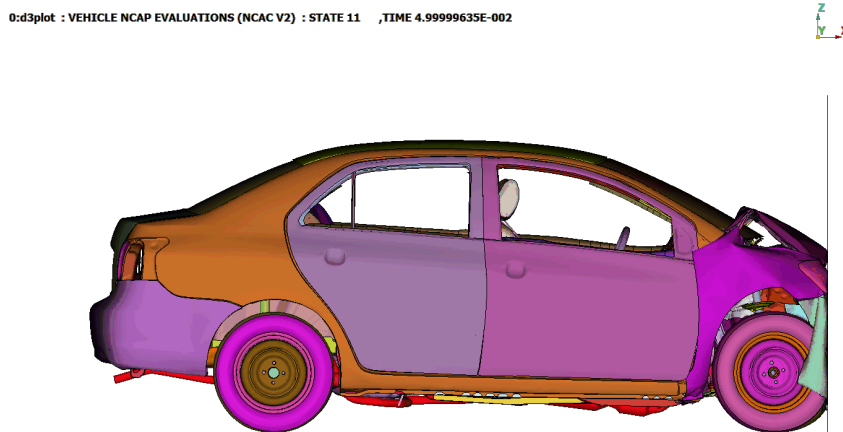


Figure 4.1: Yaris FWRB - simulation snapshot

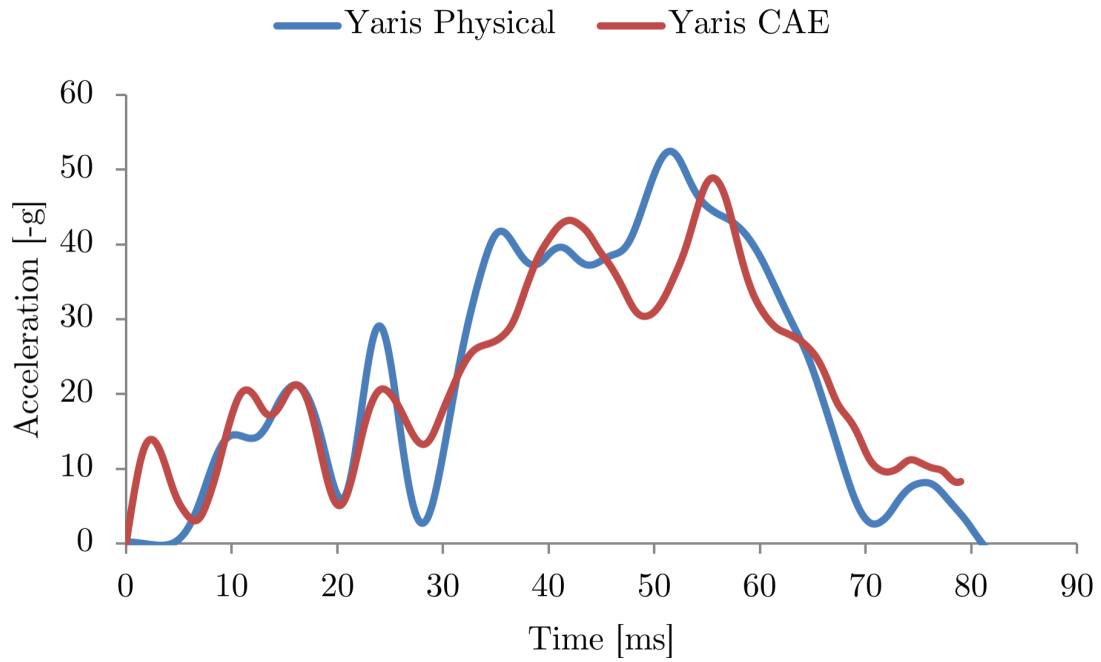


Figure 4.2: Yaris FWRB - acceleration

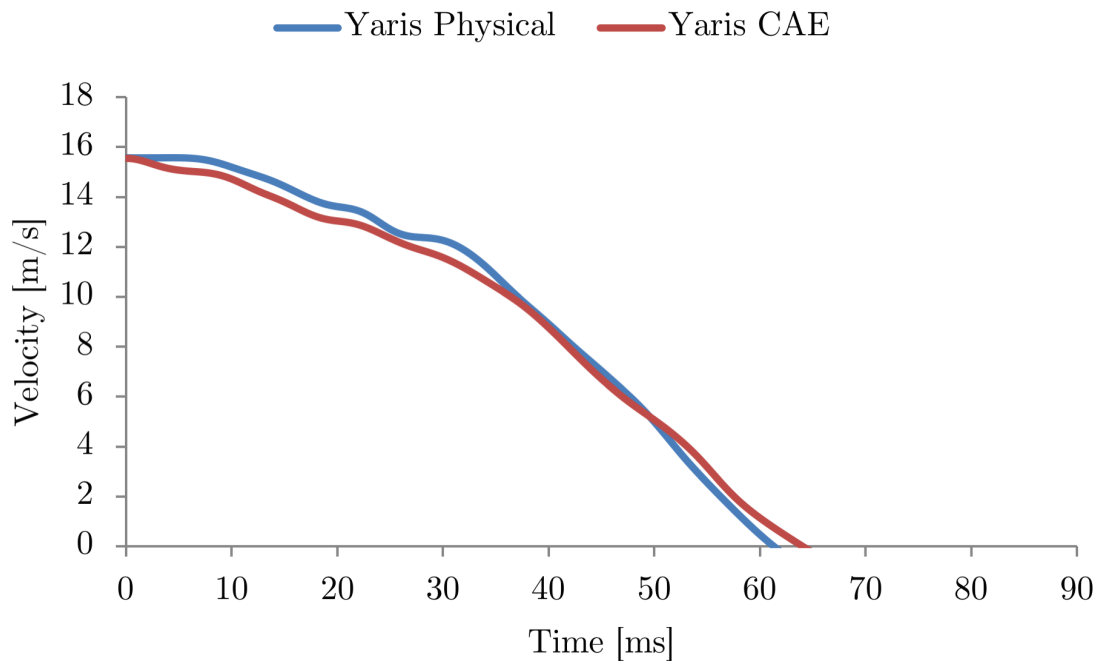


Figure 4.3: Yaris FWRB - velocity

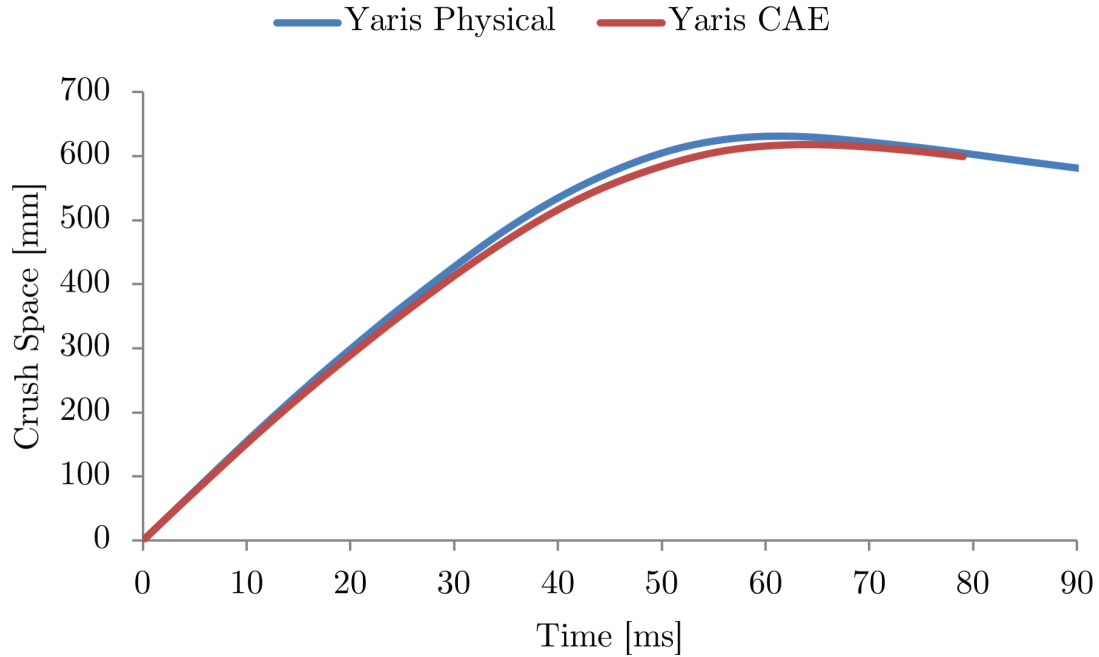


Figure 4.4: Yaris FWRB - crush space

Deformation measurements

The intrusion and deformation measurements here reported for the physical test were obtained from the official NCAP test’s final report [54]. As the values in Table 4.3 highlights, the level of discrepancy in this case is very limited. All values for door opening, wheel-base and compartment intrusion are within $3.5mm$ from the actual ones, with the greatest majority being equal or under $2mm$. These differences cannot be deemed significant, also due to the fact that the measurements were not taken by the same person or even by knowing exactly how to reproduce them to the full extent in the post processing environment. If discrepancies in the order of $10+mm$ would have appeared, that would have been definitely more relevant. Also, it has to be noted that the simulation does not include the rebound part of the crash. Therefore, the measurements are taken in two completely different moments: for the physical test, the recording occurs after the vehicle has settled in its final position and all spring effects have exhausted their energy; for the simulation, on the other end, the instant of maximum deformation is utilised. In fact, both for cost reasons and for concerns of the accuracy of the simulation of rebound and spring back effects the calculation is stopped when the impact energy reaches stability, as visible in Appendix A.

Visual analysis

For the analysis completed from the visual perspective, all relevant figures present in Report [54] were utilised and are here presented. This analysis confirms the trends understood

Table 4.3: Toyota Yaris - full width rigid barrier deformation measurements [mm]

		Physical	CAE	Difference
Door Opening Width	Left side upper	1	3	-2
	Left side lower	2	4	-2
	Right side upper	0	3	-3
	Right side lower	0	2	-2
Wheelbase	Left side	50	53.5	-3.5
	Right side	36	37.4	-1.4
Driver compartment	Inside window jam	1	1	0
	Foot rest	0	2	-2

from the previous two parts, as all the relevant deformation areas appear to be well represented. From the two side views (Figure 4.5) it is clear how the wings and bonnet deform in a very similar way, with the only critical areas being the plastic components of the front bumper and headlights, which are not modeled accurately and appear too soft. The deformation of the cabin is absolutely comparable and the small difference in crush space is evident. Looking at the underbody, the deformation of the engine subframe is similar, although the model appears to show it at a slightly higher level. The underbody rails and floor structure are mostly undeformed in both examples, as are the suspension components. Unfortunately, the physical model includes a number of plastic trim parts that don't allow the analysis of the radiator area. Finally, from the top view is again visible how the level of deformation of the front is similar and the behaviour of the front wings is reproduced accurately. Larger versions of the figures can be found in Appendix B.



Figure 4.5: Yaris FWRB - LHS and RHS comparison

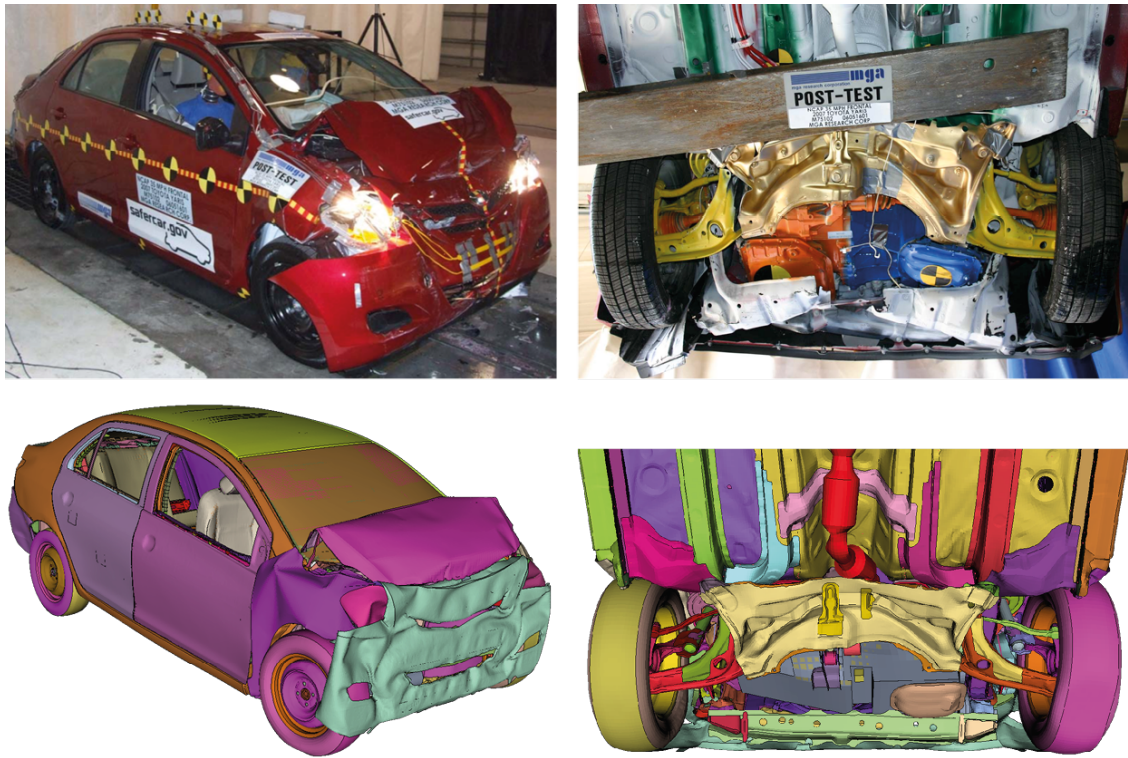


Figure 4.6: Yaris FWRB - three quarters and underbody comparison

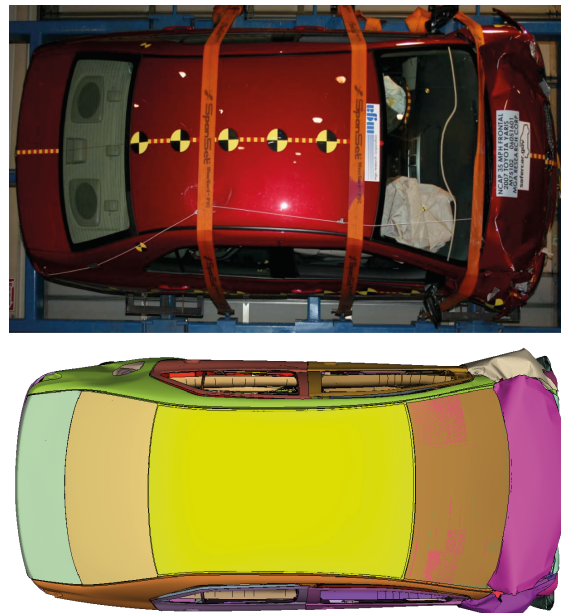


Figure 4.7: Yaris FWRB - top view comparison

4.4 Honda Accord

Model issues

In contrast with the Yaris model, the Honda Accord showed a number of issues in terms of behaviour of components and structural deformation. The first set of tests conducted highlighted how the dynamic parameters of acceleration pulse, velocity change and crush space were for the most part unrelated to the physical data. For this reason, the model's dynamic behaviour was analysed in META and two main issues were found: first of all, the main crash structures and crash boxes were not collapsing in the logical sequence. In fact, the crash boxes were not collapsing at all, while the main rails were buckling immediately after the first contact occurred, as highlighted in Figure 4.8a. This was caused due to three main factors

- the **geometry** of the right hand rail included a large, empty hole located at the mid point through its length. This feature is required in the physical model to house the engine mount, which, when inserted, confers more rigidity to the whole structure. In the model, on the other hand, this part was not represented and therefore the main rail design presented a massive weak point;
- the **engine mount** was however still modeled, which caused a further issue. This was done by creating a rigid component attached to the above mentioned hole. The rigid was, however, only connected to one side of the perforation, hence not only adding zero rigidity to the structure, but deforming the rail immediately after impact, due to the inertia of the engine mass.
- the **materials** of the crash boxes and rails were defined in an illogical manner: both were simulated as steel, but the former had a yield strength value of $500MPa$, while the latter of $180MPa$. Although their cross sections are vastly different, such a large difference is not justified, as the resulting behaviour demonstrates.

To attempt to resolve the evident issues and fix the behaviour of the model, a number of changes were made sequentially:

1. the **material definitions** were modified: a yield strength of $180MPa$ was assigned to the crash boxes components, a value of $350MPa$ was set for the main rails (and internal components). Additionally, it was also found that the main cross beam was set to a value of $1050MPa$ and was brought down to $750MPa$, after the first results were seen from the modification of the first two components;
2. the **engine mount** rigid element was branched to more nodes around the whole circumference of the hole in order to replicate the component present in the physical model to a greater extent;
3. the **geometry** of the right main rail was eventually modified, filling the hole in the outer sheet metal and in its inner reinforcement.

The last, and more intrusive, procedure was performed due to the lack of results achieved with the previous two steps: the structure wasn't behaving as required and the acceleration profile was still greatly out of line. With the last modification, the behaviour finally started

representing what is expected from front structures, as shown in Figure 4.8b. Nonetheless, the improvement in terms of crash pulse were minute: the overall shape of the curve started being more representative in terms of trend, but the main issue of the unreasonably high initial peak remained, with only a minor reduction (Figure 4.9). At this point, it was not possible to continue in the modification of the model as no support was received by its original authors and the time constraints of the project imposed to proceed further. The final results obtained in comparison to the physical model are presented in the next paragraphs.

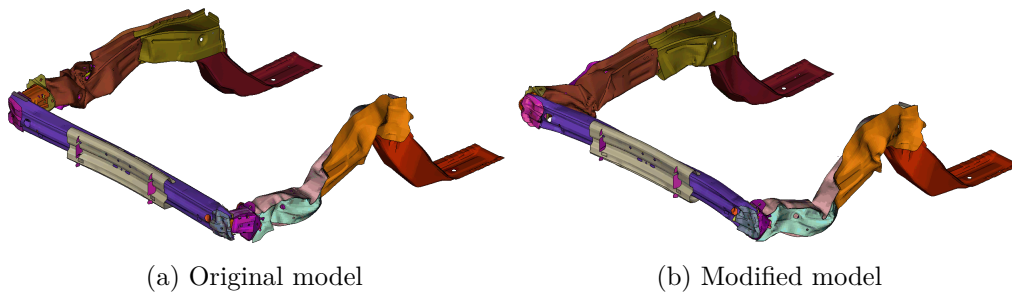


Figure 4.8: Honda Accord - front structures modification

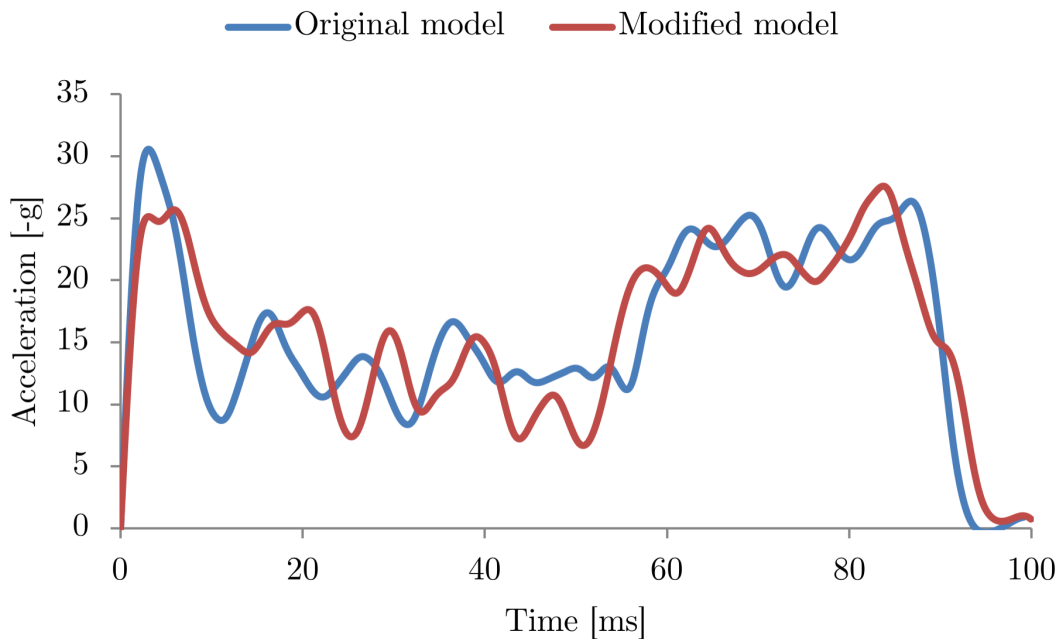


Figure 4.9: Accord - comparison of crash pulse before and after modifications

Dynamic data

Given the issues shown in the previous paragraph, it is evident that the behaviour of the model will not present a high level of accuracy. Although the overall shape of the pulse in terms of location of peaks presents a level of similarity, the amplitude of the simulated acceleration is substantially lower than that of the physical test, as demonstrated by the 15.3% and 14.3% difference in the peak and mean accelerations respectively (Table 4.4). As stated in the previous section, a difference of more than 10% is considered significant. This great discrepancy occurs mainly due to the presence of a first peak of $25g$, rising immediately at the moment of impact (Figure 4.11). The height and duration of this phenomenon dissipates a great amount of energy, which is then not present later in the crash event. Looking at the dynamic representation of the simulation, the area under observation cannot be reconducted to any visually evident deformation or movement, as it cannot be identified any relation with forces through the main structural members.

The discrepancy between the two impacts is not mitigated when the change in velocity trend is analysed. Figure 4.12 shows the influence of the first peak in the simulation, which produces an unrealistically aggressive deceleration, followed by a much milder trend that results in a delay of $11.3ms$ in reaching zero velocity.

With regards to crush space, the data relative to its maximum shows a very small difference equal to -0.3% . This is a positive result in terms of overall deformation of the vehicle, which seems to be in line with reality. However, the punctual information provided by the maxima of the lines should not be misleading when it comes to representing how the deformation occurred through the impact. The graph in Figure 4.13 shows clearly how, even though the same final level is reached, the slope of the lines is vastly different since the early stages of the crash. The progression of the deformation is therefore not simulated with the required fidelity by the model.

Table 4.4: Honda Accord - full width rigid barrier dynamic data

	Physical	CAE	Difference	% Difference
Peak acc. [$-g$]	32.56	27.58	4.98	15.29
Mean acc. [$-g$]	18.36	15.72	2.63	14.33
Max crush space [mm]	771.02	773.62	-2.59	-0.34
Time to zero velocity [s]	82.2	93.5	-11.30	-13.75

Deformation measurements

In contrast with the dynamic results, the measurements of deformation and intrusion give a more promising view. Again, the values here reported were obtained from the official NCAP test's final report [55]. All the quantities related to door opening and driver compartment intrusion are within $1-2mm$, similarly to what was found for the Yaris model. As the same limitations to the measurements explained in Section 4.3 are valid for the model under investigation as well, these differences cannot be deemed significant. The similarity between intrusions is an important fact as, although not covering up the pulse differences, it proves that the overall deformation of the model is representative of the physical vehicle.

0:d3plot : HONDA ACCORD BL MODEL (V1.1) : STATE 13 ,TIME 5.99999391E-002

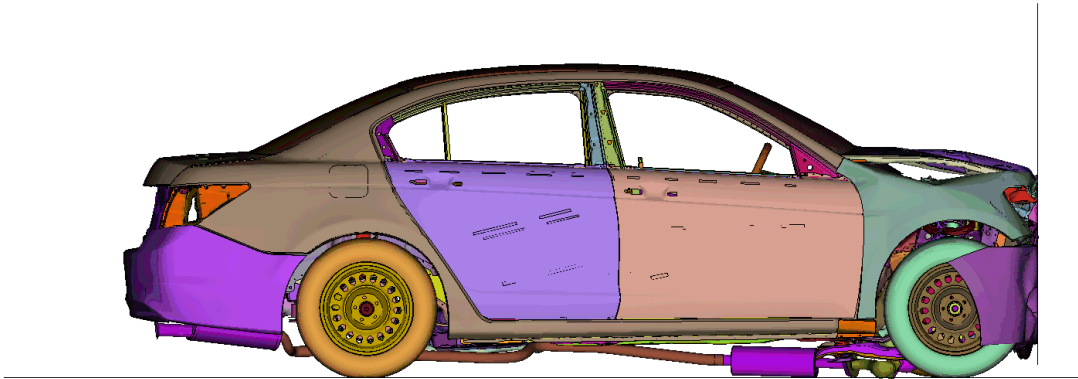


Figure 4.10: Accord FWRB - simulation snapshot

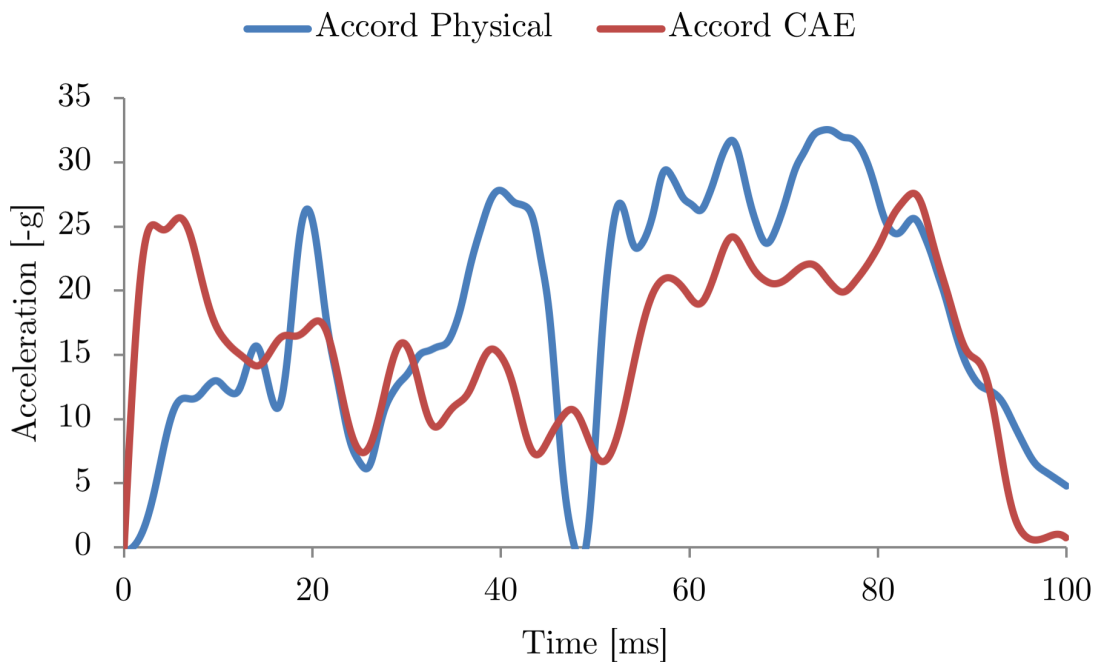


Figure 4.11: Accord FWRB - acceleration

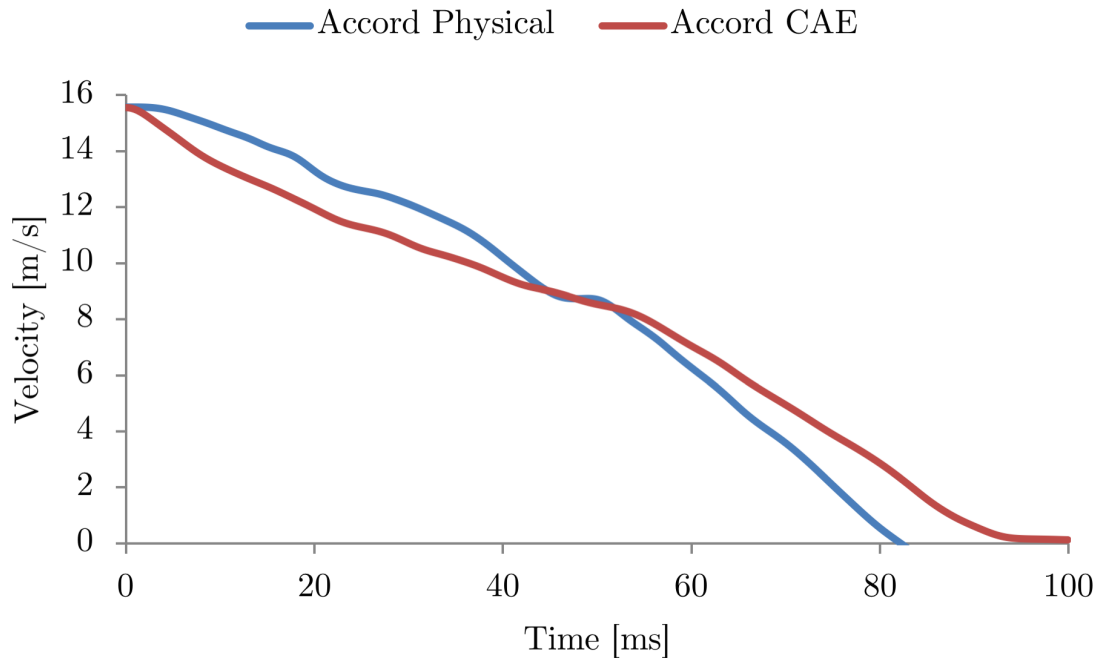


Figure 4.12: Accord FWRB - velocity

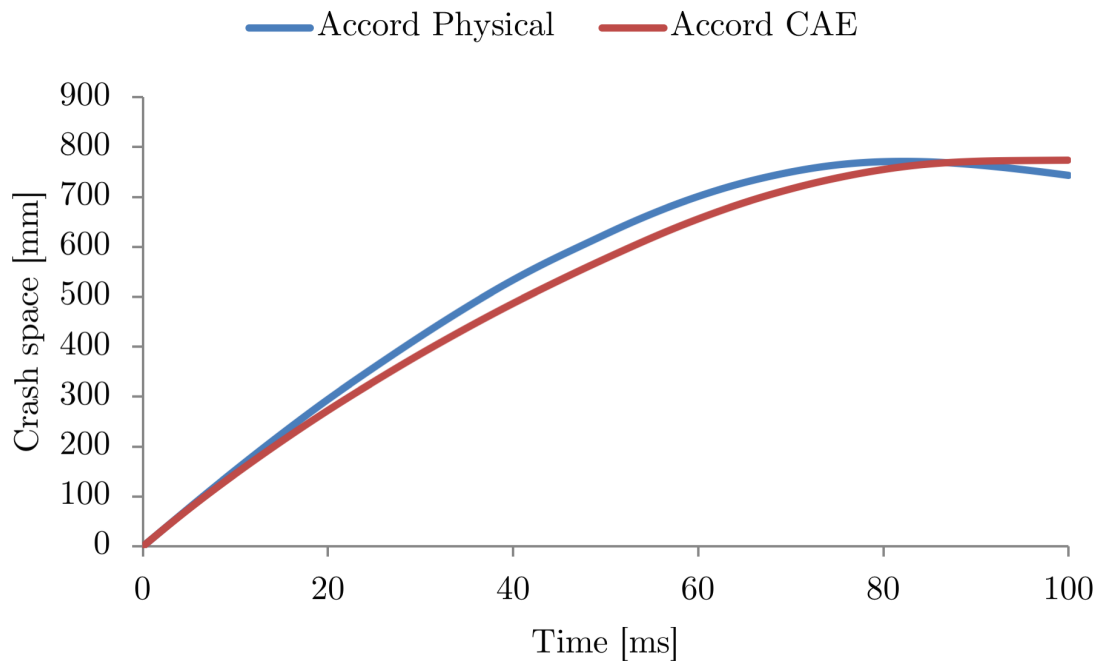


Figure 4.13: Accord FWRB - crush space

This is particularly true due to the fact that the values are for the most part distant from zero: the best example is found in the foot rest deformation, equal to $8mm$ and $10mm$ for physical and CAE respectively.

As it is evident from Table 4.5, the only clear issue has to do with the wheelbase deformation. There is a substantial difference for measurements of both sides, and there is also a large discrepancy if the difference between left and right sides of the same test are considered ($5mm$ for physical, $12.3mm$ for CAE). The reason of this lies in the fact that in the simulation the two front wheels underwent complex movements as they proceeded backwards, outwards and also rotated both in toe and camber, making it difficult to ensure that a precise measurement was taken. Furthermore, from [55] it is not clear if the same complex behaviour occurred in the physical test and even more so how the measurement was then taken.

Table 4.5: Honda Accord - full width rigid barrier deformation measurements [mm]

		Physical	CAE	Difference
Door Opening Width	Left side upper	5	4	1
	Left side lower	5	3	2
	Right side upper	5	6	-1
	Right side lower	5	4	1
Wheelbase	Left side	94	121.4	-27.4
	Right side	99	109.1	-10.1
Driver compartment	Inside window jam	2	1	1
	Foot rest	8	10	-2

Visual analysis

The figures utilised in this section, just as the data for deformations, were taken from [55]. Overall, the model deformation is similar to that of the physical model, from what can be seen in the available photographs. The deformation of the cabin is equally not present, the front wheels move backwards into the sills in a similar manner, leading to a small level of deformation of these structures, and the crumpled portion visible in Figure 4.15 is visually identical. However, a number of differences are also present:

- the **engine subframe** (Figure 4.16) in the physical test does not rupture its chassis mounts but deforms heavily, bending towards the top of the vehicle. In the CAE model, the mounts detach and the whole subframe moves backwards along the underbody by a considerable distance;
- the **bonnet** does not deform in a comparable manner: the behaviour of the hinges in the simulation leads to the metal impacting the windscreen and damaging it, while in reality this does not occur. The CAE bonnet is also much less deformed in terms of bending

- the **wings** appear less deformed in the simulation (Figure 4.14). At the end of the impact they still extend forwards further than the wheel, while in reality they bend more outwards and, as a result, protrude much less towards the front of the vehicle;

Despite these differences that affect for the most part components with little structural relevance, the most important fact is that the overall deformation is absolutely comparable and the cabin behaves in the same way, together with the frontal structures which deform to the same extent.

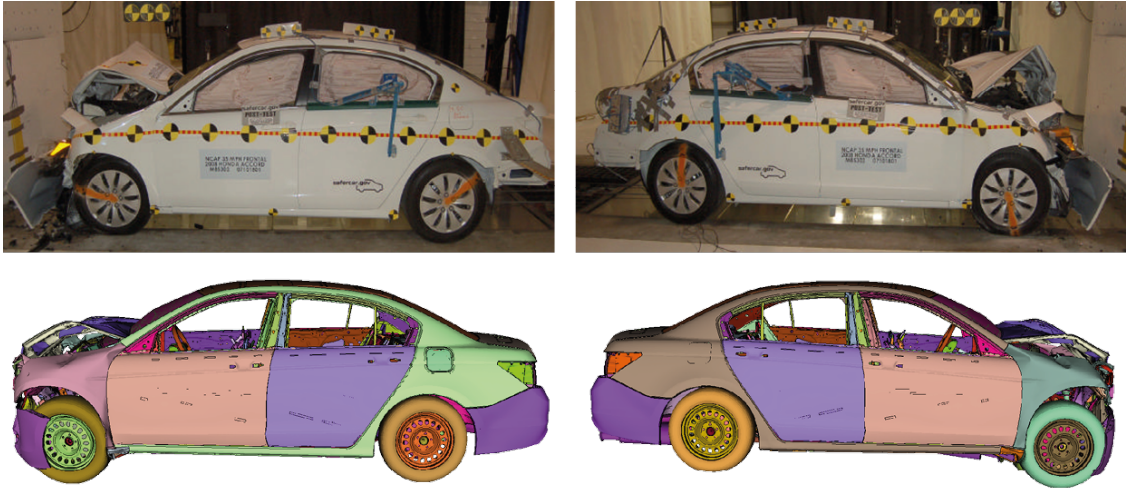


Figure 4.14: Accord FWRB - LHS and RHS comparison

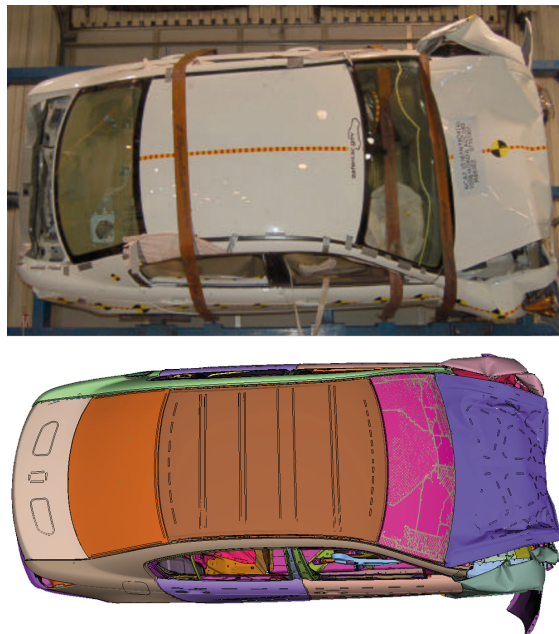


Figure 4.15: Accord FWRB - top view comparison



Figure 4.16: Accord FWRB - three quarters and underbody comparison

4.5 Chevrolet Silverado

Dynamic data

Out of the three models, the Chevrolet Silverado shows arguably the best results in terms of dynamic data. The peak acceleration is closer than that reported for the Yaris, as the difference is of $1.7g$, equal to 4.5% . Looking at the pulse in Figure 4.18, the first and second peaks (and dips) are reproduced with a good level of accuracy by the simulation, only with a slight overestimation of the initial acceleration due to failure of the front structures. The second peak also shows that the front part of the main rails of the model deforms slightly more progressively. The first substantial difference between the two events appears at around $40ms$, when the front structures reach the point of attachment of the engine cradle: in the simulation, this impact causes a mild and progressive peak as the rails and the cradle bend; in the physical test, it is assumed that the components in the engine bay pack against the engine and, in combination with a stiffer structure, cause a spike to the maximum acceleration experienced. It would be interesting to be able to analyse this particular phenomenon using footage of the crash test, but unfortunately high frame rate-high quality versions are not available for analysis. The spike at $40ms$ is followed by a second peak corresponding with the backwards movement of the engine and its subsequent

bottoming out. This part appears to be slightly offset in the simulation: the engine starts moving backwards at $50ms$ but does not encounter significant obstacles until $55ms$ and fully bottoms out in two stages around $10ms$ later. Overall, the two trends are sufficiently similar and most of the differences can be attributed to model incompleteness.

The same trend of similarity is reflected on the velocity vs time graph (Figure 4.19), as the discrepancies in pulse are smoothed out and the lines are extremely close. The time to zero velocity, reported in Table 4.6, is almost identical as only $0.4ms$ separate the modeled and the physical events. Furthermore, the difference in crush space can be explained by relating it to the pulse analysed above: the model is less efficient in terms of energy absorption at the beginning of the crash and the peak is still lower than the physical twin, therefore the result of both phenomena happening at the same time is a greater deformation of the structure, testified by the increase in crush space of $21mm$. This higher deformation is therefore mainly due to the emptiness of the engine compartment. In any case, the difference is small, at around 2.8%, and the lines overlay perfectly up until the very end of the crash, where the compacting takes place

Table 4.6: Chevrolet Silverado - full width rigid barrier dynamic data

	Physical	CAE	Difference	% Difference
Peak acc. [$-g$]	37.88	36.19	1.69	4.46
Mean acc. [$-g$]	17.72	18.16	-0.44	-2.49
Max crush space [mm]	741.48	762.45	-20.97	-2.82
Time to zero velocity [s]	79.6	80	-0.40	-0.50

0:d3plot : NSLT_BASE_NCAP_FF56 : STATE 42 ,TIME 1.00000344E-001

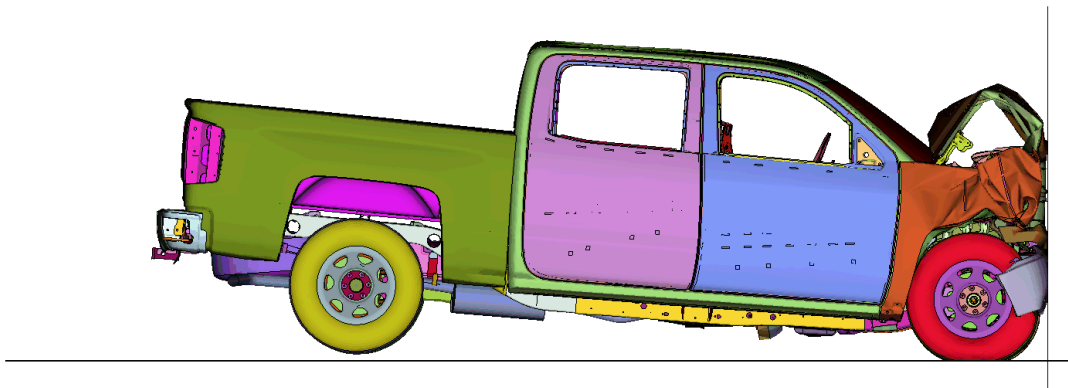


Figure 4.17: Silverado FWRB - simulation snapshot

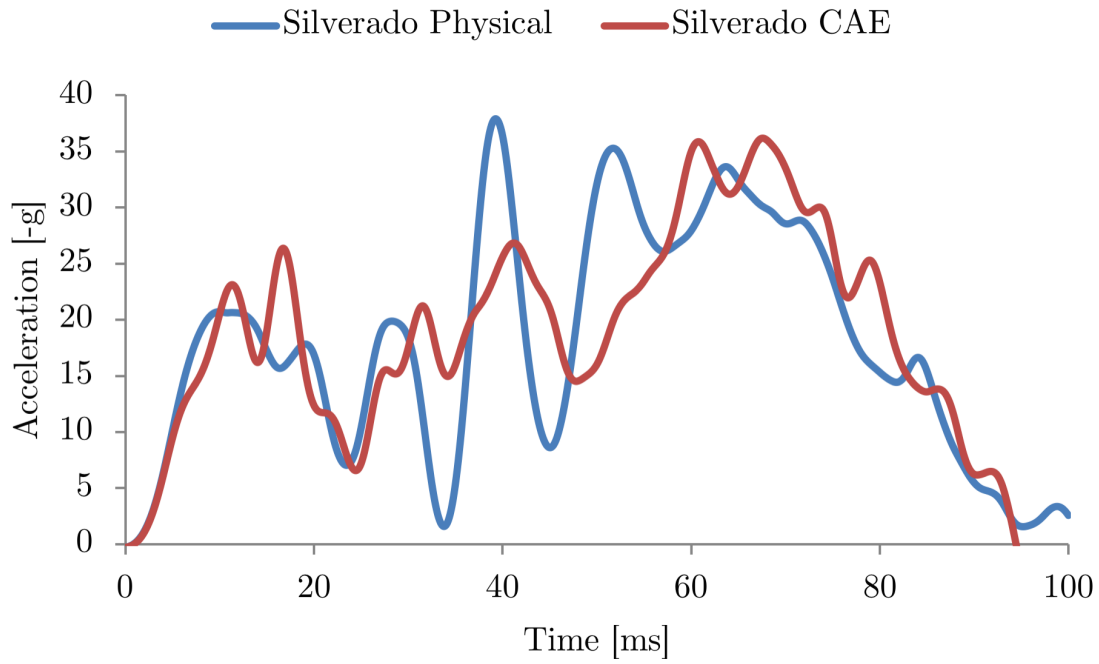


Figure 4.18: Silverado FWRB - acceleration

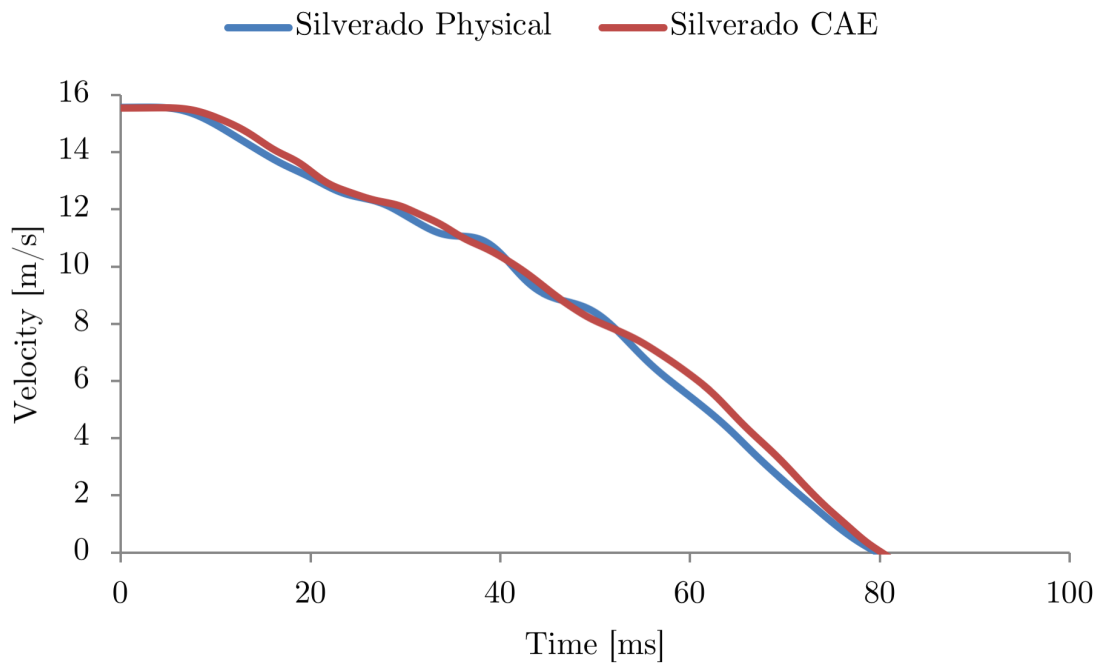


Figure 4.19: Silverado FWRB - velocity

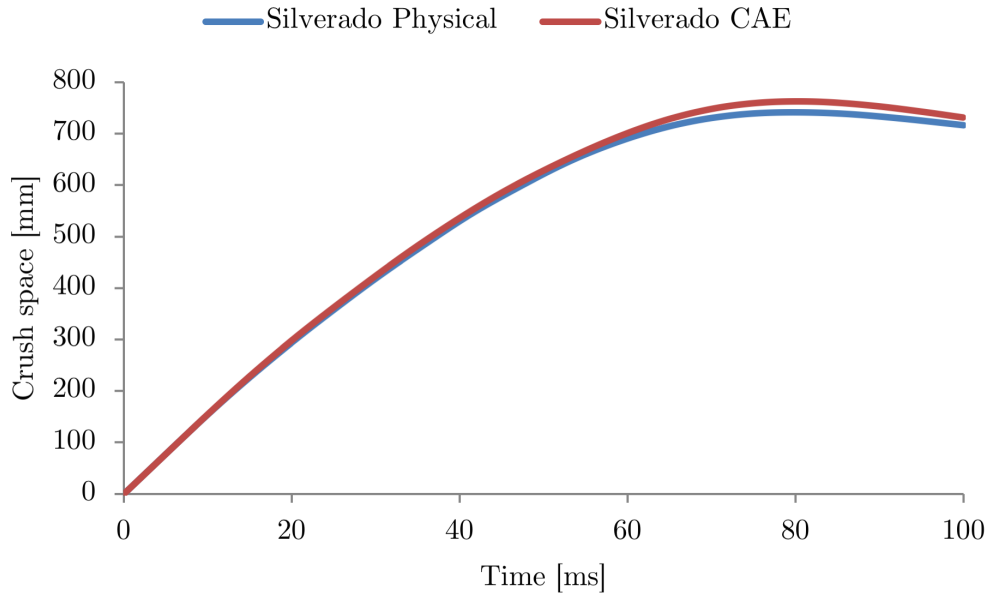


Figure 4.20: Silverado FWRB - crush space

Displacement measurements

With regards to displacement measurements, the model is again extremely representative of reality. Door opening width is almost perfectly matched, with slight overestimations for the lower part of the cabin. Unfortunately, the measurement for foot rest deformation was not available in the official report [1], but due to the small deformations present in the other fields, it is expected that it would be equal or near to zero. Finally, the wheelbase presents a small level of discrepancy, which is mainly to be attributed to the behaviour of the model's tires, which are heavily deformed at the instant of measurement (end of crash, prior to rebound), in contrast with the measurement taken on the physical model which would have been performed at rest, with the rubber being back to its original shape.

Table 4.7: Chevrolet Silverado - full width rigid barrier deformation measurements [*mm*]

		Physical	CAE	Difference
Door Opening Width	Left side upper	0	0	0
	Left side lower	0	1	-1
	Right side upper	0	0	0
	Right side lower	0	3	-3
Wheelbase	Left side	80	71.4	8.6
	Right side	85	78.4	7.6
Driver compartment	Inside window jam	0	1	-1
	Foot rest	-	1	-

Visual analysis

Analysing the photographs contained in the test report [1], it is possible to appreciate just how representative this model is. From the two side views, it is evident how front part of the vehicle is bent upwards in the real model, meaning that the car underwent a level of diving during the impact, which is perfectly represented in the simulation. The bonnet and even the front bumper show extremely similar deformation shapes compared to reality, while the wing on the right hand side seems a little too soft as it deforms very heavily. The whole ladder structure from the beginning of the cabin backwards is completely undeformed in both, similarly to the whole passenger compartment and loading bay. From Figure 4.23, it can be noted how the main components have deformed in a very similar way, with the engine tray showing bending in the two longitudinal supports, while other components such as the exhaust are untouched. The whole engine block and transmission assembly seems to have moved backwards by a comparable amount, while the attachment points of the cabin are identical. From the top view, once again, the crush space utilised is clearly shown and it is identical.



Figure 4.21: Silverado FWRB - LHS and RHS comparison

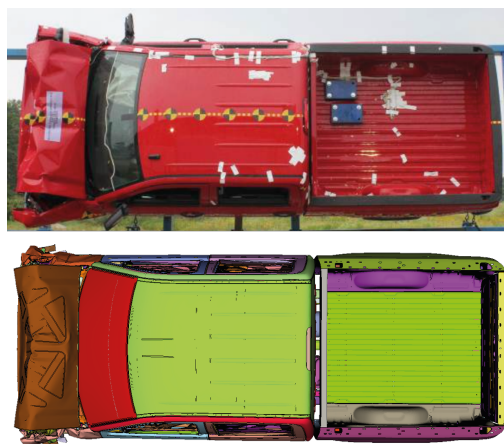


Figure 4.22: Silverado FWRB - top view comparison



Figure 4.23: Silverado FWRB - three quarters and underbody comparison

4.6 U Model

The last vehicle to be analysed, the U Model, was tested in a different manner compared to the previous three. One of the aims of the model was to complete successfully the European homologation test, which entails performing an ODB procedure at 56km/h . For this reason, a physical test was performed in the late design stages to correlate the simulation results with the production vehicle. The simulation was reproduced for this study in order to verify once again the findings. Apart for the different vehicle velocity, this simulation had the key difference of utilising an older model of the ODB barrier: as the study was completed before the release of the latest LSTC ODB models, a solid-solid formulation with shells only on the exterior skin was available at the time and was hence utilised.

Unfortunately, only a few pieces of information can be utilised for this work and they include two graphical representations, video footage and a number of cabin deformation and intrusion measurements.

As shown in Table 4.8, the great majority of the readings are representative of the physical model, especially with regards to deformations in the X direction, which all fall within 0 to 3mm and are the most relevant when analysing the level of intrusion. The same can be said for the Z direction, as all readings are within similar boundaries. On the other hand the y direction displacements show a slightly higher level of discrepancy, sign of a difference in the compression behaviour of the structure. An area that shows a greater level of discordance is that of the firewall, with almost 10mm difference for X and 4mm

for Z; in this area the intrusions are of considerable importance in the physical model and are partially underestimated by the model, mostly in terms of X.

With regards to the visual analysis, two frames are available for utilisation and are shown in Figure 4.25 . These have been analysed together with video footage of the impact, and several conclusions can be drawn:

- the deformation of the cabin in terms of upper part of A-pillar and roof is overestimated by the model. In the physical test the cabin does not deform in a visible way in this area;
- the deformation of the engine compartment is similar in terms of shape, but the extent of the crushed area is slightly underestimated by the model. The engine in the physical test moves rearwards by a visible length, while in the model this behaviour is less evident;
- the overall dynamic behaviour of the vehicle is well represented: the vehicle impacts the barrier, dives downwards and at the end of the crash starts rotating heavily in the clockwise direction. This is found to be true and accurately represented in the simulation, too;
- the front upper crash structures deform in the same way: they bend and push downwards on the top part of the barrier. The honeycomb core of the impactor is pushed outwards by these structures and a large part of it is therefore not utilised;
- the wheel backwards translation into the sill on the driver side is reproduced well, with the wheel deforming heavily and the sill absorbing the impact with little to no denting;
- the underbody area deforms in a comparable manner in terms of structural collapse.

In conclusion, although the model seems to represent well the intrusions in the cabin compartment, the analysis of the dynamic footage of the crash highlighted some points of discrepancy, such as the cabin deformation, which are not simulated entirely correctly. It was found that this could be due to an overestimation of the mass, which in the model reaches values north of 1900kg . Unfortunately, it was not possible to perform an analysis on the crash pulse to understand better the discrepancies caused by these structural and mass differences.

0:d3plot : IR30.1 AS per physical test -1 : STATE 23 ,TIME 1.09999999E-001

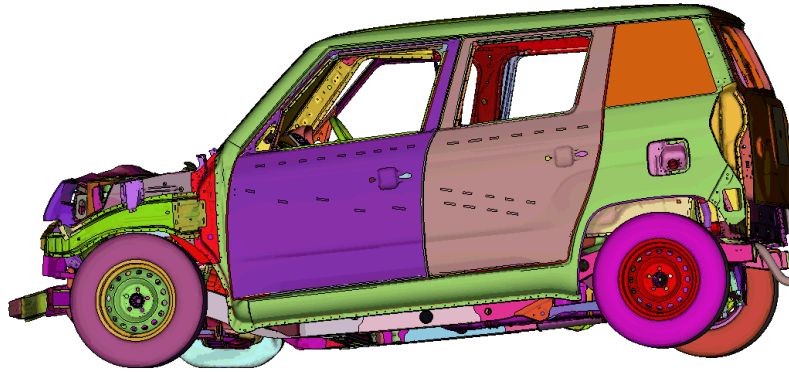


Figure 4.24: U Model ODB 56km/h - simulation snapshot

Table 4.8: U Model - ODB 56km/h intrusion measurements [2]

	Direction	Physical	CAE	Difference
Steering column	x	-1.1	-1.1	0
Right A-pillar base - top	x	1	0.5	0.5
	y	-5.7	-5	-0.7
	z	-0.9	1	-1.9
Right A-pillar base - lower	x	2.7	2.4	0.3
	y	-11	-4.8	-6.2
	z	0	1	-1
Left A-pillar base - top	x	1.4	-2	3.4
	y	-3.2	-12	8.8
	z	3.3	2	1.3
Left A-pillar base - lower	x	0.3	-0.3	0.6
	y	0.7	-10.5	11.2
	z	2.7	2	0.7
Firewall - driver side	x	48.2	40	8.2
	y	-3.6	-6	2.4
	z	26.7	23	3.7



Figure 4.25: U Model ODB 56km/h - RHS and underbody comparison

4.7 Conclusions

In conclusion, this section of the study has shown that two out of the four mathematical models under consideration are able to replicate the results of their physical counterparts very closely, while the other two show a certain level of discrepancy with respect to the real life crash tests.

In particular, the Toyota Yaris model showed to be representative both looking at crash pulse and deformations, while the visual analysis revealed positive results for the main structures and some differences in the modeling of thin surfaces. One area that remains unresolved is the low acceleration peak in the very early stages of the impact.

The Chevrolet Silverado model was the overall best in this comparison and showed that despite the simplifications in the modeling of engine compartment components and interior trim, the structural behaviour is very close to reality. Still, the crash pulse reveals that simplifications in the engine bay and a slightly different behaviour of the front structures

might have an effect on the peak locations. This however, should be verified by cross checking the acceleration data from the physical test with accelerometers placed in other rigid locations, in order to avoid a misinterpretation of the mathematical model's performance.

Talking about the models that did show a number of issues, a few of questions still have to be resolved regarding the Honda Accord model. The evident modeling flaws of the frontal structures and engine support have been fixed with a great effort in terms of working hours, but these did not give the expected results in terms of crash pulse. The high peak present at the beginning of the event remains, even though to a lesser extent. However, the intrusion measurements and the visual analysis showed positive results and the model will still be utilised as the core of this study is a comparison between the behaviour in two different tests, hence as long as the model stays the same, it can still be utilised and useful conclusions can be drawn. Nonetheless, It will have to be kept in mind that the seen results may not be highly representative of the physical vehicle.

Finally, the data available regarding the U Model demonstrates a satisfactory level of correlation, but with the lack of crash pulse data it is difficult to draw definitive conclusions. The ODB test correlation revealed that the intrusion measurements are very close, although the structure of the cabin visually behaves in a slightly different manner, with the A-pillar deforming and the roof collapsing. This does not occur in the full scale example tested, hence the model might need a level of refinement to be fully correlated. Unfortunately, it was out of the scope of this study to investigate such actions and carry them out. The U model will be utilised for the comparison as the major areas of interest are correctly represented, remembering that certain deformations might be overestimated in the simulation.

Chapter 5

Results

In this section, the results obtained from the simulations of the selected models on ODB and MPDB tests are presented. First, the models' structural performance is analysed in terms of the ODB test, to assess their strengths and weaknesses on the current Euro NCAP testing protocol. The fields under consideration are, similarly to the correlation study, the crash pulse, key deformation and intrusion measurements, and forces loading major structural areas. These are supported by an in-depth analysis of the visual side of the simulation, in order to understand the key phenomena driving the results. Next, the MPDB test is analysed with regards to the same aspects and finally a comparison between the two tests is completed. Additionally, a few interesting comparisons between different models are reported, in order to better understand the direction taken by the new protocol and the possible advantages and disadvantages for certain vehicle categories and chassis design methods.

5.1 Toyota Yaris

5.1.1 ODB test

The ODB 64km/h test showed that the Yaris, although having a compact frontal crumple zone, does in fact achieve a good level of performance, although with some cabin deformation.

As starting parameteres, the vehicle kerb weight, anticipated in Chapter 3, stands at 1050kg , to which the mass of the dummies and luggage must be added, together with the variation of fuel load to fill 90% of the fuel tank: the final test mass achieved was 1361kg . This equates to a total impact energy of 215kJ .

Crash pulse

First of all, let us analyse the acceleration, which, in combination with section forces and the dynamic visualisation of the impact, allows to understand the sequence of deformation of the structural components. In the initial 10ms the first acceleration peak of $20g$ is caused by the straightening of the cross beam and loading of the crash boxes, which do not deform axially but bend towards the centreline of the vehicle as the whole front structures

are also bending during barrier penetration, including the ones on the rhs. This appears to be due to the cross beam, which does not deform and in an attempt of transferring load between main rails pushes the whole front outwards. At this point, as the crash boxes do not perform any additional function, the crash structure is loaded and starts progressively bending inwards, keeping the acceleration low. During the same interval, a number of components in the engine bay start packing and pushing against the engine but the load on the engine support remains low. As the maximum peak of $44g$ is reached, the crash structure is loaded to its maximum capacity in bending and finally buckles together with its supporting section of the firewall and underbody rail. The engine support is subsequently loaded, but it does not detach from its mountings and does not impact with the firewall. At the same time, the barrier is completely punctured and the vehicle is now loading the rigid wall. In the further two acceleration spikes, the crash structures are completely ineffective, the sill and the outer underbody rails absorb the energy coming from the compact bulk of gearbox, wheel, suspension components and engine cradle, all in contact with the wall. The sill does not deform and slowly unloads as the impact energy dissipates.

Overall, the maximum acceleration reached in the test is quite high, with a peak of $44g$ and another two also around the $40g$ mark. This behaviour was however expected due to the limited size of the vehicle and its need to absorb as much energy as possible with only a limited front crumple zone.

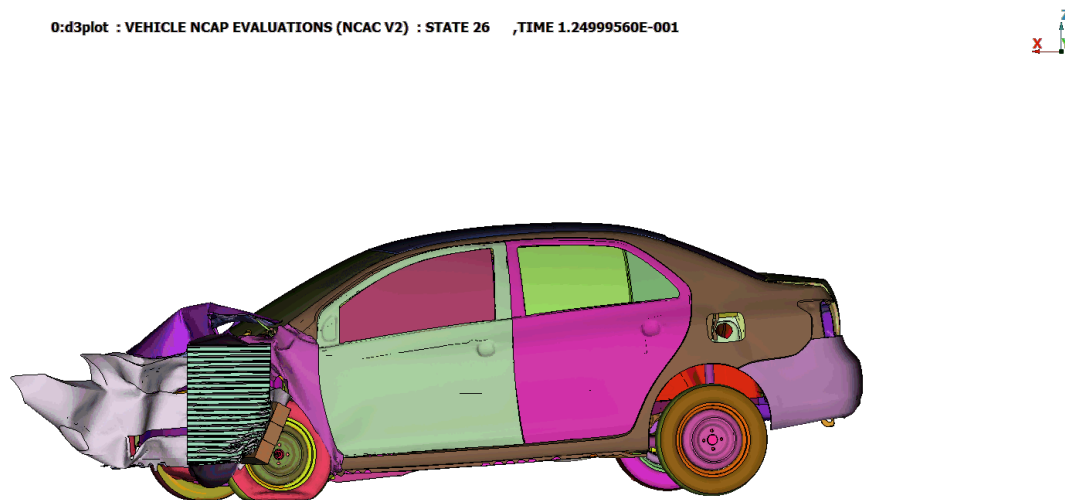


Figure 5.1: Toyota Yaris ODB - simulation snapshot



Figure 5.2: Toyota Yaris ODB - structural collapse detail

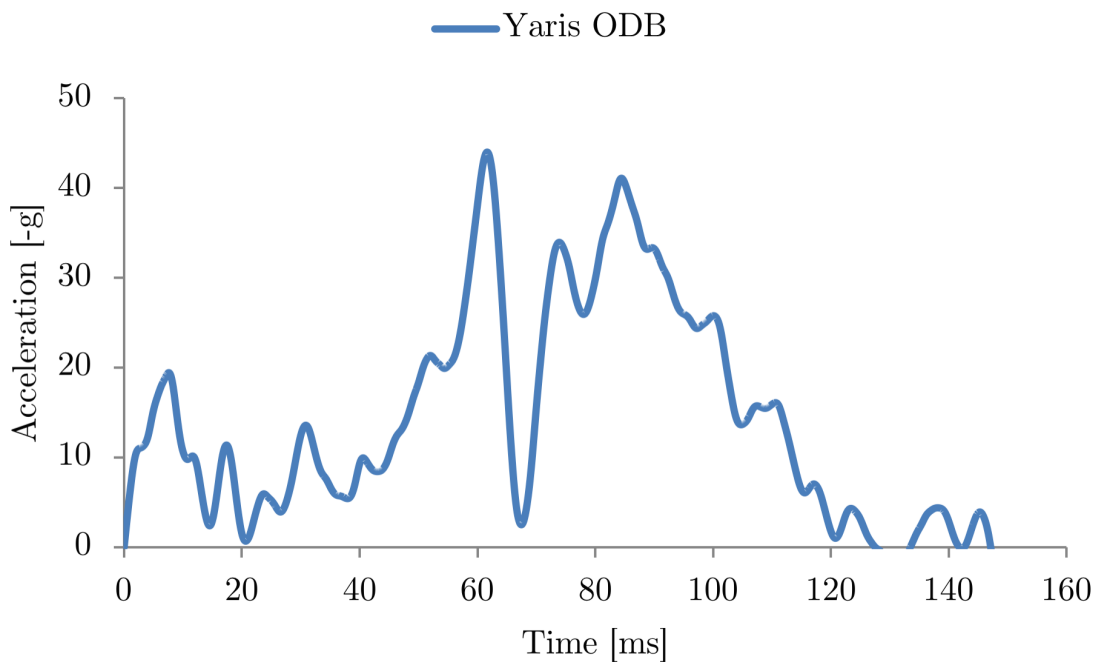


Figure 5.3: Toyota Yaris ODB - acceleration

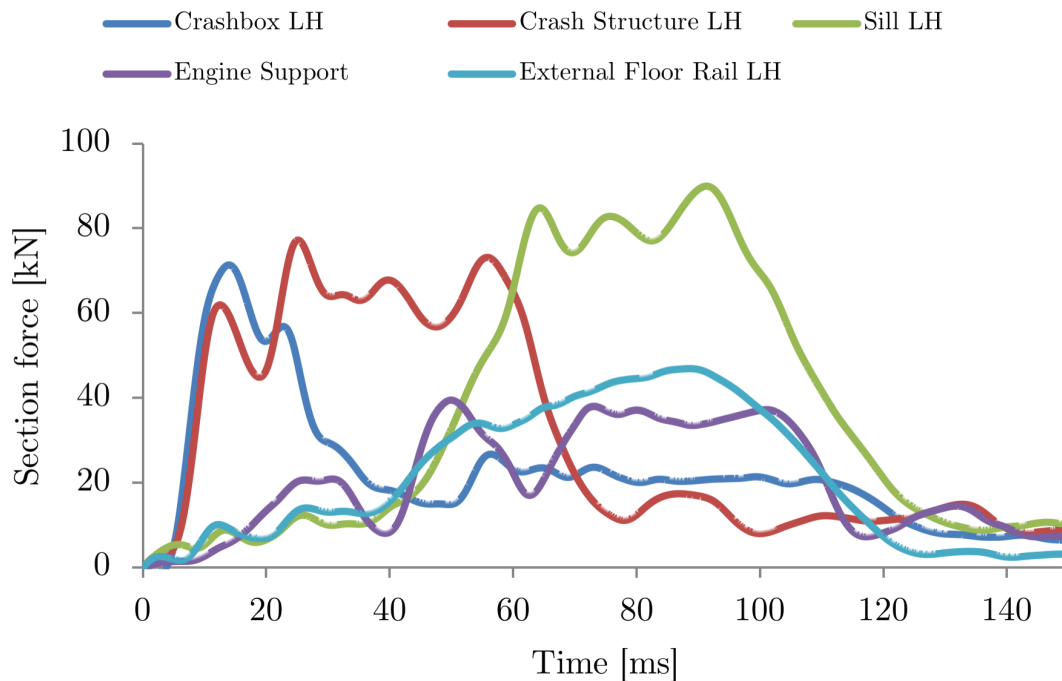


Figure 5.4: Toyota Yaris ODB - section forces

Cabin deformation

Looking at intrusion measurements, it is evident that although the vehicle performed well in Euro NCAP, the structure allows a level of intrusion in areas which do not impact heavily the loading on the ATDs. Note that all measurements given which do not have an explicit direction are taken along the X axis.

The two main areas that show high cabin deformation levels are the firewall and the A-pillar: these drive the subsequent intrusion of the other components listed in Table 5.12. Starting from the firewall, it is evident that the extensive deformation achieved is due to the positioning of the battery and brake booster: these rigid components are placed one in front of the other and during the maximum loading against the rigid barrier they are pushed against the firewall, which fails. As a result, the cross car beam deflects in its weakest spot, the centre point, and pushes the whole dashboard in the cabin. The deformation, however, interests mainly the central part and does not diminish to a large extent the space available for body deceleration. The steering column is also moved together with the dashboard and the firewall: its movement consists in rising, moving towards the passenger side and towards the driver at the same time. This measurement, however, does not include the collapsing of the steering column, which cannot occur in this simulation due to the absence of a test dummy loading the steering wheel.

The second important area of deformation, as stated above, is the lower base part of the A-pillar. Its deformation is driven by the compact mass of components crushed between the cabin and the rigid wall and by the effect of the wheel, pushing on the sill and deforming consequently the firewall. This, in turn, leads to a partial deformation of the

door, which is compressed and bends outwards, as demonstrated by the readings taken on the door opening width. Furthermore, the fixture point of the cross car beam, which is located in correspondence with the mid part of the A-pillar’s base, is pushed towards the driver, dragging with itself part of the instrument cluster. The extent of this phenomenon is, however, not substantial. With regards to the passenger side, no major deformation areas are present and the intrusion levels are near zero.

Additional areas worth noting are the floor and centre tunnel. The former is affected by the behaviour of the engine cradle and hence by the engine itself: when the vehicle loads the rigid wall completely, during the final stages of the impact, the cradle is loaded and does not detach from its mountings. These are fixed both to the inner and outer floor rails and to the sill. However, the weakest and most direct point of loading is represented by the inner rail, which is only supported by the floor. This leads to the rails moving backwards and deforming the floor area around it, as shown in Figure 5.9. On the other hand, the central tunnel is affected by the firewall deformation and also by the floor deformation just highlighted, resulting in its frontmost part crumbling.

Table 5.1: Toyota Yaris ODB - intrusion measurements

	Direction or Position	Intrusion [mm]
Steering column	x	29
	y	36
	z	19.5
A pillar	upper	6
	lower	32
Firewall	upper	118
	lower	49
Door opening width - driver side	upper	-14
	lower	-17
Door opening width - passenger side	upper	-3
	lower	-1
Cross car beam - fixture point	x	8
	y	14.4
	z	-0.1
Cross car beam - max deformation	x	37
	y	17.2
	z	9.5

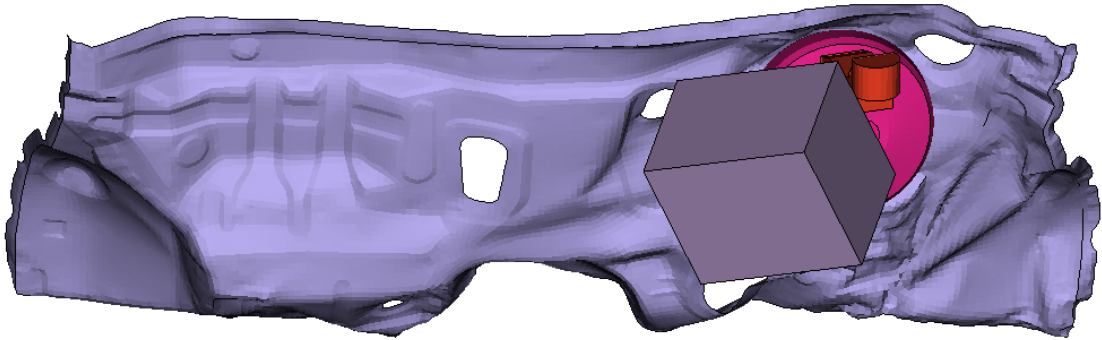


Figure 5.5: Toyota Yaris ODB - firewall intrusion

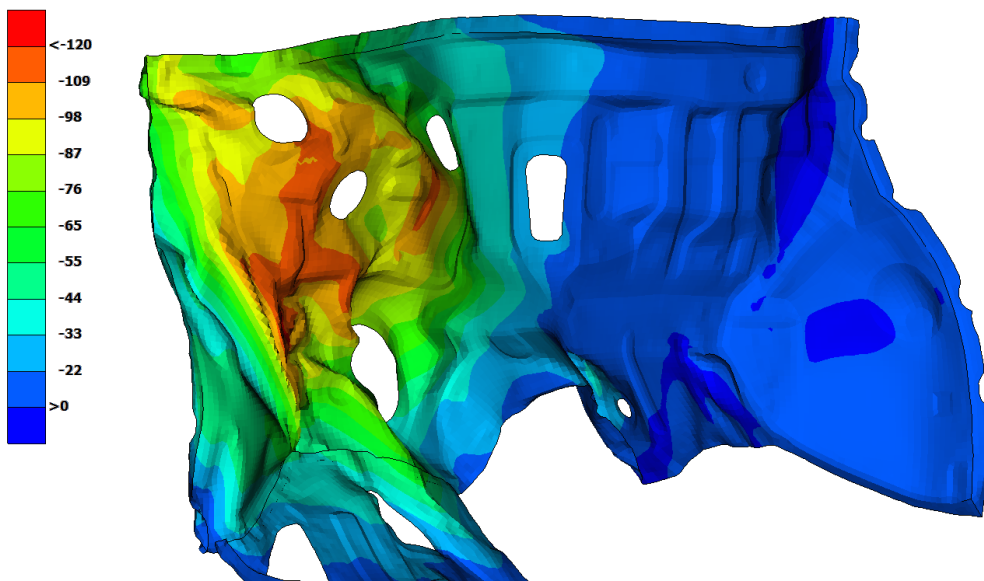


Figure 5.6: Toyota Yaris ODB - firewall deformed region

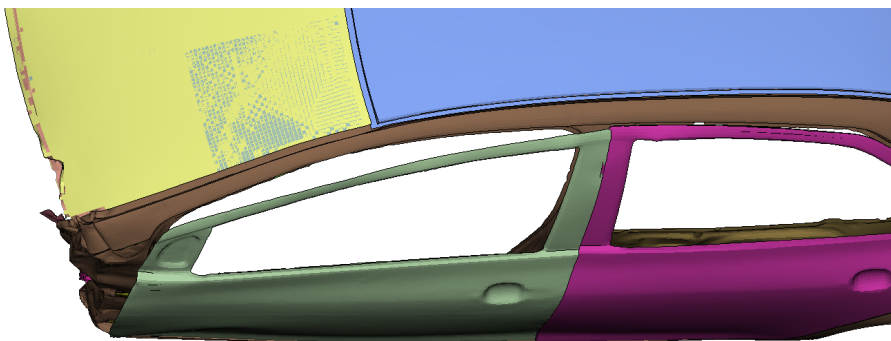


Figure 5.7: Toyota Yaris ODB - driver door opening deformation

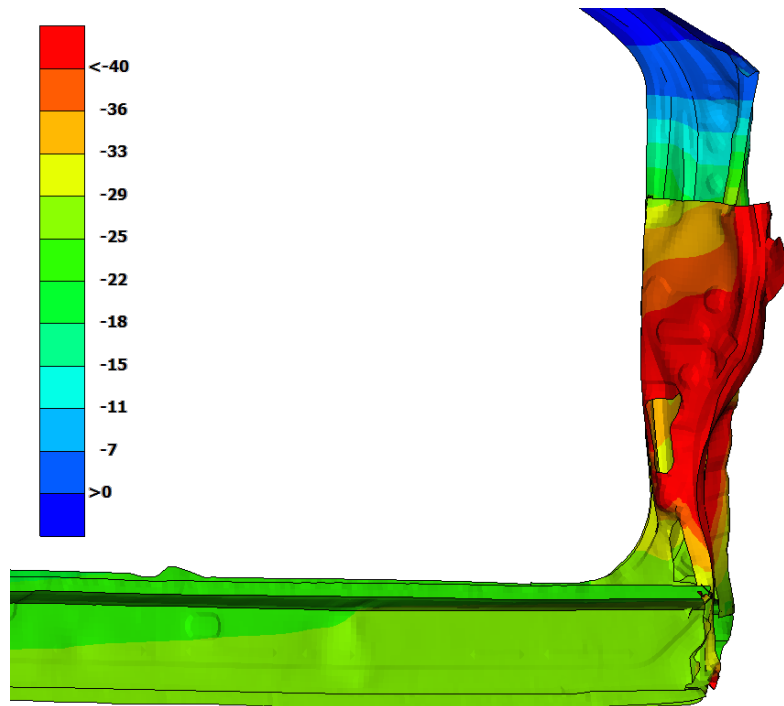


Figure 5.8: Toyota Yaris ODB - A-pillar deformation

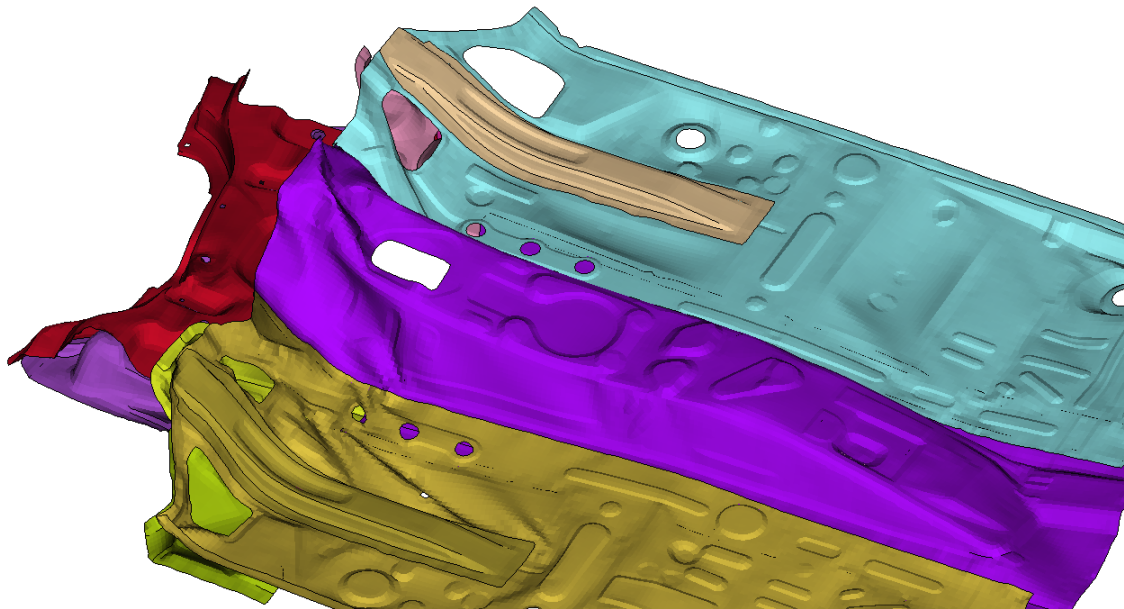


Figure 5.9: Toyota Yaris ODB - floor and tunnel deformation

5.1.2 MPDB test

As expected, the performance of the B-segment vehicle in the MPDB test was vastly different compared to ODB, as the Yaris shows major intrusions and an overall poor performance against the mobile barrier.

The test mass in this case was set at 1345kg due to the lower weight of the two front THOR test dummies; the mass of the barrier as tested (model provided by LSTC) was equal to 1452.9kg . This equates to an overall energy of 269kJ .

Crash pulse

Looking at the crash pulse, the first peak of $25g$ is caused by the initial impact with the mobile barrier, which results in straightening of the cross beam and immediate deformation of the upper components such as the bonnet and bonnet latch structure. In correspondence with the first dip, the simulation shows the failure of the left hand side crashbox, which then is loaded again with the second $10g$ peak and fails completely in the following dip. At this stage the radiator, headlights and air intake have all been crushed by the top part of the impactor, as the rail remains intact and is loaded by perforating the first layers of honeycomb and reaching the second, stiffer and progressive block. This behaviour is clearly visible in Figure 5.13, where the crash box section force reaches a peak and starts tapering down, while the load on the main rail continues its rise. The trend continues until the 25ms mark, where the rail fails axially near the firewall. In the following part the front structure cannot sustain any more force and collapses onto the firewall. Now, the vehicle has reached the third block of the MPDB. The behaviour of the main rail actually creates a problem for the cabin, as its front part buckles and maintains a straight position that allows high loading of the firewall. At the same time, the engine cradle, the engine, the battery, brake booster and all other components in the front compartment continue pushing on the firewall and A-pillar, which are able to sustain very limited load and immediately fail. The highest peak reached dissipates almost entirely through the cabin: the deformed front rail pushes heavily on the inner underbody rail and makes the entire structure fail. Also part of the energy goes through the sill, which does absorb a large portion of it with little deformation.

The main issue in this instance seems to be represented by the incorrect failure sequence of the front structure: the rail fails in a single spot, even if loaded mostly axially, which is too far into the engine compartment to be effective. Immediately after, the whole structure supporting it collapses, causing extensive cabin damage. It has to be noted that the behaviour of the supporting structures is hindered also by the engine cradle pushing on its mounts during the same instants.

Finally, the vehicle is pushed backwards at the end of the impact by the trolley, while the trolley continues to move forwards in its direction of movement, until it reaches rest.

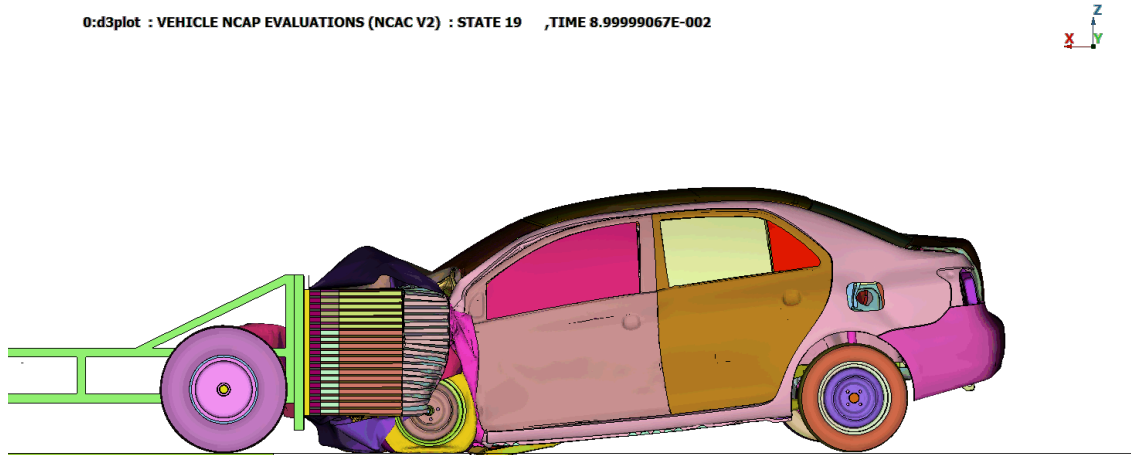


Figure 5.10: Toyota Yaris MPDB - simulation snapshot

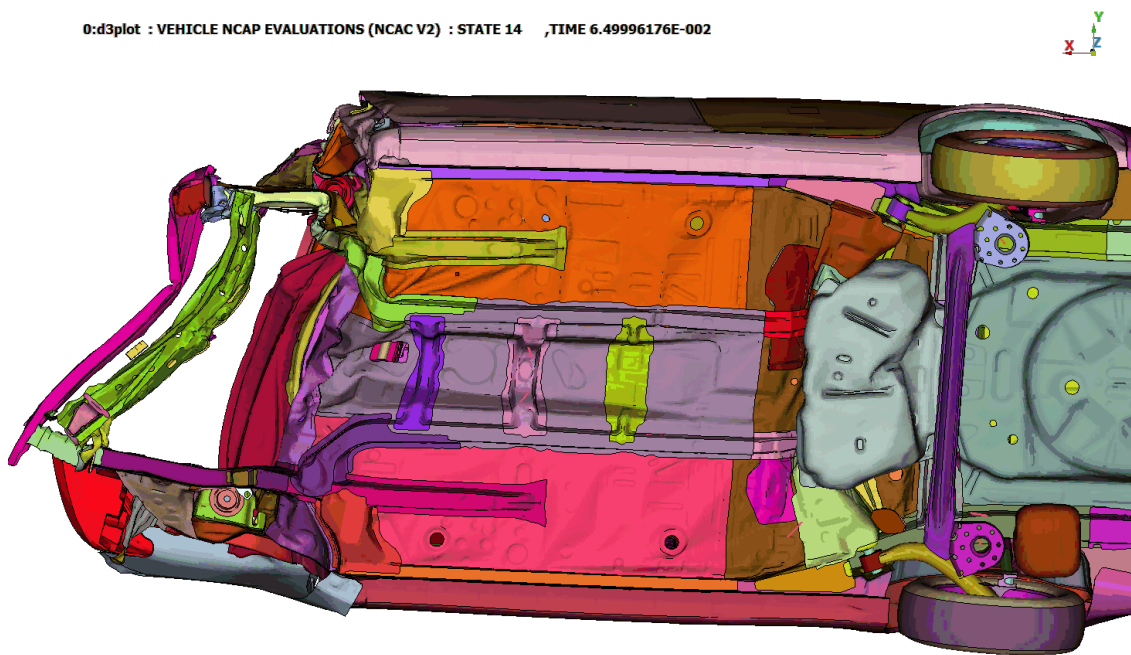


Figure 5.11: Toyota Yaris MPDB - structural collapse detail

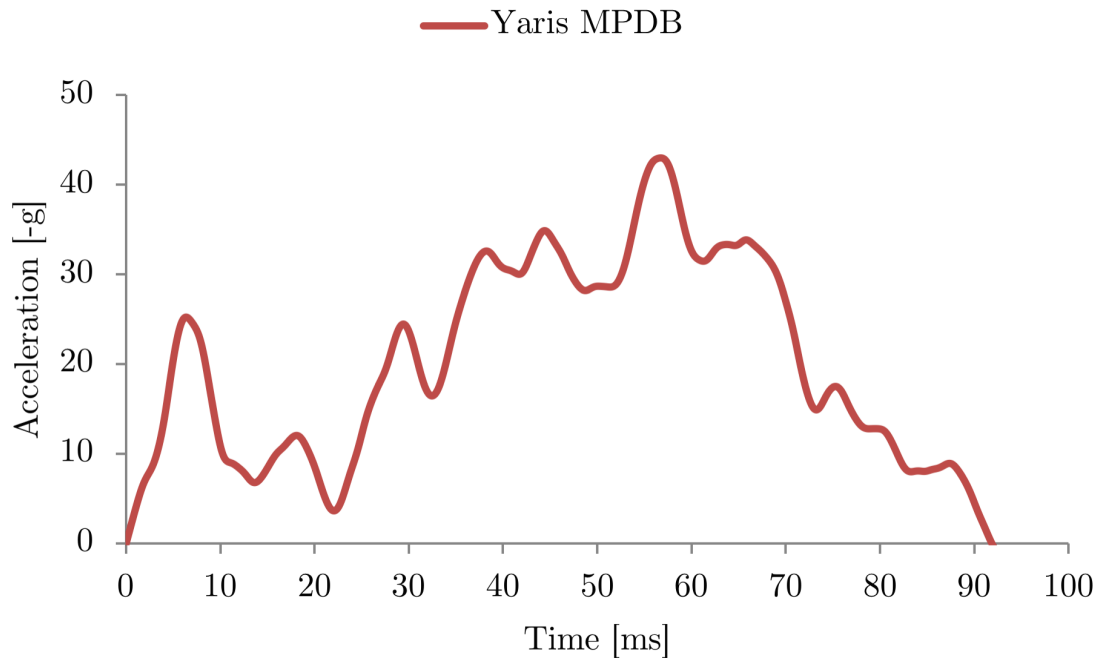


Figure 5.12: Toyota Yaris MPDB - acceleration

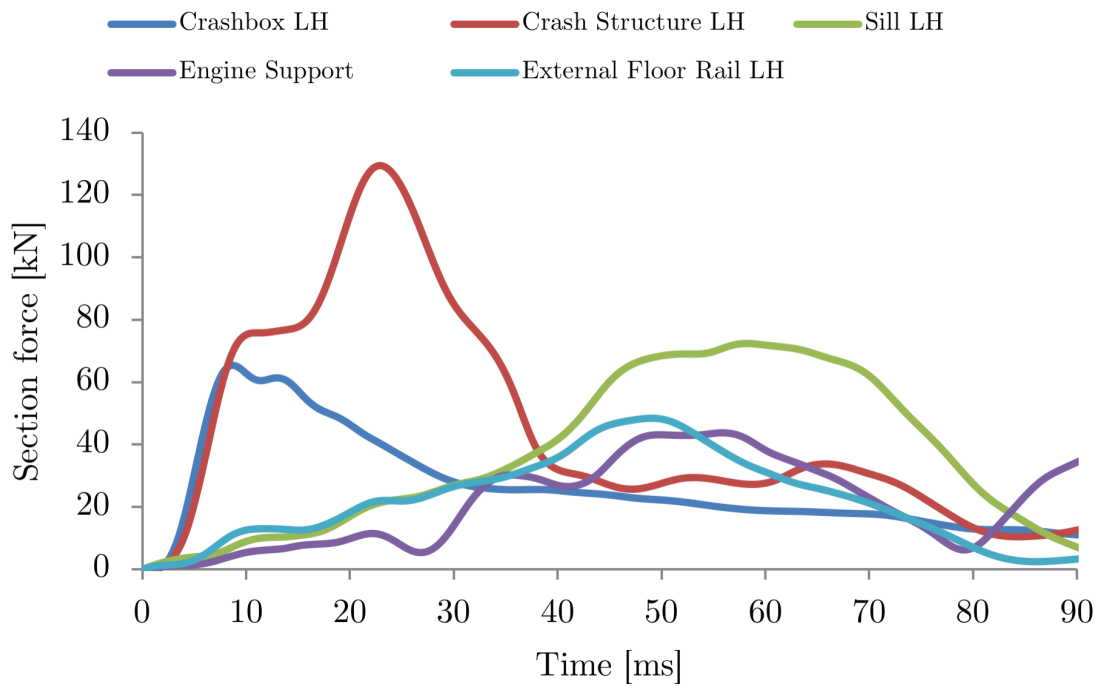


Figure 5.13: Toyota Yaris MPDB - section forces

Cabin deformation

Concerning cabin deformation, there are several criticalities to point out, as the intrusion levels are extremely high and the cabin stability is compromised. First of all, the firewall and A-pillar are still critical points, to which the windshield and floor are added as key areas.

As anticipated in the description of the crash pulse, the firewall area is compromised by the behaviour of the front crash structures and of the engine cradle, as well as by the positioning of the battery and brake booster. The area of highest damage is the upper section: the two components mentioned above are pushed by the barrier heavily into the firewall and bend it completely: in fact, by the end of the event the battery is for the most part inside the cabin, past the windshield, while the brake booster is directly pushing on the cross car beam. The brake master cylinder assembly also enters the cabin and the resulting level of intrusion is above $300mm$. This massive deformation drives the backwards movement of the cross car beam, of the whole dashboard and steering column, no space is left for the occupant that in such a crash would not survive. A considerable level of intrusion is achieved also on the passenger side, which sees the distance between the dashboard and the seat being shortened. Furthermore, as the barrier pushes forwards, the bonnet is also crushed onto the windscreen, which is not supported by its frame and gets shattered.

Considering the lower part of the footwell, the intrusion level reaches here a concerning $169mm$ of deformation: this is the location where the main rail is attached, hence the point where the barrier is pushing mostly towards the end of the impact. If the pedals were present, they would move backwards considerably and the room for the driver's legs would be almost non-existent.

With regards to the A-pillar, an X displacement of $36mm$ is found at the top of the base structure, which deforms together with the top of the firewall at the very end of the crash. At this moment, the cabin is absorbing more residual energy than it can take and it is possible to notice the onset of deformation of the upper section of the pillar, in correspondence with the top of the driver's door. The cross car beam fixture point is moved inwards by $45mm$, together with the pillar. The situation at the bottom end of the pillar is, however, much more critical. The wheel and barrier load this section together with the sill, which in this case shows to be failing in the frontmost part of the door opening. Resulting from this failure, the opening width for the driver door is reduced by $45mm$ in its lower part and by $24mm$ in its upper half. The passenger side shows a non negligible level of deformation as well, with a maximum of $10mm$ at H node height.

Finally, the floor area and the central tunnel undergo substantial levels of deformation, too. As depicted in Figure 5.16, the area corresponding to the outer and front inner underfloor rail crumbles, moving in -X direction by more than $60mm$. The deformation, however, is not only limited to this area: the whole driver side of the floor is damaged until the area of the rear seats, together with the central tunnel and, to a lesser extent, the floor under the passenger side of the cabin. This shows that the entire passenger compartment undergoes at least a slight level of deformation, up until the area corresponding with the fuel tank.

Table 5.2: Toyota Yaris MPDB - intrusion measurements

	Direction or Position	Intrusion [mm]
Steering column	x	110
	y	95.9
	z	68.8
A pillar	upper	36
	lower	92
Firewall	upper	301
	lower	169
Door opening width - driver side	upper	24
	lower	45
Door opening width - passenger side	upper	10
	lower	5
Cross car beam - fixture point	x	45
	y	-1.4
	z	-19.4
Cross car beam - max deformation	x	153
	y	21
	z	6.6

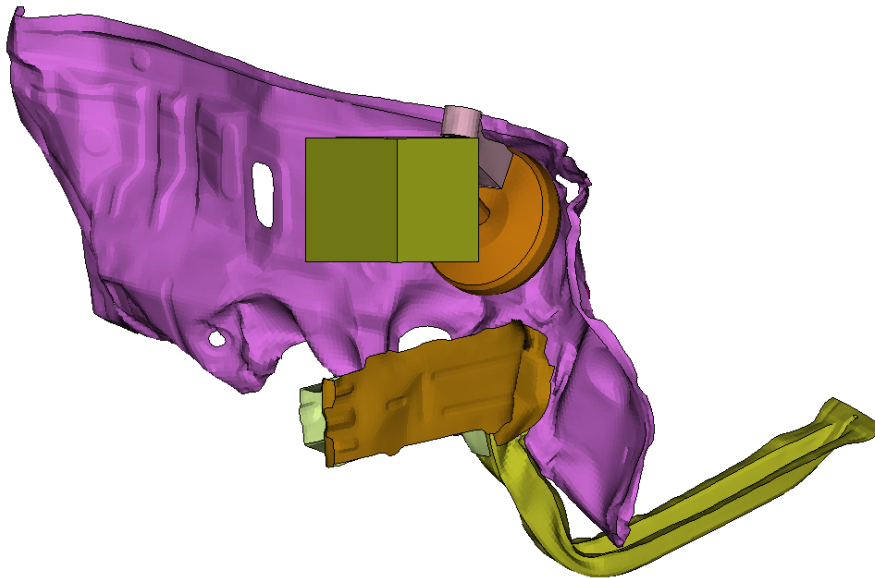


Figure 5.14: Toyota Yaris MPDB - firewall intrusion

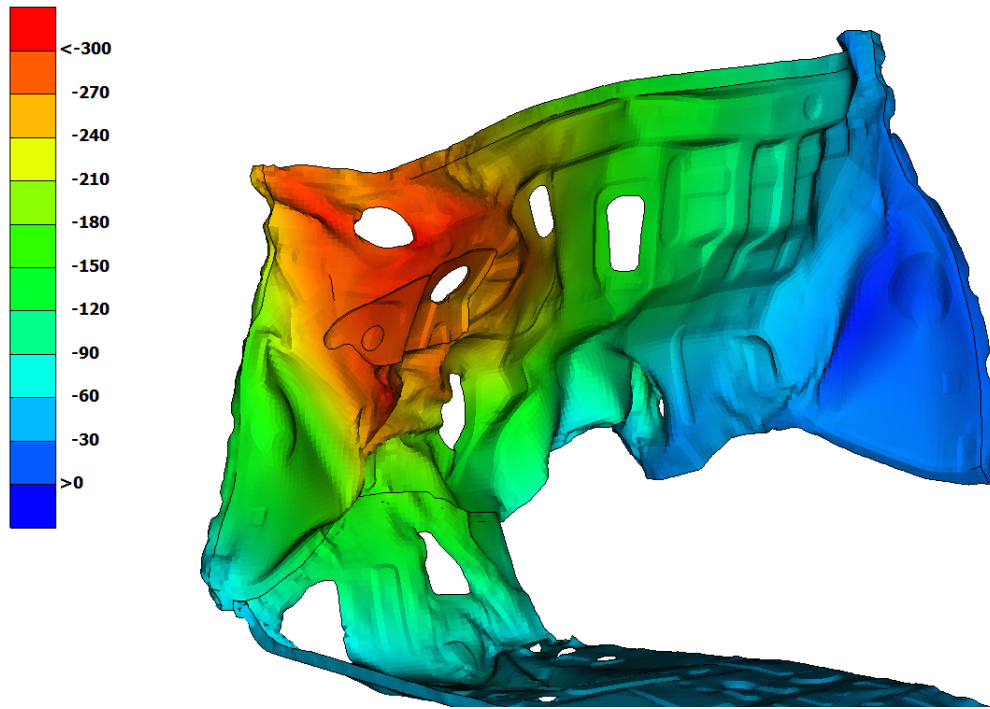


Figure 5.15: Toyota Yaris MPDB - firewall deformed region

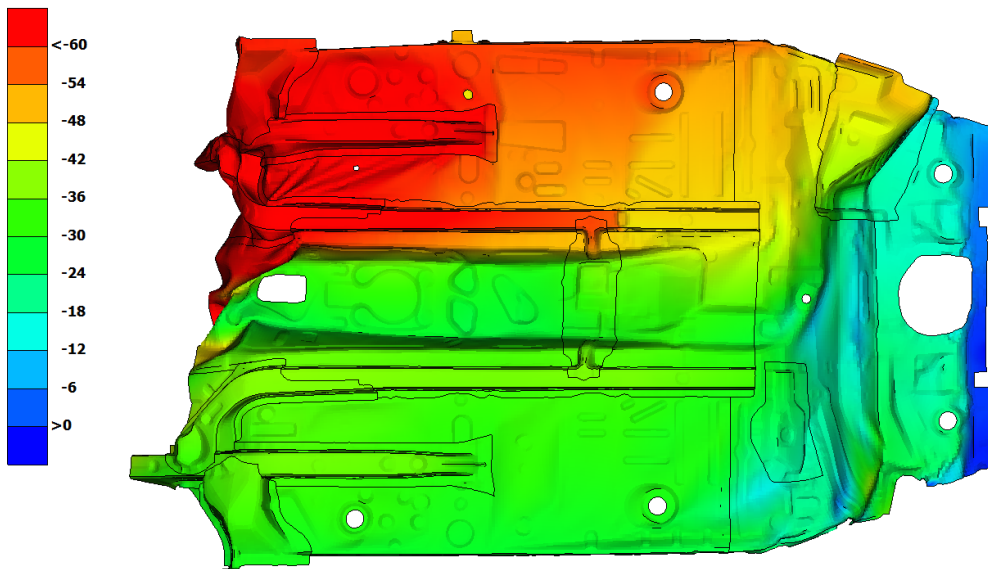


Figure 5.16: Toyota Yaris MPDB - floor and tunnel deformation

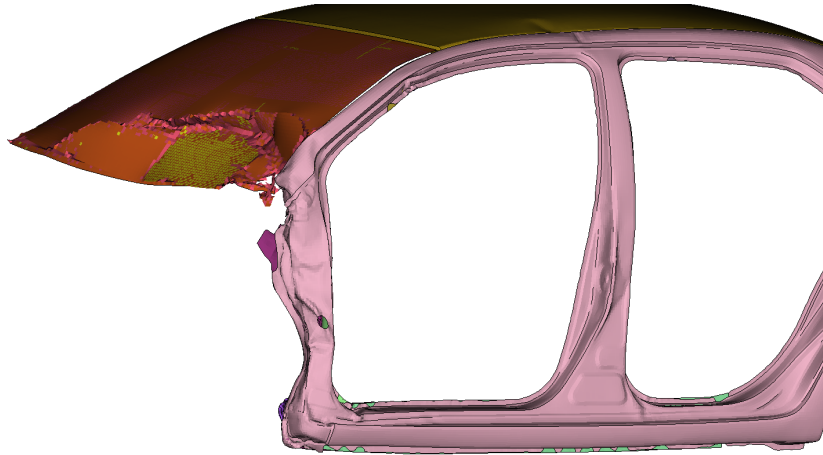
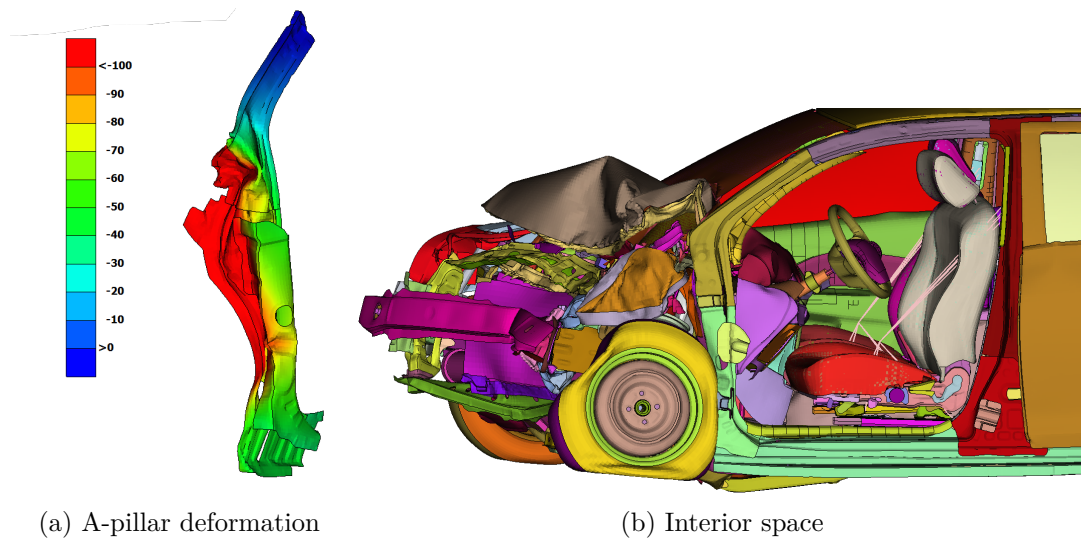


Figure 5.17: Toyota Yaris MPDB - driver door opening deformation



(a) A-pillar deformation

(b) Interior space

Figure 5.18: Toyota Yaris MPDB - deformed pillar and interior

5.1.3 Comparison

Energy content

Comparing the results from the two tests, the first consideration to make is in regard to the difference in energy between procedures. The ODB test total energy is roughly $215kJ$, while for the MPDB the level was at $265kJ$, resulting in a difference of $50kJ$ or around 19%. The energy of the impact is also dissipated much quicker in the MPDB, as shown in Figure 5.19: the current test takes between 100 and 110ms to reach stability, while this occurs in the new procedure in just 70-80ms. In these terms, it is possible to see how the MPDB is much harsher for a vehicle of this segment, even with non extreme weight deficit of around $100Kg$ compared to the impactor in test conditions - $1345Kg$ vs. $1452kg$.

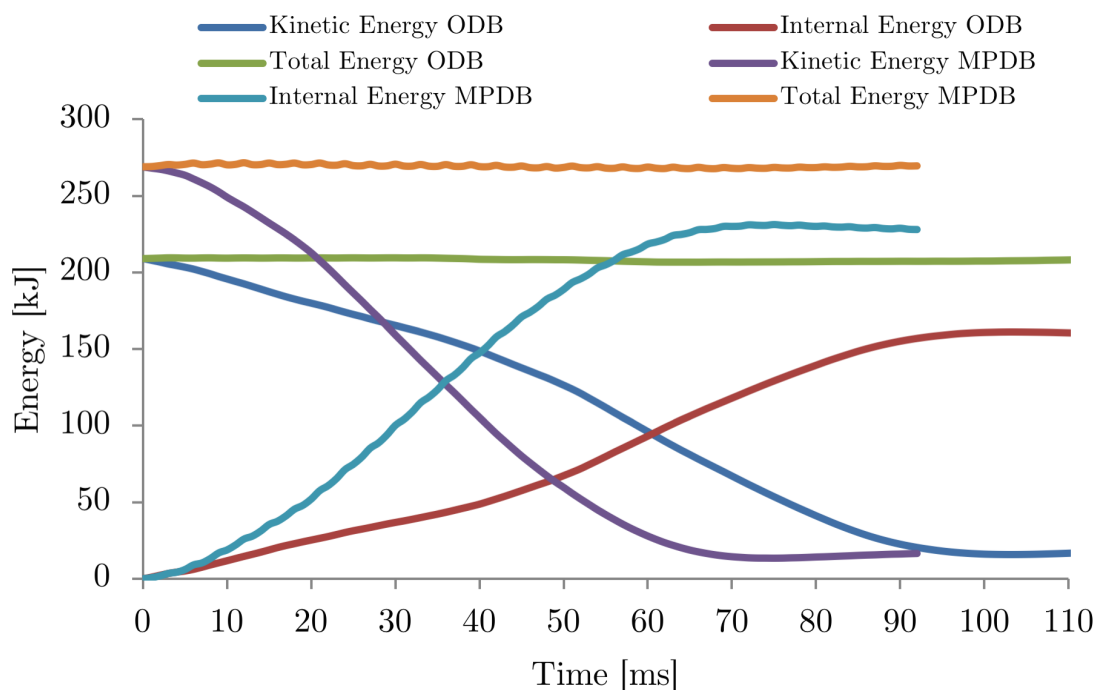


Figure 5.19: Toyota Yaris - comparison between ODB and MPDB energy content

Crash pulse

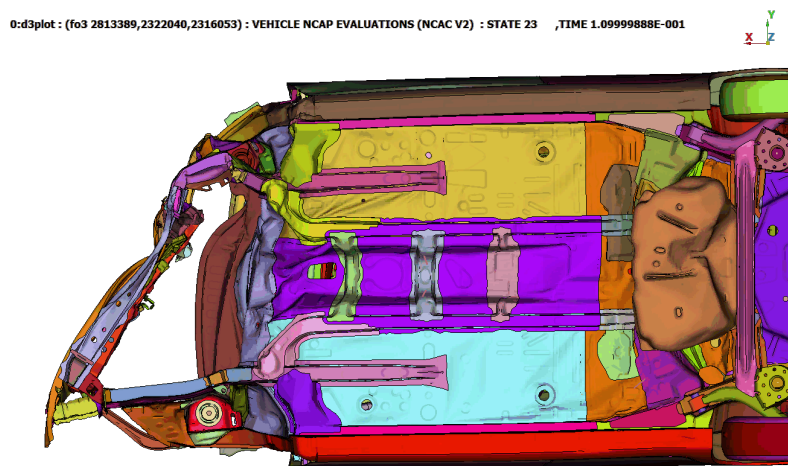
Looking at dynamic data, the first aspect to notice is that the peak acceleration is virtually identical between the two tests, with a maximum of $44g$ for ODB and $43g$ for MPDB. The peak occurs in both tests between 55 and $60ms$, with the difference that for the MPDB this corresponds with the end of the crash, while for ODB it is only at $2/3$ of the duration. A bigger difference is represented by the average acceleration which is around 20% higher in the mobile barrier offset test. This is confirmed by Figure 5.22: even though the two procedures have different starting velocity, it is possible to compare the overall change in velocity trend by analysing the slope of a line of best fit, which gives an idea of the difference in harshness. The inclination difference in this case is around 19%.

The main aspects to notice, however, are found when considering the crash pulse in its details. During the first $20ms$ the behaviour of the structures appears to be similar in terms of acceleration: in both the initial peak represents the straightening of the cross beam and the following failure of the crash box, although the ODB test seems more gentle as the peak corresponding to the initial barrier deformation stops at $20g$, against the $26g$ of MPDB. The similarities end here, at $20ms$ the mobile barrier loads the front structures much more heavily and drives the collapse of the main rails within $15ms$. On the other end, the soft core of the deformable barrier allows penetration of the main rail with a more gentle slope and the failure occurs only at $60ms$. It has to be noticed that the force direction on the crash structure is different between the two tests: in the current procedure it fails due to bending towards the centre line of the vehicle, while in MPDB the failure is due to axial loading. The early failure of the rail in the mobile barrier test also leads to

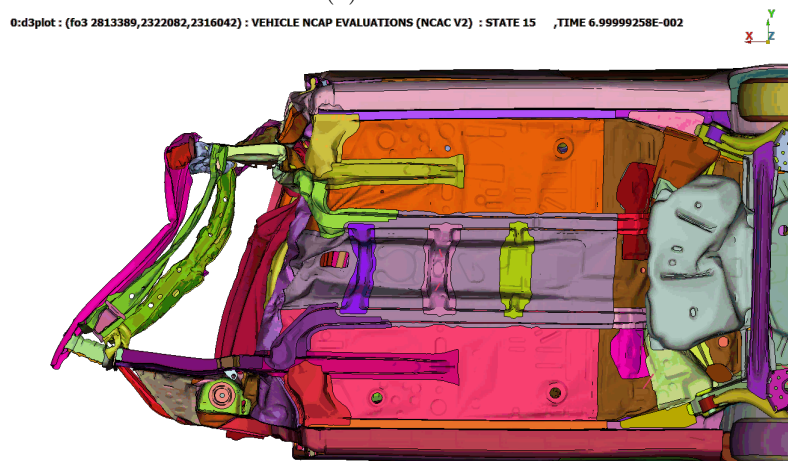
the maximum acceleration peak being reached with the front structures not being able to absorb any more energy, hence leading to higher level of deformation in other components, I.E. the cabin.

Table 5.3: Toyota Yaris - ODB vs MPDB dynamic data

	ODB	MPDB	Difference	% Difference
Peak acc. [$-g$]	44.01	43.01	1	2.26
Mean acc. [$-g$]	18.25	22.18	-3.93	-21.54
Time to zero velocity [s]	99.2	63.8	35.4	35.68



(a) ODB



(b) MPDB

Figure 5.20: Toyota Yaris - front structures behaviour comparison

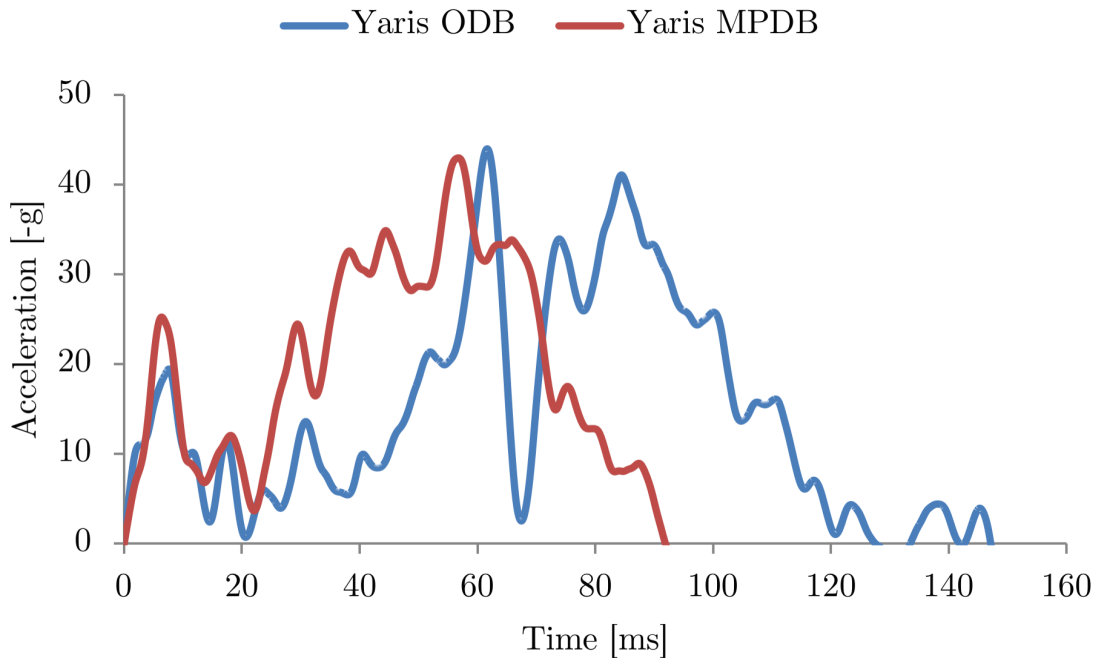


Figure 5.21: Toyota Yaris - crash pulse comparison

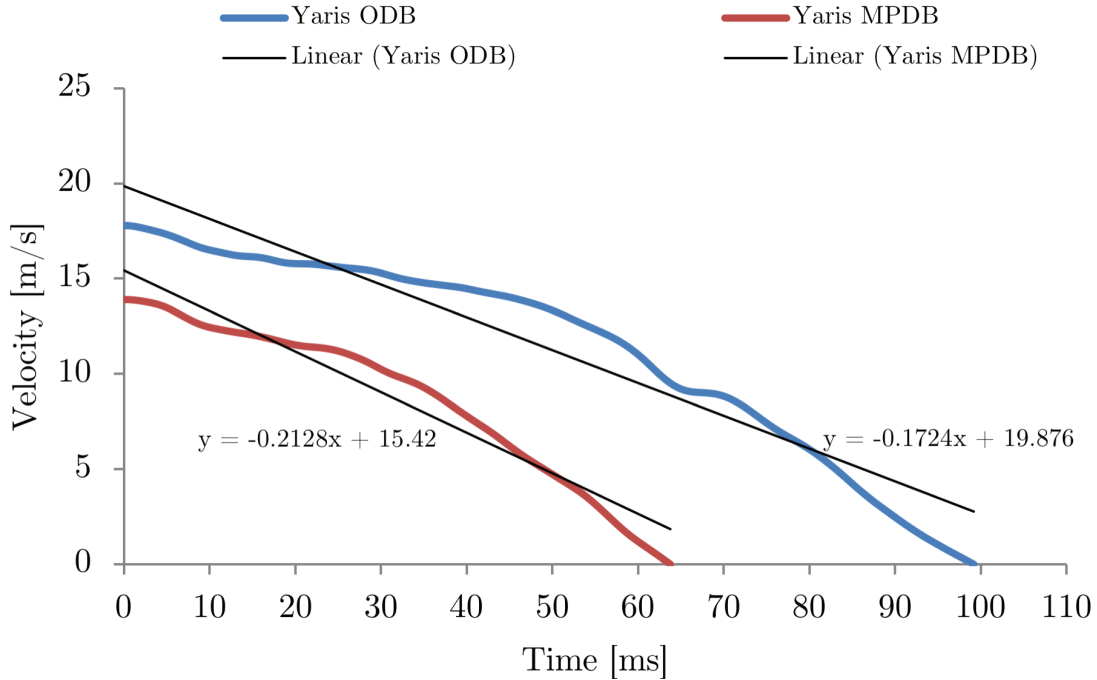


Figure 5.22: Toyota Yaris - velocity trend comparison

Section forces

In support to the statements made above regarding the failure of the structures of the Yaris, the section forces across the most relevant load paths are here compared. The crashbox, as shown in Figure 5.23a, fails in a similar manner in both tests, with the MPDB failure beginning at a slightly lower load due to a more axial direction of force. Regarding the main rails, Graph 5.23b makes absolutely evident that in ODB the box section is loaded in a different direction, as it supports a considerably lower amount of force and fails very gradually up to the point of clear rupture. The same element withstands a force almost twice as high in the MPDB and ruptures abruptly without oscillation, no more load is supported after the first failure.

Furthermore, it is possible to make considerations about the sill and underfloor rail: after the failure of the front rail, in the current test the load path through these two components continues to support a high amount of force with no deformation, dissipating the residual energy. In the mobile barrier test this occurs as well, as the sill and underfloor rail are loaded initially and support a relevant amount of energy. In this case however, the process occurs in a shorter timeframe and the different loading mode causes their failure.

Intrusions and cabin deformation

As anticipated in the previous sections, in terms of intrusions the Toyota Yaris achieves very different results in the two tests. As it is possible to see in Table 5.4, the MPDB procedure causes a much higher deformation in all fields. The most relevant areas of difference are, once again, those of the firewall and A-pillar, from which the other ones derive. From Figure 5.26 it is possible to see the very large deflection of the firewall in the mobile barrier test, which is not only limited to a spot of maximum but interests the whole driver side, while being much less extensive in spread and depth in the ODB. Figure 5.4 shows the resulting effects of this failure: the dashboard, steering wheel and instrument cluster that already show a level of movement in the current test are pushed against the driver heavily in MPDB. Also, front passenger side sees a considerable level of intrusion and a reduction of the survival space.

Furthermore, the A-pillar is pushed backwards five times more at the H node and three times more in its lower part, suffering also due to the failure of the sill. The higher part of the A-pillar, already showing some minimal damage in ODB, seems to fail more noticeably in the MPDB. In accordance with the rest of the structure, also the windscreen undergoes complete failure, while it shows no shattering in the former test. Moreover, an interesting aspect to remind is the extensive difference in floor deformation, showing how the whole front of the cabin is pushed backwards by mass of the barrier.

In conclusion, structure of the Toyota Yaris shows great shortcomings in terms of occupant protection, both for the driver and for the front passenger. The results are far worse than expected and a vehicle showing this level of performance would have to undergo important actions of redesign in order to obtain the same rating achieved in the ODB, after MPDB implementation in 2020. Even without having completed simulations with anthropometric devices, it is evident that the results would be highly concerning.

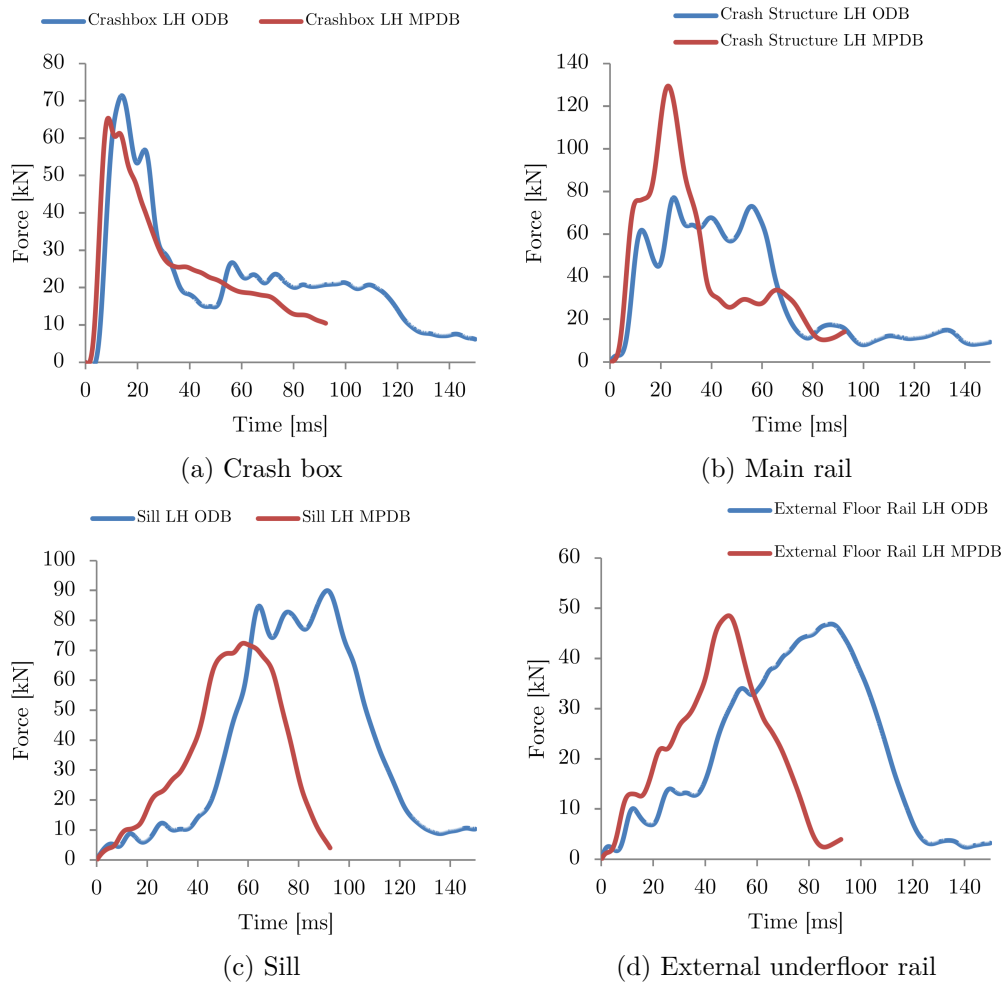


Figure 5.23: Toyota Yaris - section forces comparison

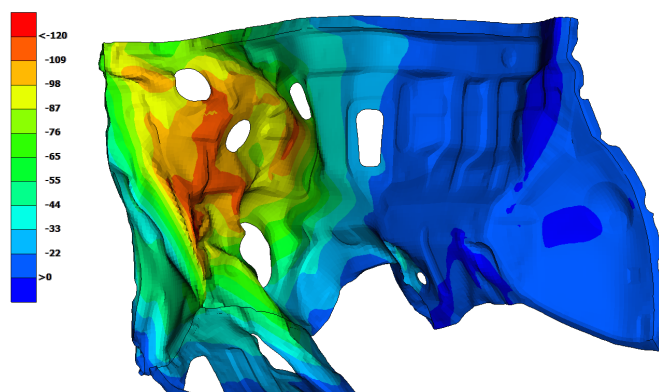


Figure 5.24: Toyota Yaris - ODB firewall deformation

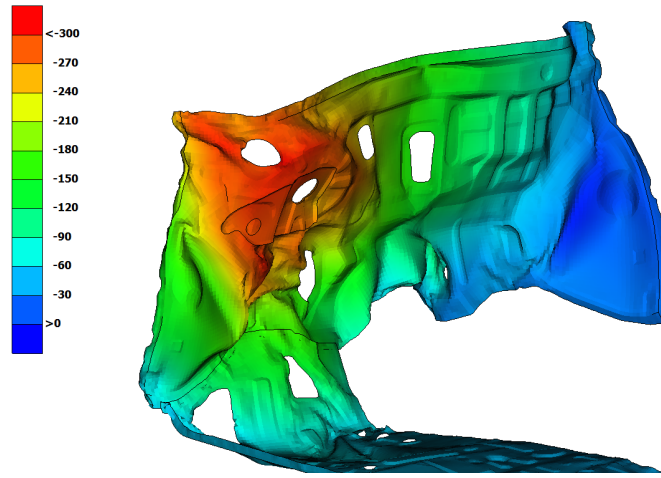
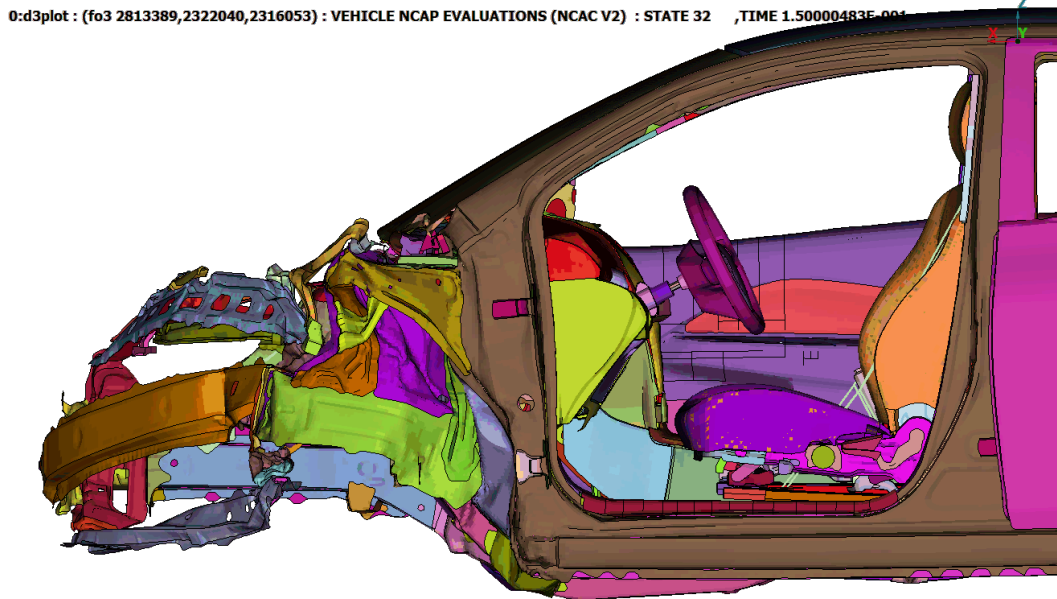


Figure 5.25: MPDB

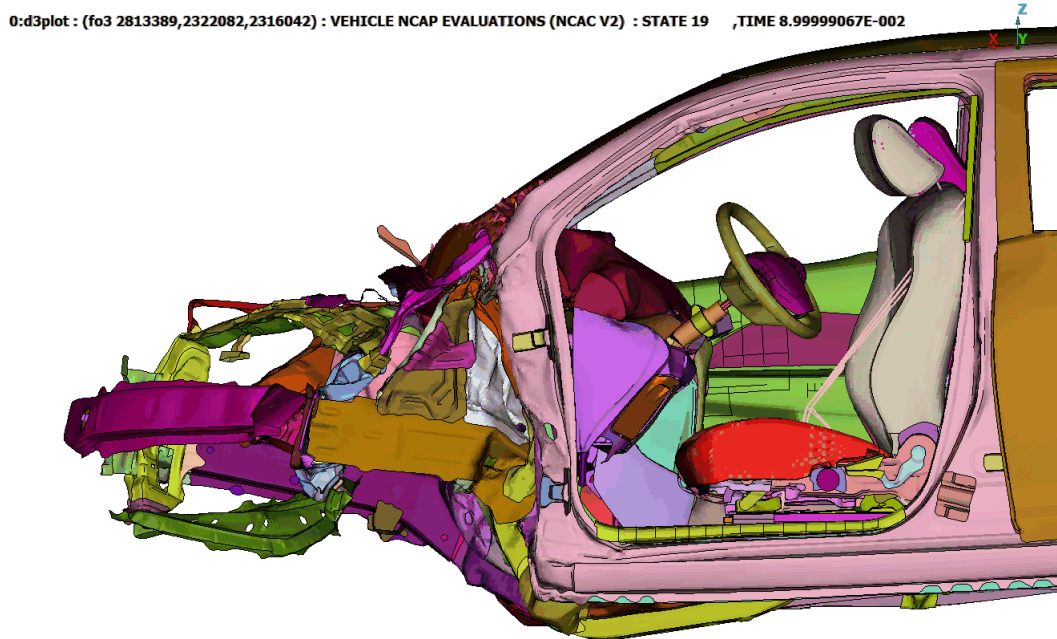
Figure 5.26: Toyota Yaris - MPDB firewall deformation

Table 5.4: Toyota Yaris - intrusion measurement comparison

	Direction or Position	ODB [mm]	MPDB [mm]	Difference [mm]
Steering column	x	29	110	81
	y	36	95.9	59.9
	z	19.5	68.8	49.3
A pillar	upper	6	36	30
	lower	32	92	60
Firewall	upper	118	301	183
	lower	49	169	120
Door opening width - driver side	upper	14	24	10
	lower	17	45	28
Door opening width - passenger side	upper	3	10	7
	lower	1	5	4
Cross car beam - fixture point	x	8	45	37
	y	14.4	-1.4	-15.8
	z	-0.1	-19.4	-19.2
Cross car beam - max deformation	x	37	153	116
	y	17.2	21	3.8
	z	9.5	6.6	-2.9

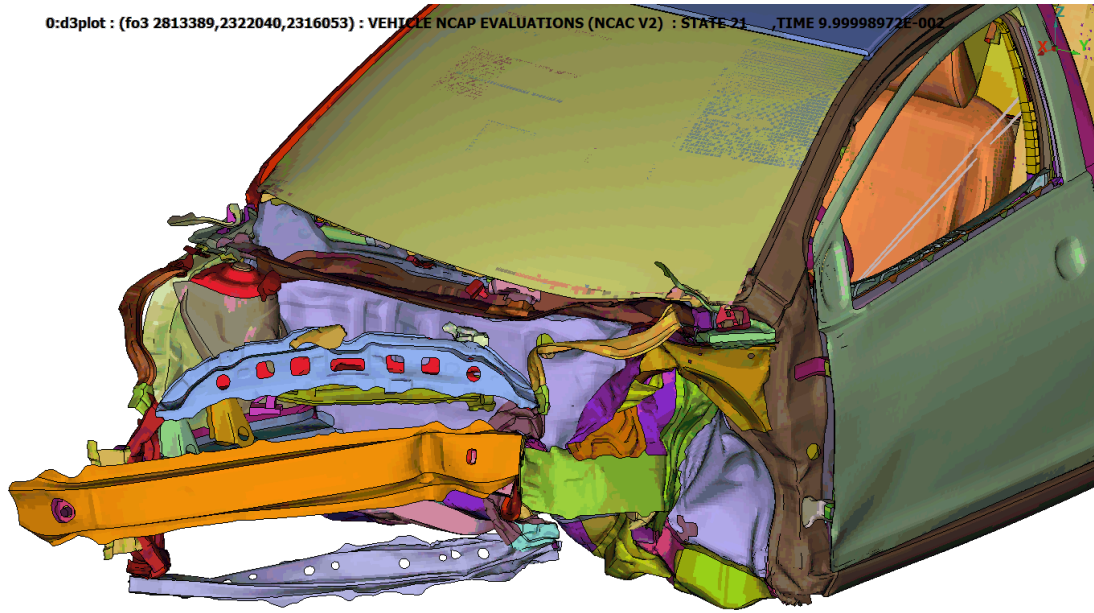


(a) ODB

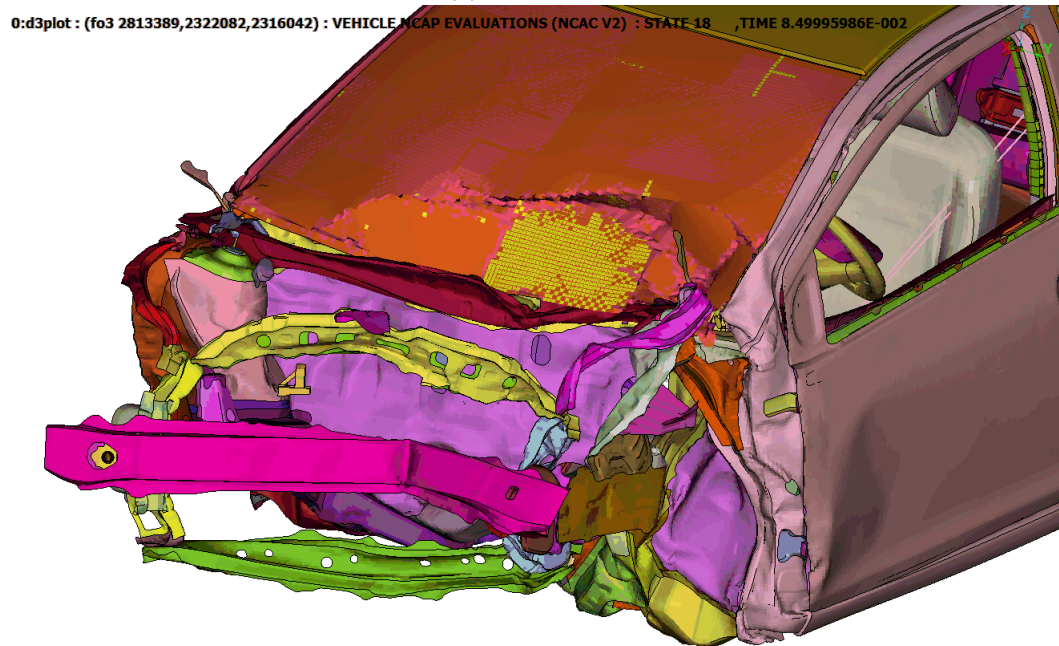


(b) MPDB

Figure 5.27: Toyota Yaris - interior intrusion comparison



(a) ODB



(b) MPDB

Figure 5.28: Toyota Yaris - front deformation comparison

5.2 Honda Accord

5.2.1 ODB test

The performance of the Honda Accord on the ODB test is in line with the expectations coming from the five star rating given by Euro NCAP. The occupant protection level in terms of intrusions is optimal and the front structures behave correctly. Unfortunately, due to the issues highlighted in the correlation study, it is hard to reach significant conclusions regarding the crash pulse, hence the analysis is limited to intrusions and visual phenomena. The mass of the model as tested, with all instrumentation and dummies, was $1570kg$, which translates into a total energy of $248kJ$.

Pulse and forces considerations

As stated above, it was not possible to analyse the crash pulse and section forces and reaching meaningful conclusions due to the unexpected high peak occurring in the first $4ms$ of the impact. As Figure 5.29 shows, there's little relation between the loading of the main structural components and this spike, as in the same timeframe the vehicle is only just coming in contact with the barrier. The rest of the pulse results compromised due to the high amount of energy dissipated in the first instants and shows maxima of $15-16g$ which are unrealistic. The only event happening in the initial hit with the barrier is a questionable backwards movement of the engine block, due to a definition issue of its mounts which was not resolved in the restricted timeframe of this project. It is however unlikely that just the movement of the block can cause a peak of $45g$ in $4ms$.

Furthermore, the force on the front part of the sill at the end of the crash is double compared to that experienced by the main rail, and this also seems unrelated to the dynamics shown in the simulation graphical representation: the front tire is pushed between the barrier and the sill but a force level of $100kN$ is unreasonably high, also due to the fact that there is still a considerable space available for the wheel at this point.

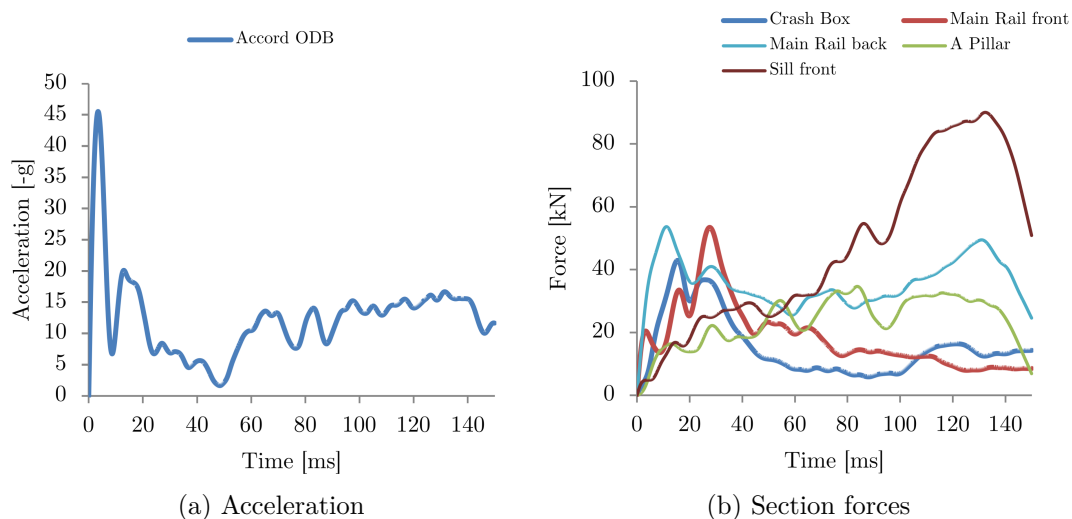


Figure 5.29: Honda Accord ODB- acceleration and section forces

Front structures behaviour

The frontal part of the Accord, as expected, works very differently compared to the Yaris, sharing the impact on multiple load paths thanks to the ACE layout. During the first $15ms$, the cross beam deforms and starts pushing on the crash box; at the same time, a level of controlled deformation is visible on the fixture point of the main rails on the firewall, hence the whole frontal section moves backwards without getting damaged. A portion of load is transmitted by the cross beam to the rhs main rail, as it is initially loaded and fails at the attachment point with the firewall. After this initial phenomenon, the crash box is loaded axially to its maximum strength and buckles almost perfectly. Consequently, the main rail is loaded again and shows the first failure: due to its variable cross section, the weakest point corresponds to the thinnest section, located slightly in front of the firewall. At the same time, the upper load path starts bending inwards. The following $20ms$ see the consequent collapse of the main rail in two other points, further towards the front of the vehicle, as the initial collapse does not make the structure bend, maintaining it straight and forward facing. The points of failure are again corresponding to the changes in cross section. The engine cradle is now reached by the barrier and its mountings fail, sliding the cradle backwards without damaging the floor of the cabin. When the room for motion has ran out, due to the engine hitting the firewall, the front part of the support is loaded as well and bends upwards.

At $60ms$, after further pushing on the barrier, the several failure points of the main rail make it bend out of shape completely - partly downwards and outwards, partly inwards; the upper structures fail bending downwards and the whole frontal part is at this point a flat and compact metal shield pushing on the remaining branches of box section.

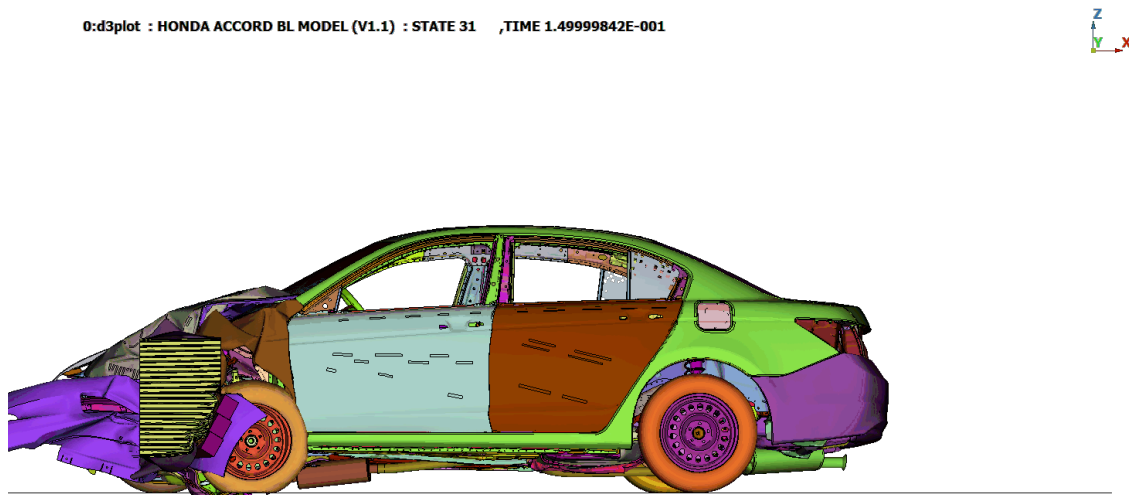


Figure 5.30: Honda Accord ODB - simulation snapshot

In the final stages of the crash, the shortening of the engine compartment causes the engine to push with more energy on the firewall, causing it to deform slightly in its top part. However, at this point the amount of energy left is not enough to cause major failures. Finally, the wheel, which has been pushed outwards during the event by the deformation of the upright mounting points, is squeezed between the barrier and the sill and the whole structure of the cabin lifts by a few tens of *mm*. One important factor to be noted is that the vehicle never punctures the barrier, but makes use of two thirds of the honeycomb's width compacting it evenly. The vehicle bumper, main structures and the bumper element of the barrier remain in line for most of the impact, pushing one on the other. Furthermore, at the end of the crash the upper structures still have a branch which has not been crushed, while the space in the engine compartment is reasonable. These two final considerations show that, overall, the ACE system seems to work properly both for occupant and for partner protection. This will be further emphasized by the level of intrusions explained in the next subsection and by the partner protection analysis in Chapter 6.



Figure 5.31: Honda Accord ODB - structural collapse detail

Intrusion measurements

With regards to intrusion levels, the Accord performs well as the deformations occurring do not substantially diminish the survival space inside the cabin. The only two measurements of intrusion which seem to be worth discussing are the deformation of the firewall and the movement of the steering wheel. Starting from the latter, it is noted that during the impact the lower joint of the steering column, placed in correspondence with the exit through the firewall towards the steering rack, fails due to the deformation of the rack itself. This stops the steering wheel being pushed towards the driver, but allows a certain degree of movement of the whole column in other directions. Therefore, under the acceleration of the impact, the column pivots around the cross car beam, changing by a few centimetres the positioning of the airbag.

The most relevant deformation, however, affects the firewall. The highest levels of intrusion are found in the top half of the metal sheet, where the main rail is supported and connected to its underfloor continuation. As highlighted in the previous section, the initial and unsubstantial denting occurs quite early in the event. The pushing continues for the entire duration of the crash, hence there's a slow and progressive deformation. Although the maximum reached is around 100mm , this does not compromise the space available for the driver or the movement of the cross car beam, hence it is supposed that the dashboard would not move substantially as well. The design of the cabin makes it so that the space between the beam and the firewall is generous, allowing the firewall's central parts to deform without pushing directly on other components. In addition, the point of attachment of the pedals does not correspond with the restricted area undergoing heavy deformation, therefore their movement is virtually null. Nonetheless, the behaviour here described should be verified by conducting a simulation on a model containing all the interior components to verify that what is here hypothesized occurs effectively. Considering the lower part of the firewall, corresponding to the footrest area, the intrusion level is very low, with the area of maximum being deformed by $10\text{-}12\text{mm}$. Moreover, it has to be noted that the passenger side of the firewall is also deformed due to the impact with the engine: the intrusion is located in the area behind the dashboard and reaches values of 50mm .

The last aspect to point out regards the windshield, which gets shattered by the impact with the bonnet. The sheet metal is pushed from the front backwards and the deformation achieved does not stop the latches from lifting and pushing it into the glass, causing an unwanted effect and some intrusion as well. It has to be noted that the dynamics of deformation of the latches appeared to be different from reality in the correlation study, hence this could be an issue caused by the model.

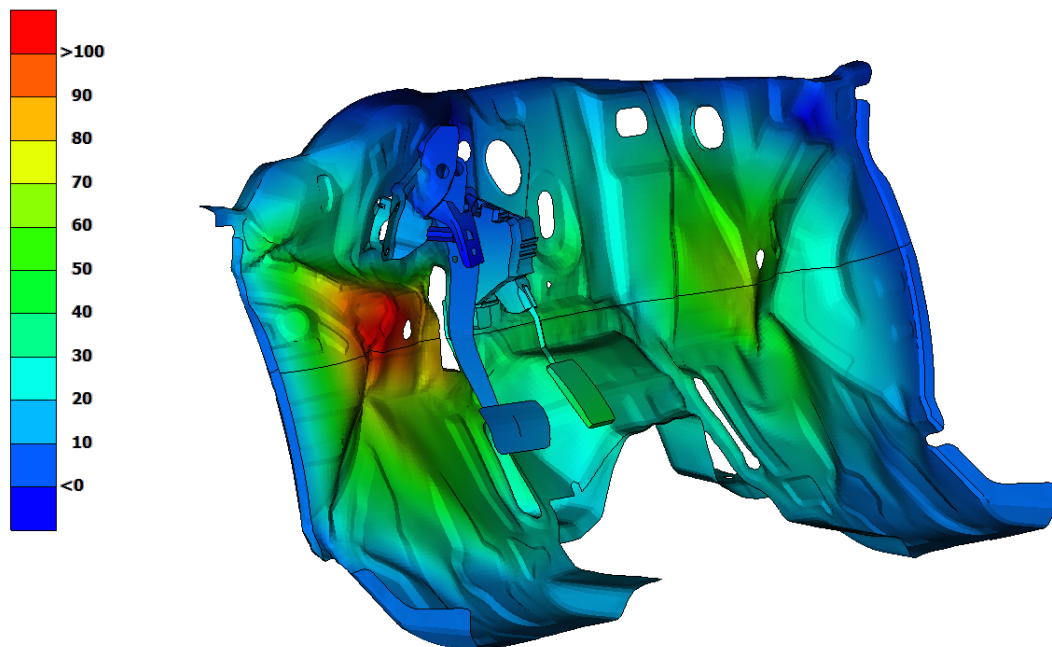


Figure 5.32: Honda Accord ODB - firewall deformation

Table 5.5: Honda Accord ODB - intrusion measurements

	Direction or Position	Intrusion [<i>mm</i>]
Steering column	x	-3
	y	13.3
	z	31.6
A pillar	upper	1
	lower	5
Firewall	upper	101
	lower	12
Door opening width - driver side	upper	4
	lower	3
Door opening width - passenger side	upper	1
	lower	0
Cross car beam - fixture point	x	1
	y	3
	z	-5.6
Cross car beam - max deformation	x	2
	y	2.7
	z	0.8

5.2.2 MPDB test

In the MPDB test the Accord also performs as expected, with slightly higher level of intrusion which still do not compromise its occupant protection to a large extent. In this case, as in the ODB, the crash pulse does not lead to meaningful conclusions hence it will not be considered. Regarding the total energy of the impact, the mass of $1554kg$ results in a value of $288kJ$.

Pulse and forces considerations

The resulting pulse from the impact with the mobile barrier still shows the initial high peak, this time reaching $30g$. The rest of the pulse shows peaks at the same level, but they cannot be reconnected to visible behaviours. The same considerations made for the ODB test are still valid in this instance as well, also regarding the section forces. The sill still shows unrealistically high loading, above $120kN$. The two graphs are shown in Figure 5.33 for reference.

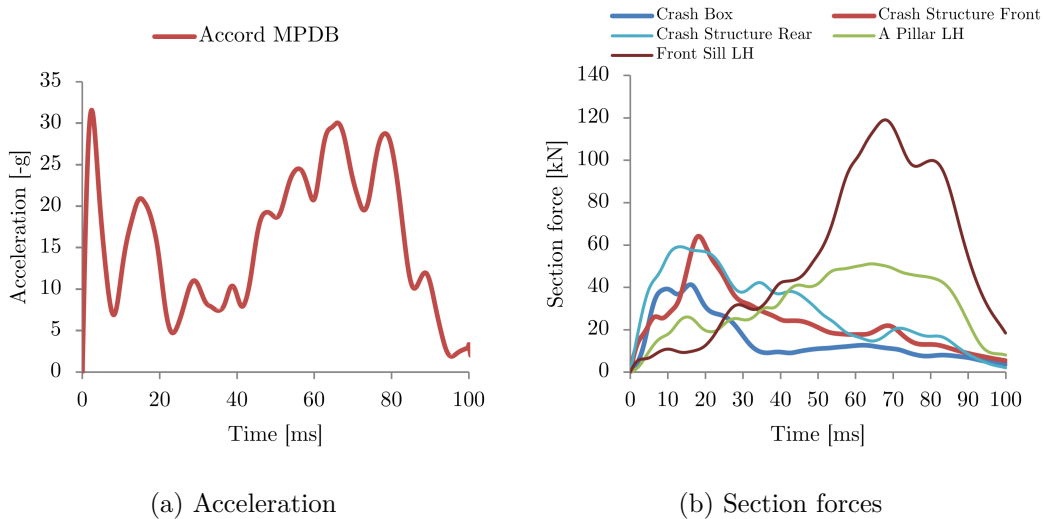


Figure 5.33: Honda Accord MPDB - acceleration and section forces

Front structures behaviour

Analysing the animation of the simulation, it is clear the the ACE design works quite well with the MPDB setup. At the moment of impact, the bumper immediately penetrates through the first core layer of the barrier, loading the cross beam and the crash box as well. The latter buckles axially in a fairly ideal way, as the vehicle reaches the initial part of the second core. It takes $15ms$ to get to this point, plus the initial $5ms$ of the two bodies travelling towards each other. In the next $5ms$, the main rail is loaded, the point of connection at the cabin pushes backwards the firewall and the box section fails in two separate points along its length, both of which correspond to the previously mentioned width changes. At the same time, the top load path is loaded and pushed backwards - without downwards deflection - by the top part of the barrier, hence making it work

appropriately. Next, among the failure of higher level components, the barrier hits the engine subframe, which detaches and bends upwards absorbing damage at the same time, showing how quickly the impact occurs in MPDB. In the final instants of the crash, the main rail continues to deform in the two initial failure points and shortens in an S shape, while the same behaviour seen in the ODB occurs for the front structures. In this section the level of force applied to the firewall is high, and the shield deforms substantially at the point of contact with the main rail. The compact face of metal that is created by the deformation of the frontal parts allows to utilise well the honeycomb of the PDB's second block, making the barrier absorb a substantial amount of energy. At the very end, the front honeycomb block comes in contact with the wheel and pushes it onto the sill, the tire deforms the barrier face and reaches the second layer just as the impact energy is completely dissipated. The loading on the base of the A-pillar is however considerable as the structure deforms when in contact with the rim, which gets squeezed in an oval shape. The face of the door sill also gets damaged in the process. The amount of space left in the engine compartment is very low in its top half, while towards the mid section, in correspondence with the main rail, it opens up leaving some room for engine and gearbox. This testifies how the upper section of the PDB does in fact have a considerable effect on the structures and a secondary load path to exploit this part of honeycomb is needed.

Intrusion measurements

The MPDB stresses the cabin of the Honda Accord in a substantial way, however the deformations remain within reasonable limits, with a few issues that would need to be resolved to reach top level performance.

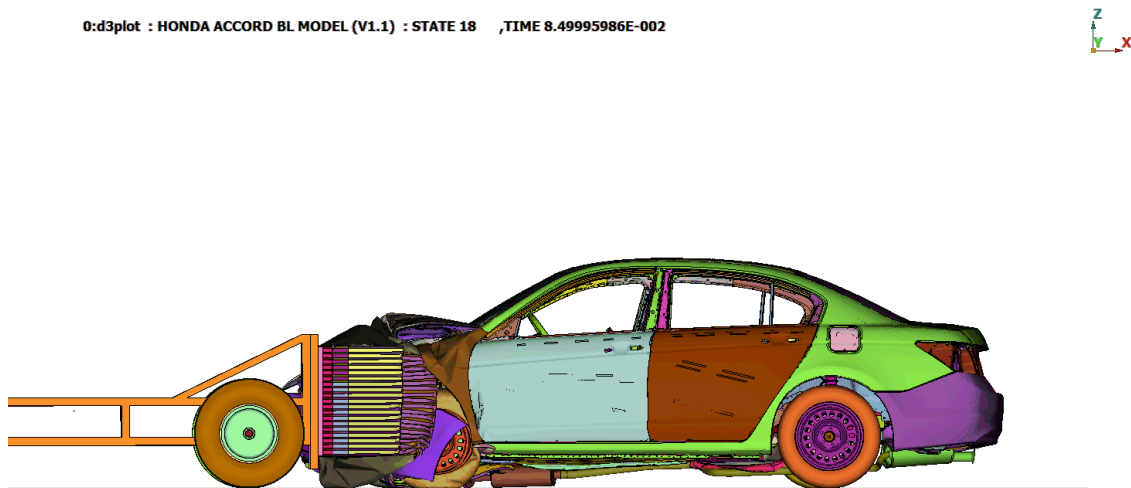


Figure 5.34: Honda Accord MPDB - simulation snapshot



Figure 5.35: Honda Accord MPDB - structural collapse detail

The areas of most interest are the firewall and the A-pillar, which undergo noticeable deformation. Considering the firewall, the area of highest deformation is again located in correspondence with the main rail attachment. As the crash occurs in a very low amount of time, the denting is quite abrupt and most of the deformation occurs in the final instants of the event. The area interested by deformations around 120mm is small and confined to the top part of the main rail's box section, as it is pushed upwards and backwards by the barrier. However, there is a vast area enclosing most of the mid section of the metal plate which gets pushed towards the occupants by $60\text{-}70\text{mm}$, including the locations where the pedals are fixed. As a consequence, the pedals too are moved backwards by 50mm for the brake and 80mm for the accelerator. The area of the lower footwell remains mostly undeformed, showing that the overall performance is not absolutely critical. Regarding the steering wheel, the joint at the bottom of the column fails in this instance as well, ensuring that the distance between driver and airbag remains unchanged.

The second area of interest, as stated at the beginning, is the A-pillar and mostly the bottom part of its base. The increased aggressiveness of the barrier pushes the wheel and rim with high force against the base of the pillar, which, as shown in Figure 5.37a, is dented in its lower part by more than 50mm . This is however of minor importance as the whole pillar does not move backwards by the same amount: the front face takes most of the deformation without collapsing. The whole pillar, however, moves by a more modest 20mm , which is enough to cause the cross beam to shift by the same amount in $-X$ direction. The door opening width is also diminished and the door itself is damaged, bending outwards and creating a gap between the top part of the A-pillar and the window frame. Furthermore, the windscreen gets damaged by the bonnet, with consequent intrusion of the part in the cabin by a considerable amount, as shown in Figure 5.37b.

Table 5.6: Honda Accord MPDB - intrusion measurements

	Direction or Position	Intrusion [mm]
Steering column	x	9
	y	5.3
	z	14.1
A pillar	upper	20
	lower	26
Firewall	upper	117
	lower	41
Door opening width - driver side	upper	19
	lower	14
Door opening width - passenger side	upper	4
	lower	1
Cross car beam - fixture point	x	22
	y	3.7
	z	-2.7
Cross car beam - max deformation	x	21
	y	3.9
	z	-16.4

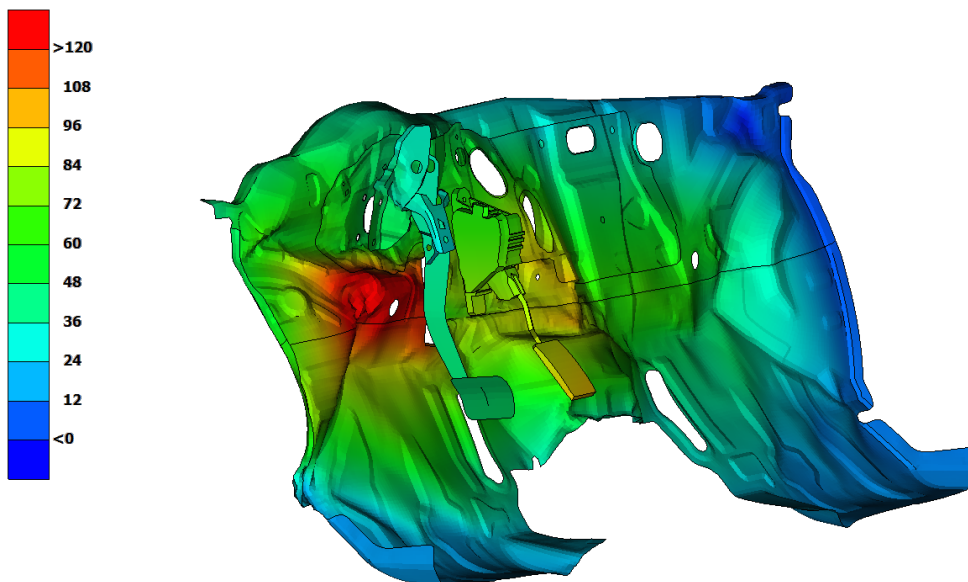


Figure 5.36: Honda Accord MPDB - firewall deformation

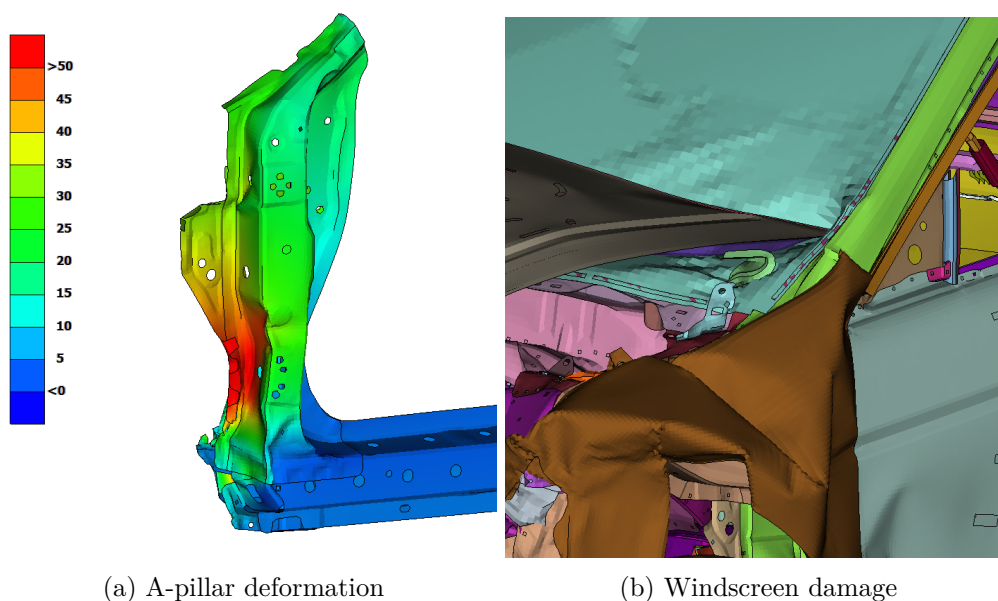


Figure 5.37: Honda Accord MPDB - A pillar and windscreen deformation

5.2.3 Comparison

Overall, the performance of the vehicle appears to be comparable in the two tests, mainly due to the mass of the vehicle and the advanced frontal structures that this model already uses. However, the MPDB still seems to be harsher on the structure in terms of deformation depth and spread. In fact, although the mass of the vehicle in test conditions is higher than that of the barrier, the energy of the mobile barrier crash is still higher, with a difference of roughly 14%. The new test is also much harsher in terms of duration, as the impact is over in $85ms$ while the ODB lasts for more than $140ms$.

In terms of how the sequence and way in which the structure deforms, the two tests show extremely similar results, with both ODB and MPDB following the same trends, as explained in the previous two sections. The main issue from this side is the rate at which the deformations occur and the slightly higher amount of energy to be dissipated in the crash. As shown in Figure 5.42, both crash boxes, main load path and second load path have similar failure modes: the crash box axially, the main rail by failing in the two weakest points and deforming into an S shape, and the higher load path by being sequentially deformed downwards. In both instances, at the end of the crash the deformed parts form a compact face that pushes on the barrier and the wheel is squeezed between the barrier and the sill.

Intrusion and cabin deformation

The noticeable differences appear when looking at the intrusions, the key areas affected by the mobile barrier are the firewall and A-pillar. Starting from the former, from the data shown in Table 5.11 it might seem that the difference is not substantial, and in terms of maximum deformation it actually is not critical: the highest value achieved differs only by

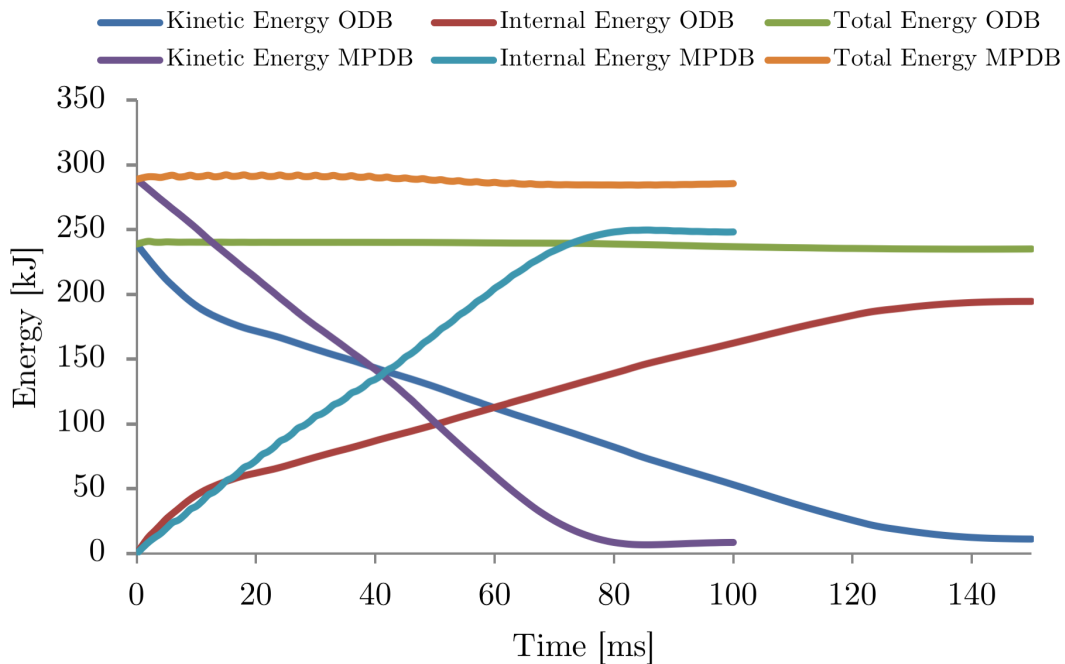


Figure 5.38: Honda Accord - energy content comparison

16mm out of over 100mm. However, the key difference is made clear by the representations in Figures 5.39 and 5.41, where it is evident that the spread of the denting is completely different. In ODB the interested area is limited to the contact point with the main rail and, to a lower extent, to a few spots where the engine comes into contact. The pedals are not at all affected by the impact and so is the lower footwell section. In MPDB, on the other hand, the area is much wider both laterally and vertically, as the engine pushes on this structure in a much more evident way. The maximum remains located where the crash structure is supported and highlights that the added energy content does cause higher intrusion. Furthermore, the pedal fixtures move by around 60mm and the accelerator pedal plate, due to the length and inclination of the arm, increases this value to 80-85mm. The trend here explained is testified also by the value of maximum footwell deformation which is now more than triple, increasing from 12 to 41mm.

Considering the A-pillar, the deformation has less of an impact compared to that of the firewall. In ODB, the deformation of this section is absolutely negligible, as there are no external forces exerted on it apart for the support of the top load path, which is not stiff enough to cause any deformation. Moreover, the rim and tire do not push on it due to the fact that the whole cabin lifts on top of them, causing only minor denting in the sill. In MPDB, on the other hand, the wheel gets trapped between the barrier and the pillar, causing the peak of deformation shown in Table 5.11. The overall displacement of the pillar is much lower than the highest value shown, but it still causes the cross car beam to move and the door opening to be reduced by 15mm. Finally, the windscreen gets shattered in both tests, with slightly more intrusion by the bonnet in the mobile barrier procedure.

In conclusion, the ACE structure performs very well in the new procedure, ensuring a high level of occupant protection and also a reasonable level of partner protection, as will be discussed in the next chapter. The deformations here reported would need to be addressed if the MPDB test was to be undertaken, but an adjustment to the strength of the rail's connection with the firewall using internal reinforcements should be enough to reduce the maximum deformation area. At the same time, a slightly stiffer crash structure could ensure that the energy carried by the engine onto the firewall is diminished to the point where deformation returns at the levels of the ODB test. The effect of such countermeasures would have to be checked with a model that is able to produce a significant crash pulse, in order to verify that the acceleration levels do not reach unsafe levels.

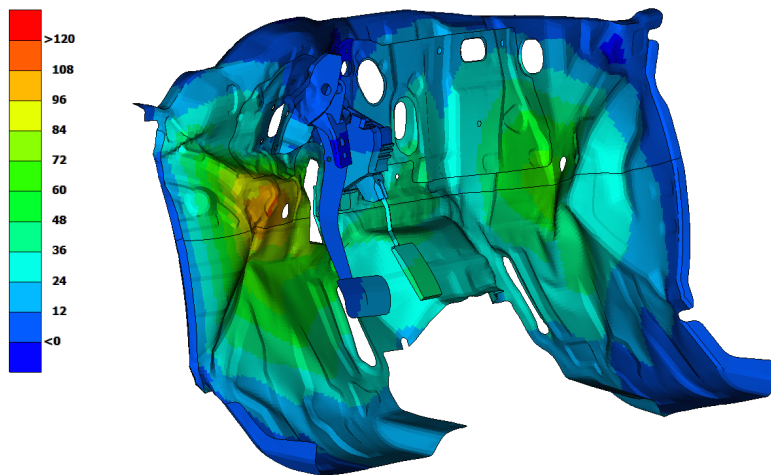


Figure 5.39: Honda Accord - ODB firewall deformation

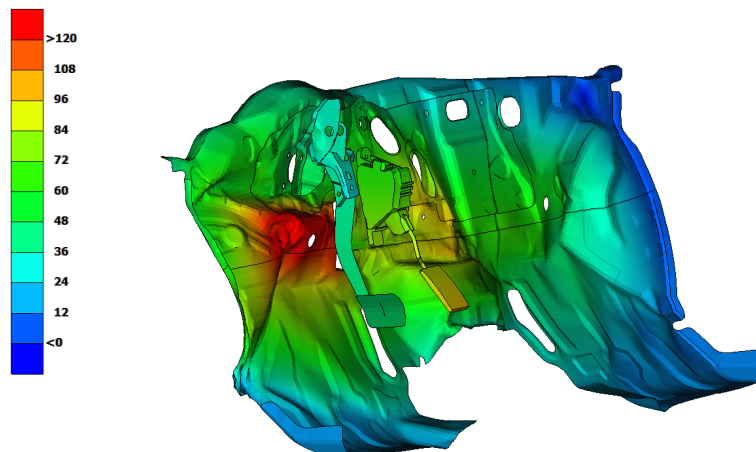
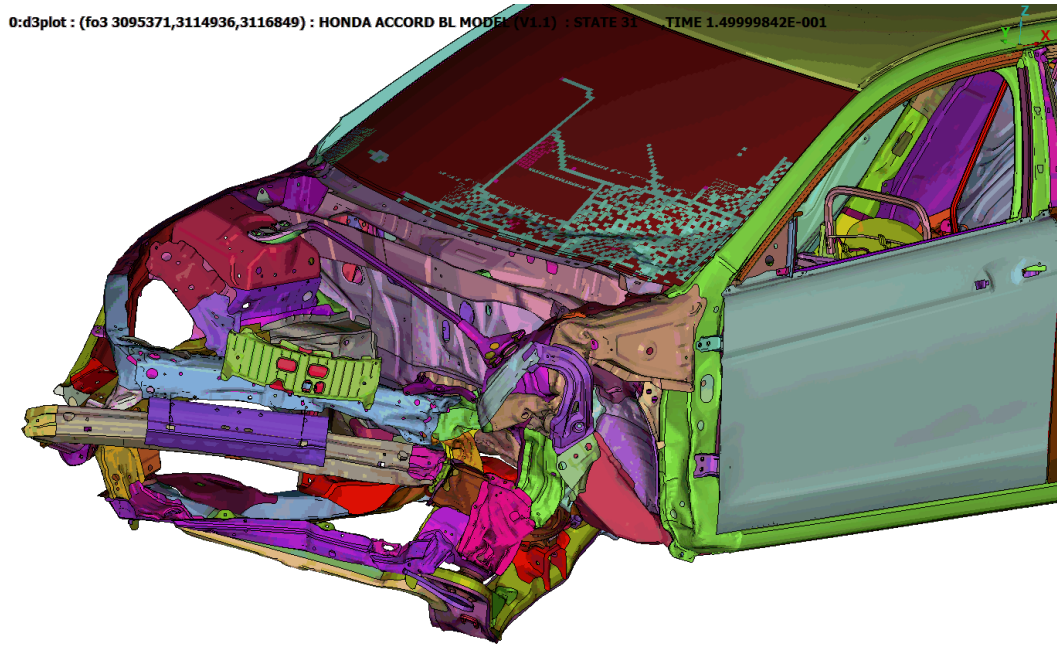
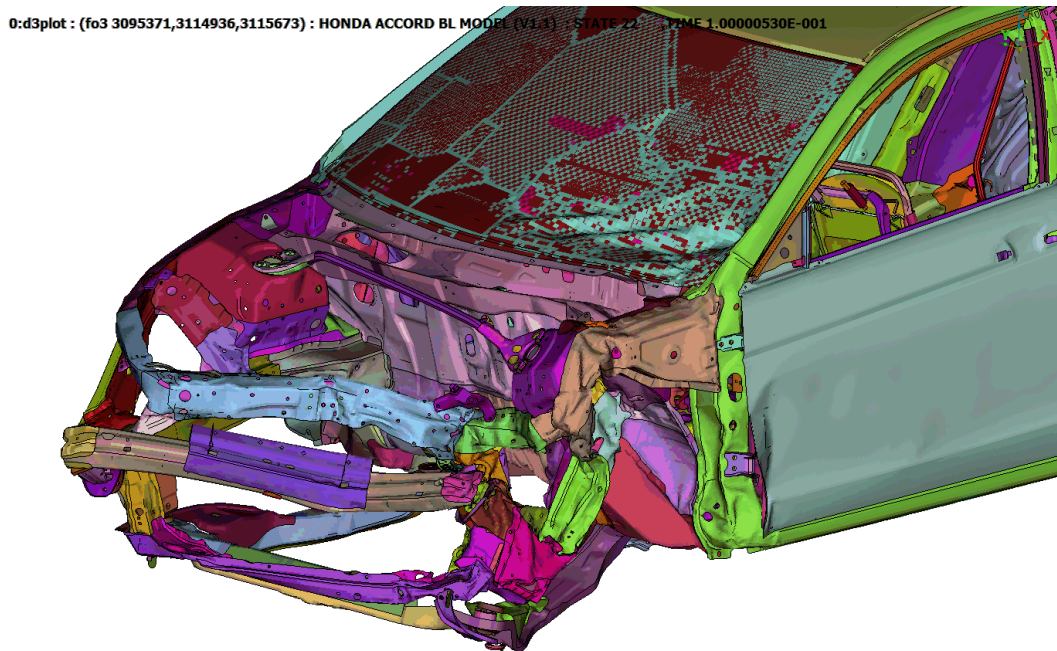


Figure 5.40: MPDB

Figure 5.41: Honda Accord - MPDB firewall deformation



(a) ODB



(b) MPDB

Figure 5.42: Honda Accord - front deformation comparison

Table 5.7: Honda Accord - intrusion measurement comparison

	Direction or Position	ODB [mm]	MPDB [mm]	Difference [mm]
Steering column	x	-3	9	12
	y	13.3	5.3	-8
	z	31.6	14.1	-17.5
A pillar	upper	1	20	19
	lower	5	26	21
Firewall	upper	101	117	16
	lower	12	41	29
Door opening width - driver side	upper	4	19	15
	lower	3	14	11
Door opening width - passenger side	upper	1	4	3
	lower	0	1	1
Cross car beam - fixture point	x	1	22	21
	y	3	3.7	0.7
	z	-5.6	-2.7	2.9
Cross car beam - max deformation	x	2	21	19
	y	2.7	3.9	1.2
	z	0.8	-16.4	17.2

5.3 Chevrolet Silverado

5.3.1 ODB test

The Chevrolet Silverado pickup was designed with a completely different philosophy compared to the previous two models, its ladder chassis construction includes only one main load path and its large mass is expected to be quite problematic in the ODB $64km/h$ test. The long crumple zone and the efficient work of the crash structures limit the damage, but the results for occupant protection are still not optimal, as shown in this section. The starting parameters for the test are of a mass equal to $2757kg$ and a total energy of $436kJ$.

Crash pulse

Due to the simple structural configuration of the vehicle, its behaviour and the consequent analysis of the crash pulse are fairly straightforward. There is exact correspondence between the peaks shown in the acceleration trend and the section forces of progressive stages of the main crash structure and hence of the components positioned in the same lengthwise location, such as the engine. It has to be noted that the three locations shown in Figure 5.47 correspond to Main Rail front, Main Rail mid and Main Rail rear starting from the front of the vehicle and moving towards the back.

During the first 40ms of the impact, almost no deformation occurs due to the fact

that the vehicle penetrates the barrier completely without experiencing the level of force necessary to initiate buckling. The only parts that deform are the front bumper, lights and part of the bonnet, together with the small "crash box" placed in front of the rail. This already shows how aggressive a vehicle of this mass and construction can be. Also, the bumper element of the barrier is so low compared to the vehicle's rail that it is simply pushed out of the way with no effect at all. When the main rail finally comes into contact with the rigid block supporting the barrier, the event actually starts taking place in terms of deformation. In the first section described until here, it is possible to see that also in terms of acceleration the crash is mild, with a single peak of $15g$ and the others fluctuating below $7g$. Between 40 and $55ms$ the main rail is loaded to the point of failure of the three triggers placed in its frontmost part. Only the rear two fail, with the front section remaining intact. The direction of the force is completely axial, hence the behaviour of the box section which buckles is as ideal as possible. During this timeframe, the accelerations exerted on the vehicle are still very low and do not exceed $10g$, showing that in fact the amount of energy dissipated is not particularly high. At this stage the weak part of the main rail has been utilised fully and the zone where the engine cradle and suspension attach is reached. The strength added due to these reinforcements makes the average acceleration increase to $20g$ and the rail buckles in correspondence with the rear cradle fixing area, right before the firewall. In addition, the frontmost part of the rail is finally crushed as well. The engine starts moving towards the firewall slightly but hasn't been directly loaded, as shown in Figure 5.46. In the following instants the rail keeps crumbling in the same spot, hence the engine accelerates towards the cabin more heavily and, at $85ms$ starts bottoming out. As it is pushed into the firewall, the gearbox inclines towards the ground and brings with it two of the cross members, which in turn pull both left and right rail inwards. At $100ms$ the left rail fails in correspondence with the mid point of the driver's door: this point appears to be the weakest along its length, due to several holes and a large notch being present. At the same time, the engine loads the cabin even more, causing the peak of acceleration of $48.5g$ to occur. Figure 5.46 shows clearly this sequential behaviour and the loading on the engine occurring mostly at the very end of the crash.

Furthermore, the front cross member pulls the right rail inwards as well and this fails in bending only where the triggers are placed. The whole ladder structure is acquires an S shape which continues until the loading bay, but this deformation does not appear to be plastic after the midpoint of the vehicle.

In conclusion, the peak acceleration achieved is quite high, and it appears to be mostly due to the fact that the foremost part of the main rails does not absorb a considerable amount of energy at the beginning of the crash, leaving a large portion of it to be dissipated by the area where the engine is located. As a consequence, the force with which the block is pushed into the firewall is too high to cause only minor deformation. Hence, not only the firewall is deformed, but also the main rail buckles right underneath the cabin, which will surely affect it, as will be discussed in the next paragraphs.

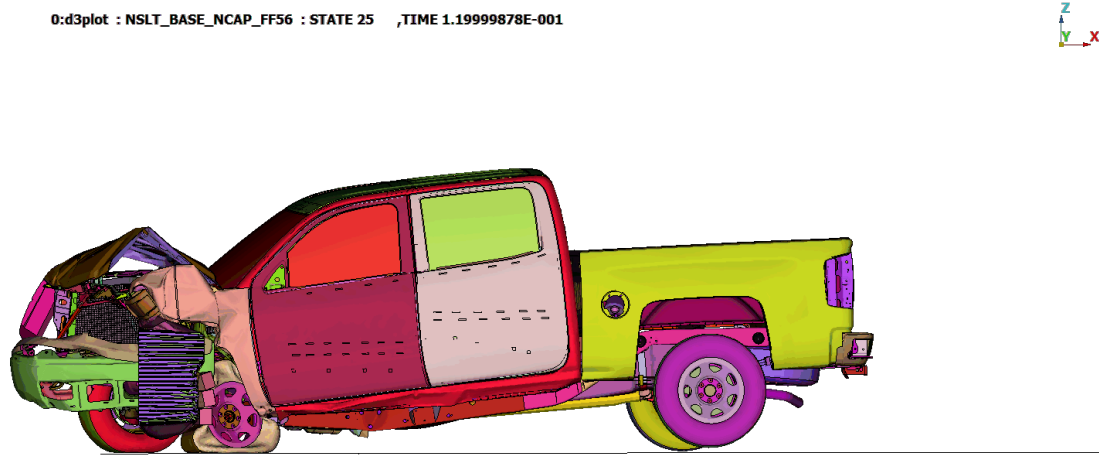


Figure 5.43: Chevrolet Silverado ODB - simulation snapshot

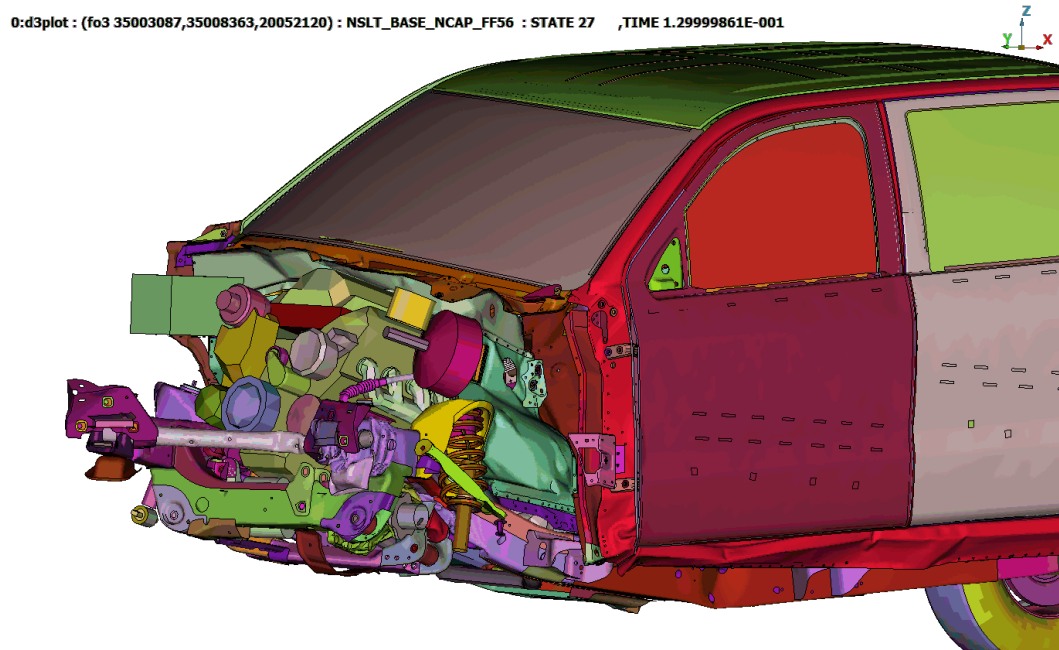


Figure 5.44: Chevrolet Silverado ODB - structural collapse detail

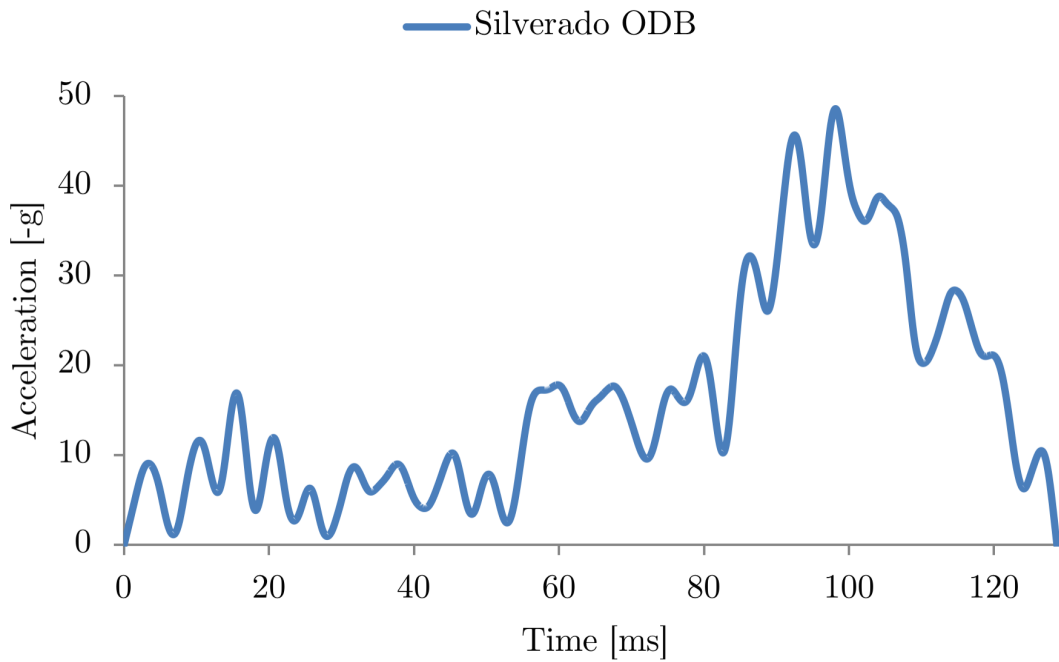


Figure 5.45: Chevrolet Silverado ODB - acceleration

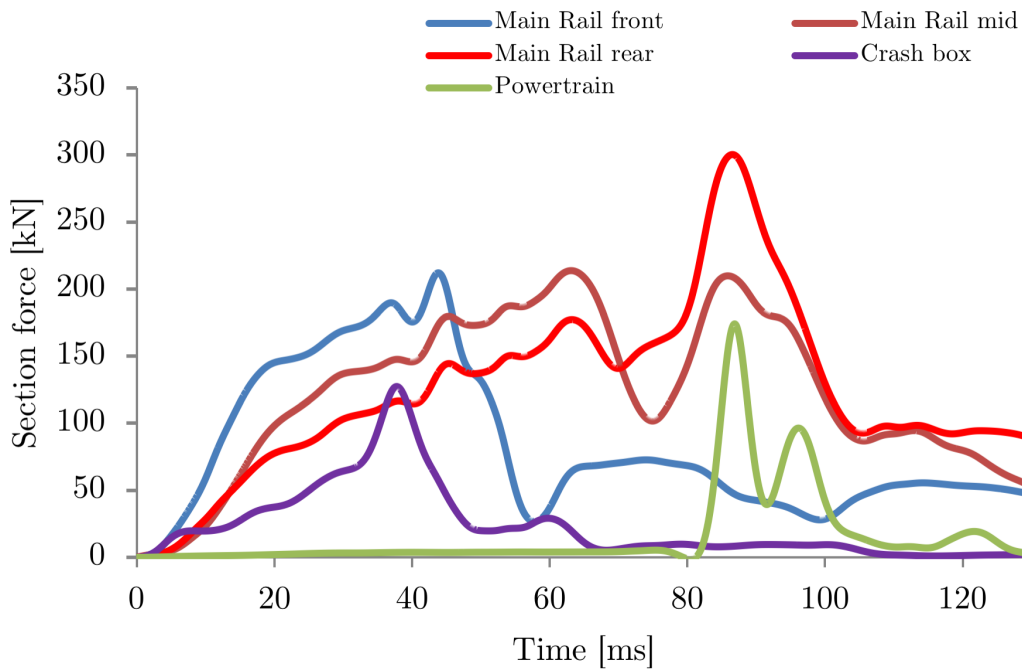


Figure 5.46: Chevrolet Silverado ODB - section forces

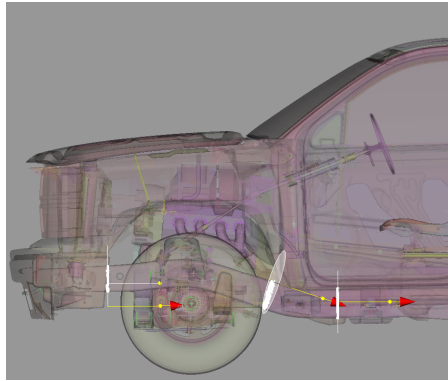


Figure 5.47: Chevrolet Silverado ODB - cross section location

Intrusions and cabin deformation

Due to the trends explained above, the main drivers for intrusion and cabin deformation are the impact of the engine with the firewall and the failure of the main rail underneath the cabin. Regarding the first one, the level of intrusion is worryingly high, especially in the area occupied by the front passenger: on the driver side, the entire area deforms by $100\text{-}110\text{mm}$, while on the passenger side the peak deformation is above 190mm , with an average values all above 100mm . This difference seems to come from the fact that the block is not pushed straight into the firewall but, due to the reduced overlap of the barrier, it is pushed with an angle and results more inclined towards the passenger area. These high levels of intrusion, however, do not affect greatly the pedals, as the length of the engine makes sure that a space is left between the barrier and the brake booster, which does not push on the firewall. Furthermore, the area which shows values around 100mm , just below the pedal attachment point is caused by the impact with the suspension spring and its mounting, which are also pushed into the firewall. Luckily, the pedals are in an unaffected area and move by an amount limited to $20\text{-}25\text{mm}$, considerably less than the majority of the other firewall zones. The intrusion of the firewall in this instance seems not to cause a considerable reduction in occupant survival space, as the cross car beam and steering column only move by a few millimetres; nonetheless, it has to be remembered that the model does not show all the dashboard components and these could be pushed towards the driver.

In second instance, the entire structure of the cabin results deformed due to the failure of the ladder supporting it. In fact, the front left cabin fixture location moves in $-X$ direction by approximately 90mm , remaining attached to the front half of the main rail. As a consequence, the driver's side sill bends and twists in several locations along its length and the floor attached to it loses support and cannot properly hold the weight of the seats. Although a level of collapse is expected with this kind of structural behaviour, the floor of the model seems to over exaggerate this possibility, showing very large waves forming in the material and a consequential inclination of the front seats. This might be a problem of the model that will need to be resolved. Nonetheless, the failures here reported will definitely cause an unwanted level of instability in the floor and would have to be addressed. The base of the A-pillar results also affected and shows mainly a rotational deformation, as its

lower part is dragged backwards by the cabin's mounting point, the twist of the cabin itself makes the top part of the component move slightly forwards. The resulting door opening deformation is however small and the cabin remains sealed all around. The only opening occurs at the sill, more due to its twist than to door damage.

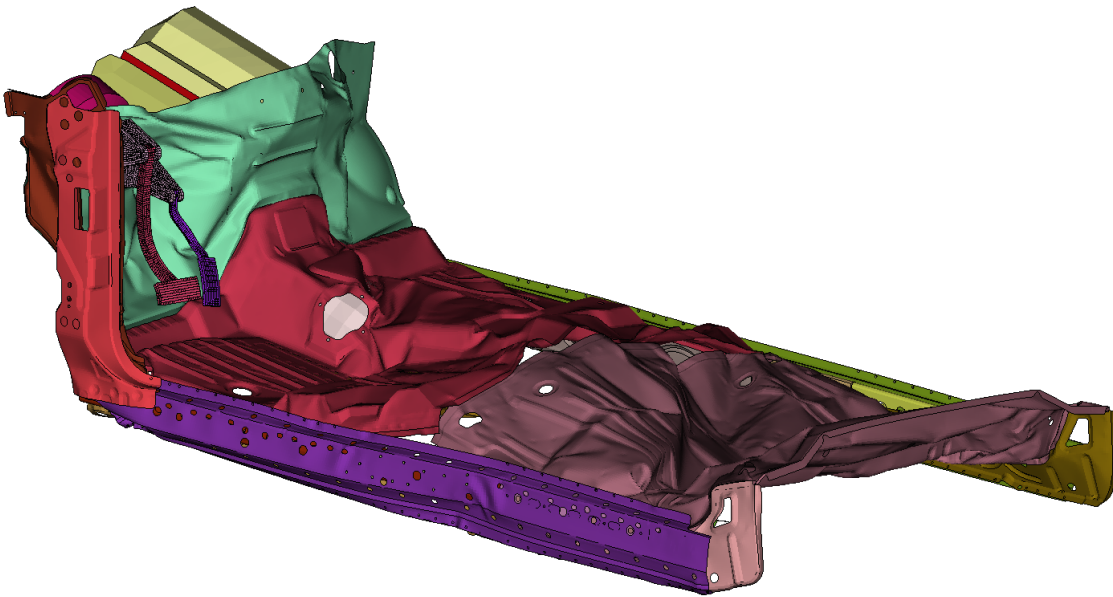


Figure 5.48: Chevrolet Silverado ODB - overall cabin deformation

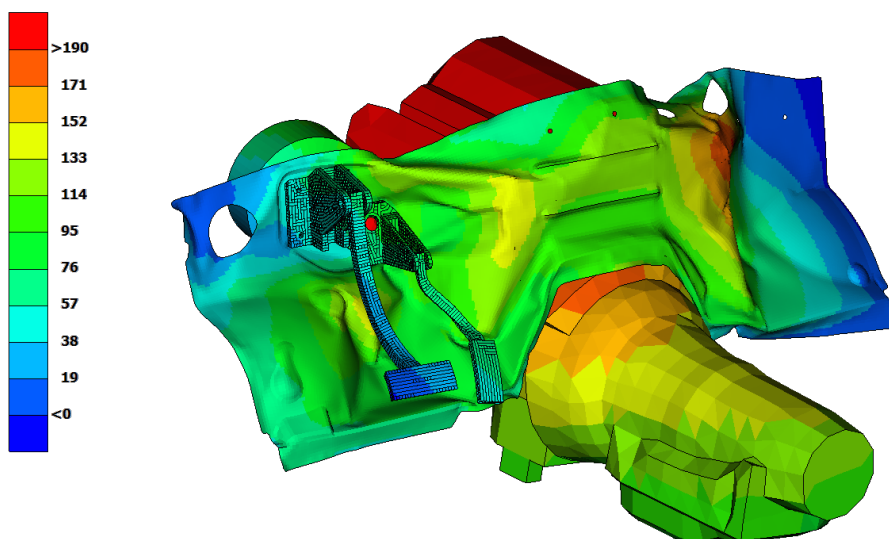


Figure 5.49: Chevrolet Silverado ODB - driver side firewall intrusion

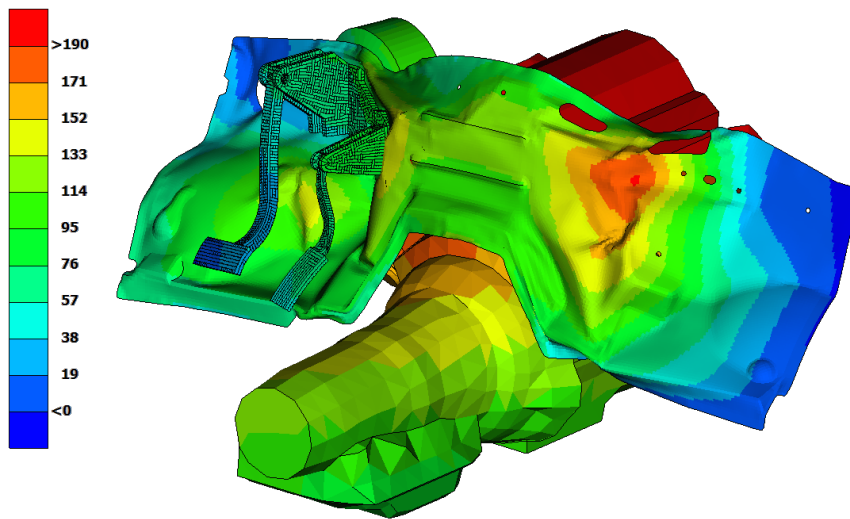


Figure 5.50: Chevrolet Silverado ODB - passenger side intrusion

Table 5.8: Chevrolet Silverado ODB - intrusion measurements

	Direction or Position	Intrusion [mm]
Steering column	x	-6
	y	24.3
	z	7.6
A pillar	upper	-19
	lower	33
Firewall	upper	100 - 193 passenger
	lower	112 - 103 passenger
Door opening width - driver side	upper	4
	lower	11
Door opening width - passenger side	upper	-1
	lower	1
Cross car beam - fixture point	x	-17
	y	-
	z	-
Cross car beam - max deformation	x	-18
	y	-
	z	-

5.3.2 MPDB test

In the MPDB test, the Chevrolet Silverado performs very well in terms of occupant protection, with very low levels of intrusion and reduced acceleration peaks. This is in fact as expected, due to the very large mass of the pickup, far greater than the 1400kg of the mobile barrier. The weight of the vehicle was 2741kg and the total energy roughly 399kJ.

Crash pulse

The first fact to notice about the crash pulse of the MPDB is the fact that the peak experienced by the vehicle is quite low, with a maximum value of 35g. Regarding the details of the various peaks, the initial part occurring in the first 30ms corresponds to the rail initially penetrating the barrier and collapsing just behind the crash box - which does not collapse at all -, followed by the loading of the section in front of the engine cradle, where the triggers are located. These start buckling at at 25 ms and end their function at 35. In this instance as well, the deformation is completely axial: the bumper pushes on the barrier and creates a flat surface on which the rail can be loaded in an ideal way. At the 30ms mark, the part of the rail behind the suspension mounting point starts absorbing energy and the deformation is onset soon afterwards, in a very similar manner to that showed in the ODB test. Its failure is progressive and it continues its function for around 15ms, where the rear section of the rail starts supporting most of the load. The engine cradle moved the engine towards the firewall since the initial deformation of the "mid" rail section, however, as shown in Figure 5.54 it is never considerably loaded during the event. The peak acceleration is reached as the residual energy gets dissipated by the section of the rail underneath the cabin. This point corresponds to the engine bottoming out against the firewall, although this occurs with little residual energy pushing on the block. The main rails do not show any sign of deformation in the cabin section: the last deformed part is that behind the engine cradle. At the end of the crash, the kinetic energy of the barrier has been exhausted completely, but that of the vehicle has not, hence the barrier starts moving backwards compared to its initial velocity. One aspect to notice in Figure 5.54 is the trend of the crash box section force: interestingly, this component does not fail at all during the impact as it penetrates the barrier deeply, remaining completely intact.

Overall, the shape of the vehicle remains unchanged, the rhs rail is bent in a minor way and does not show any sign of plastic deformation. The entire length of the ladder rails is also undeformed, keeping the cabin and the loading bay in line with no twisting. Furthermore, the engine is not loaded directly by the components in the engine bay, compacted by the barrier: in fact, the only reason why it bottoms out against the firewall is the deformation of the rail which makes its support slide backwards. At the end of the crash, the block springs back by a visible distance, unloading the firewall.

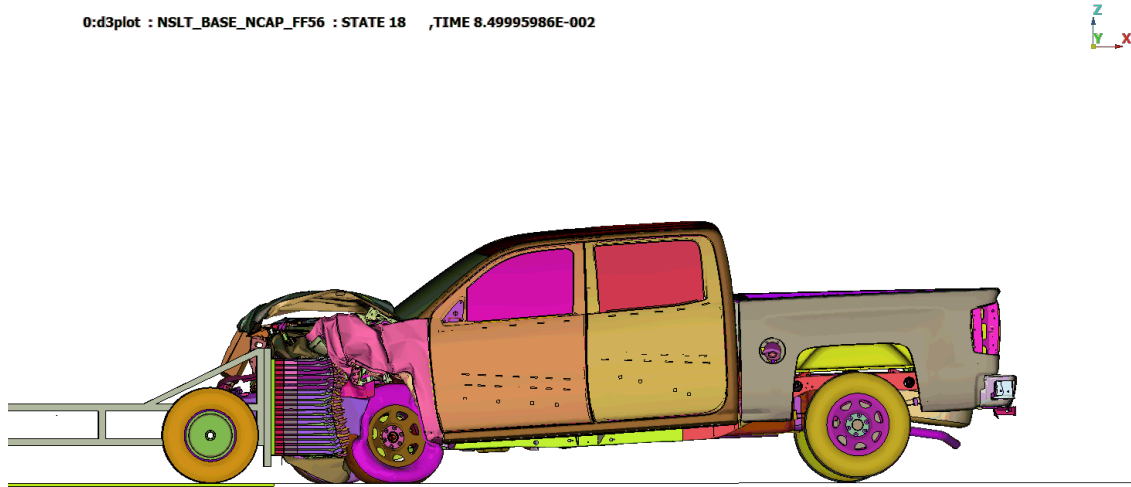


Figure 5.51: Chevrolet Silverado MPDB - simulation snapshot

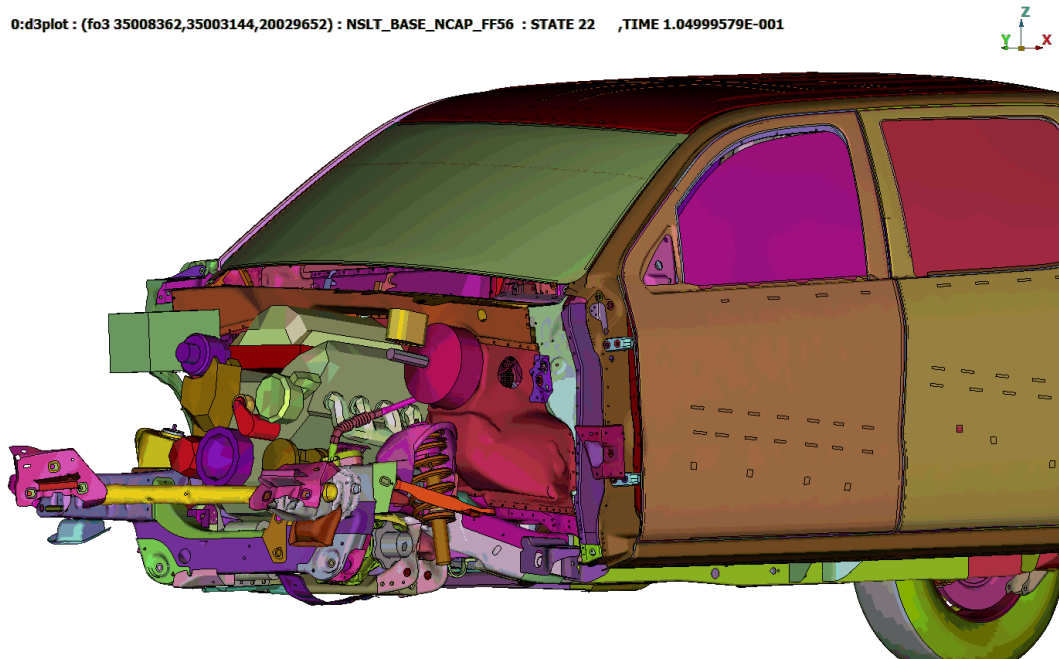


Figure 5.52: Chevrolet Silverado MPDB - structural collapse detail

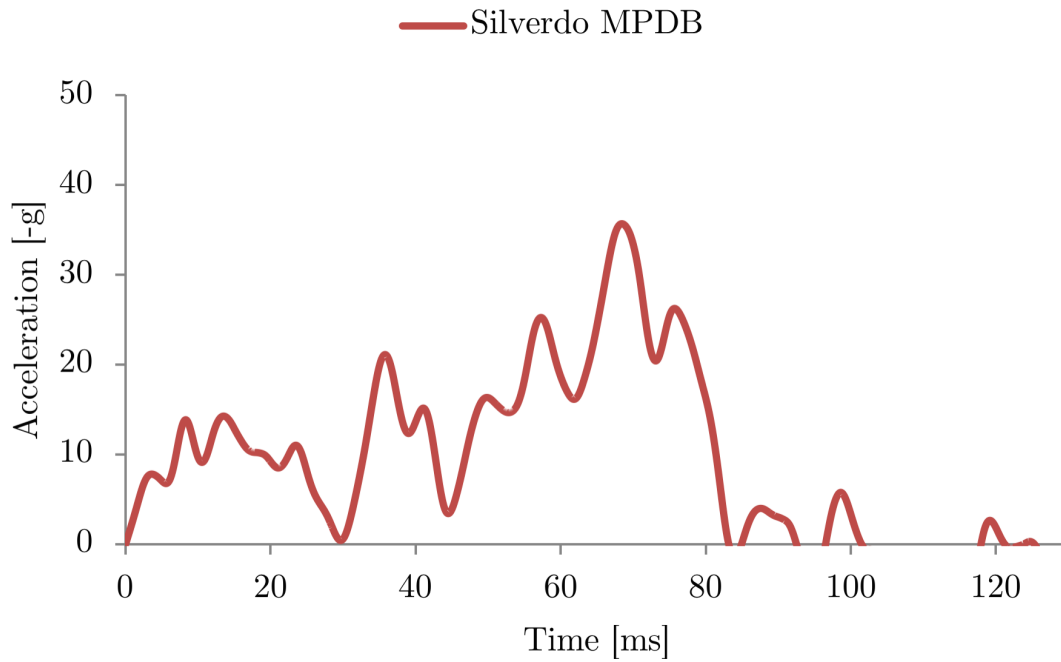


Figure 5.53: Chevrolet Silverado MPDB - acceleration

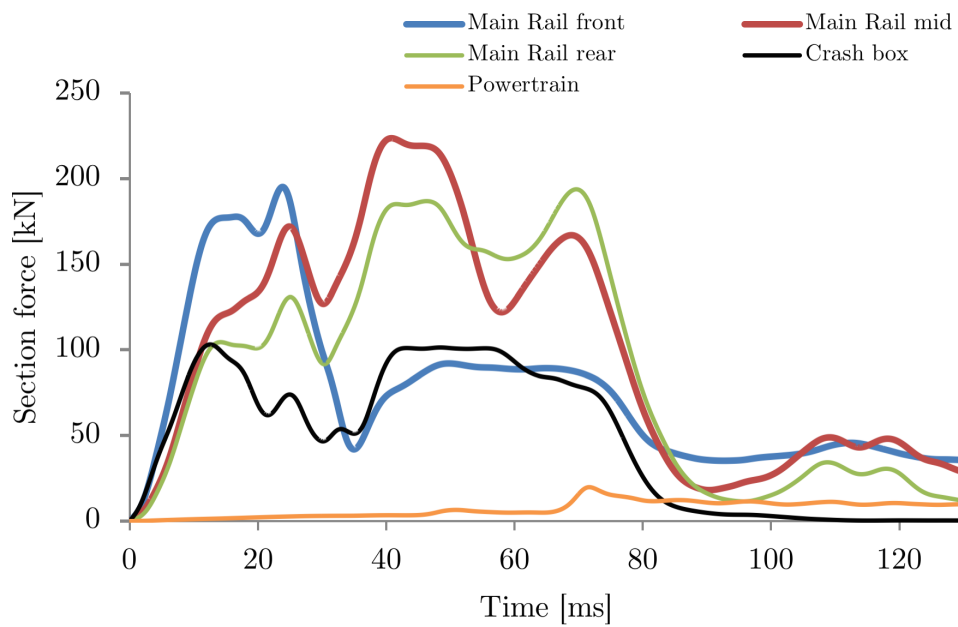


Figure 5.54: Chevrolet Silverado MPDB - section forces

Intrusions and cabin deformation

With regards to intrusion, Table 5.9 depicts a very clear picture of the situation: the cabin undergoes virtually no deformation in all its parts, apart for the firewall. The engine is driven against the firewall at the end of the crash due to the failure of the structure maintaining the cradle in position. The offset of the barrier, as in ODB, pushes the block at an angle and this hits the firewall first on the passenger side, hence the greater intrusion level. The pedal attachment point is completely untouched and the pedals do not move. The only area where the intrusion can be considered relevant is the central one, which corresponds to the space between passenger and driver and would not interest the survival space in a significant manner. This behaviour is expected to be true even when the vehicle is completely equipped with dashboard and interior trim. For what concerns the rest of the cabin, the door openings are not affected, the A-pillar doesn't move and also the floor is for the most part as it was prior to the impact. The rear area of this component shows a level of deformation which seems unreasonable, as there is no displacement in the components surrounding it and the damage appears since the very first *ms* of impact.

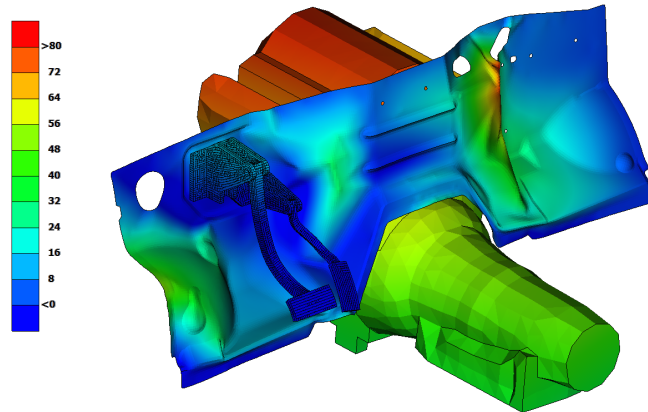


Figure 5.55: Chevrolet Silverado MPDB - driver side firewall intrusion

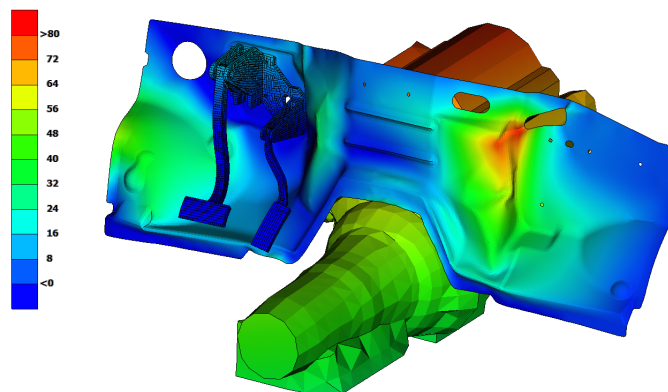


Figure 5.56: Chevrolet Silverado MPDB - passenger side intrusion

Table 5.9: Chevrolet Silverado MPDB - intrusion measurements

	Direction or Position	Intrusion [mm]
Steering column	x	-11
	y	-11.5
	z	-8.6
A pillar	upper	0
	lower	0
Firewall	upper	33 - 81 passenger
	lower	4 - 23 passenger
Door opening width - driver side	upper	0
	lower	0
Door opening width - passenger side	upper	0
	lower	0
Cross car beam - fixture point	x	-4.1
	y	2.3
	z	3.1
Cross car beam - max deformation	x	-
	y	-
	z	-

5.3.3 Comparison

Energy content

Starting from the total energy of both tests, the Chevrolet Silverado is the first vehicle out of the three analysed for which the total value of this parameter is higher for the ODB test: the current procedure shows a value of $435kJ$, while the MPDB reaches a maximum of $399kJ$. The difference between the two tests is roughly equal to 10%. This is clearly due to the very large mass of the vehicle, which surpasses greatly that of the barrier. This is the main reason for the differences in the results shown in the previous sections. The crash duration is still vastly different, as it was for the previous two vehicles: the ODB impact lasts for $130ms$, while in the new procedure it ends at $75ms$, but the reduced pulse amplitudes show that the new test is substantially easier for this vehicle

Crash pulse

With regards to dynamic data, the first evident difference is the peak acceleration achieved in the two tests: the MPDB reaches a value around 26% lower than ODB, with a peak of $36g$ against $49g$. In both procedures the maximum point is reached at the very end of the crash, but while in the current one it is due to the engine loading heavily the firewall, in the future test this occurs due to the final loading of the main rail. In terms of average

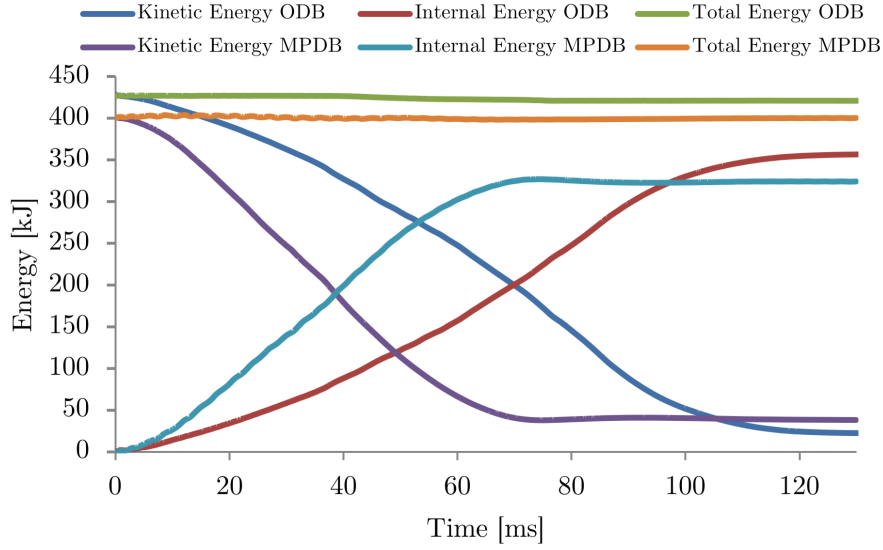


Figure 5.57: Chevrolet Silverado - ODB vs MPDB energy content

acceleration, however, both show a value around $13g$, as after the initial section in which the triggers work in a virtually identical way, the main rail is loaded much more quickly by the mobile barrier and the buckling of the mid section of the structure is restricted to around $15\text{-}20\text{ms}$. This effect can be attributed mainly to the nature of the PDB, which is substantially stiffer and does not get penetrated as deeply as the ODB, inducing high enough loads earlier. Therefore, where the ODB causes a peak much higher, this effect is balanced in the average by a higher acceleration throughout the final $2/3$ of the impact with the mobile barrier. Another substantial difference is represented by the time to zero velocity. The zero point is crossed after 113.2s in the current test, while it is not reached at all in the new procedure: the Silverado achieves a stable velocity of 2.1m/s after 101.5s and it does not decelerate further, accelerating the obstacle in reverse direction. The delta of velocity is therefore even lower than 13.8m/s .

The difference in energy and between the two procedures drives substantial disparity in the failure of the ladder chassis as in one test the rail fails heavily at the end of the crash underneath the cabin, while in the other it does not show any sign of damage in this area. This, together with the loading on the engine, results in very different intrusion levels, as will be explained later in this section.

Table 5.10: Chevrolet Silverado - ODB vs MPDB dynamic data

	ODB	MPDB	Difference	% Difference
Peak acc. [$-g$]	48.57	35.71	12.86	26.47
Mean acc. [$-g$]	13.39	12.92	0.47	3.51
Time to zero velocity [s]	113.20	(101.50)	(11.70)	(10.33)

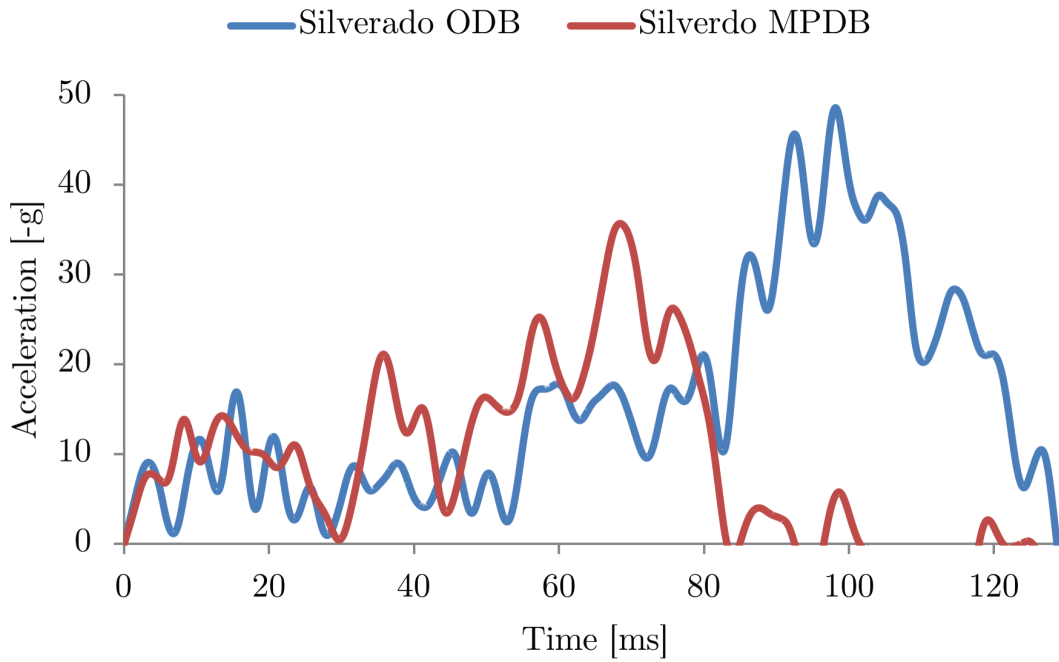


Figure 5.58: Chevrolet Silverado - crash pulse comparison

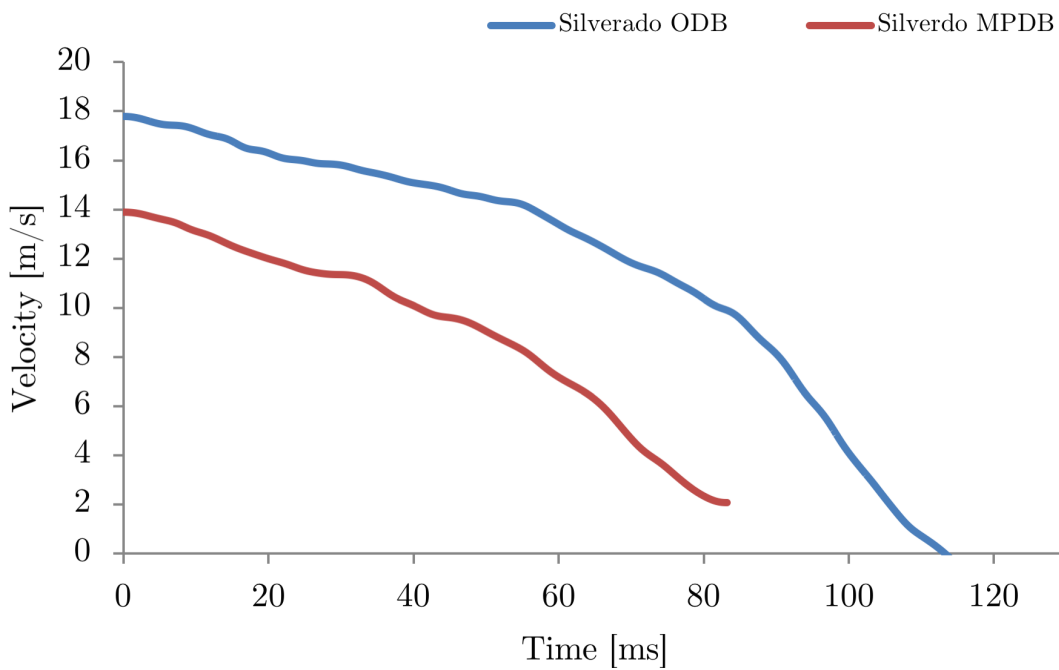
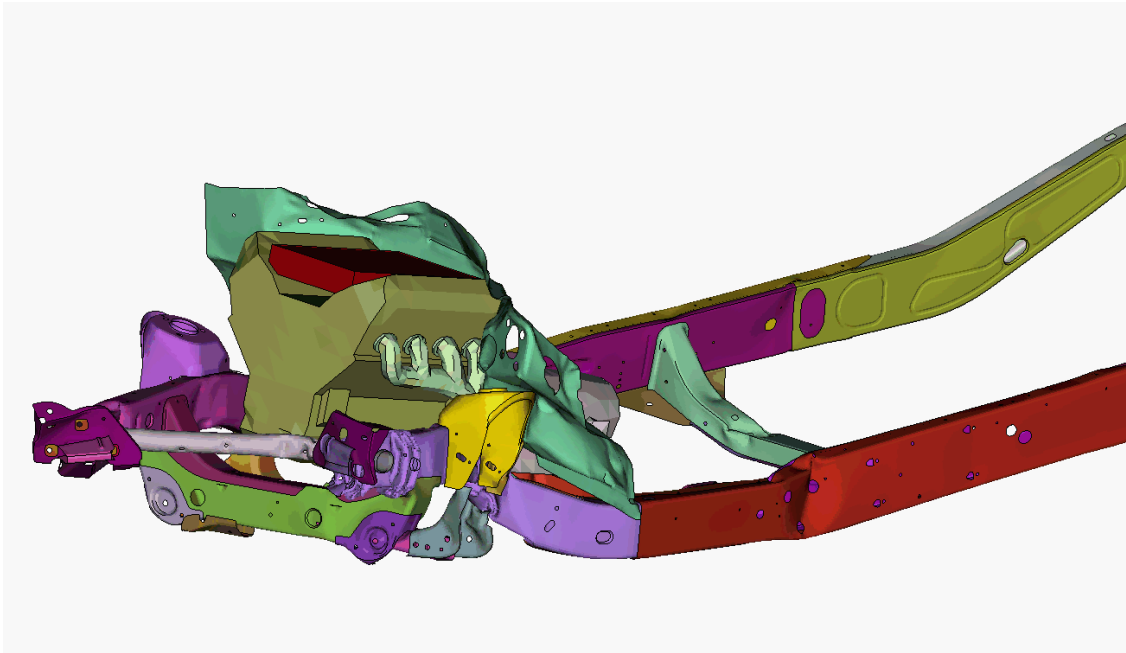
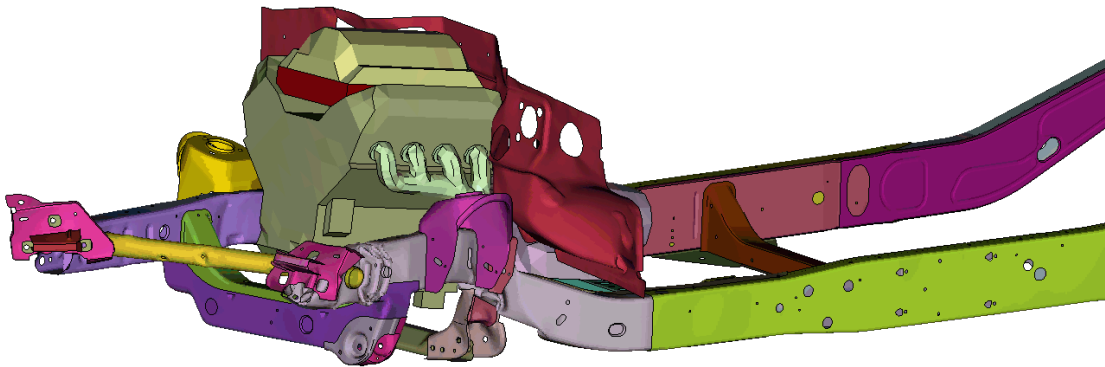


Figure 5.59: Chevrolet Silverado - velocity trend comparison



(a) ODB



(b) MPDB

Figure 5.60: Chevrolet Silverado - main rail deformation comparison

Section forces

The comparison of section forces shown in Figure 5.61 supports what has been said above. In fact, both the front part and mid part of the main rail show the same maximum level of force sustained before buckling, the main difference being the timeframe in which the loading and buckling occur. In addition, the mid part of the structure fails in three fast, consecutive instances when loaded by the mobile barrier, while in the ODB it loads slowly and fails once - the second time corresponds to the loading of the rear section. The real differences begin to show when looking at the just mentioned rear section and at the powertrain loading. The level of force sustained by the former part is considerably higher in ODB, with a difference of more than $110kN$, which is more than enough to cause catastrophic failure. Similarly, a discrepancy of more than $160kN$ is registered for the powertrain loading, which justifies the completely different behaviour in terms of intrusion as the extra force is only counterbalanced by the cabin.

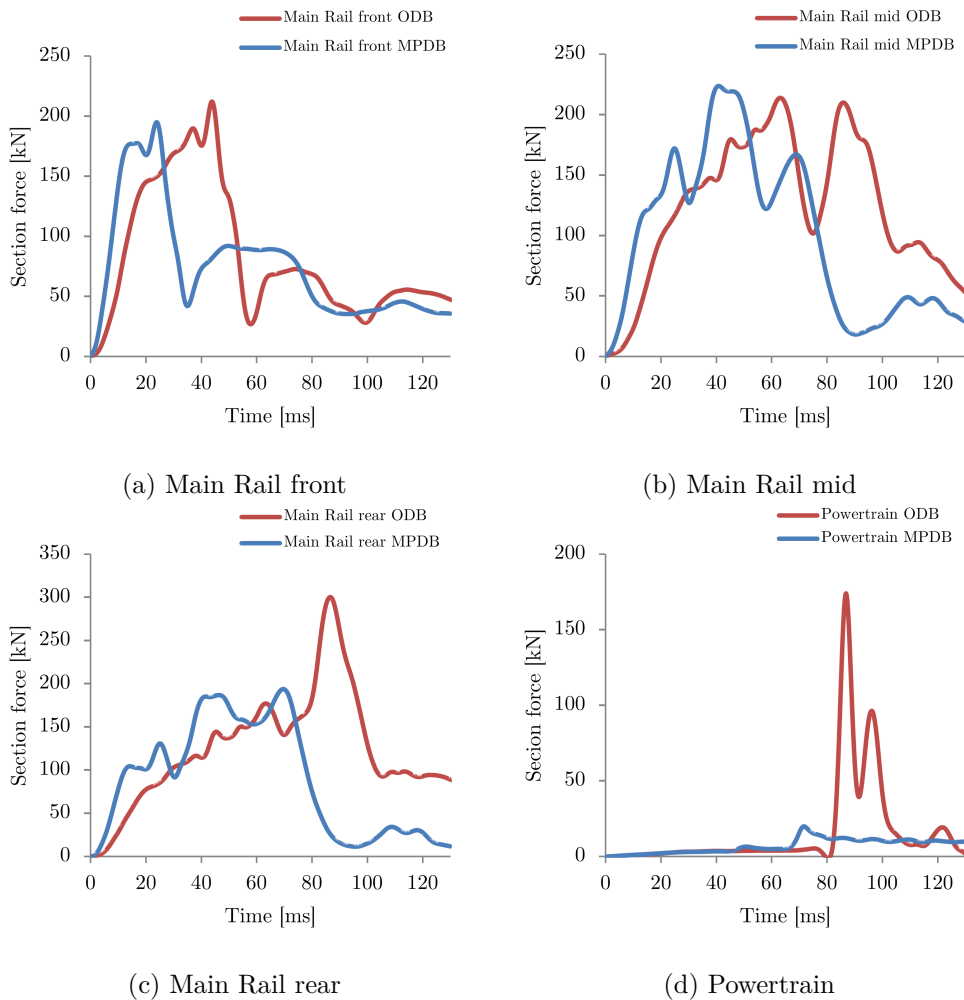


Figure 5.61: Chevrolet Silverado - section forces comparison

Cabin deformation and intrusion

As anticipated above, the intrusion and cabin deformation levels show a large improvement in MPDB due to the reduced amount of energy carried by the engine block during the impact. In Figure 5.62 the difference is made evident by the extensive deformed area in the ODB, which affects not only the back of the central dashboard section but also the pedals, the footwell and the passenger footwell. The two figures could not be put on the same colour scale as the latter would result looking completely undeformed. It has to be remembered that, despite these results, the vehicle obtained a GOOD rating in IIHS moderate overlap test. The intrusion measurements reported in [56] match up with the model, hence proving that those are not overestimated. This means that the available space behind the instrument cluster is so large that the vehicle has been designed to absorb a large portion of the impact energy with the firewall itself. Clearly, this necessity will not be present if the Silverado will be tested in MPDB, if the front structures stiffness was to remain unchanged. In any case, the high deformation of the rails in the ODB test causes a number other issues, such as the deformation of the floor (overestimated) and the rotation of the A-pillar, which translates into a minor decrease in door opening width.

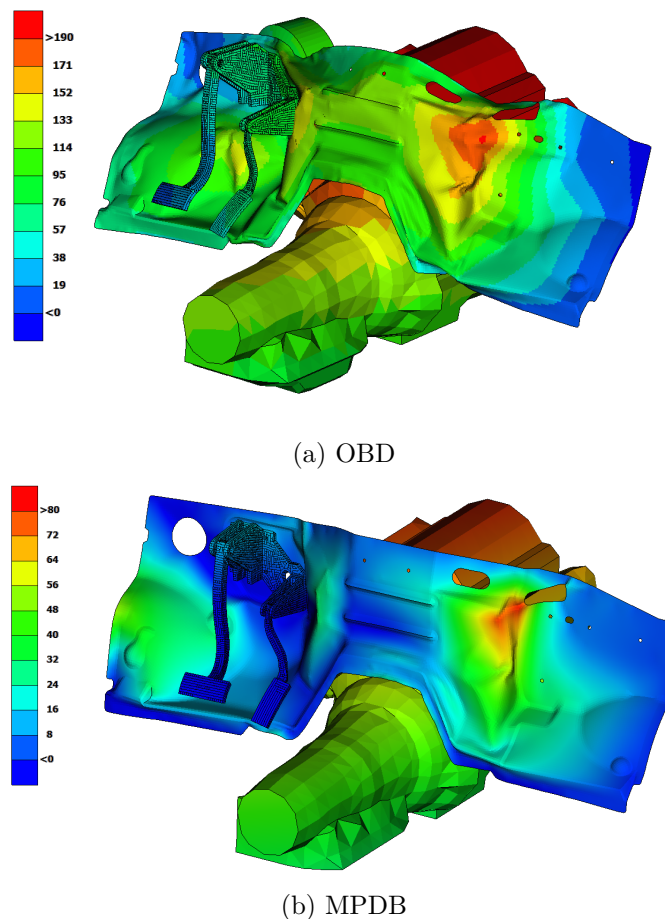


Figure 5.62: Chevrolet Silverado - firewall intrusion comparison

In conclusion, it is clear that the reduced amount of energy of the test and the fact that the PDB, although being theoretically more difficult to load appropriately, allows the same level of axial buckling as the rigid wall behind the ODB create a more favourable situation for the occupant protection devices of the Silverado. This was in fact one of the expected results from the introduction of the mobile barrier test and will allow the manufacturers to modify the frontal structures in order to achieve the same - or better - level of self protection achieved in ODB, while focusing more on the partner protection side of the matter. Partner protection is clearly the flip side of such optimal performance in occupant protection for this vehicle, as will be discussed in the next chapter.

Table 5.11: Chevrolet Silverado - intrusion measurement comparison

	Direction or Position	ODB [<i>mm</i>]	MPDB [<i>mm</i>]	Difference [<i>mm</i>]
Steering column	x	-6	-11	-5
	y	24.3	-11.5	-35.8
	z	7.6	-8.6	-16.2
A pillar	upper	-19	0	19
	lower	33	0	-33
Firewall	upper	100 - (193)	33 - (81)	-77 - (-112)
	lower	112 - (103)	4 - (23)	-108 - (-80)
Door opening width - driver side	upper	4	0	-4
	lower	11	0	-11
Door opening width - pass. side	upper	-1	0	1
	lower	1	0	-1
Cross car beam - fixture point	x	-17	-4.1	-12.9
	y	-	2.3	-
	z	-	3.1	-

5.4 U Model

5.4.1 ODB test

The U Model, being designed for the asian market where no test similar to Euro NCAP is present, performs poorly in the ODB test. The level of deformation of the passenger compartment is extreme and the survival space is greatly reduced. In the current form, it would score a low star rating for occupant protection. Similarly to the Silverado, the vehicle is constructed with a ladder chassis and a separated cabin mounted on top. This vehicle, however, has a more complex cabin design that incorporates a secondary load path developing from the H node. The mass of the model in this test was of 1940 *kg*, which translates to 306*kJ* in terms of total energy.

Crash pulse

Due to the nature of the structural design and to the fact that the model has no front bumper, no bonnet and no wings, the first 35*ms* of impact do not show any deflection, apart for the deformation of the two frontal cross beams and the consequent bending of the upper load path. These components are fairly soft and their deflection causes a peak of only 7.5*g*, as show in Figure 5.65. During this timeframe, the barrier's honeycomb core is pushed from the top down by the second load path and also sideways by the lower cross beam. This causes a great part of the barrier to be literally pushed out to the right, allowing the structures to hit the rigid block supporting it before undergoing any deformation. In fact, the first component that starts to get pushed backwards is the tire, together with the suspension components: the only part of honeycomb showing a high residual thickness is located in this area. At 35*ms* the crash box is finally loaded up and the acceleration of the vehicle starts increasing, while 7*ms* afterwards the same component buckles axially. It is interesting to note that at the same time, the main rail also shows signs of failure in correspondence with the upper wishbone mount (front wheel - rear mount). In the next 10*ms*, the buckling of the crashbox and of the ladder rail continues, while in this component two other points of failure becomes visible. This time they are further back: one in correspondence with the cabin fixture point and the other just in front of it, the seem to be arising in coincidence due to the S shape of the rail in this location. At 57*ms* the main rail reaches its maximum load and the initial point of failure buckles completely: this causes the rim and tire to be pushed heavily against the outer part of the firewall and door sill, while the engine is also finally hit and accelerated towards the cabin. After this cut off point, no other structure can support the load caused by the residual energy still present. The ladder rail fails in the two locations mentioned above and the engine hits the firewall causing the second peak of maximum acceleration of 36*g*. The tire is squeezed between the wall and the A-pillar base, the force with which this occurs is enough to cause high deformation and the top part of the pillar starts to fail. This behaviour continues until the energy is completely exhausted: the engine deforms the firewall even more, the sill fails, the roof fails as well. The cabin has to absorb such a level of energy that the deformation is visible until the rear wheel arch, with the rear passenger door being pushed backwards noticeably and the roof completely collapsed. During the impact, the upper load path deformed in several points absorbing part of the energy, hence the H point was not damaged as much as the sill, which was pushed by the tire. In addition, the left side

rail fails in two points as well, due to bending caused by the cross beams pulling it towards the centre of the vehicle, overall it is not loaded significantly in a useful way.

Moreover, the peak accelerations achieved highlight the possibility of positive results in terms of biomechanical loading. These are however counterbalanced by the high level of intrusion, which is expected when a vehicle of this mass, crumple zone length and design shows such comforting crash pulses in the ODB procedure.

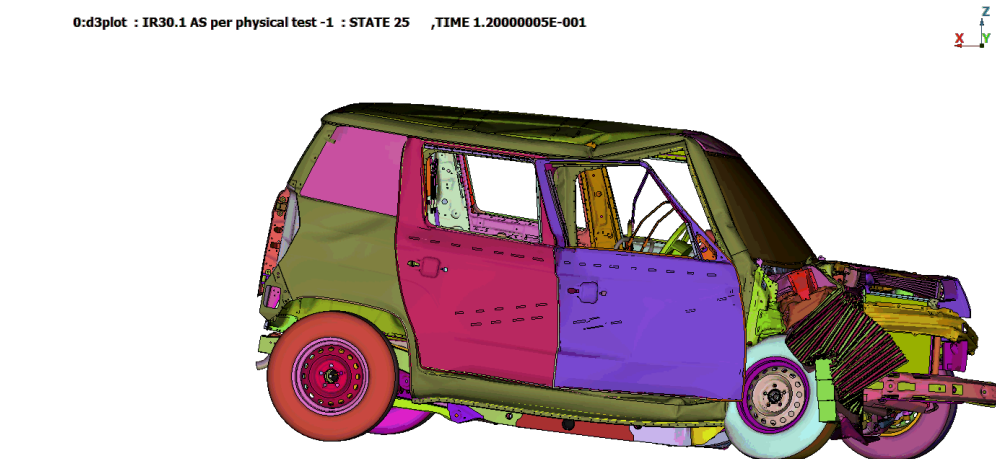


Figure 5.63: U Model ODB - simulation snapshot

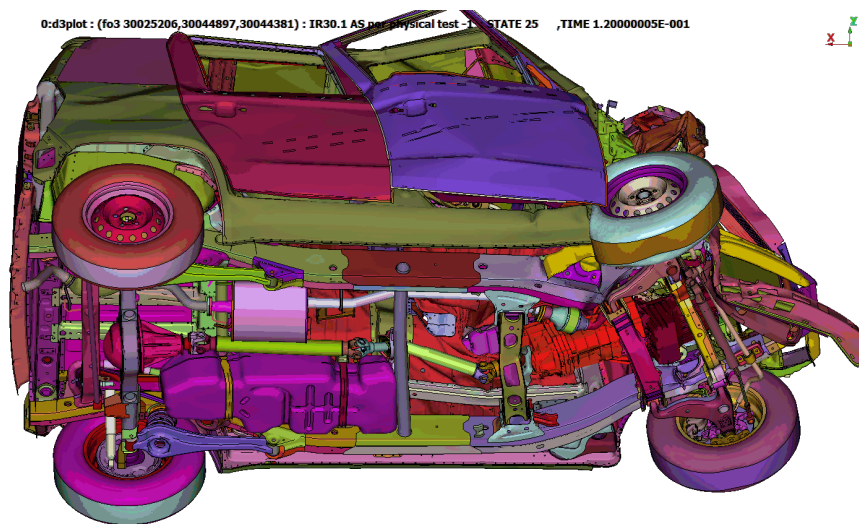


Figure 5.64: U Model ODB - structural collapse detail

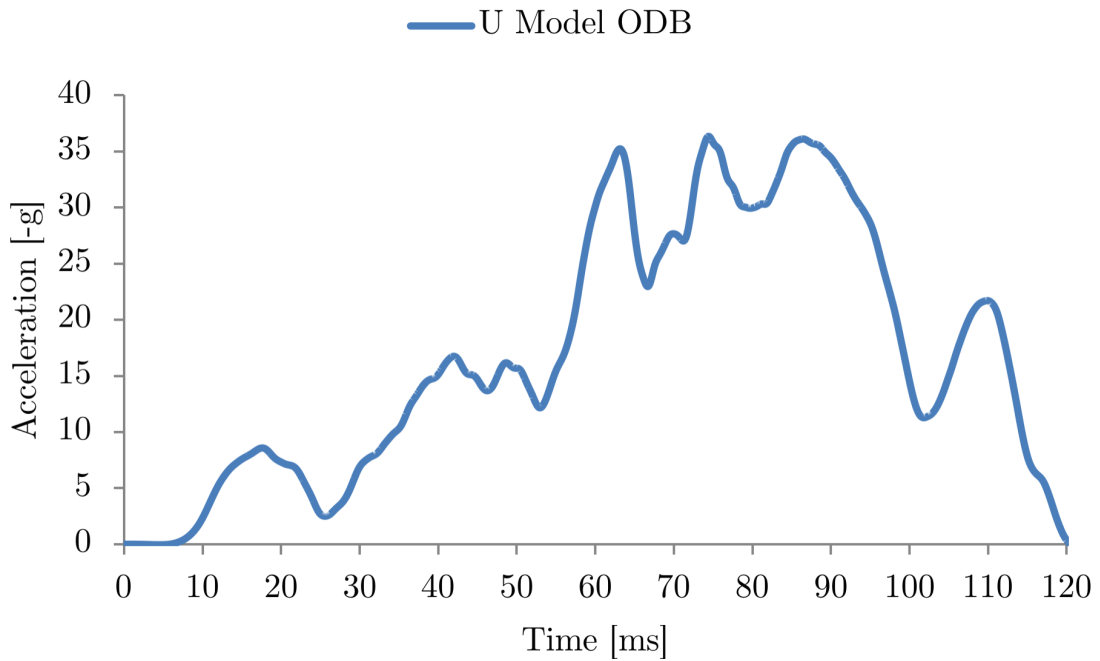


Figure 5.65: U Model ODB - acceleration

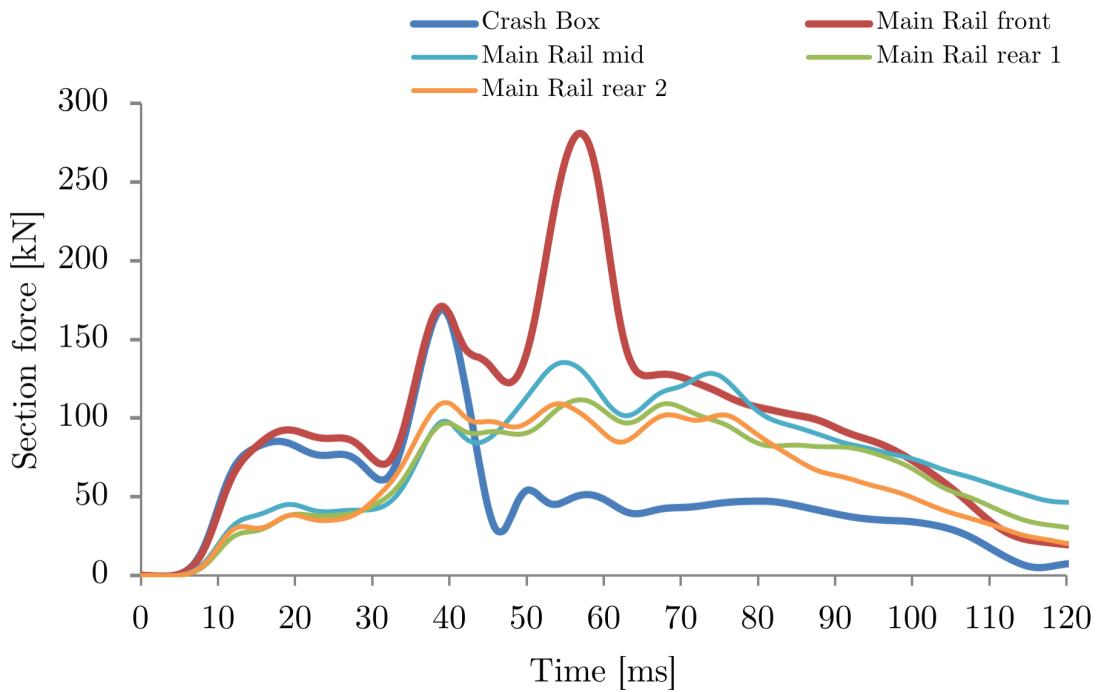


Figure 5.66: U Model ODB - section forces

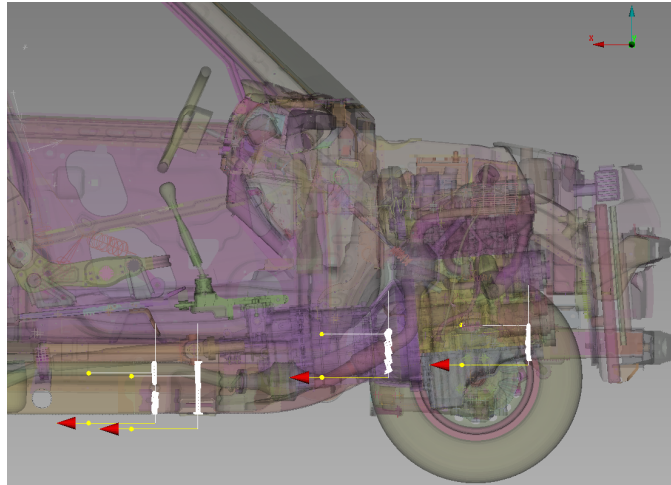


Figure 5.67: U Model ODB - cross section location

Intrusion and cabin deformation

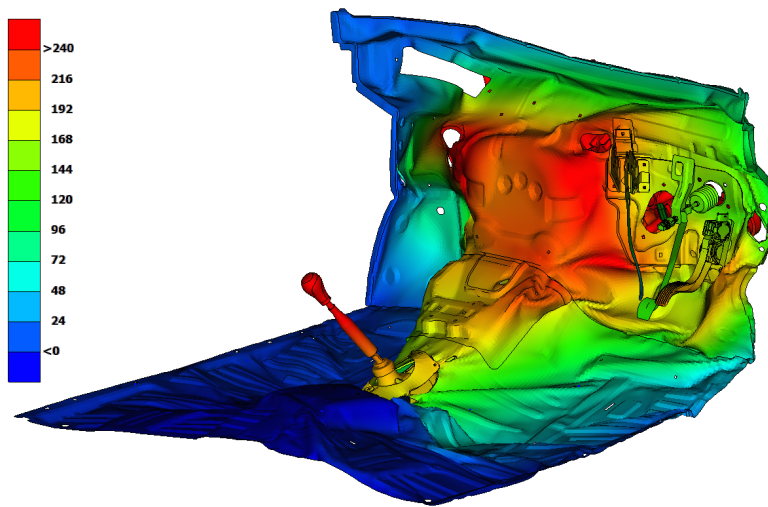
As anticipated above, extremely high levels of deformation and intrusion interest all parts of the cabin. The firewall, shown in Figure 5.68, undergoes maximum deformation in its central section with more than 240mm on both the driver and passenger sides. The areas of the footwells are not as critical, but still record displacements above 100mm , which are highly concerning. As a result, the accelerator pedal is pushed back by 180mm , the brake by 120mm and the clutch cannot be quantified as in the model it detaches from its mount. The damage to this component is caused, in order of importance, by the engine block, the tire and the brake booster. In the same figure it is possible to denote how the floor of the vehicle also undergoes extensive failure. Although this is expected when the structures surrounding it fail as heavily as in this case, the factor of highest relevance in this phenomenon is represented by the gearbox and it is, in fact, an issue of the model: the bracket holding the gearbox and the gear selector together should fail under load, while in the model the failure criterion is not set and the two components remain attached.

The second area of main interest is the base of the A-pillar, together with the adjacent section of sill. The former segment gets damaged solely by the wheel which loads it heavily in its lower part during the second half of the crash. The point of failure corresponds to the area above the lower door hinge, which records a deformation of 109mm that makes it bend clearly. The top part does not appear to be damaged, but due to the failure of the supporting structures, i.e. the sill, it still moves backwards by 70mm . The mentioned damage to the sill occurs just subsequently to the pillar damage, causing the door opening width to shorten by roughly 100mm both on the top and bottom. The door then detaches from the front hinges and at the end of the crash appears to cover part of the front wheel: this gives a clear idea of the importance of the deformation. The rear door is affected too, as it gets pushed by roughly 30mm towards the rear of the vehicle.

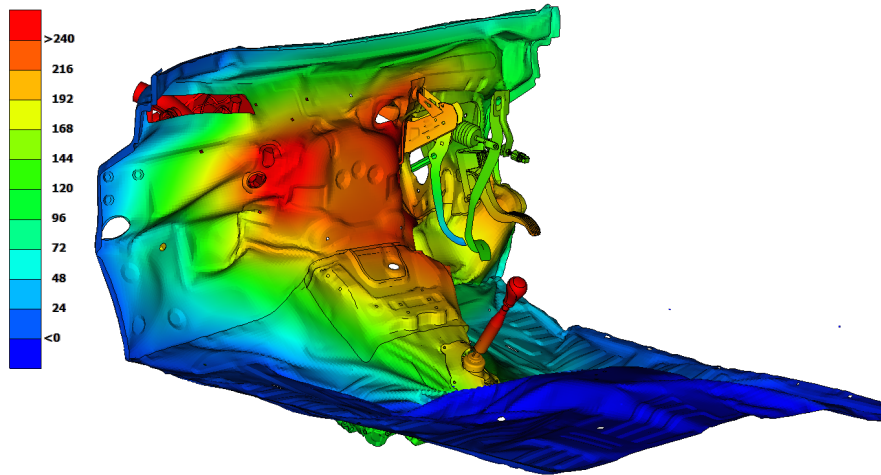
The behaviour just described is also the cause to the extensive damage caused to the roof. Just as the sill starts failing and the A-pillar moves backwards, the same occurs to the roof rail just in front of the B-pillar, which bends and collapses. As a consequence, the

angle between the A-pillar base and the windscreen section increases greatly, the B-pillar undergoes damage and the whole rear half of the upper structures bends towards the front. In addition, the roof panels detach from the roof rail as well.

In conclusion, all the factors here analysed combine to the result of a greatly diminished survival space, as the entire dashboard, instrument cluster, steering wheel and overall trim are pushed towards the driver. In order to withstand the loads caused by the ODB 64km/h test the vehicle frontal structures would need to be reworked and allowed to absorb much more energy in the initial phases of the impact.

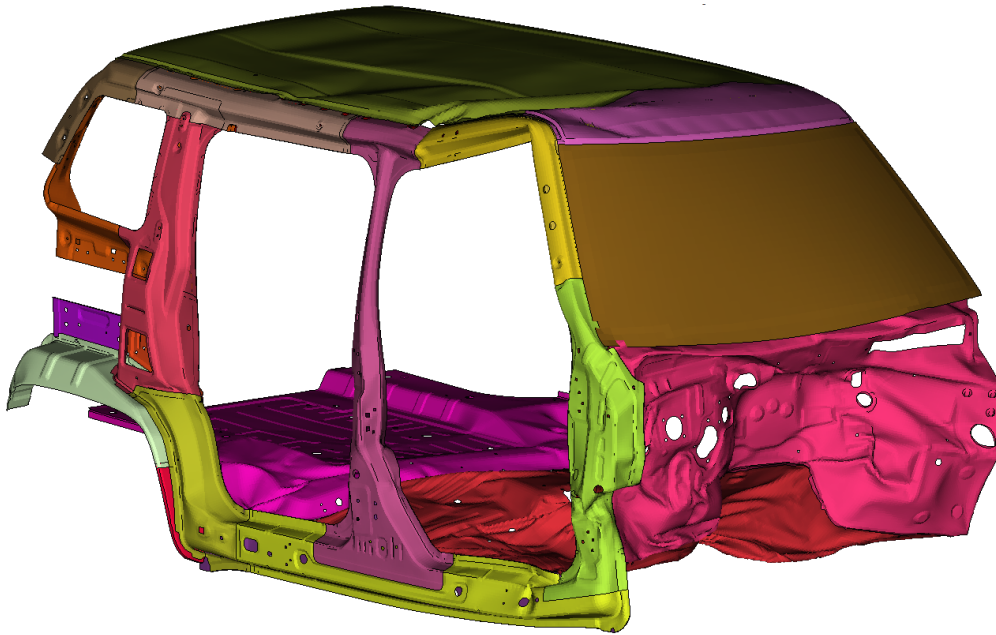


(a) Driver side

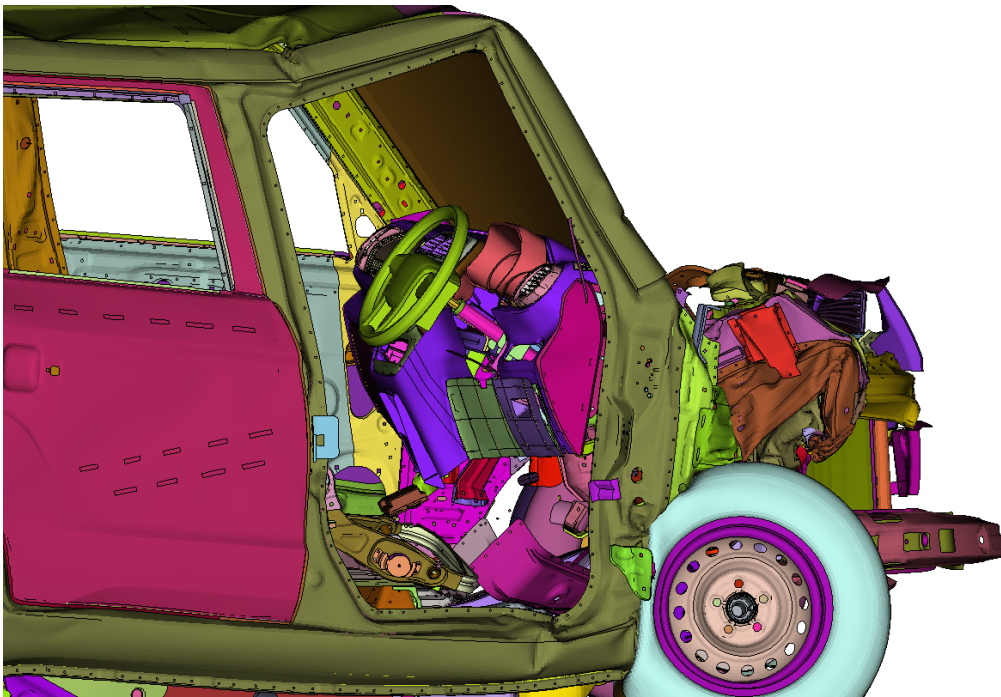


(b) Passenger side

Figure 5.68: U Model ODB - firewall intrusion



(a) Cabin structure



(b) Driver side intrusion

Figure 5.69: U Model ODB - cabin deformation and interior intrusion

Table 5.12: U Model ODB - intrusion measurements

	Direction or Position	Intrusion [mm]
Steering column	x	108
	y	-10.5
	z	72
A pillar	upper	71
	lower	109
Firewall	upper	190
	lower	181
Door opening width - driver side	upper	99
	lower	91
Door opening width - passenger side	upper	9
	lower	9
Cross car beam - fixture point	x	103
	y	-7.9
	z	91
Cross car beam - max deformation	x	109
	y	-3.4
	z	54

5.4.2 MPDB test

In the mobile barrier procedure the U Model, which improves greatly compared to ODB, does not achieve a high standard of occupant protection. In fact, intrusions levels are considerable and the survival space is diminished. Parts of the cabin that should remain intact such as the roof are affected and the overall performance has to be considered poor. The mass of the model as tested was 1921 *kg*, equating to 302 *kJ* of total energy.

Crash pulse

In the first 15*ms* of impact the barrier face impacts with the vehicle and loads a large area which includes both cross beams and the radiator. The crash box is loaded, but the overlap level allows the load to be shared with the right hand crash box too and the softer initial core of the PDB does not make it fail. In addition, the structures supporting the top cross beam and the upper load path all fail, taking part of the load. This process causes the high acceleration peak of 31*g* shown in Figure 5.72. In the next 10*ms*, however, the main rail and crash box penetrate the barrier until the second core, while the lower cross beam pulls the rail towards the centre of the vehicle. This causes the crashbox to fail prematurely in bending, hence at a much lower load compared to the axial mode seen in ODB. This occurs

in correspondence with the lower $15g$ peak at $20-25ms$. Next, the main rail starts taking most of the load and immediately fails both at the cabin mounting point (major damage) and at the lower wishbone support (minor denting). For this reason the oscillation visible between 30 and $40ms$ occurs. At this point the wheel is pushed against the sill and the engine starts loading the firewall, the main rail is not sustaining a high level of force and the left hand side rail, which has been loaded since the beginning, reaches the axial point of failure in two points: the first at the rear engine cradle attachment, and the second on the top face of the box section, just under the cabin. The final peak of acceleration of $35g$ occurs as the engine and the wheel load firewall and A-pillar, dissipating the final portion of energy. During this final section the passenger compartment starts deforming noticeably, with the roof partially collapsing above the driver's door. The deformation is plastic only to a certain extent, as during the unloading phase part of the roof rail springs back. By the end of the event, the main rail has punctured the barrier reaching the end of the second honeycomb block, just a few millimetres in front of the last core. Also, the top part of the PDB pushes against all the components in the engine bay located above the wheelarch, deforming around them, hence at the end of the crash the honeycomb has reached a point very close to the A-pillar and firewall.



Figure 5.70: U Model MPDB - simulation snapshot

0:d3plot : (fo3 30025206,30044897,30044381) : IR30.1 AS per physical test -1 : STATE 25 ,TIME 1.20000005E-001



Figure 5.71: U Model MPDB - structural collapse detail

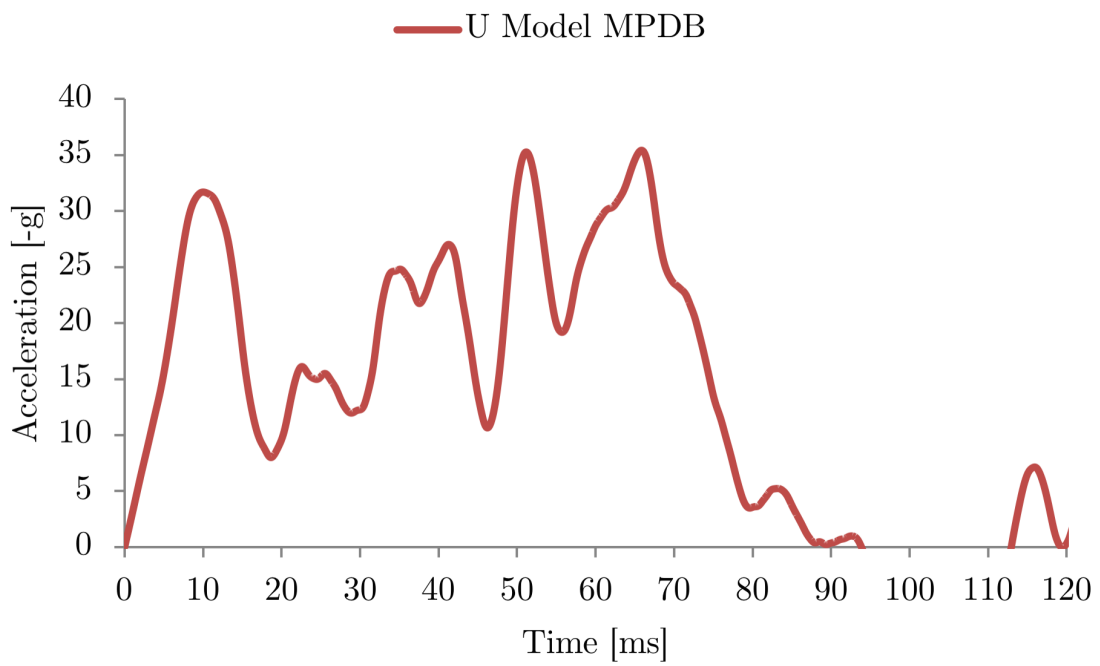


Figure 5.72: U Model MPDB - acceleration

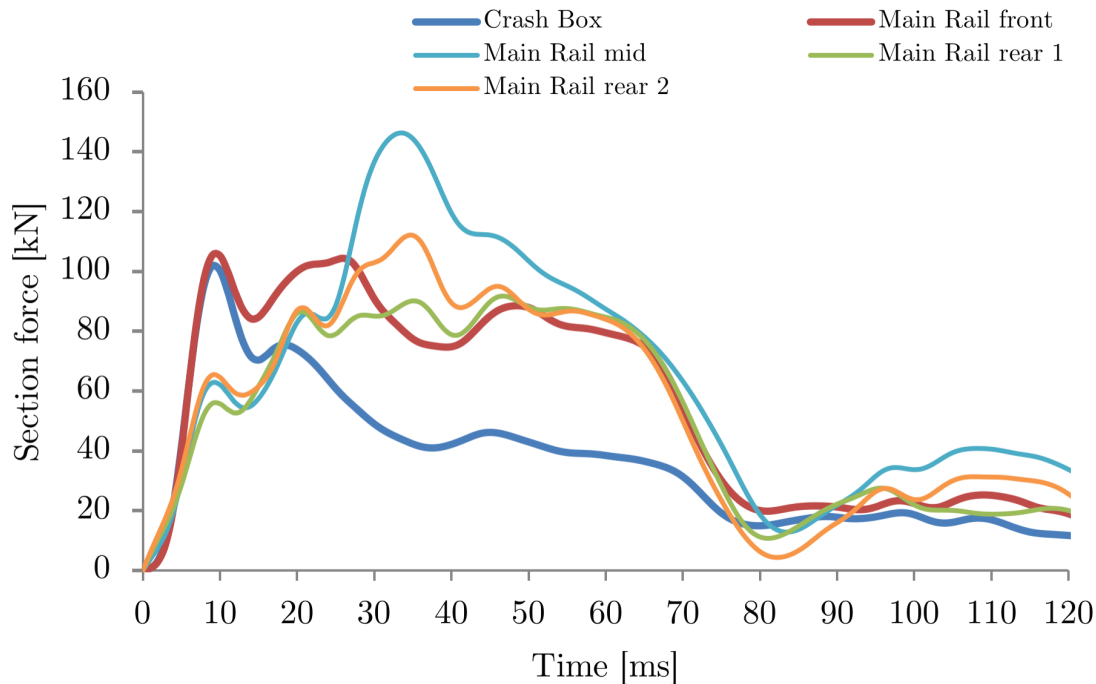


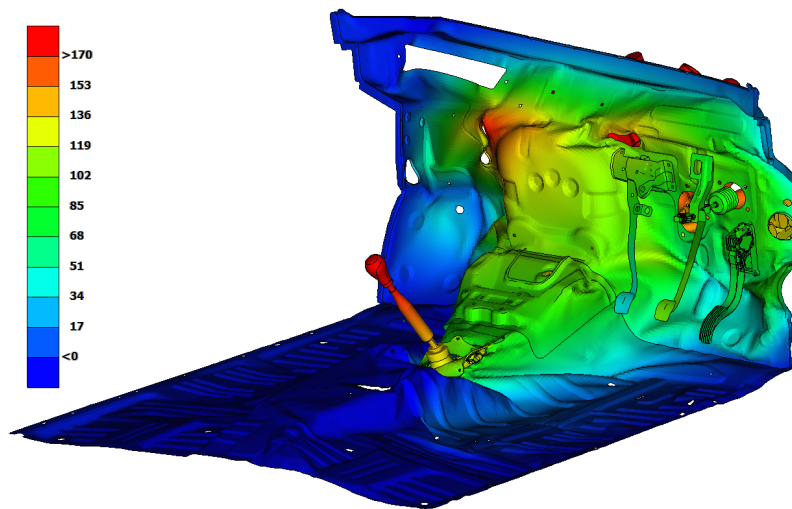
Figure 5.73: U Model MPDB - section forces

Intrusions and cabin deformation

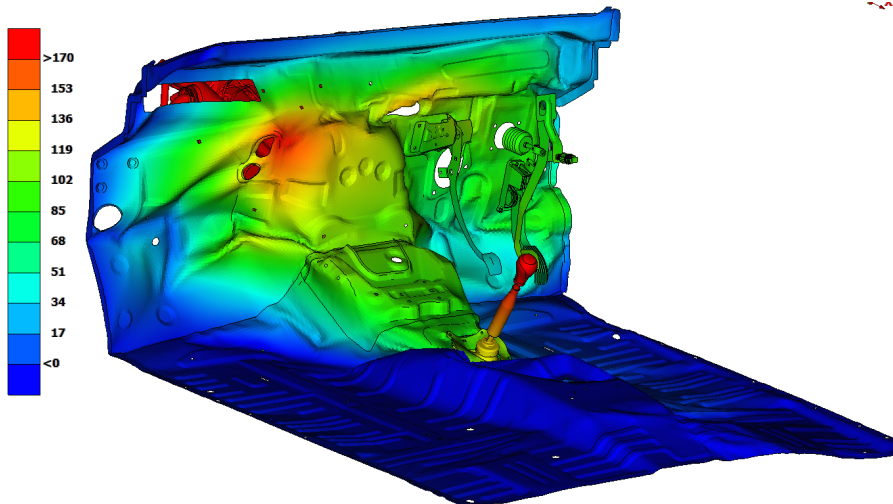
With regards to intrusion, the U Model shows quite high values throughout the cabin, making it poor in terms of occupant protection in this test as well. The firewall is impacted by the engine block and by the wheel, as in the ODB test, and shows peak values of 171mm on the passenger side and 135mm on the driver's. The pedal fixing area in this case is pushed backwards by roughly 85mm all around, causing the pedals to move towards the occupant by a minimum of 51mm and a maximum of 93mm , which is seen for the accelerator pedal. The wheel has a reduced effect due fact that gets squeezed against the honeycomb, sharing part of the loading through deformation of the PDB. As a result, the area of the firewall adjacent to the wheel arch is deformed by a more limited, although still considerable, amount. Due to the same reason, the base of the A-pillar undergoes a deformation of 42mm in correspondence with the tire, while the sill shows signs of initial deformation at the point of maximum loading of the cabin. These however do not translate into catastrophic failure and this part of the structure remains intact, apart for a small dent just behind the connection with the A-pillar. In a similar fashion to the ODB test, the movement of the A-pillar pushes on the roof rail and makes it collapse in front of the B-pillar. The maximum deformation showed appears to be in part elastic, as during the rebound the angle between pillar and rail increases again, resulting in a less critical situation. The floor is again deformed by the gear selector lever, hence its damage is for the most part overestimated. Finally, the deformation of the firewall and pillar still causes the dashboard to move by a worrying amount towards the driver, which sees the distance between the seat and the steering wheel reduced by a maximum of 66mm - not considering

the collapse of the steering column. The area of the knees is also greatly affected due to the way in which the bottom part of the dashboard is pushed backwards.

In conclusion, the vehicle would not achieve positive results for occupant protection even if the MPDB test was to be carried out. The front structures of the vehicle, during the first three quarters of the impact work in a reasonably positive manner and absorb a big part of the energy of the crash. This is, however, still not enough to prevent the cabin from being burdened with the task of absorbing a too large portion of energy for it to be safe.

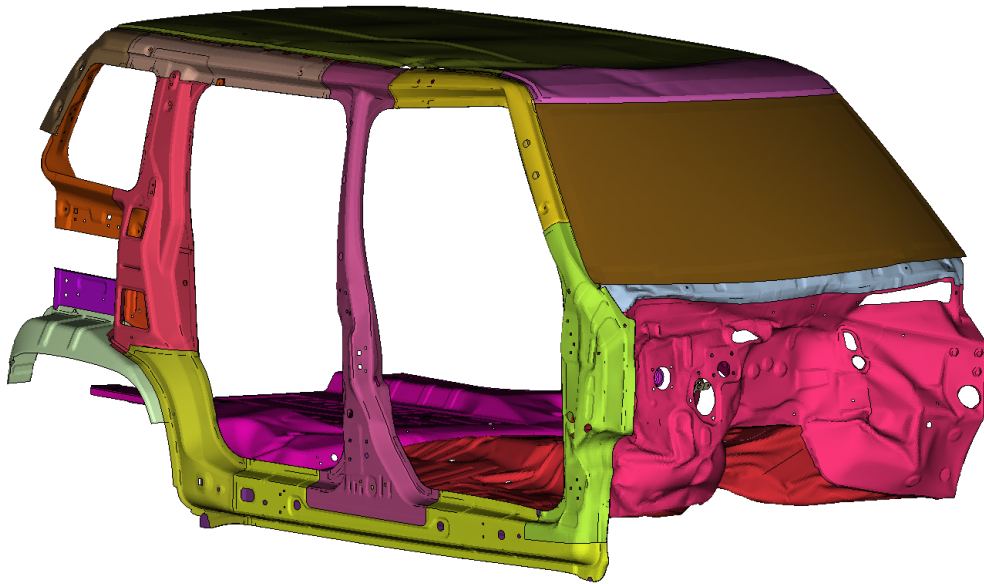


(a) Driver side



(b) Passenger side

Figure 5.74: U Model MPDB - firewall intrusion



(a) Cabin structure



(b) Driver side intrusion

Figure 5.75: U Model MPDB - cabin deformation and interior intrusion

Table 5.13: U Model MPDB - intrusion measurements

	Direction or Position	Intrusion [mm]
Steering column	x	66
	y	-5.6
	z	36
A pillar	upper	29
	lower	42
Firewall	upper	135
	lower	73
Door opening width - driver side	upper	35
	lower	14
Door opening width - passenger side	upper	4
	lower	1
Cross car beam - fixture point	x	63
	y	-6.2
	z	39
Cross car beam - max deformation	x	68
	y	-5.4
	z	25

5.4.3 Comparison

Energy content

In terms of energy, the mass of the model makes the two tests very similar, with the current procedure having a total energy of $306kJ$ against the MPDB's $303kJ$. This accounts for a difference just under 1%. In reality, however, the amount of energy absorbed by the vehicle structures in the two tests appears to be substantially different: in the ODB test the barrier is pushed to the side and the large majority of the honeycomb structure is not compressed at all but only moved in the Y direction. Clearly, this mode of deformation requires a lower amount of energy compared to axially crushing the aluminium cells. On the other hand, apart for requiring more energy to be compressed from a purely theoretical standpoint, the PDB is loaded as it is supposed to be: the cores are sequentially compressed axially and the whole frontal part of the vehicle is utilised to perform this deformation, which in turn takes up part of the impact energy. Therefore, the considerable difference seen in the damage to the structures and to the cabin seems to be due more to the dynamics of the crash test itself than to a large difference in energetic content. Furthermore, a possible issue of the model affecting the differences seen will be investigated in the next paragraph.

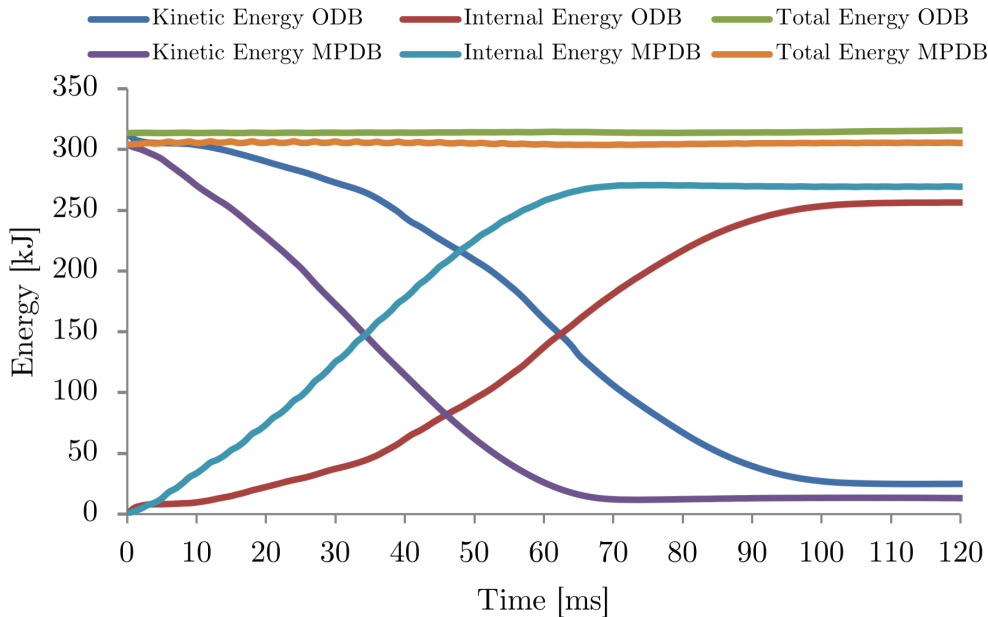


Figure 5.76: U Model - energy content comparison

Crash pulse

Looking at the crash pulse, the behaviour mentioned above is made even more evident: in the first 20% of the MPDB crash, the vehicle has already gone through a high peak of acceleration, deforming the barrier front core and part of the middle core, damaging a great part of the upper front structures and also loading both main rails and crash boxes. In ODB, during an equal percentage of the crash, the vehicle is only lightly loaded as it moves the barrier laterally and after 35ms (35%) finally hits the rigid wall and the lower structures start being loaded. The maximum acceleration peak achieved is similar for both tests, with a difference of only 1g, while the average is substantially higher for the MPDB, still mainly due to the peak occurring at the beginning of the crash. This is visible also in Figure 5.80, where the slope of the line is much steeper for the new procedure in the initial stages of the impact, while the ODB shows a flat line. In addition, another substantial difference is represented by the behaviour of the engine mounts and consequent movement of the engine block. In the first ms of the crash the force exerted by the mobile barrier on the vehicle causes the engine mounts to deform and partially detach from their position, allowing the engine to move and hit the firewall. Part of the initial high peak can be attributed to this phenomenon, which affects the subsequent stages of the crash. This does not occur in ODB due to the softer initial contact with the barrier. It has to be further investigated if what is seen in the MPDB is in fact realistic. The two models are identical as they have not been modified in any way, apart for the dummy masses, between one procedure and the other, hence it seems that the comparison is meaningful; however, the engine mounts could have modeling issues which are made evident only in the new procedure.

With regards to the differences in deformation of the crash structures, it has to be

noted that the crash box appears to be working properly only in the ODB, as in the mobile barrier test it is pulled inwards by the cross beam and fails due to bending rather than axially. On the other hand, the load direction caused by the rigid block behind the barrier makes the component buckle perfectly in the current procedure. Furthermore, the main rail undergoes a much higher level of deformation, as it is the only element supporting the load against the rigid block. In MPDB the left hand side rail shares part of the load, failing axially only a few *ms* after the left hand one starts to buckle. These differences in behaviour of the main rails drive another point of discrepancy between the two tests, which consists in the loading of the sill and firewall by the wheel and tire assembly. In the ODB this component sees a much more reduced space and a high force being applied to it as it is squeezed between a rigid block and the cabin of the vehicle. In MPDB this is still present but to a lesser extent as the main rail has not been shortened as much, and the tire is blocked between the sill and the barrier's deformable element.

The results of all the differences here reported cause major discrepancies between the loads that the cabin has to sustain at the end of the crash and the consequent levels of deformation and intrusion that will be shown at the end of this section.

Table 5.14: U model - ODB vs MPDB dynamic data

	ODB	MPDB	Difference	% Difference
Peak acc. [$-g$]	36.32	35.40	0.92	2.52
Mean acc. [$-g$]	15.96	20.76	-4.80	-30.11
Time to zero velocity [s]	103.10	69.50	33.60	32.59



Figure 5.77: U Model ODB - structural damage

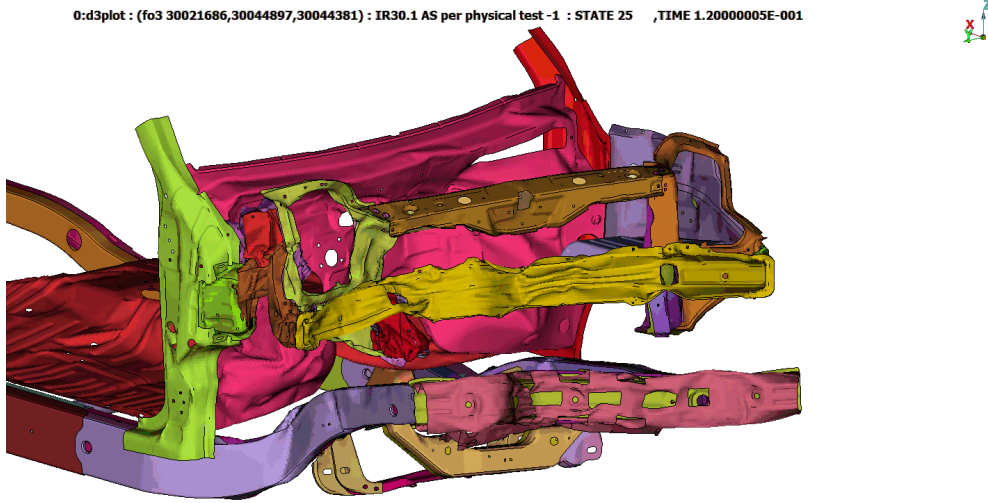


Figure 5.78: U Model MPDB - structural damage

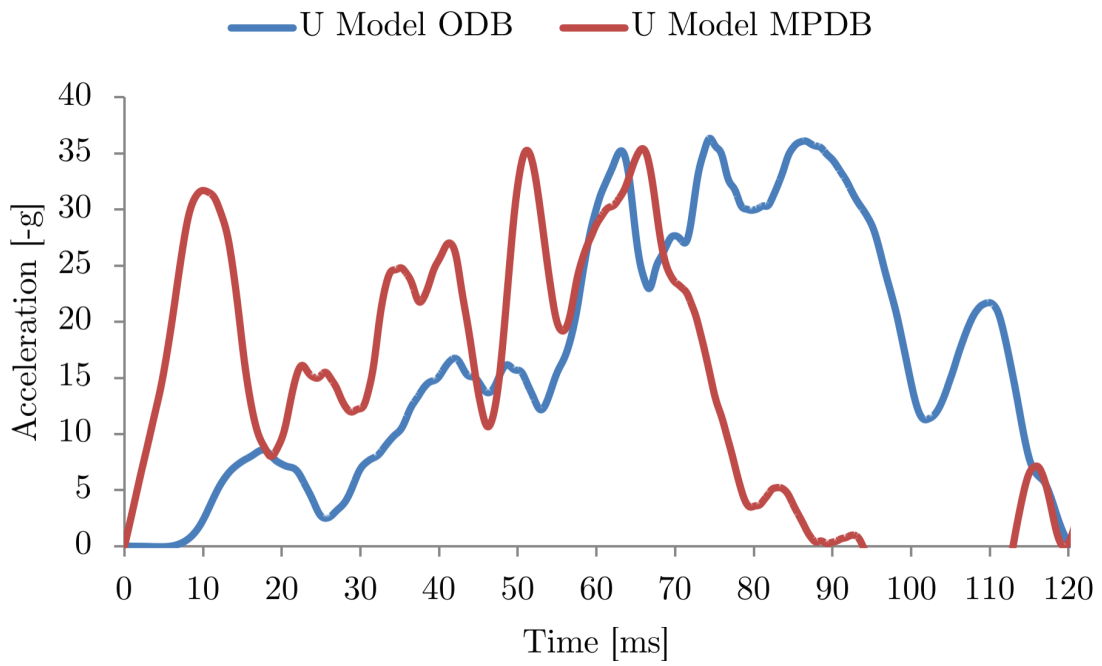


Figure 5.79: U Model - crash pulse comparison

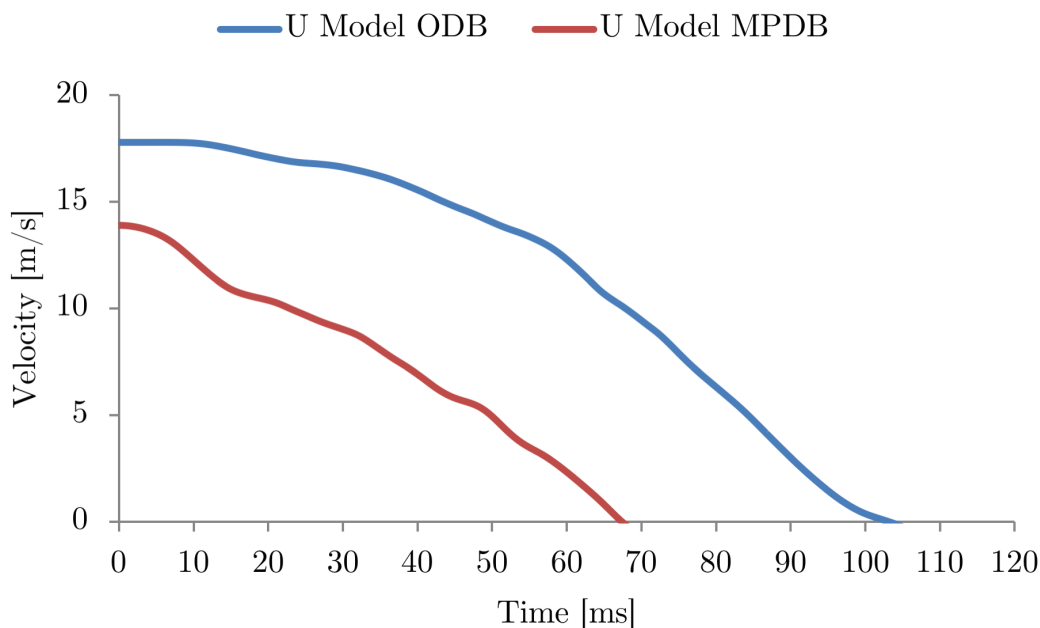


Figure 5.80: U Model - velocity comparison

Section forces

The section forces comparison shown in Figure 5.81 highlights better the trends analysed in the previous paragraph, concerning the right hand side crash structures. The crash box in the MPDB procedure clearly has to support a much lower loading compared to that seen in ODB and its point of failure is not under the maximum allowable load that the component was designed for, but due to an incorrect failure mode. The front part of the main rail also sees a much lower force, which justifies the lower level of deformation in this section of the structure. Finally, the rear section forces appear to be similar in the peak force under which they collapse. A more interesting trend, however, is presented in Figure 5.81: it is possible to see how the left hand side rail is loaded in a relevant way during the MPDB impact. During the initial phases of the crash, this part of the structure is experiencing about 60% of the force of the directly loaded rail; in the final part of the crash, the structure is loaded again to about half the values seen by the rear segment of the rhs structures. In the ODB, on the other hand, this does not occur at all: the loads are extremely low for the whole duration of the impact, up until the point where the rail is pulled towards the centreline of the vehicle and fails due to bending. The overall contribution of this structure towards energy absorption and limitation of the damage to the cabin seems to be vastly different between the two tests. This trend was visible in the previous vehicles as well, but its significance was absolutely marginal, while in this case it is definitely worth noting. Regarding the section force trends for the locations further down the rail, the same behaviour can be found, but the difference between the two tests goes diminishing due to decreased values seen in the MPDB, while the ones for ODB remain very low throughout.

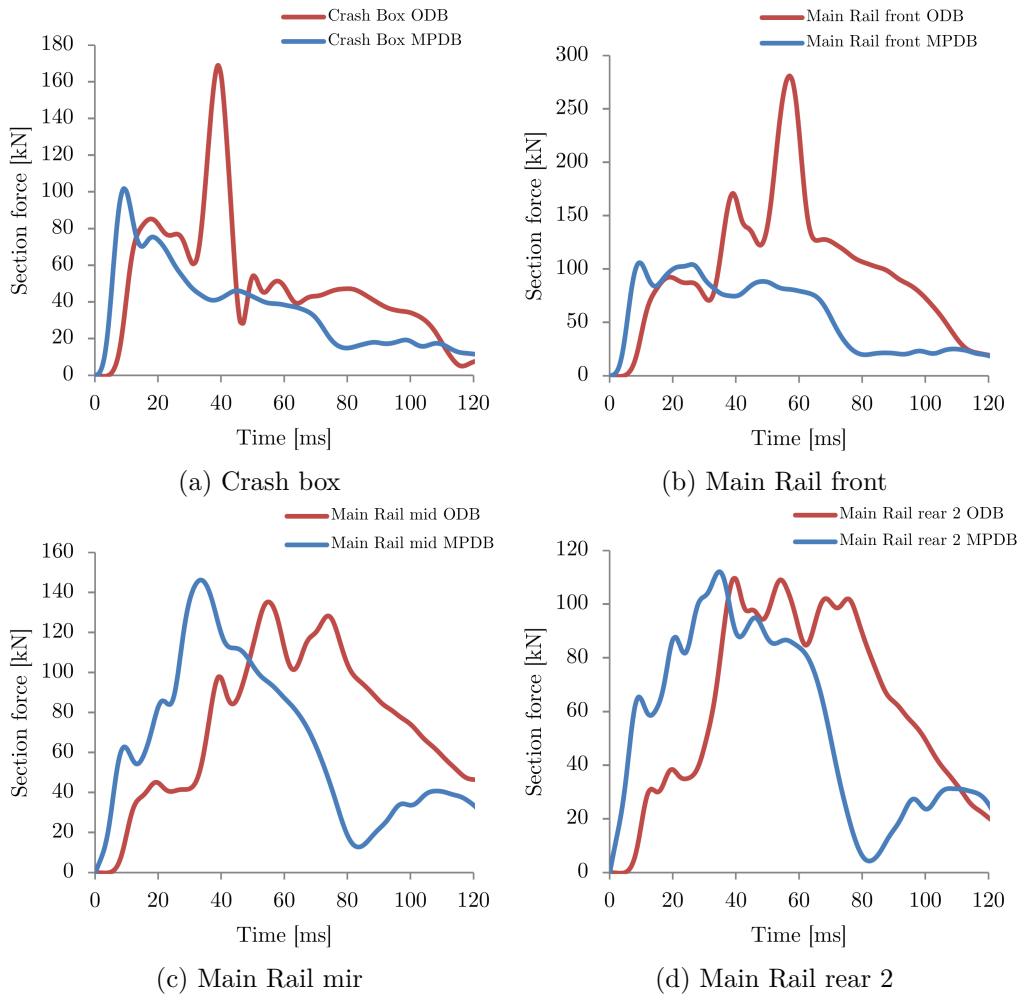


Figure 5.81: U Model - RHS section force comparison

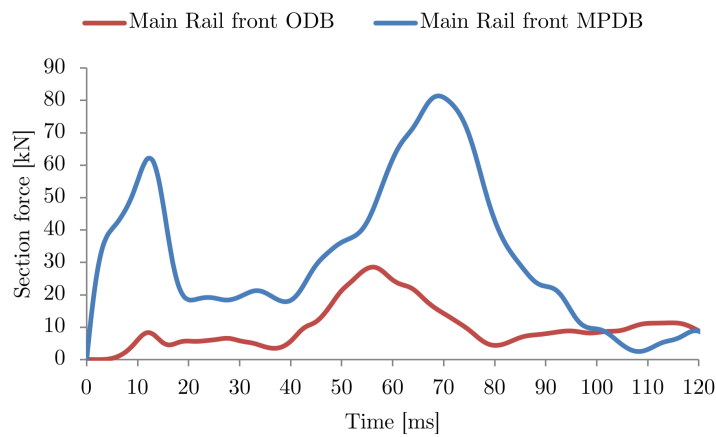


Figure 5.82: U Model - LHS rail section forces comparison

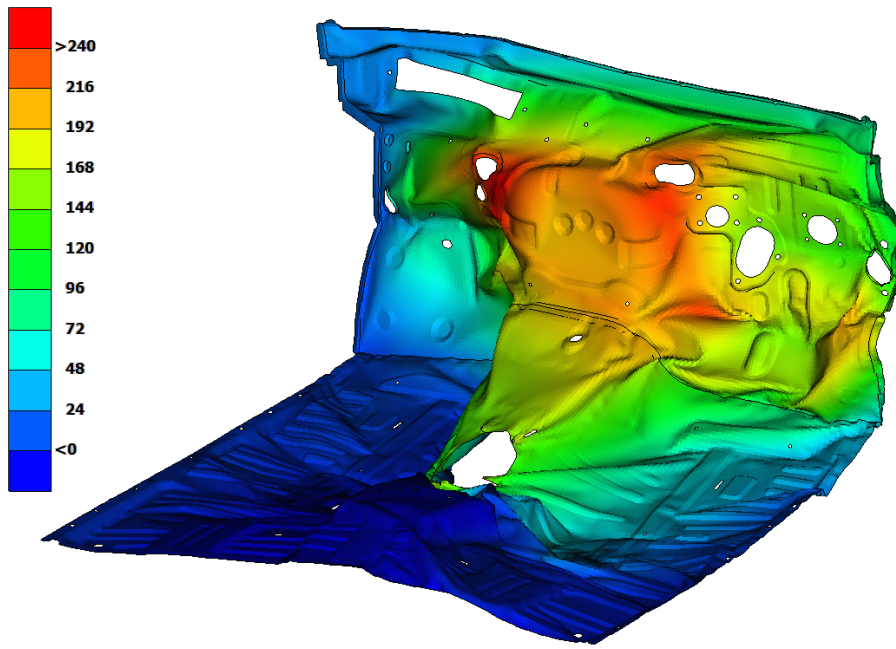
Intrusion and cabin deformation

As already mentioned, the deformation and intrusion levels of the U model are all around very high. The results of the ODB test however are considerably worse than those obtained from the mobile barrier procedure, under every aspect. Table 5.15 shows the comparison between the values recorded for the two tests and there is no area showing a small discrepancy, while no value is low in the first place. The firewall deformation reaches values above $240mm$ for the current test procedure, with the pedals and the passenger area all being greatly affected, while the same deformation in the MPDB shows maxima of $170mm$ and a lower pedal backwards movement. Furthermore, it is evident that the deformation of the A-pillar, sill and consequent failure of the roof are much more pronounced in the ODB, where the deformation shows its effects until the rearmost parts of the cabin's side and top panel. The B-pillar is also affected in the offset deformable barrier test, while it shows no damage at all in the new procedure. These phenomena result in much larger intrusion of the dashboard, steering wheel and instrument cluster, both on the upper section and in correspondence with the knee area, as it is visible in Figure 5.84.

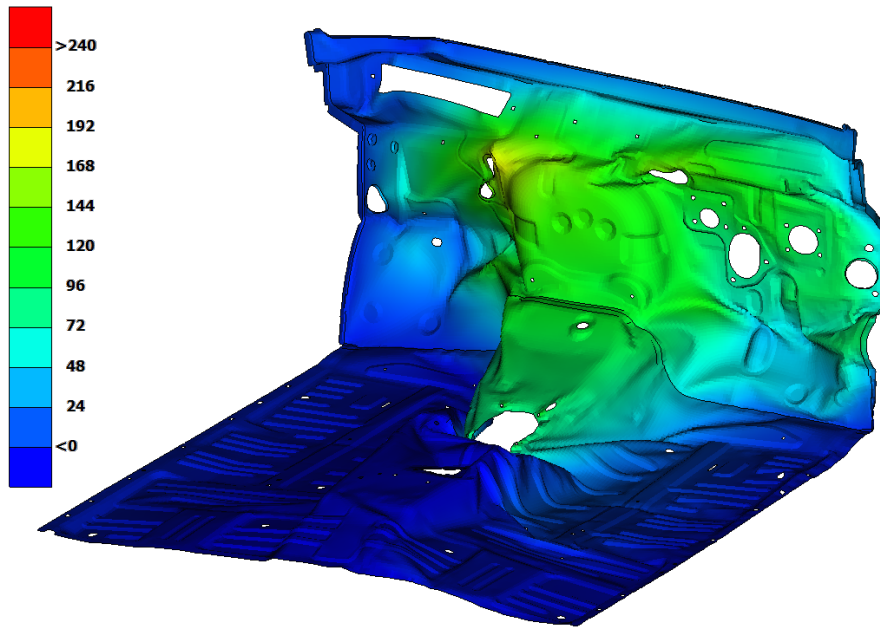
In conclusion, the vehicle's performance is not adequate in both procedures. The results, however, show that the vehicle would need a more limited number of actions in order to achieve a satisfactory level of occupant protection, due to the lower intrusions and reduced cabin collapse obtained through MPDB procedure. Nonetheless, the whole frontal structure would have to be highly revisited to achieve this objective. A completely different problem is represented by the issue of partner protection, as the vehicle clearly deforms heavily the barrier with the main rail puncturing it deeply.

Table 5.15: U Model - intrusion measurement comparison

	Direction or Position	ODB [mm]	MPDB [mm]	Difference [mm]
Steering column	x	108	66	-42
	y	-10.5	-5.6	-4.9
	z	72	36	-36
A pillar	upper	71	29	-42
	lower	109	42	-67
Firewall	upper	190	135	-55
	lower	181	73	-108
Door opening width - driver side	upper	99	35	-64
	lower	91	14	-77
Door opening width - passenger side	upper	9	4	-5
	lower	9	1	-8
Cross car beam - fixture point	x	103	63	-40
	y	-7.9	-6.2	-1.7
	z	91	39	-52



(a) ODB
1



(b) MPDB

Figure 5.83: U Model - firewall intrusion comparison



(a) ODB



(b) MPDB

Figure 5.84: U Model - interior intrusion comparison

5.5 Conclusions

Given the results of this section of the study, it is clear that the findings are in line with the expectations set by the analysis of the existing literature, for the most part. Overall, the mobile barrier test results show equal or lower values in terms of accelerations peaks achieved, moving the issue on increased levels of intrusion for light vehicles, which are those for which the new procedure proves to be harsher than the Euro NCAP ODB. In terms of overall crash pulse, however, the MPDB proved to be consistently harsher due to the reduced amount of time between start and end of the event. The trend of correlation between test severity and vehicle mass was also confirmed. In fact, the lightest analysed vehicle, the Toyota Yaris, showed significantly higher damage when crashed following the new procedure, as the much higher energy involved in the crash could not be absorbed by the frontal structures in an efficient manner. When this vehicle was new and tested by Euro NCAP it achieved a five star rating. If it was to be tested in 2020, it would achieve a significantly lower star rating. The intrusion measurements recorded for the MPDB were several multiples above those of the ODB and the survival space was diminished to a critical point. The structure of the light city car would need to be reworked heavily in order to achieve even moderately positive results. This is in fact a very important result, as it proves that the step taken by Euro NCAP is in fact going in the right direction and representing real world crash dynamics in a more representative way.

In second instance, the D-segment vehicle with a mass similar to the barrier showed to be affected in a much less dramatic way by the mobile barrier. The total energy of the impact is still greater for MPDB but the increased portion absorbed by the PDB makes the results in terms of intrusion fairly similar. It has to be noted that this vehicle includes frontal structures which were designed not only to perform well in the ODB but also to initiate the process of improving partner protection, hence with the mindset directed towards car-to-car crashes. The design will have to be improved under certain aspects in order to achieve the same results seen for ODB after 2020, such as the zone of the firewall supporting the frontal structures. Unfortunately, in this project it was not possible to analyse the dynamic behaviour of this vehicle in terms of acceleration pulse, due to issues with the creation of the model that could not be resolved. Further investigation in vehicles of this segment will have to be carried out to obtain trustworthy results.

Concerning the third vehicle simulated, the trend seen for the Yaris was completely reversed. In fact, the large mass of the Chevrolet Silverado, in conjunction with its not so sophisticated structural design, resulted in considerable damage in the ODB test, with evident deformation of the cabin and considerable intrusion in the passenger compartment. The MPDB in this case proved to be much simpler to withstand for the vehicle structures mainly due to the diminished amount of energy involved in the crash. The maximum acceleration achieved was also considerably lower than that caused by ODB. In this case, while no issues will be experienced in terms of occupant protection, the attention will have to be directed towards partner protection and the balance between the two aspects will be the challenge for structural redesign.

With regards to the last vehicle, which was not designed to be tested in the Euro NCAP ODB procedure, the results of both tests were negative, but with some key differences. In the ODB test the structure of the vehicle collapsed heavily, the intrusion of the firewall and consequent displacement of all interior equipment towards the driver are a major concern,

together with the significant collapse of the roof rail and A-pillar. In the MPDB test, the same trends were seen but the recorded values of intrusion were significantly lower, in most cases at least halved. In this instance the mass of the vehicle is so that the theoretical amount of energy in the crash is extremely similar, but the PDB clearly absorbs a higher amount of energy and justifies the different results. Although the performance is still critical, the new test shows that less extensive design changes would have to be made to make the SUV achieve good results in the new Euro NCAP test. It must be noted that, in order to confirm these findings, the model would have to be tested again including the front bumper, bonnet and wing panels. In this way, the offset deformable barrier could potentially be loaded in a more efficient way.

The test ran on the U model highlighted another important aspect which consists in difference in loading of the opposite side rail. In the ODB test, as for all other vehicles, the section force achieved across the rail not directly lined up with the barrier was negligible, with the only seen failure mode being due to bending. In the MPDB, the different configuration of the deformable element and the increased overlap made it possible to increase substantially the force on the LHS main rail, which in contributed to decreasing the amount of energy left at the moment of direct impact with the firewall. This behaviour is present in the results from the other three vehicles as well, but not quite to such a substantial extent: modifications to the frontal structures, in combination with the new overlap level, could try to apply measures to exploit such phenomenon in a more efficient way than it was possible for ODB and improve the occupant protection results.

Finally, a less expected result was noticed in terms of direction of loading of the crash structures and crash boxes. From the theoretical knowledge achieved in the initial chapters, the progressive deformable barrier was meant to create a much more complex loading environment for the frontal structures of vehicles. However, in three out of four simulations the frontal part of the vehicle was loaded in a very similar way to ODB, with the crash boxes failing due to axial load and the crash structures behaving comparably to the previous test. The biggest contributors to this factor seem to be the bumpers, which remain partially intact while penetrating the first PDB block, and the nature of the barrier itself, which generally starts collapsing the structures as soon as the second, stiffer core is reached. The only vehicle for which this behaviour was not present was the U Model, as the crash box bent out of shape and did not collapse axially. As stated above, the model did not have a front bumper, a factor that could change this result if the assumptions here explained were to be realistic. However, the sample of vehicles tests would have to be increased in order to establish a clear and convincing trend.

Chapter 6

Partner protection analysis

In this chapter, the work completed in order to gain an understanding of the partner protection level of the tested vehicles is reported. Initially, a proposition found in literature for the procedure that will be used in Euro NCAP's assessment is explained in the details available to date; next, a brief description of the methodology used to apply this procedure in the simulation study is given. The results of barrier deformation and acceleration obtained from the MPDB simulations of the four vehicles utilised until this point are analysed in order to highlight criticalities and positive achievements. Finally, the performance of the four vehicles is compared to draw conclusions on the findings.

6.1 Partner protection in Euro NCAP 2020

In Chapter 2, it was anticipated that a second important change will be made to the Euro NCAP rating system, in order to include an evaluation of the partner protection performance of the tested vehicles. This is a critical point for the consumer testing programme, as it is the first time that such a rating is introduced in any kind of official and extensive crash procedure. The driver for this change, as explained in Chapter 2, is the need to evaluate clearly what vehicles perform better at protecting the opponent, without limiting the effectiveness of their safety structures to occupant protection. An official or draft procedure regarding the methods that will be utilised to perform this part of the rating has not been published yet, but several studies have been completed to find a suitable proposal. The most relevant and reliable source is represented by the publications of Volker et al. [19] and the criteria for assessment utilised in their study were the starting point for the results reported in this chapter. The method to assess partner protection is based on the higher rigidity of the PDB, which has been developed in order to deform in a less substantial way compared to ODB; this allows to obtain an accurate idea of the aggressiveness of the frontal structures of the tested vehicle by analysing the deformation of the honeycomb. In the physical tests, the deformed barrier is inspected at the end of the crash and a 3D scan of the face of the barrier is performed. A grid of points evenly spaced in the Y-Z plane is placed in correspondence with the undeformed barrier face position, $790mm$ from the trolley face. The grid is then projected on the deformed barrier and the displacement of the point to reach the deformed face is recorded. These values are then analysed to

perform a homogeneity assessment: the average intrusion depth and the standard deviation are calculated to give a quantitative parameter for the evaluation. A higher value for standard deviation entails that the discordance between the deformation of different parts of the barrier is higher, hence resulting in an imbalance between more and less aggressive zones of the crumple zone. The average, on the other hand, gives an idea of the portion of energy that the vehicle has been able to absorb through the deformation of its own crash structures, hence being less harsh on the barrier - or partner vehicle. In order to obtain meaningful results, a limited area of the barrier has been selected: due to the kinematics of the impact, which include the rotational motion of the vehicle and barrier at the end of the event, the edge of the barrier placed at the centreline of the vehicle is deformed more deeply than the rest of the element. In an opposite manner, the area in proximity of the opposite vertical edge will be most likely much less deformed than the rest of the barrier. The inclusion of these areas in the measurement would lead to unrealistically poor results which would not be meaningful for the representation of a car-to-car crash. Therefore, corridors of a predefined width from each of the vertical edges of the barrier will be left out from the evaluation. The same rationale is used also for the very top and bottom parts of the PDB, which will be left out to take into account only the most significant area.

Furthermore, the rating criteria also include the assessment of the change in velocity of the trolley. The procedure of barrier assessment described above does not take into account the total amount of energy involved in the crash, due to the fact that it does not take into account the whole barrier deformation. For this reason, an additional criterion is added in the form of an addition or subtraction to the score: a change in velocity lower than 50km/h is seen as a positive, while a value above the starting velocity is regarded as a negative. In addition to what is presented in [19], the acceleration of the trolley will also be taken into account and compared to that of the vehicle.

6.2 Analysis methodology in simulation

As the procedure described above is designed for a physical test, a method to reproduce it in simulation had to be established. First of all, the deformed barrier element was extracted from the MPDB simulation of each vehicle through META. The element was saved as a model suitable for utilisation in the pre-processor and was hence imported in ANSA. Here, the model was cleaned from any elements that had detached from the honeycomb during the impact, in order to have a clean working surface, as it would be after the end of the crash, when all components have settled. At this point, the area of interest of the barrier had to be defined and it was decided to disregard corridors of 200mm width from each vertical edge and corridors of 100mm from the top and bottom edges. These limits were set in ANSA and all the nodes of the frontal face of the barrier were selected. Due to the fact that the solver was set to delete overly deformed elements in order to avoid simulation failure, cleaning of the selected nodes had to be performed: in portions of the barrier where the frontmost face presented holes due to deleted elements, the nodes seen by the software as the ones closer to the surface were in fact far inside undeformed layers and had to be manually deselected. Next, a new reference frame was created in correspondence with one of the corners of the barrier's support plate and the coordinates of the model were shifted to this custom position. In this way, the reading of the X coordinate of the selected

nodes represents the length of undeformed barrier still left behind the node. Finally, the array of coordinates was exported and processed in order to obtain the opposite value, corresponding to the X displacement of each node in relation to the original location of the barrier face. This process allowed to have very accurate readings for average and standard deviation, as the minimum number of collected data points was 35'000. In addition, the accelerometer readings of the trolley were analysed in the same manner as those reported in the previous chapter to understand change in velocity and crash pulse.

6.3 Partner protection results

6.3.1 Toyota Yaris

The Toyota Yaris shows very poor results in terms of compatibility. The average deformation level is set at $329.3mm$, which is considerable given the low mass of the vehicle, while a standard deviation value of $143.4mm$ highlights very high unevenness between barrier areas. Analysing the crash animation, it is clear that a great deal of deformation is caused by the wheel and tire assembly and by the engine block, both of which push heavily on the honeycomb in the final parts of the crash. The greatest level of unevenness is however due to the behaviour of the main load path and cross beam: the main rail fails in a point closer to the firewall and its frontal section remains mostly straight, pointing at the barrier, while the cross beam deforms very close to the rail, accentuating the spear-like effect of this structure. In addition, due to the complete failure of the supporting structures, most of the rigid components in the engine compartment come into contact with the barrier blocks in the final part of the event, deforming other parts of the honeycomb in a significant way. Figure 6.1 shows the areas of max deformation and it is easy to notice how the central area, affected by the main rail is considerably more deformed than the surrounding parts, reaching maximum values above $600mm$. The low deformation caused by the bonnet and the low front end of the car also caused zones of the area of interest to be deformed by only $13mm$, hence contributing further to the increase in standard deviation. It will have to be established through a more specific procedure if a threshold is to be set for such low values, in order to avoid unreliable conclusions. On a side note, the colour scheme shown in Figure 6.1 is the same used in [19], where values above $480mm$ are all considered in the worst possible category. This will presumably be the limit utilised for additional penalties in the evaluation. Furthermore, it has to be noted that the areas of the figure that show very low deformation values, surrounded by red zones, are to be considered red as well: those areas correspond to regions where the elements were deformed too much and had to be deleted. The software only reads displacement of nodes, hence the visible ones correspond to deeper layers which were not interested by the deformation but are exposed due to the deletion of ones further in front.

Moving the attention onto dynamic data, the situation appears to be better than that depicted by the barrier deformation analysis. The change in velocity of the trolley is equal to $49 km/h$ at the end of the simulation, as the vehicle gets pushed backwards by the barrier, which slowly exhausts its kinetic energy during the final ms of the crash. However, if the velocity of the barrier is assessed at the instant where the vehicle velocity crosses zero and is reversed, it is possible to see that the change in velocity is in fact only $10.64m/s$, or $38km/h$. When comparing the acceleration pulse of the Yaris and of the

barrier, the latter is substantially lower, with maximum values of $24.5g$, against the peaks of $43g$ previously shown for the vehicle.

In conclusion, the structure of the yaris showed very poor performance in terms of barrier deformation and it will have to be redesigned with this goal as well. The MPDB test clearly showed that both aspects of partner and occupant protection need to be addressed heavily, contrary to what was shown by the ODB test both in simulation and in Euro NCAP physical testing. The low levels of barrier acceleration are comforting, although they were expected due to the reduced mass of the vehicle.

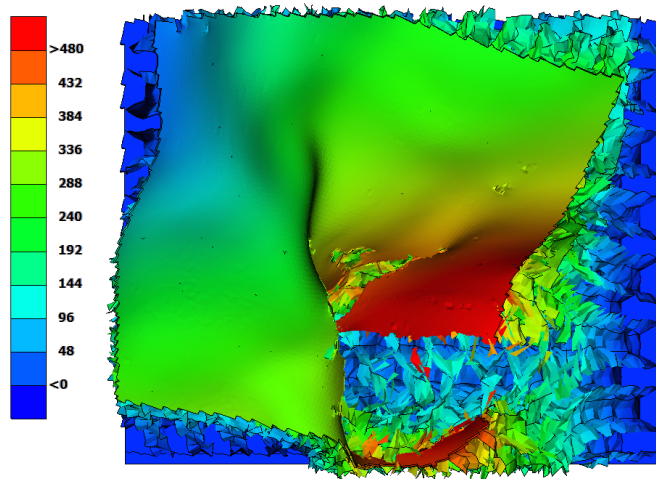


Figure 6.1: Toyota Yaris - barrier deformation in area of interest

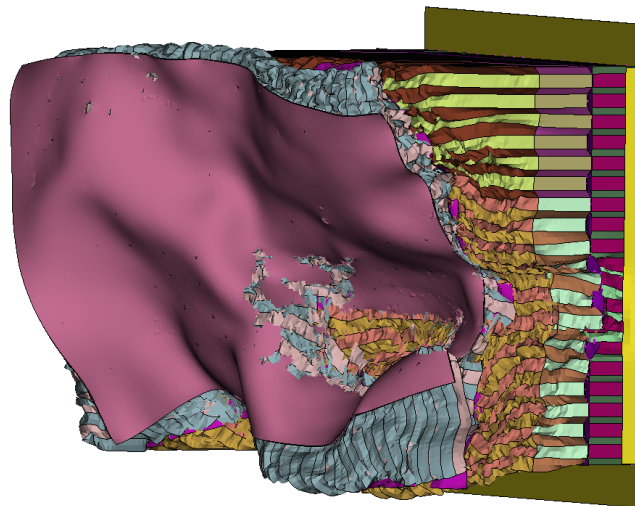


Figure 6.2: Toyota Yaris - overall barrier deformation

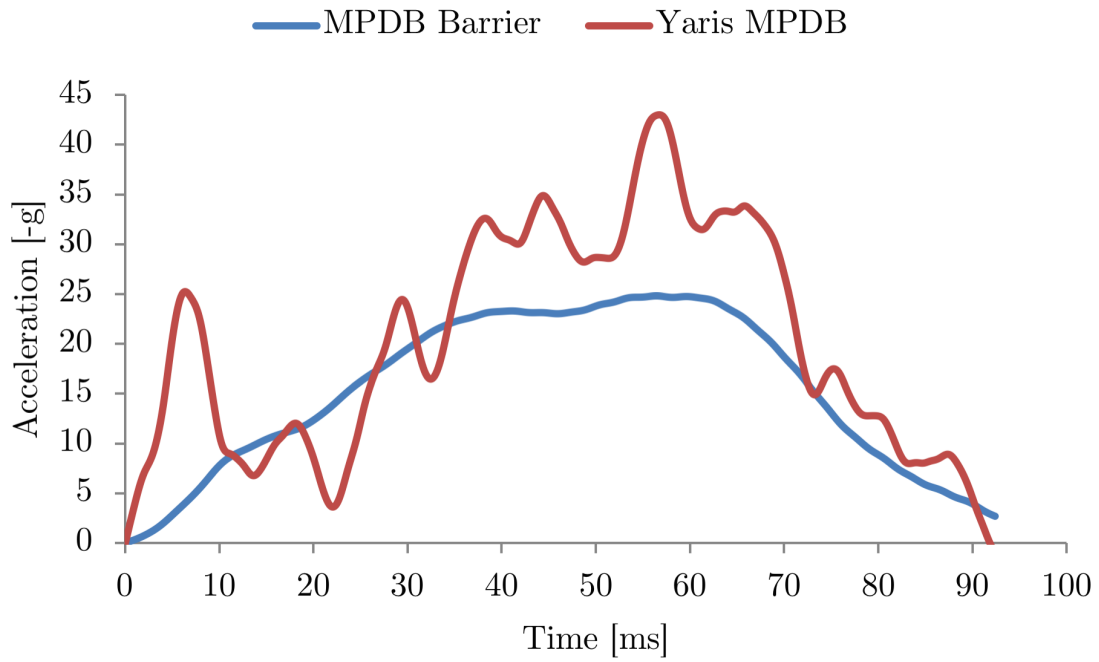


Figure 6.3: Toyota Yaris - barrier and vehicle acceleration comparison

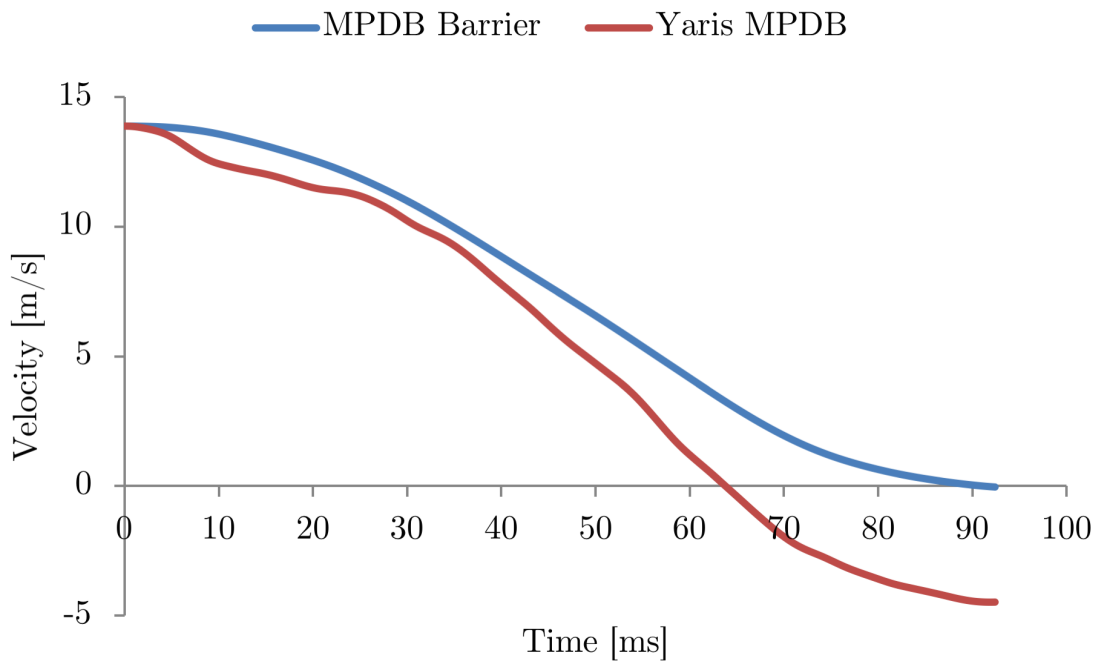


Figure 6.4: Toyota Yaris - barrier and vehicle velocity comparison

6.3.2 Honda Accord

Considering the second vehicle, which is also the one that showed the most balanced results between the two tests, the performance level achieved for partner protection is substantially better than that of the Yaris, mostly in terms of barrier deformation. In fact, the average intrusion level was limited to 290mm and the standard deviation to 71.4mm , the lowest values seen in this study. In combination, the vehicle achieved a maximum value of 542.2mm , and a minimum of 138.4mm . Although these levels will surely be improved by the time the new test is put in place, they show that the initial design efforts produced to improve compatibility are moving in the right direction, as the ACE structure works well by loading the impactor much more evenly than a vehicle with one single load path, such as the Yaris. In the sections dedicated to the explanation of the structural behaviour it has already been highlighted how the multiple load paths create a more or less flat face when undergoing heavy deformation, and this greatly helps loading the partner vehicle evenly. Furthermore, the bonnet acts as an effective shield between the deformable honeycomb and the engine block and rigid engine bay components. The main rail also deforms in multiple points, moving back to the same level of the other metal parts and without poking outwards. In fact, Figure 6.5 shows that in this simulation very few elements were deformed to the point of being deleted and the front cladding sheet of the PDB is almost completely intact: another sign of the positive manner of loading by the vehicle. Nonetheless, the structure is still not perfect and some critical points are evident: the tire is still playing a considerable role in the unevenness, but most importantly the main cross beam is behaving in a way far from ideal. During the impact, this component is pushed upwards and twisted along its longer axis, rather than just being pushed backwards into the the engine bay. This causes the most visible irregularity section and it should be addressed in order to achieve better results, as these will be certainly required if the achievement of a five star rating is the goal.

With regards to acceleration pulse, it is difficult to compare the one of the barrier with that of the vehicle, due to the model issues already mentioned. However, it can be noticed that both the barrier and the vehicle reach zero velocity and rebound in opposite direction at the end of the crash, with the vehicle being pushed back first and the barrier velocity showing a flat trend at -1.21ms , or -4.36km/h , and the vehicle stabilising around -5.8km/h . If the instant in which the vehicle crosses the zero velocity line is considered, the barrier shows to be still moving in its initial direction of motion with a velocity of 3.6km/h . The maximum acceleration achieved is of $27.8g$, which is also lower than the $31g$ achieved by the vehicle, although this final value cannot be considered reliable.

Overall, the Accord design strategy seems to give the intended results, although the path to achieve the best possible results is still not finished. The design direction taken in terms of multiple load paths and connecting segments between them loads the barrier in a more homogeneous way compared to the other designs present in this study. A vehicle of this kind could already achieve decent results if tested on MPDB and with further developments of the ACE structure a high star rating is not out of reach.

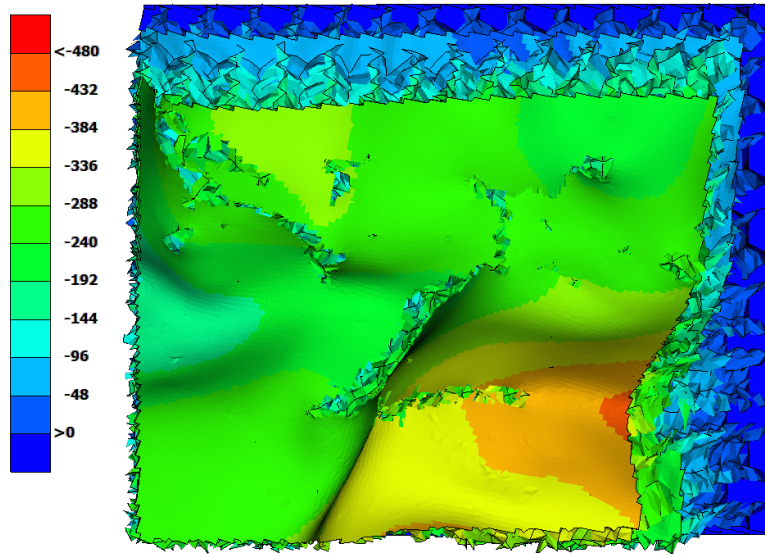


Figure 6.5: Honda Accord - barrier deformation in area of interest

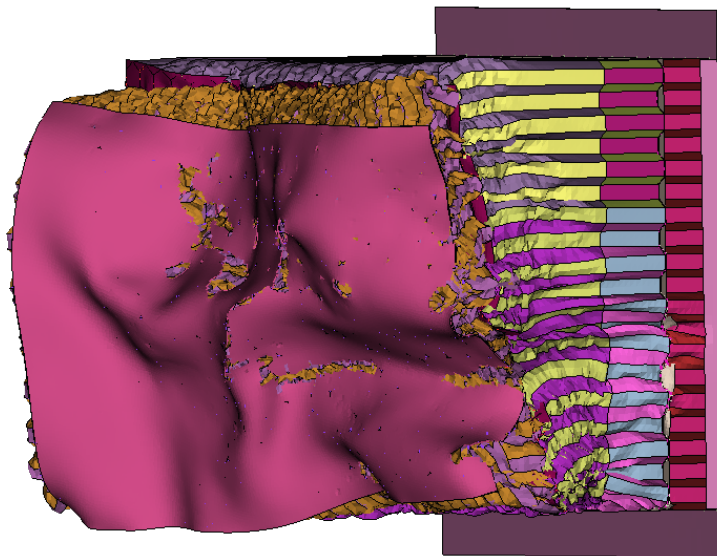


Figure 6.6: Honda Accord - overall barrier deformation

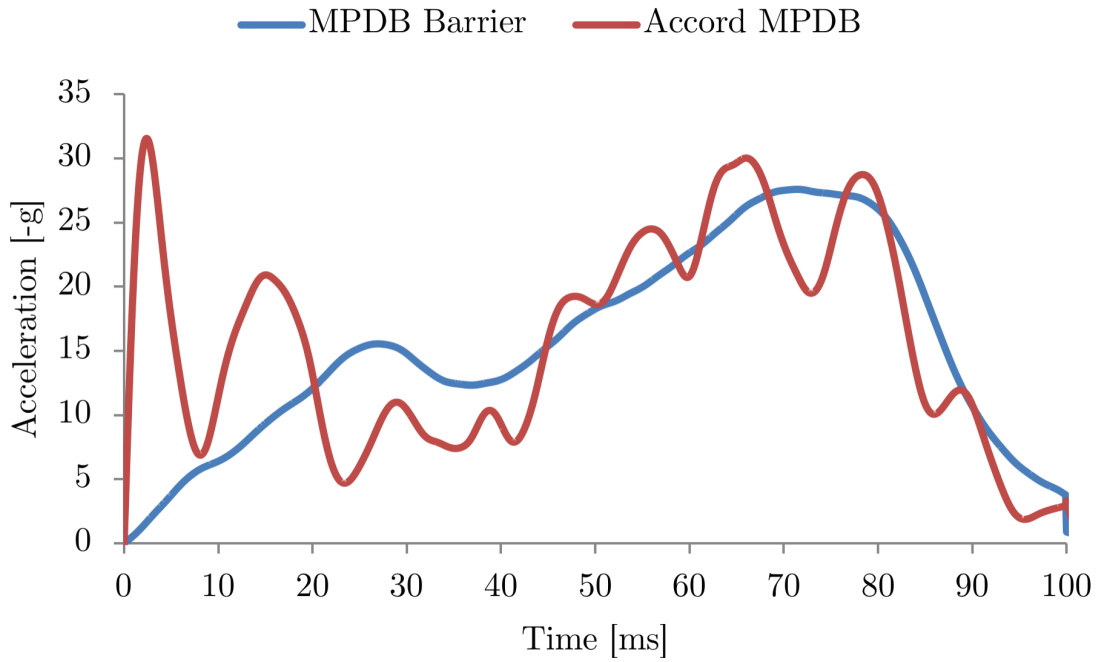


Figure 6.7: Honda Accord - barrier and vehicle acceleration comparison

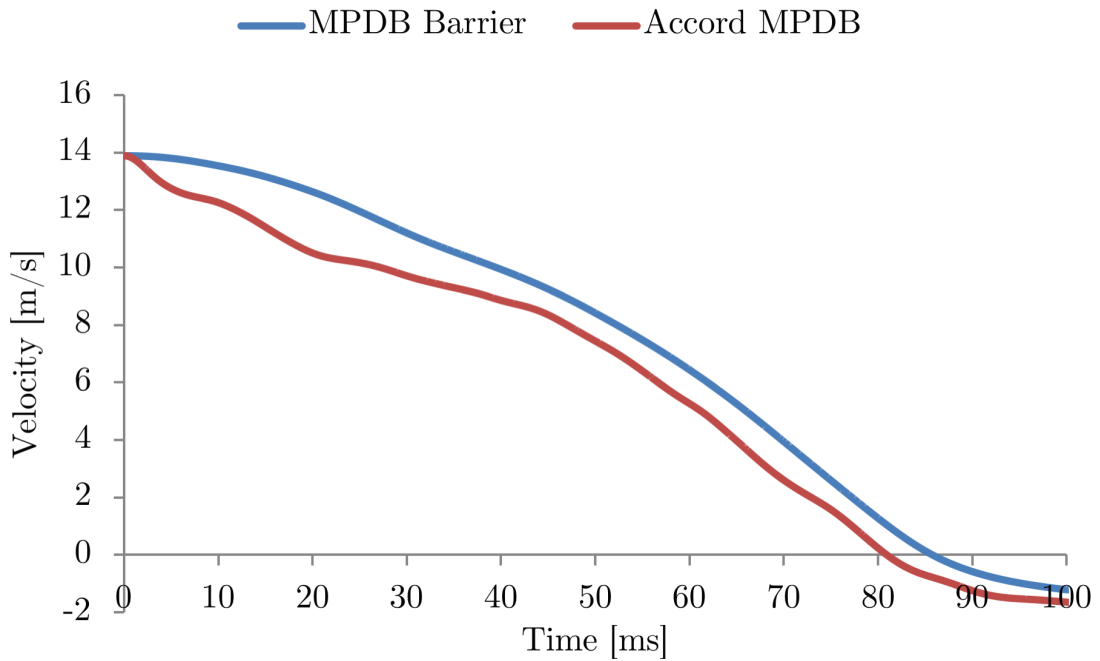


Figure 6.8: Honda Accord - barrier and vehicle velocity comparison

6.3.3 Chevrolet Silverado

The Chevrolet Silverado, as expected due to its ladder chassis construction, achieves very poor results when considering compatibility. The mean value is the highest seen in this study, with 457.1mm of deformation, while the standard deviation is lower than that of the Yaris, but still at a very high level of 100.3mm . The maximum point reached by the vehicle's structures is also the deepest among the four vehicles, at 696.1mm . It is only 3.9mm in front of the last, 90mm deep, honeycomb core. The minimum recorded value, on the other hand, was 204.8mm . The deformation inflicted to the PDB is due, for the most part, to the main rail, the cross beam, the engine cradle and the very large metal plate positioned in front of the crash structure. Also, the metal component which should act as a crash box is far too stiff to deform properly and punctures the barrier very deeply. In the lower section, the honeycomb material that wraps around the cross beam is then crushed by the engine cradle, which is considerably high off the ground and hits the barrier in the area of interest. In addition, the higher structures of the vehicle do not perform any support function and, in fact, they mainly push downwards on the top of the barrier, due to the height of the vehicle and to their low stiffness. One of the main reasons for which the standard deviation is not much higher is the fact that the bumper performs a positive function, effectively spreading - as much as it can - the load on a wider area. If the material of the bumper was softer, the main structures would probably puncture the barrier until the rigid face of the trolley. It is difficult to predict how the ladder chassis structure could be improved to increase the level of partner protection, as adding other load paths is more difficult and the design of the cabin would have to undergo major advancements in order to be able to sustain the loads of other paths. This kind of structure is less and less used in vehicles circulating on European roads, but a great deal of off roaders, heavy duty passenger cars and light commercial vehicles still use this design, especially in markets outside of the EU. Nonetheless, a test of the likes of MPDB could be implemented on the US market as well, forcing the manufacturers either to stop using this design or to improve it vastly, including large shield structures supported in multiple points at the leading edge of the vehicle.

In terms of velocity delta and acceleration, the Silverado shows a very poor performance as well; as expected, it is the worst out of all four vehicles, mainly due to its large mass. The velocity delta in this case is far above 50km/h , as it reaches a final value of -5.4m/s (19.44km/h), hence achieving an effective final change in velocity of 69.44km/h . The acceleration of the trolley is also slightly higher compared to that of the vehicle, with the first achieving a peak of $36.5g$ and the second topping at $35.7g$. It is also noted that the peak point for the barrier is reached much earlier compared to the vehicle, as shown in Figure 6.11.

In conclusion, the extremely positive results shown for occupant protection are, as anticipated, balanced by equal and opposite results for partner protection. The extreme mass of the pickup and the stiffness of the front structures are the exact reason why crashes between cars of very different size in the real world show results that are not closely comparable to laboratory tests, and shows the clear need for an assessment of this type in consumer testing and even more so in legislative regulations.

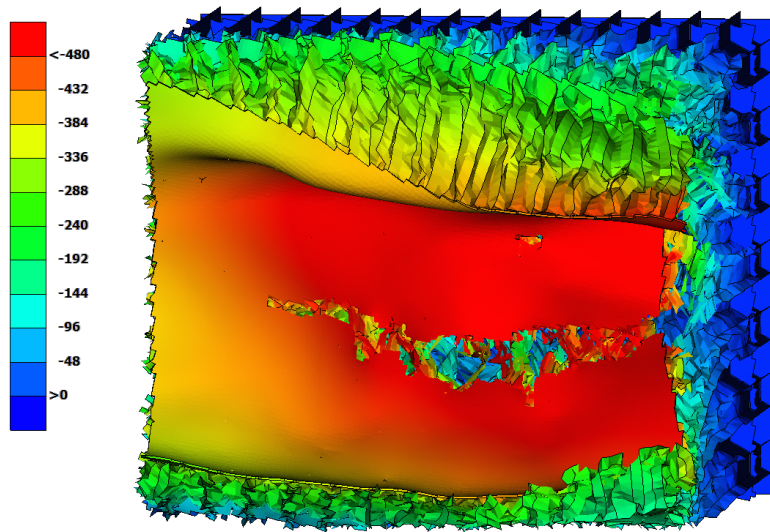


Figure 6.9: Chevrolet Silverado - barrier deformation in area of interest

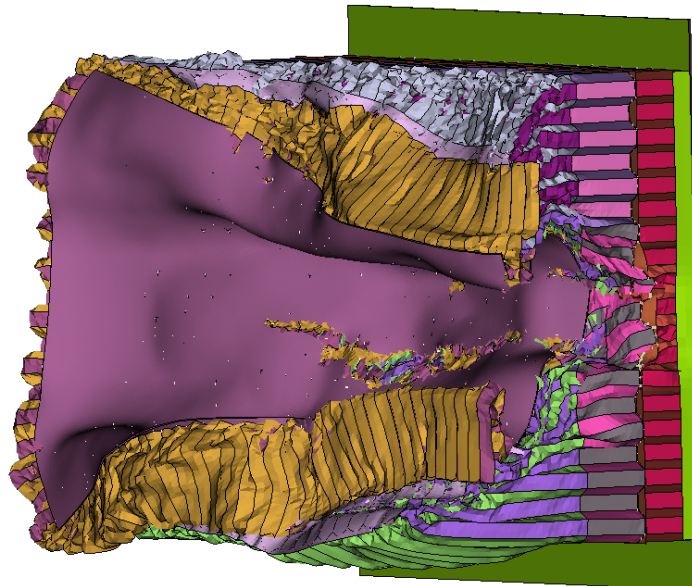


Figure 6.10: Chevrolet Silverado - overall barrier deformation

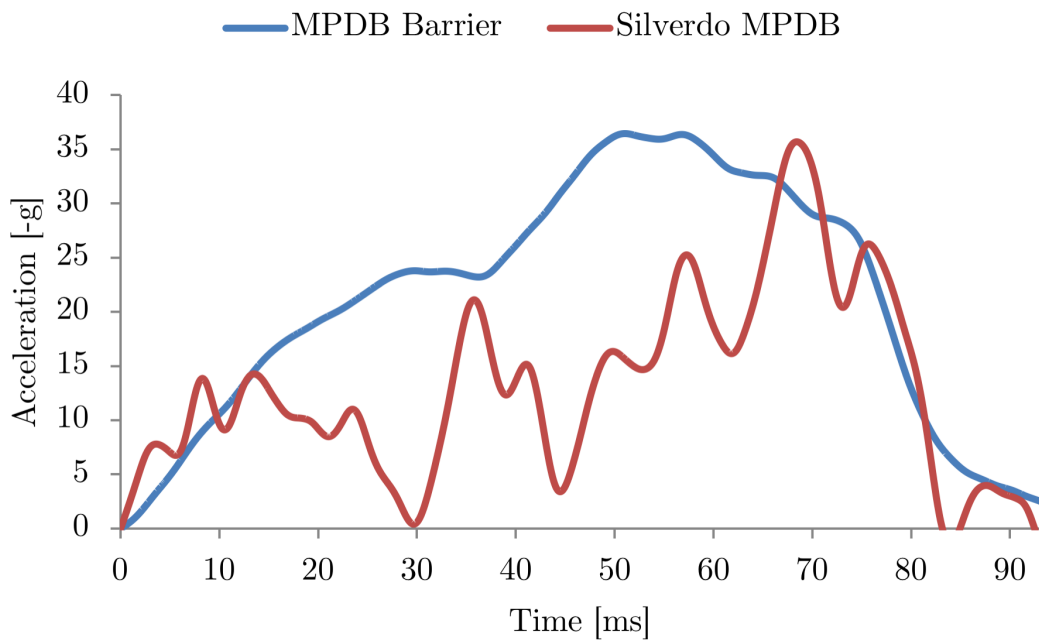


Figure 6.11: Chevrolet Silverado - barrier and vehicle acceleration comparison

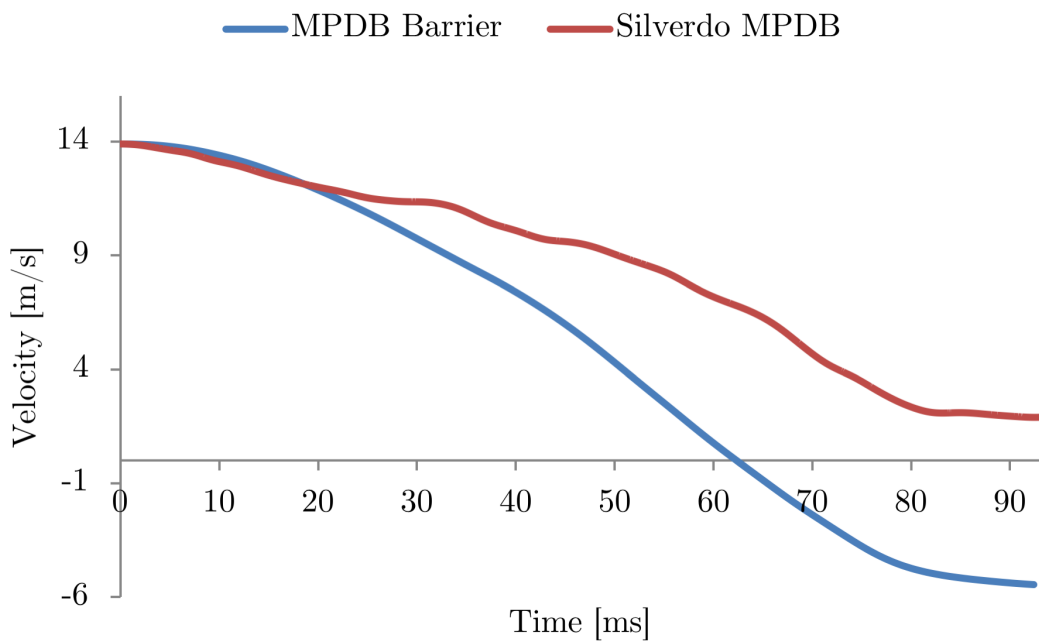


Figure 6.12: Chevrolet Silverado - barrier and vehicle velocity comparison

6.3.4 U Model

The last model tested showed a behaviour in certain ways similar to that of the Silverado, as could be expected from its structural design. The mean deformation is lower to that of the previous vehicle, with a value of 400.2mm . The standard deviation is considerably higher and reaches 110.7mm , while the maximum value is a nearly identical 695.4mm . The minimum value achieved is of 184.2mm . The two main issues with this vehicle are the RHS main rail and the tire-wheel assembly: the former extends for a long distance in front of the other compacted components of the engine bay, as the bending of the pronounced crash box only shortens it by a few mm and the cross beam wraps around it, expanding the area of the barrier that is evidently punctured. The main rail itself does not collapse in a way that reduces its initial length significantly, and the combination of these factors produces the effect shown in Figure 6.13, where the whole area affected by these components shows deleted elements and deep deformation. In addition, the tire pushes heavily on the barrier, deforming it in a substantial way. It is also possible to notice how there is a clear area with lower deformation between the mark left by the wheel and the puncture by the main rail. This is due to the fact that the tested model was not equipped with a front bumper, hence making all the results seen here less significant. The presence of a full front end, namely bumper, bonnet and front wings, would have made the damages to the barrier certainly more homogeneous, although the overall trends would have most likely remained the same. As discussed in the previous chapter, the structure of the U Model shows a higher level of complexity compared to that of the Silverado, with an upper load path that should theoretically produce a more homogeneous deformation of the barrier and this should definitely be verified by using a finalised and complete model. Having this in mind, the failure of the main rail would still need to be redesigned in order to avoid the visible mark left in the honeycomb and spread the load on a larger area.

With regards to the velocity change, in this instance the results are more promising, due to the lower vehicle mass and also to the high levels of structural deformation undergone by the vehicle as a whole. As shown in Figure 6.16, both the vehicle and the trolley move backwards compared to their initial direction of motion and the moment in which they cross the zero line is only 2.4ms apart in favour of the trolley, meaning that the effective delta of velocity is equal to 48km/h . Considering the final velocities reached, on the other hand, the vehicle stabilises at a value of -2.29ms - or -8.2 km/h - while the trolley at a lower -5.4km/h . Looking at the crash pulse comparison, the barrier peak acceleration is of $31.9g$ against a vehicle maximum of $35.4g$.

To sum up, more reliable results will be obtained when a complete model will be available; however, given the severity of the deformations inflicted to the barrier, it is reasonable to assume that major reworking will have to be done with the partner protection design goal in mind as well. The vehicle underperforms heavily under both of the aspects of interest of this study, as it is understandable given that its structure was not designed to undergo such harsh testing. The positive takeaway from this simulation is the fact that having a structure which is not overly stiff can ensure low levels of acceleration for the partner vehicle. At the moment this is done at the expense of occupant protection and a more balanced solution must be found, together with a design that limits the perforation of the barrier.

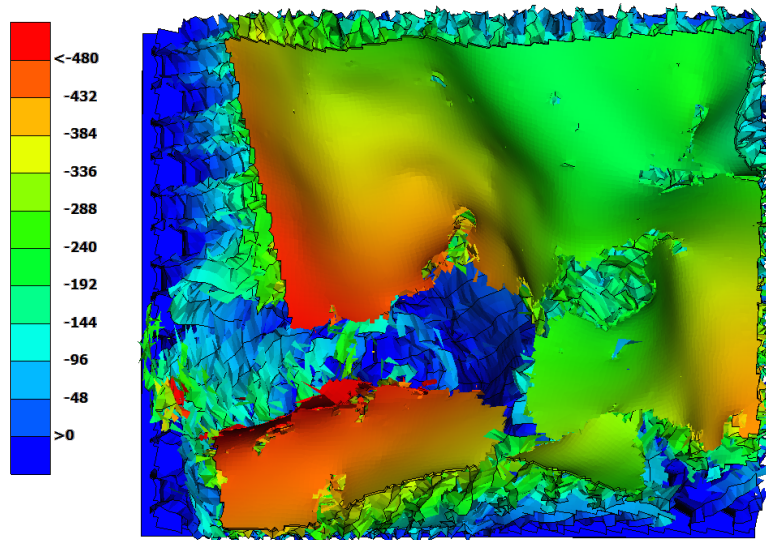


Figure 6.13: U Model - barrier deformation in area of interest

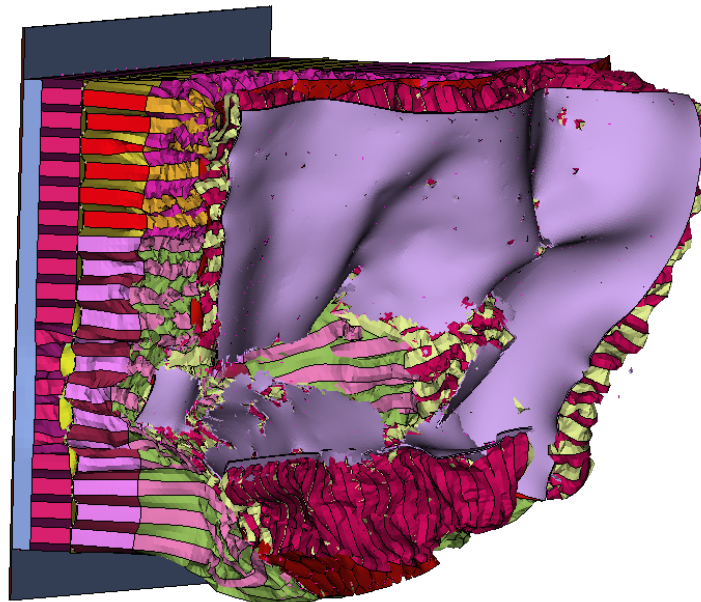


Figure 6.14: U Model - overall barrier deformation

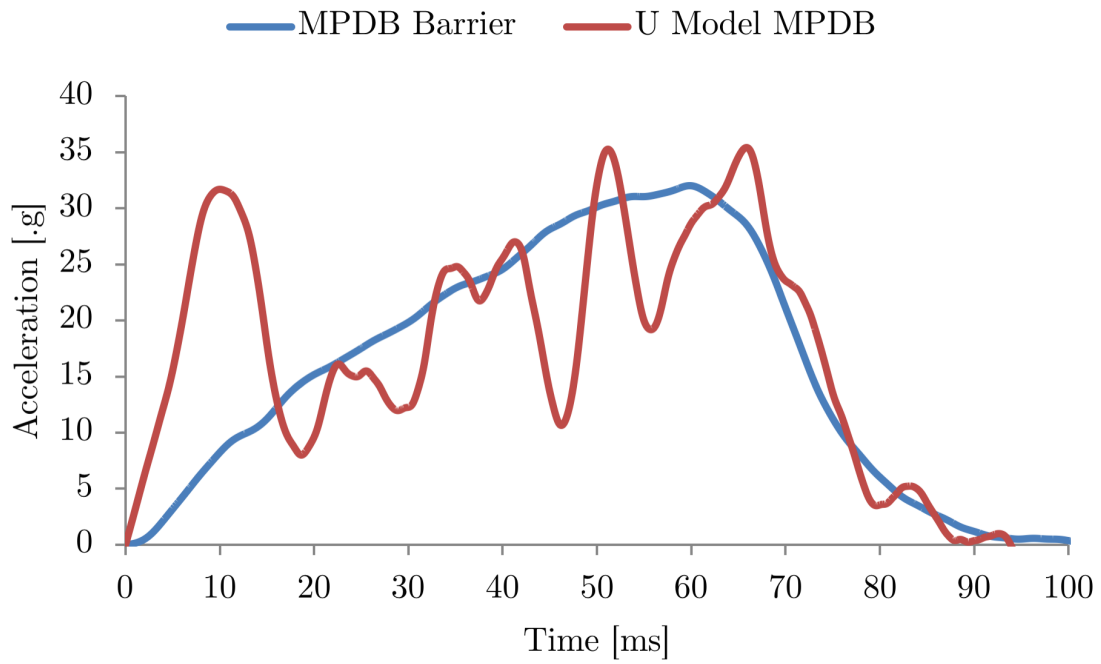


Figure 6.15: U Model - barrier and vehicle acceleration comparison

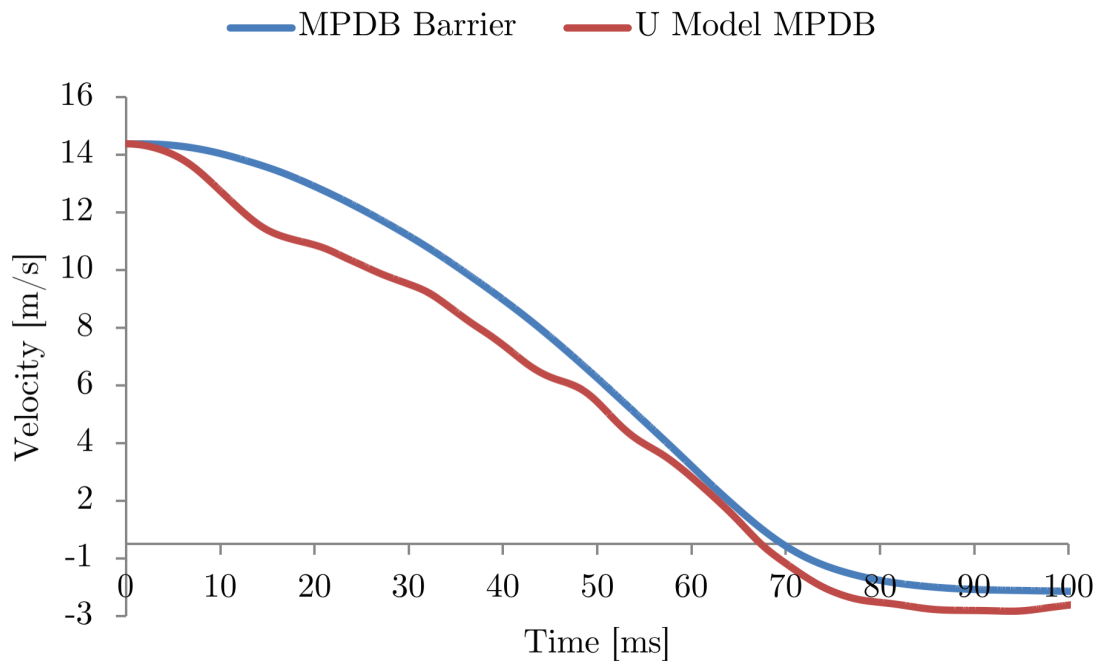


Figure 6.16: U Model - barrier and vehicle velocity comparison

6.4 Conclusions

In conclusion, this part of the study has shown some interesting trends in relation to the partner protection assessment that will be included in the new Euro NCAP procedure. Although the parameters are still not finalised, it is safe to assume that the analysis methods used for this work are close to those that will be implemented by the consumer safety assessment programme. A part that was unfortunately completely missing from literature is the relationship between the results obtained through the mean and standard deviation calculations and the thresholds that will be put in place, meaning that it is hard to relate these results with the specific rating that would be given. Nonetheless, it has been possible to understand that the major factor in partner protection is in fact the design of the frontal structures of the vehicle, rather than it being primarily related to the mass of the vehicle and the stiffness of the front rails. This was demonstrated by the Toyota Yaris, which, despite being light, achieved extremely poor results both in terms of mean deformation and standard deviation. This was due to the incorrect behaviour of its main rail and the presence of only one load path. On the opposite end of the scale, the Honda Accord showed the ability to achieve positive results all around, thanks to the more complex front end design which was the only example of a first step towards compatibility-driven structural engineering. Its increased mass also didn't produce significantly higher acceleration pulses through the trolley. With regards to the other two vehicles analysed, their shortcomings were very evident and highlighted the fact that the ladder chassis design will pose a very difficult challenge for the future, if they will be used in partner protection assessments. Furthermore, the Silverado, although not being a vehicle present on European roads, could be in a way compared to the vast majority of the light commercial vehicles circulating on EU roads due to its chassis design and overall mass, with the main difference being the distance of the cabin from the leading edge of the bonnet. Its performance in the compatibility assessment highlights how important it will be to modify the structural designs of those types of vehicles too, in order to achieve an overall higher safety level of the circulating fleet.

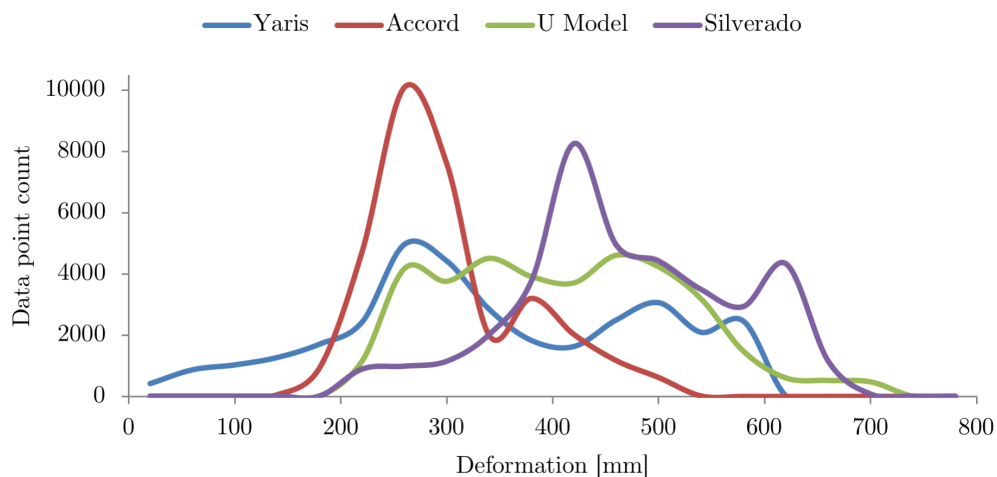


Figure 6.17: Comparison between analysed vehicles

Chapter 7

Conclusions and further work

In this final chapter, the conclusions reached in each part of the study are summed up in order to give a clear idea of the findings. The points of criticality in the work performed are also highlighted, while the steps that would be required to improve and extend the findings that have been here reported are explained.

7.1 Simulation study conclusions

The overall aim of gaining a deeper understanding of the effect of the Euro NCAP MPDB test procedure on vehicles with different masses and chassis designs was achieved by conducting comparative simulations on four different models and two different structural philosophies. The main aim of the study entailed three separate objectives that had to be reached, in order to obtain a clear and comprehensive picture.

The first was the correlation of the models used with their physical counterparts, so that a sufficient level of reliability could be proved, with regards to the results that would have been later obtained. The correlation study was hence developed for the first three vehicles - Yaris, Accord, Silverado - using a full width rigid barrier procedure at 56km/h . The findings were that two out of the three mathematical models considered were closely representative of reality, with intrusion levels in a close range to those reported by NHTSA and crash pulse peaks that achieved the same maxima and, with some tolerance, similar locations in the crash timeframe. The differences observed were attributed mainly to the partial model completeness in terms of equipment in the engine compartment and to imperfections in the definition of materials of non structural components. On the other hand, the model of Honda Accord was found to have a number of issues: although the intrusion measurements were on the boundaries of the expected tolerance, the crash pulse was completely unrelated to that resulting from the physical test. The overall behaviour of the front structures was also found to be problematic and great effort was put into modifying the model to obtain a more significant simulation. This was only partially achieved, as the structural collapse sequence improved, but the crash pulse was for the most part unvaried. Regarding the fourth model, the correlation was performed by analysing the data gathered by Pininfarina s.p.a. in an internal study. The U Model was tested in the ODB 56km/h procedure and showed positive results in terms of intrusion, but also

highlighted some criticalities as the overall deformation of the cabin was overestimated with a collapsing roof rail.

The second, and most relevant, objective was to compare the current ODB 64km/h test with the new MPDB procedure with regards to occupant protection, performing both simulations on all four vehicles. The obtained results showed how the trend of increased harshness of the mobile barrier procedure with decreasing mass of the vehicle can be confirmed. The lightest vehicle - Toyota Yaris - suffered an extreme increase in the levels of intrusion, to the point where the survival space was completely compromised. In this instance, the energy difference between the two tests was around 20%, in favour of the ODB. The Honda Accord, which not only has a mass similar to that of the trolley but also a more sophisticated structural design compared to the Yaris, achieved a comparable performance in both tests, with the MPDB proving to be marginally more severe than ODB. The difference in energy was still at 14%, but the vehicle managed to load the barrier in a more efficient way and its front end complexity ensured limited intrusion levels. This also gave an initial insight in the importance of the differences in the design of crash structures, the effects of which will have to be investigated further with vehicles of equal mass. Considering the heaviest vehicle out of the three, the trend seen for the Yaris was completely reversed. The Chevrolet Silverado pickup achieved poor results in terms of deformation in the ODB test, suffering from important collapse of the ladder's main rail, which in turn affected the cabin. In the MPDB, on the other hand, the severity was so diminished that almost no intrusion was recorded, apart for the deflection of the central part of the firewall. The energy difference in this case was of 10%, with the MPDB being the lower. These findings proved that such a heavy vehicle, despite its unrefined and simple front end, would be much safer for its occupants in a real world crash not only compared to the Yaris, but also to the Accord, with its advanced and complex ACE design. Clearly, this conclusion is limited to conditions of partial overlap frontal impacts, with a mass difference in a similar region. Finally, the U Model presented a clear improvement in terms of occupant protection when tested on the new procedure, despite the results of both tests being highly negative due to the fact that the vehicle was not designed to undergo the Euro NCAP assessment. In this case, the total energy present in the two impacts was very similar, with a discrepancy of only 1%. However, the vehicle loaded in a substantially better way the PDB, while it did not exploit at all the energy dissipation capacity of the ODB. This resulted in a limitation of the firewall intrusion, A-pillar displacement and resulting survival space reduction. The roof of the vehicle still showed signs of collapse but their extent was definitely milder. Overall, the levels of acceleration showed by the four vehicles on the MPDB test were very similar or lower than those experienced in ODB in terms of peak, but the crash severity was increased in all of them due to the reduced total time of the event. In addition, an unexpected result was found in the mode of loading of the frontal structures of the models: from literature, the PDB was predicted to offer a much more complex loading platform for the crash boxes and main rails, with the result being an incorrect failure, for example from bending rather than axial buckling. This was not the case in this work, as only one of the four vehicles showed signs of improper failure of the crash box and it was the U Model, which did not have a front bumper to help in the correction of the direction of loading. However, the sample of models tested should be increased before finalising the significance of this finding.

Thirdly, the aspect of partner protection was also investigated, as it will be a central

topic for Euro NCAP with the 2020 modifications. This was done by following the proposed procedure published by ADAC [19], which contemplates a post-crash analysis of the barrier element to quantify the mean and standard deviation of the honeycomb's deformation. The procedure, developed for physical testing, was adapted to the simulation environment in order to obtain results as significant as possible. The change in velocity of the trolley and its acceleration were also analysed and compared to those of the vehicles. The findings demonstrated that the major role for the unevenness of deformation of the barrier is played by the design of the crash structures, as the worst standard deviation result of $143mm$ was achieved by the Yaris, the lightest vehicle of the lot. The same factor is the most influential for the maximum penetration in the honeycomb as well, as the Silverado and the U Model achieved a very similar value around $695mm$ despite their vast mass difference. Both vehicles punctured the PDB due to the ladder chassis construction. The Honda Accord showed the best results all around due to its more advanced front end, which spread the load evenly on the barrier face, causing the lowest mean deformation, lowest standard deviation and lowest maximum penetration. On the other hand, when considering velocity change and acceleration, the correlation with the vehicle mass is very strong. The Yaris was accelerated by the barrier in negative direction heavily, proving to be very light on the partner also in terms of peak acceleration. The Accord and the U model both showed similar results, as the barrier was pushed back only after the vehicle also crossed the zero line. At the opposite end of the scale, the Silverado was extremely harsh on the trolley, as it accelerated it backwards up to almost $20km/h$ while continuing on its direction of movement. Overall, the results of the U Model and Silverado proved that it will be critical to modify the ladder chassis construction for the new compatibility requirements and that a great deal of work will have to be performed on large vehicles such as SUVs to ensure a reduction in the energy transferred to the structures of lighter partners in car-to-car accidents. In addition, to bring these findings closer to the European roads, the results of the Silverado can give an initial idea of the criticalities that light commercial vehicles present in real world crashes for the average passenger car, as their mass and the widespread use of ladder frames can cause damages similar to those seen for the US pickup, if no additional and more sophisticated load paths are employed.

All in all, the utilisation of the ODB procedure in consumer testing brought positive results since its year of establishment, but the comparison with the MPDB test highlighted that it also created a trend of misleading beliefs about occupant protection, especially with respect to the many small cars achieving a five star rating, which proved to the public a safety level far above reality. It is safe to say that the new Euro NCAP procedure will bring an important improvement in terms of representativeness of real world impacts, giving to the consumers a more reliable view of the safety of their vehicle, which is ultimately the whole purpose of consumer testing. As demonstrated in the past, this will drive manufacturers towards substantial improvements in occupant protection and the same is expected for compatibility and partner protection as well, where larger vehicles will be most interested.

7.2 Further work

In order to expand the findings here presented and achieve even more significant results, a few actions should be taken:

- first of all, the issues with the Honda Accord model should be resolved, repeating the correlation study throughout the process of modification of the mathematical model to achieve a higher level of representativeness. The objective should be to replicate the crash pulse as closely as possible, maintaining the sequence of collapsing structures as it is at this moment;
- the missing bumper, wings and bonnet of the U Model should be added and the comparative study should be repeated, together with the analysis of the barrier for partner protection. Only in this way it is possible to ensure that the findings are effectively related to the vehicle behaviour;
- the final procedure for the partner protection assessment, which will be published in 2019, should be used to repeat or improve the compatibility study and understand the rating level that would be achieved with the values resulting from these four vehicles;
- additional models should be tested, mainly with the aim of utilising two vehicles with similar mass and different front end construction, in order to verify the importance of the impact that the structural features have, both on occupant and on partner protection;
- mathematical models of more modern vehicles should be sourced in order to get a better understanding of the performance of the current technological level, trends that have arisen in the recent years and areas still to improve before 2020. This is however difficult to achieve and possibly unrealistic, as the availability of complete vehicle models is extremely scarce.

Bibliography

- [1] “NHTSA NCAP - Frontal Barrier Impact Test report - 2014 Chevrolet Silverado 1500 4WD LT Crew Cab,” tech. rep., 2014.
- [2] Pininfarina, “U Model - ODB correlation report,” tech. rep., 2014.
- [3] M. Van Ratingen, A. Williams, A. Lie, A. Seeck, P. Castaing, R. Kolke, G. Adriaenssens, and A. Miller, “The European New Car Assessment Programme: A historical review,” *Chinese Journal of Traumatology - English Edition*, vol. 19, no. 2, pp. 63–69, 2016.
- [4] EEVC Working Group 11, “EEVC Working Group 11 Report on the Development of a Front Impact Test Procedure,” no. 94, pp. 94-SS-0-05, 1994.
- [5] C. Hobbs and P. McDonough, “Development of the European new car assessment programme (Euro NCAP),” *Regulation 44*, no. 1, p. 3, 1998.
- [6] J. Martins, R. Ribeiro, P. Neves, and F. Brito, “Accident Reconstruction Using Data Retrieval from Crash-Test Video Images,” *SAE Technical Papers*, no. April, 2016.
- [7] “Argos International, <https://www.argosyinternational.com/>.”
- [8] E. del Pozo de Dios, I. Lázaro, P. Delannoy, R. Thomson, T. Versmissen, and E. van Nunen, “Development of a structural interaction assessment criteria using progressive deformable barrier data,” pp. 1–13, 2013.
- [9] R. Baxter, N. Hastings, A. Law, and E. J. Glass, “Evaluation of moving progressive deformable barrier test method by comparing car to car crash test,” *Honda R&D Co., Ltd. Automobile R&D Center*, 2017.
- [10] J. Ellway, “Euro NCAP Mobile Progressive Deformable Barrier Face Specification,” *TB022*, 2017.
- [11] “2010 Toyota Yaris Sedan, <https://www.motortrend.com/cars/toyota/yaris/2009/>.”
- [12] “Toyota Yaris engine compartment, <http://www.mbzponton.org/n2awa/yaris.html>.”
- [13] “2011 Honda Accord, <https://www.motortrend.com/cars/honda/accord/2010/>.”
- [14] “Honda Accord engine compartment, <https://www.cargurus.com/Cars/2011-Honda-Accord-Overview-c22452>.”
- [15] “Honda Accord front BIW, http://www.hondanews.com/releases/2010-honda-accord-crosstour-safety?page=47&page_size=20&query=nears.”
- [16] “2014 Chevrolet Silverado, <https://www.motortrend.com/cars/chevrolet/silverado-1500/2014/>.”
- [17] “Chevrolet Silverado engine compartment, <http://www.trucktrend.com/truck-reviews/163-1312-2014-chevrolet-silverado-z71-double-cab-4x4-first-test/>.”
- [18] ERSO, “Annual Accident Report 2017,” tech. rep., 2017.

-
- [19] S. Volker and R. Andreas, "MPDB-Mobile offset progressive deformable barrier," *Proceedings of the 24th Technical Conference on the Enhanced Safety of Vehicles*, pp. Paper Number 15-0389, 2015.
- [20] A. Kullgren, A. Lie, and C. Tingvall, "Comparison Between Euro NCAP Test Results and Real-World Crash Data," *Traffic Injury Prevention*, vol. 11, no. 6, pp. 587-593, 2010.
- [21] "About Euro NCAP, <https://www.euroncap.com/en/about-euro-ncap/>." 2015.
- [22] Euro NCAP, "2020 Roadmap - European New Car Assessment Programme," 2015.
- [23] D. Krayterman, "Comparative Analysis of THOR-NT ATD vs . Hybrid III ATD in Laboratory Vertical Shock Testing," 2013.
- [24] E. NCAP, "Euro NCAP 2025 Roadmap," 2018.
- [25] H. CA, "The rationale and development of the offset deformable frontal impact test procedure," *SAE International*, vol. 950501, no. 41 2, pp. 151-158, 1995.
- [26] UN, "Addendum 93: Regulation No. 94 - Revision 3," 2017.
- [27] EuroNCAP, "Euro NCAP - Offset Deformable Barrier Frontal Impact Testing protocol," no. Version 7.1.2, 2017.
- [28] M. J. Edwards, R. W. Cuerden, J. Price, J. Broughton, M. Wisch, C. Pastor, and T. Adolph, "Estimation of the benefits for potential options to modify UNECE Regulation No. 94 to improve a car's compatibility," 2011.
- [29] T. Adolph, J. Ott, B. Eichhoff, and H. Johannsen, "What is the Benefit of the Frontal Mobile Barrier Test Procedure?," 2015.
- [30] J. M. Nolan and A. K. Lund, "Frontal offset deformable barrier crash testing and its effect on vehicle stiffness," *Insurance Institute for highway safety; United States of America*, p. Paper no. 487., 2001.
- [31] L. Chang Min, S. Jang Ho, K. Hyun Woo, P. Kun Ho, and P. Young Joon, "Study on car-to-car frontal offset impact with vehicle compatibility," *Hyundai Motor Company*, 2017.
- [32] T. Versmissen, J. Welten, and C. Rodarius, *FIMCAR X – MDB Test Procedure : Test and Simulation Results*, vol. 9. 2013.
- [33] H. Johannsen, T. Adolph, M. Edwards, I. Lazaro, and R. Thomson, "Proposal for a Frontal Impact and Compatibility Assessment Approach Based on the European FIMCAR Project," *Traffic Injury Prevention*, 2013.
- [34] V. Sandner, J. Ellway, and M. V. Ratingen, "Euro NCAP Frontal Impact Working Group Report," 2017.
- [35] T. Adolph, H. Schwedhelm, I. Lazaro, T. Versmissen, M. Edwards, and R. Thomson, "Development of compatibility assessments for full-width and offset frontal impact test procedures in FIMCAR," *International Journal of Crashworthiness*, 2014.
- [36] M. J. Edwards, P. de Co, C. V. der Zwepp, and E. Al., "Improvement of Vehicle Crash Compatibility through the Development of Crash Test Procedures," 2007.
- [37] I. Lazaro, N. Vie, R. Thomson, and H. Schwedhelm, "FIMCAR V – Off-set Test Procedure : Review and Metric Development," tech. rep., 2013.
- [38] C. Min, H. Woo, K. Ho, and Y. Joon, "Study on car-to-car frontal offset impact with vehicle compatibility," *Hyundai motor company*, 2017.
- [39] H. Johannsen and R. Thomson, "Compatibility assessment: Can the current ADAC MPDB test properly assess compatibility?," *2016 IRCOBI Conference Proceedings - International Research Council on the Biomechanics of Injury*, pp. 635-636, 2016.

- [40] M. Wolkenstein, G. D’Addetta, and P. Luttenberger, “A Mobile Deformable Barrier Test for the Front Crash Assessment of Future Urban Microcars,” pp. 1–11, 2015.
- [41] S. M. Summers and W. T. Hollowell, “Nhtsa’s Crashworthiness Modeling Activities,” *17th ESV*, pp. 1–5, 2001.
- [42] E. L. Fasanella and K. E. Jackson, “Best Practices Simulation for Crash Modeling and Simulation,” *Nasa Sti*, no. 211944, pp. 1–99, 2002.
- [43] “BETA CAE Systems, <https://www.beta-cae.com/>.”
- [44] “LSTC LS-DYNA, <https://www.dynamore.it/en/products/dyna>.”
- [45] “NHTSA LS-DYNA models, <https://www.nhtsa.gov/crash-simulation-vehicle-models>.”
- [46] S. Ridella, “Fleet Safety Evaluation Methodology: Application to Lightweight Vehicle Designs,” 2013.
- [47] “Honda ACE, <https://www.honda.com/safety/safety-by-design>.”
- [48] “LSTC Barriers, <http://www.lstc.com/products/models/barriers>.”
- [49] S. Bala, “LSTC ODB Barriers - presentation.”
- [50] D. Bhalsod and R. Chivukula, “Progressive Deformable Barrier,” 2015.
- [51] N. H. T. S. A. NHTSA, “Laboratory Test Procedure For New Car Assessment Program Frontal Impact Testing,” Tech. Rep. September, 2012.
- [52] “NHTSA Ratings Database, <https://www.nhtsa.gov/ratings>.”
- [53] “NHTSA NCAP Test Database, <https://www-nrd.nhtsa.dot.gov/database/VSR/veh/QueryTest.aspx>.”
- [54] “NHTSA NCAP - Frontal Barrier Impact Test report - 2007 Toyota Yaris,” tech. rep., 2007.
- [55] “NHTSA NCAP - Frontal Barrier Impact Test report - 2011 Honda Accord LX 4-Dr Sedan,” tech. rep., 2011.
- [56] IIHS, “2014 Chevrolet Silverado 1500 IIHS Report,” tech. rep., 2014.

Appendix A

Simulation energy charts

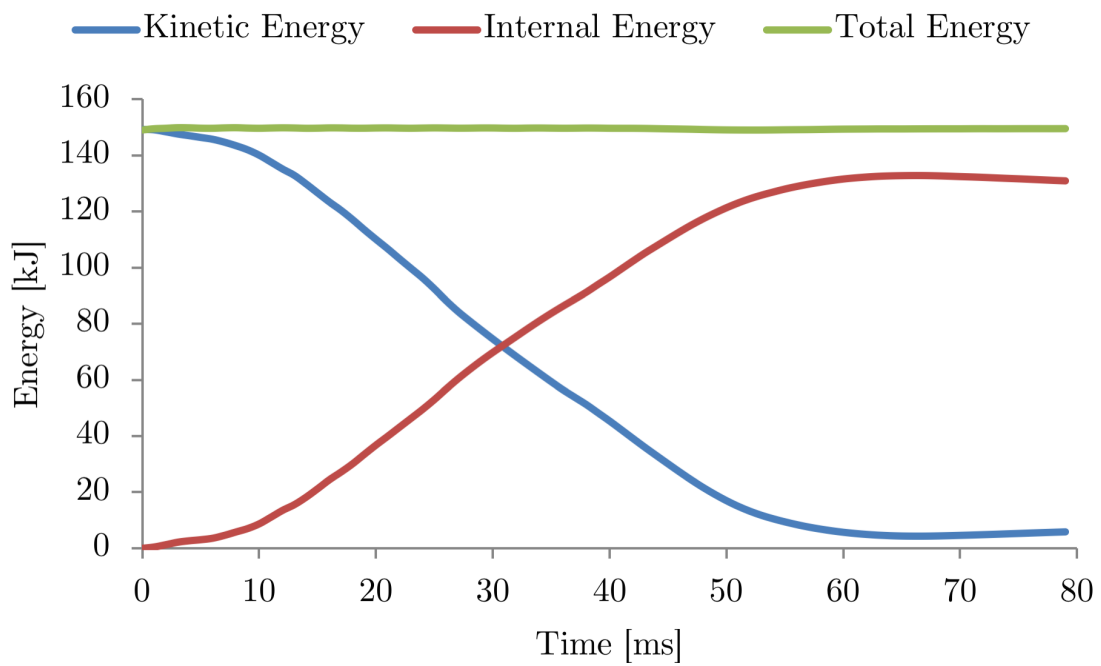


Figure A.1: Toyota Yaris FWRB - simulation energy

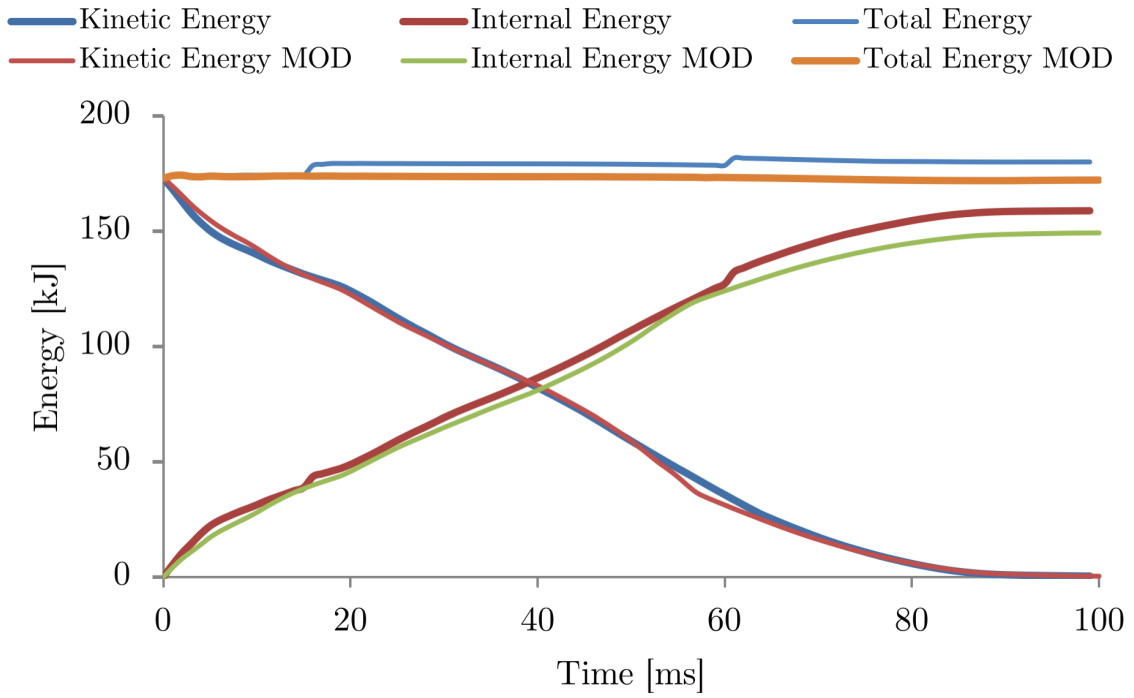


Figure A.2: Honda Accord FWRB - simulation energy

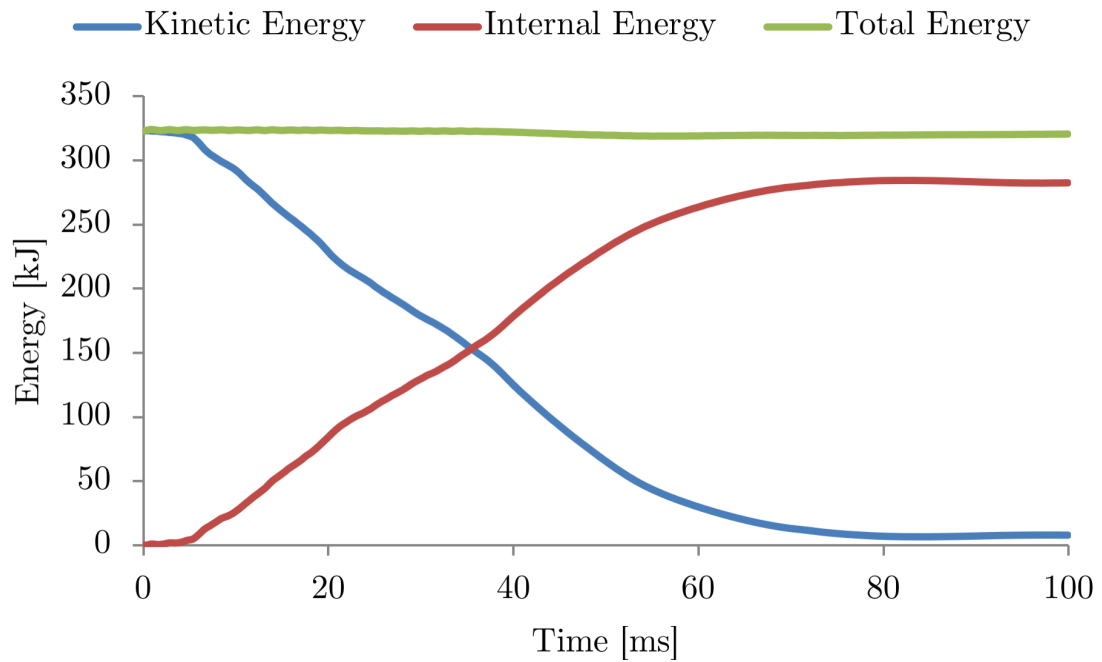


Figure A.3: Chevrolet Silverado FWRB - simulation energy

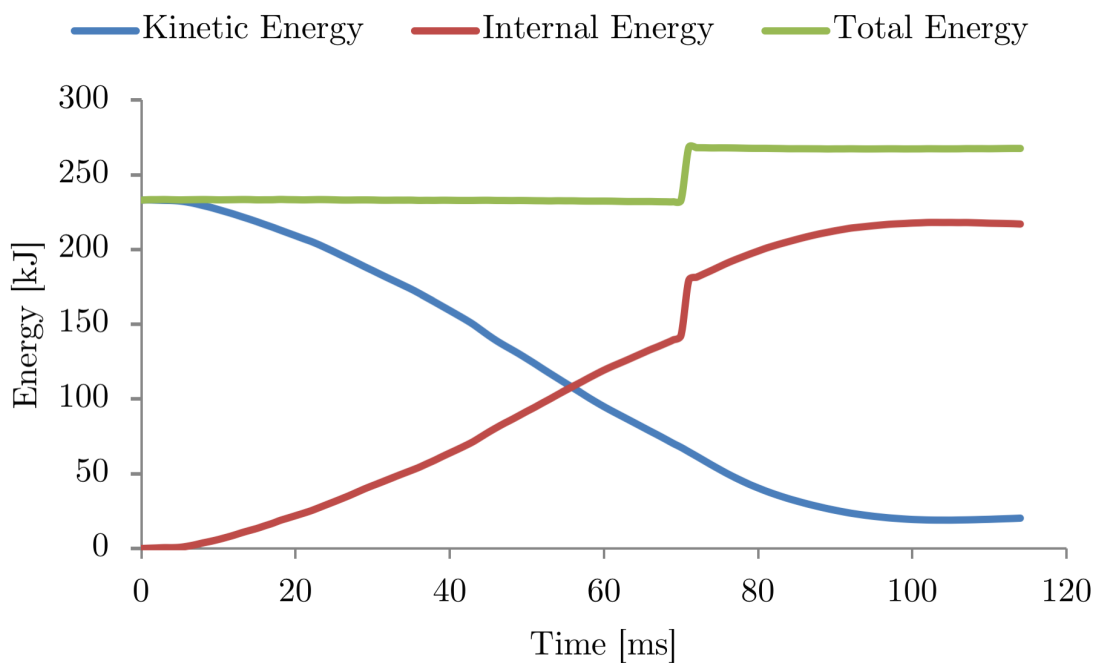


Figure A.4: U Model ODB 56km/h - simulation energy

Appendix B

Correlation study photographs

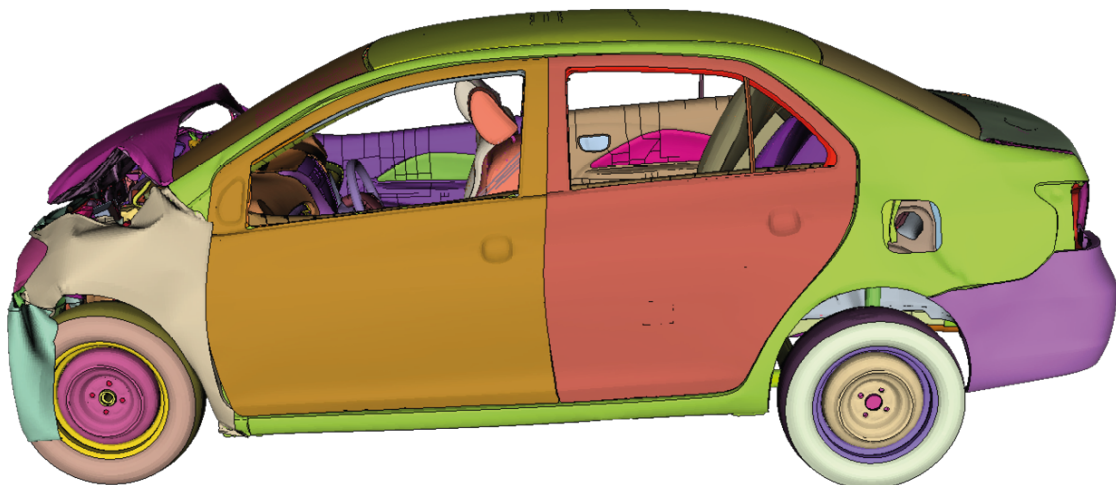


Figure B.1: Toyota Yaris FWRB - LHS comparison

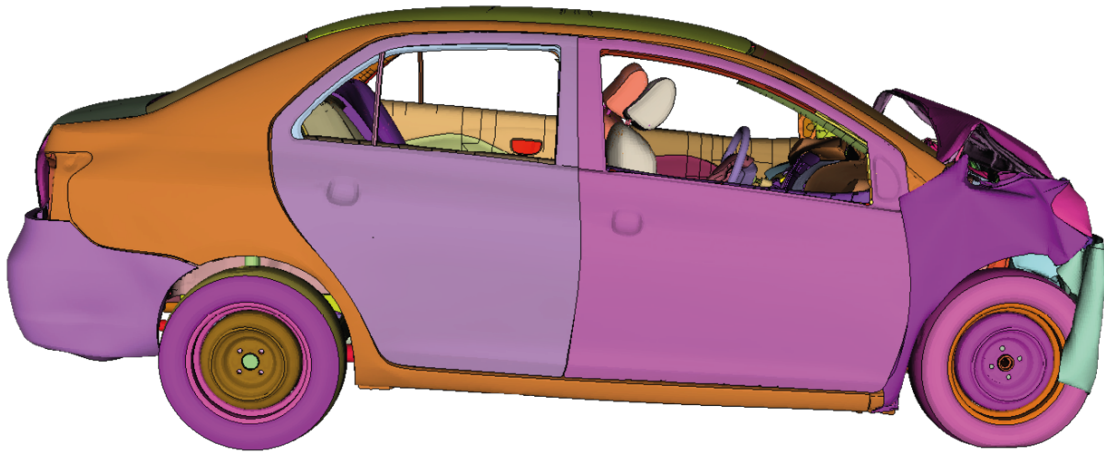


Figure B.2: Toyota Yaris FWRB - RHS comparison

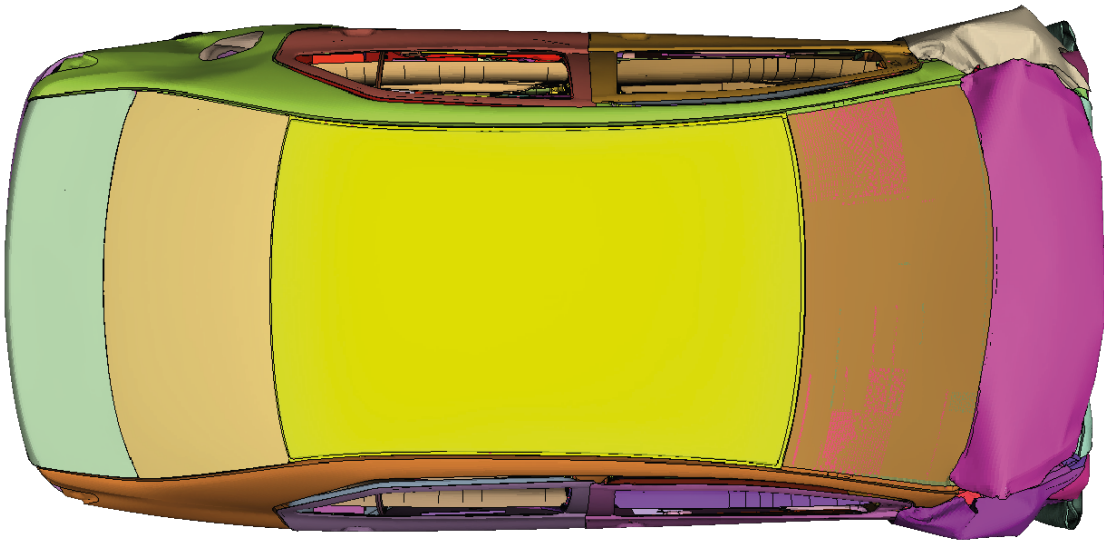
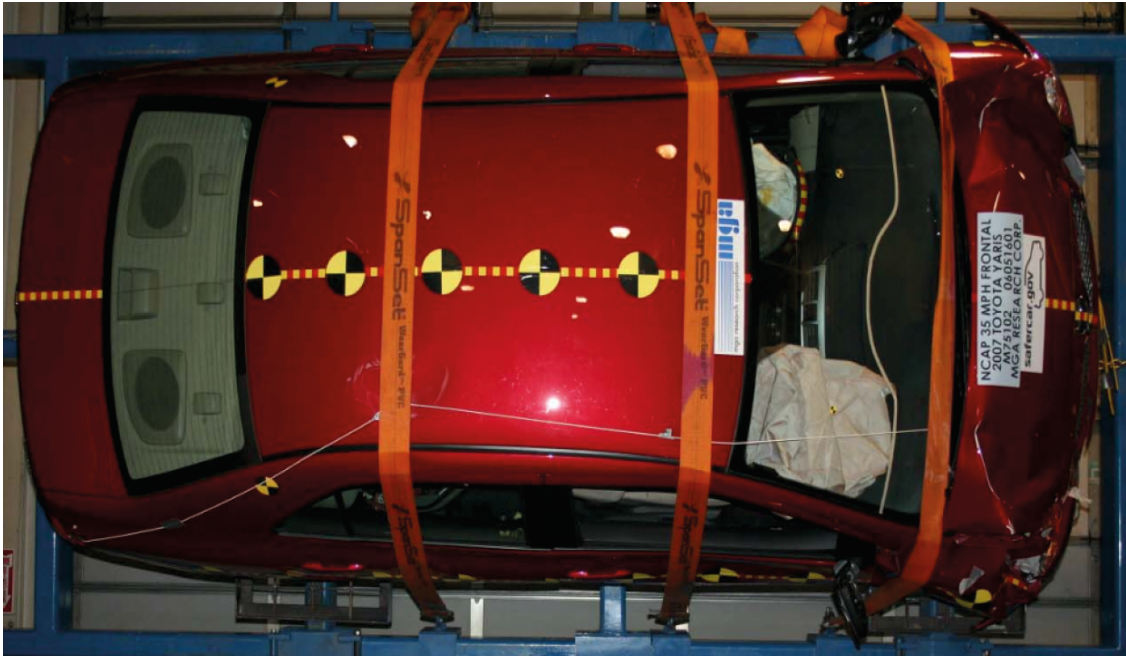


Figure B.3: Toyota Yaris FWRB - top view comparison

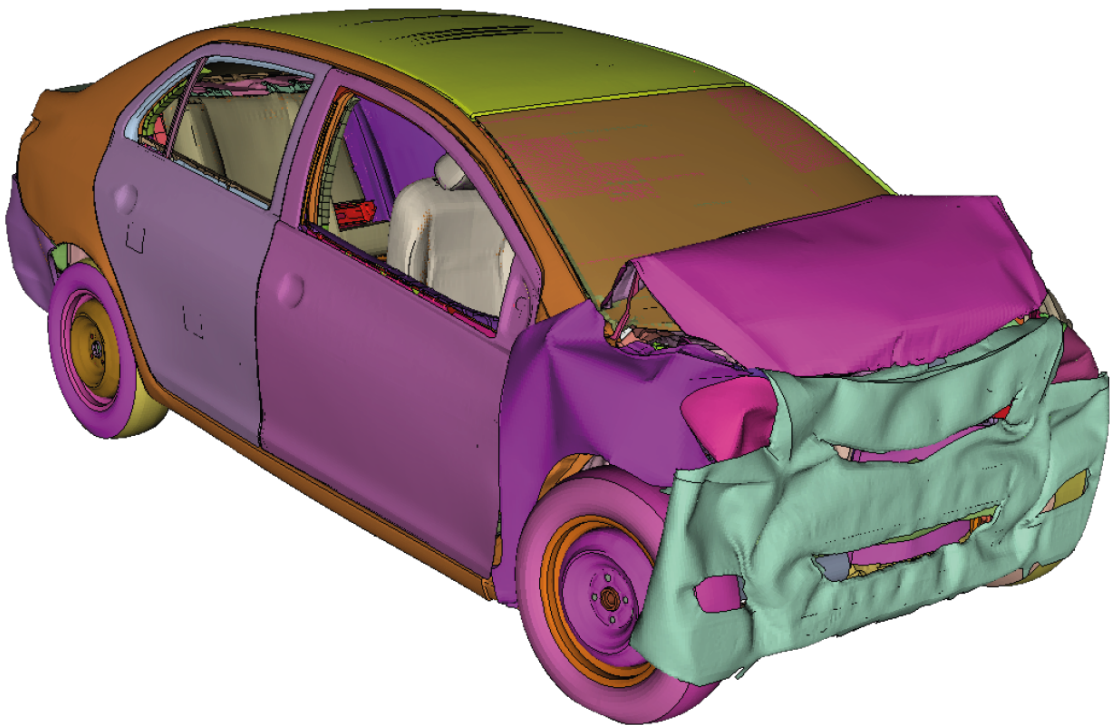


Figure B.4: Toyota Yaris FWRB - three quarter view comparison

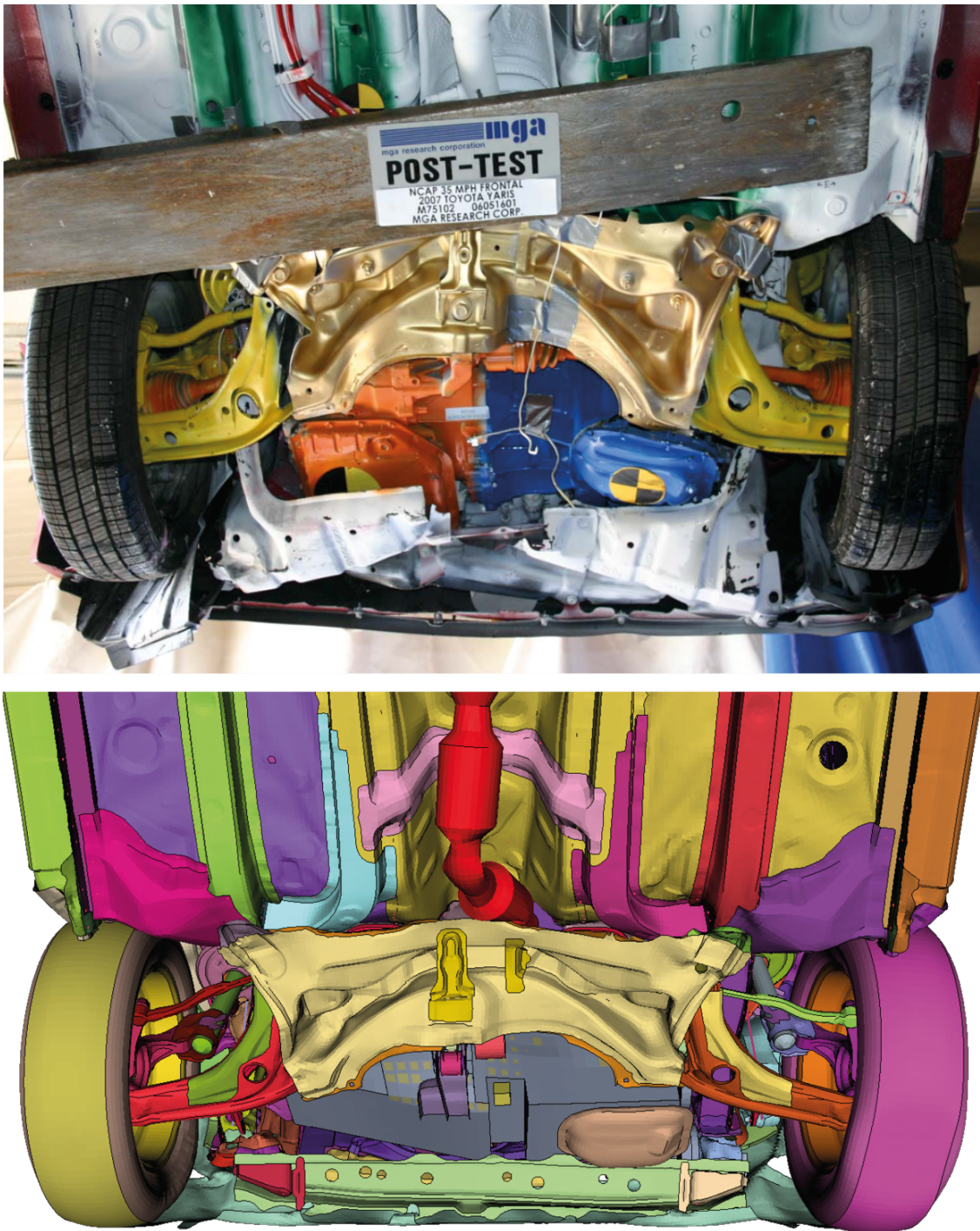


Figure B.5: Toyota Yaris FWRB - underbody comparison



Figure B.6: Honda Accord FWRB - LHS comparison



Figure B.7: Honda Accord FWRB - RHS comparison

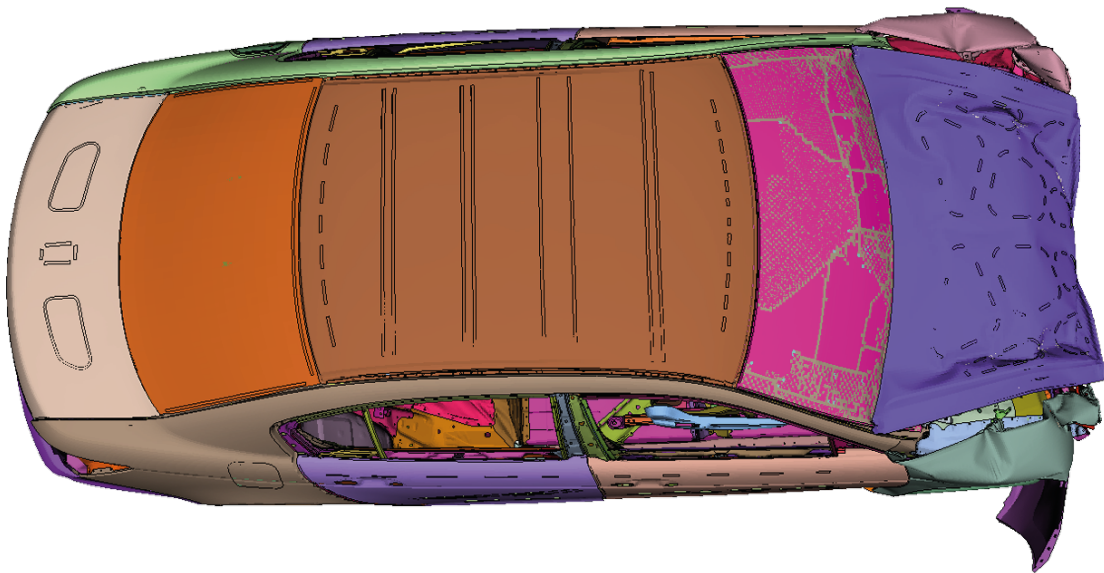


Figure B.8: Honda Accord FWRB - top view comparison

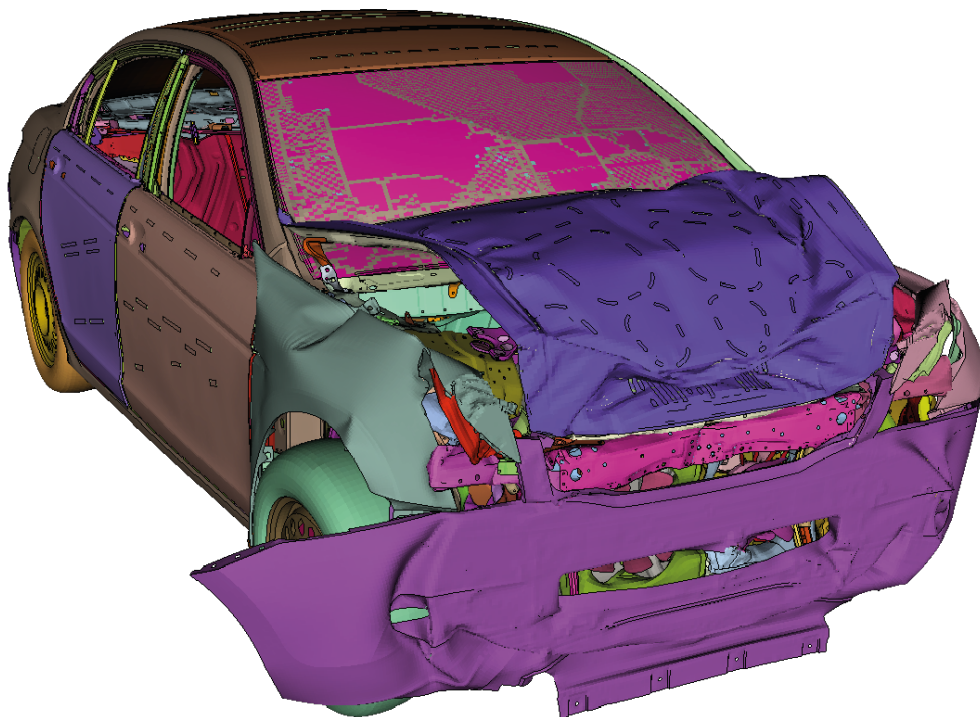


Figure B.9: Honda Accord FWRB - three quarter view comparison

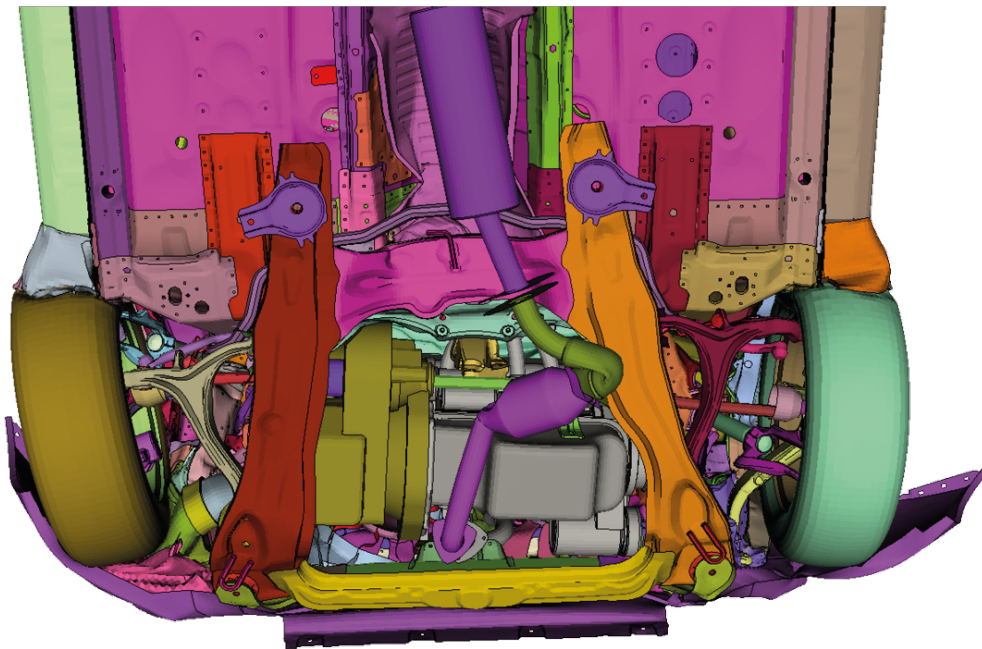


Figure B.10: Honda Accord FWRB - underbody comparison

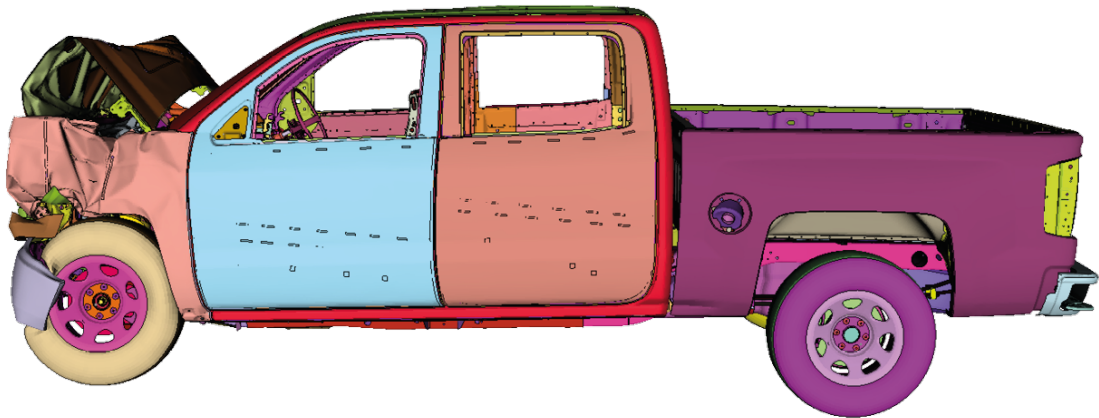


Figure B.11: Chevrolet Silverado FWRB - LHS comparison

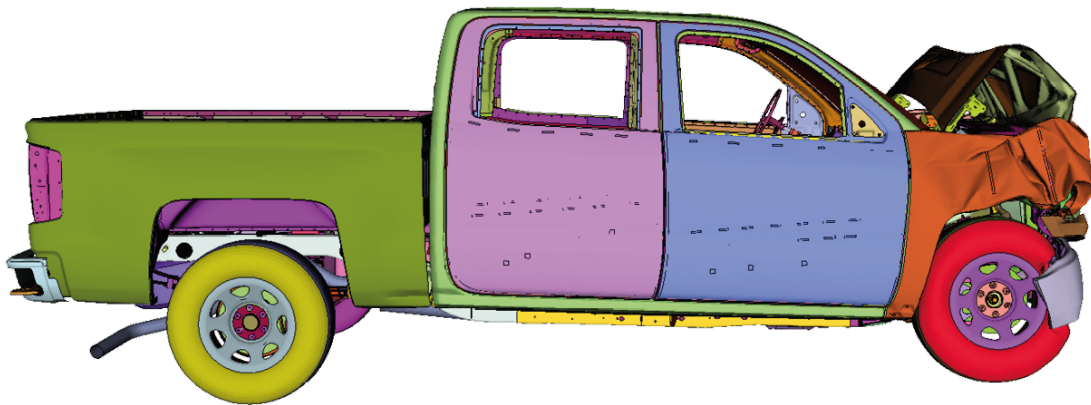


Figure B.12: Chevrolet Silverado FWRB - RHS comparison

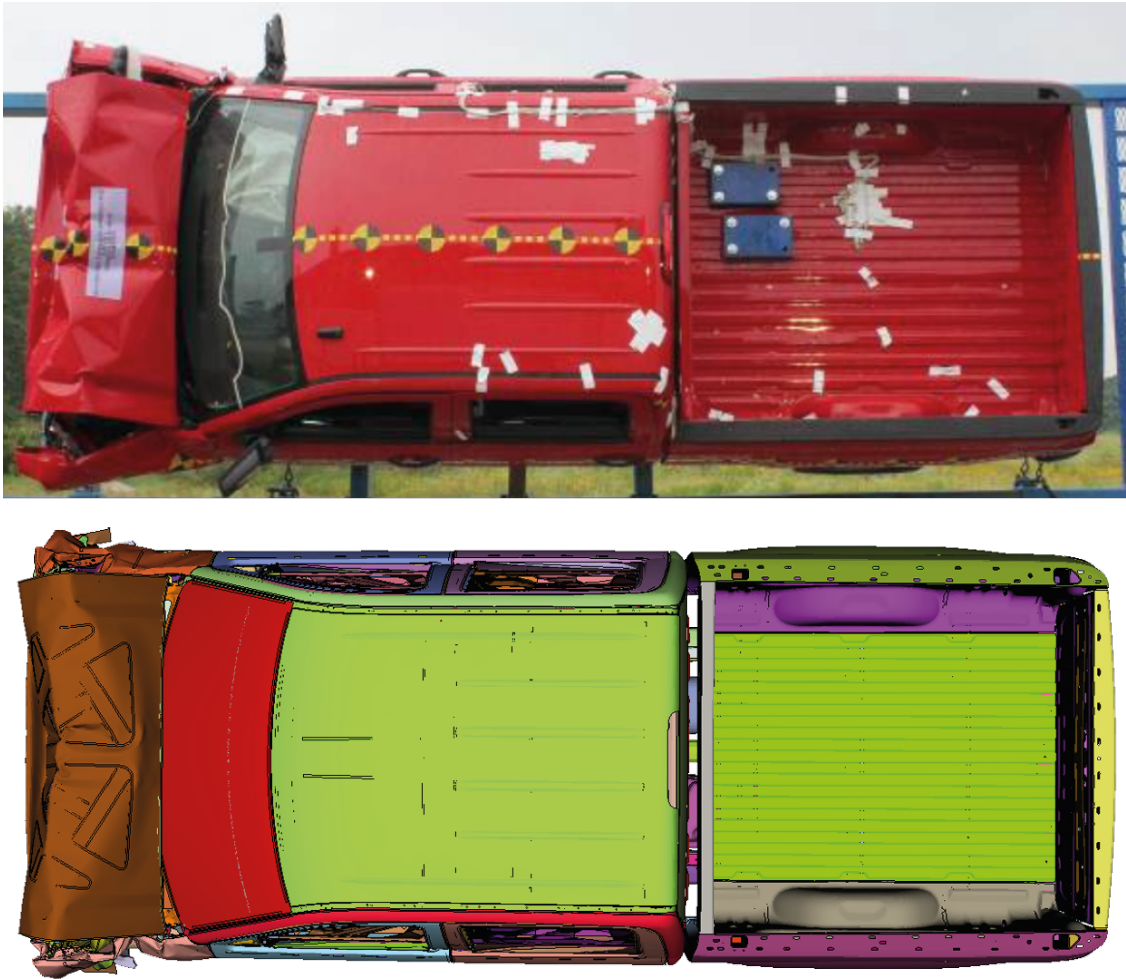


Figure B.13: Chevrolet Silverado FWRB - top view comparison

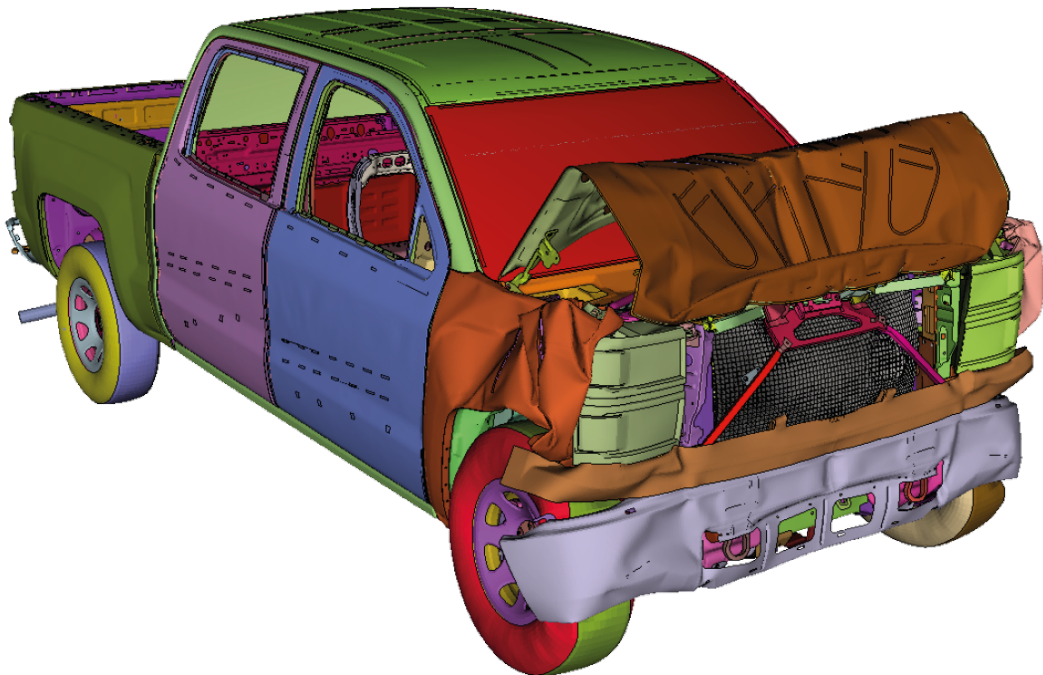


Figure B.14: Chevrolet Silverado FWRB - three quarter view comparison

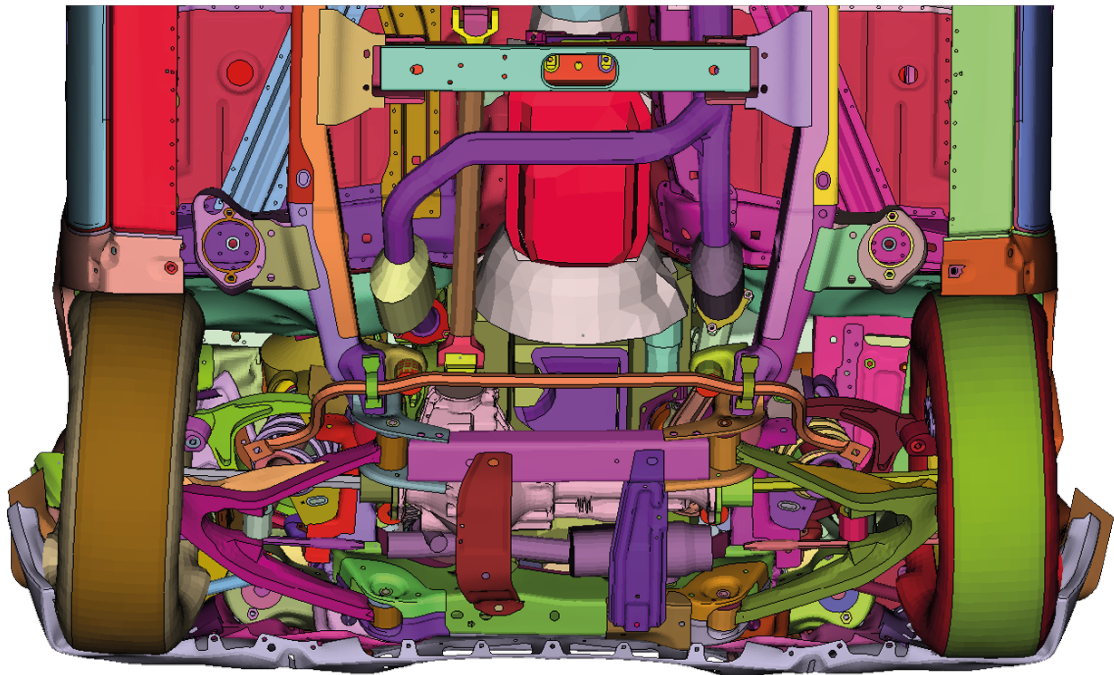


Figure B.15: Chevrolet Silverado FWRB - underbody comparison

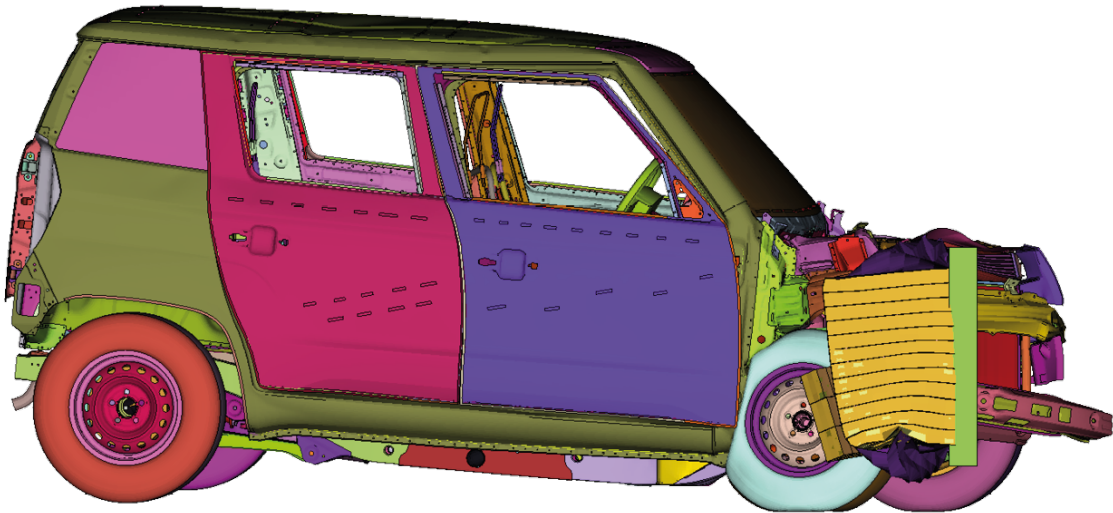


Figure B.16: U Model ODB 56km/h - RHS comparison

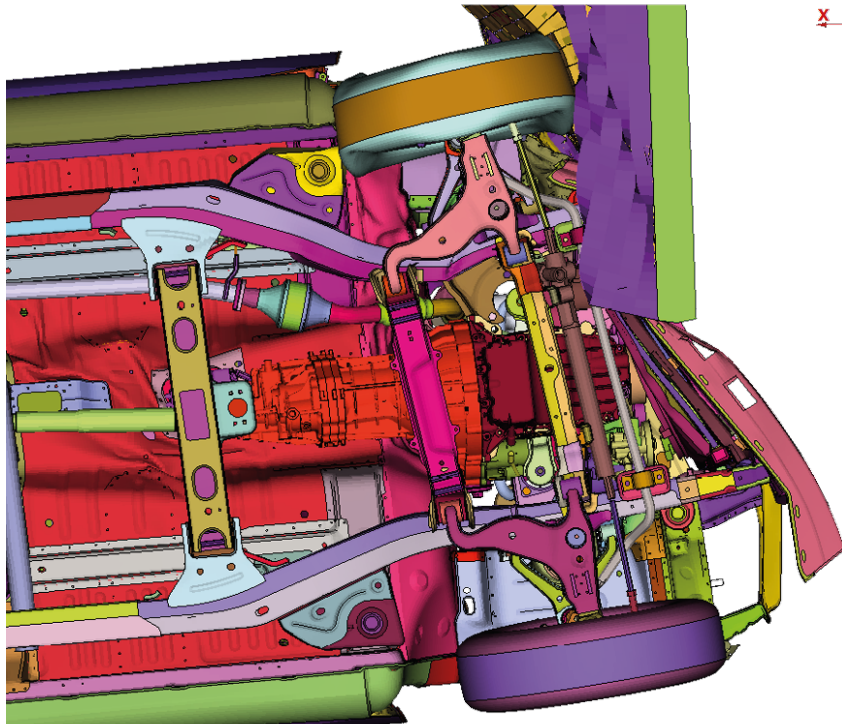
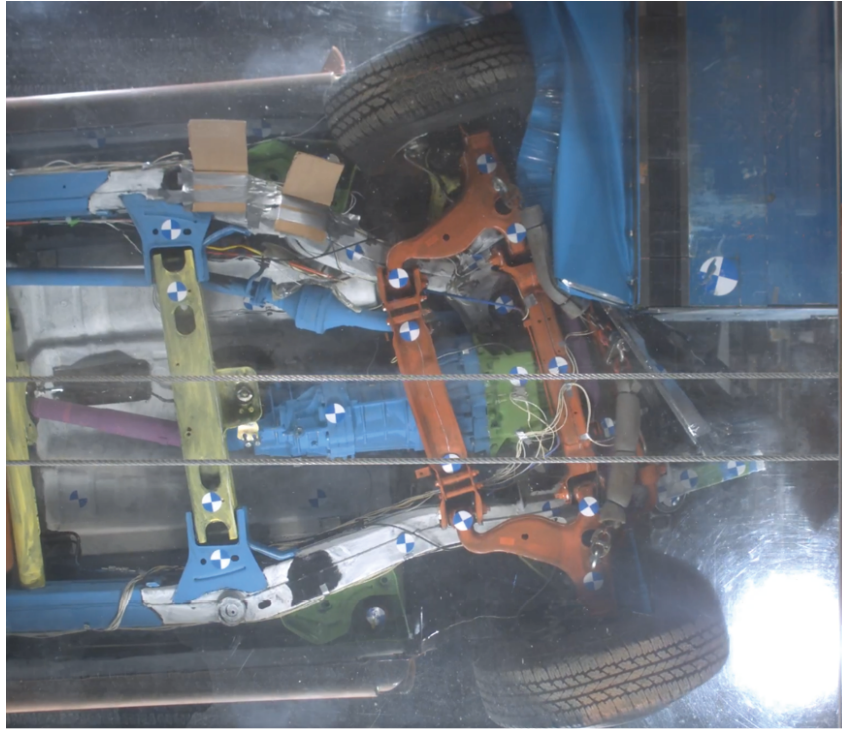


Figure B.17: U Model ODB 56km/h - underbody comparison